THE ROLE OF ADAPTOR PROTEIN GADS

IN CD8$^+$ T CELL-MEDIATED IMMUNITY

BY

Elizabeth Yan Zhang

Submitted to the graduate degree program in Microbiology, Molecular Genetics and Immunology and the Graduate Faculty of the University of Kansas in partial fulfillment of the requirements for the degree of Doctor of Philosophy.

Dissertation Committee:

_____

Chairperson: Thomas M. Yankee, Pharm. D., Ph.D.

_____

Stephen H. Benedict, Ph.D.

_____

Michael J. Parmely, Ph.D.

_____

Jianming Qiu, Ph.D.

_____

Charlotte M. Vines, Ph.D.

Date defended: August 23rd, 2011

The Dissertation Committee for Elizabeth Yan Zhang

certifies that this is the approved version of the following dissertation:

THE ROLE OF ADAPTOR PROTEIN GADS IN CD8$^+$ T CELL-MEDIATED IMMUNITY

_____

Chairperson: Thomas M. Yankee, Pharm. D., Ph.D.

Date approved: August 23rd, 2011

Abstract

$CD8^+$ T cells are the branch of the adaptive immune system responsible for recognizing and killing tumor cells or cells infected with intracellular pathogens, such as *Listeria monocytogenes* (LM). However, when $CD8^+$ T cells target our own tissues, they can cause autoimmune diseases, such as type I diabetes, rheumatoid arthritis. For $CD8^+$ T cells to fulfill these functions, the T cell receptors (TCRs) on $CD8^+$ T cells must recognize pathogens or antigens presented on the surface of target cells. TCR ligation triggers multiple signaling pathways that lead to the activation and proliferation of $CD8^+$ T cells. The goal of our research is to define the TCR-proximal signaling events that regulate $CD8^+$ T cell-mediated immunity. To accomplish this goal, we are focusing on an adaptor protein Gads, which is critical for optimal TCR-mediated calcium mobilization. We reported the first analysis of the function of Gads in peripheral naïve $CD8^+$ T cells.

To examine the function of Gads in $CD8^+$ T cell mediated immune responses, we crossed $Gads^{-/-}$ mice with mice expressing an MHC class I-restricted transgenic TCR recognizing ovalbumin (OVA). The transgenic mice are called ovalbumin-specific T cell receptor-major histocompatibility complex class I restricted (OT-I) mice. We investigated the effect of Gads on the proliferation of $CD8^+$ T cells following stimulation with peptide antigen *in vivo* and *in vitro*. We stimulated splenocytes from $Gads^{+/+}$ OT-I and $Gads^{-/-}$ OT-I mice with the peptide agonist. The experiments revealed that Gads is required for optimal proliferation of $CD8^+$ T cells. The regulation of Gads is most evident at the early time points of proliferation. Then we demonstrated that $Gads^{-/-}$ $CD8^+$ T cells have impaired TCR-mediated exit from G_0 phase of the cell cycle. In addition, $Gads^{-/-}$ $CD8^+$ T cells have delayed expression of c-myc and the activation markers CD69 and CD25, upon stimulation with peptide antigen.

Next, we investigated how Gads affects $CD8^+$ T cell-mediated immunity in the context of infection with LM. We adoptively transferred naïve $CD8^+$ T cells from $Gads^{+/+}$ OT-I mice and/or

Gads$^{-/-}$ OT-I mice into congenic wild-type hosts. Then the recipient mice were infected with recombinant LM expressing ovalbumin (rLM-OVA). The CD8$^+$ T cells from OT-I mice recognize and respond to the ovalbumin provided by this strain of LM. By using this system, we investigated how Gads regulates the activation of antigen-specific CD8$^+$ T cells as well as the expansion and memory phases of CD8$^+$ T cell-mediated immune responses following infection with rLM-OVA. We also examined the recall response of CD8$^+$ T cells after the secondary encounter with the same pathogen. Our data demonstrated that Gads regulates the expression of activation markers CD69 and CD25 of antigen-specific CD8$^+$ T cells but Gads is not required for the onset of accumulation of antigen-specific CD8$^+$ T cells following infection. However, Gads is critical to sustain the expansion of CD8$^+$ T cell-mediated immune response following infection. Although the differentiation of naïve CD8$^+$ T cells into memory cells is independent of Gads, Gads is required for an optimal recall response.

Our data indicating that Gads regulates the initiation of proliferation of CD8$^+$ T cells upon TCR ligation by peptide antigen seemed to contradict with our *in vivo* infection data showing that Gads is not required for the initiation of expansion of CD8$^+$ T cell population. In order to explain the “discrepancy”, we hypothesized that the homotypic interactions among CD8$^+$ T cells compensate for Gads deficiency at the initial stage of accumulation of antigen-specific CD8$^+$ T cells upon infection. Our data indicated that the need for Gads in cell cycle progression of CD8$^+$ T cells when total splenocytes were stimulated could be overcome by stimulating purified CD8$^+$ T cells. These data suggested that the homotypic interactions among CD8$^+$ T cells facilitate the TCR signaling so as to compensate for Gads deficiency in promoting cell cycle entry and proliferation.

To conclude, the role of Gads in TCR-mediated activation and proliferation of CD8$^+$ T cells is dependent on the interactions of CD8$^+$ T cells and their partners. Interestingly, if CD8$^+$ T cells interact with non-CD8$^+$ T cells, Gads regulates the kinetics of cell cycle entry; however, if CD8$^+$

T cells interact with other $CD8^+$ T cells, Gads is dispensable for cell cycle entry of $CD8^+$ T cells. Overall, these studies will help us better understand how TCR-proximal signaling regulates the activation of $CD8^+$ T cells.

Acknowledgements

I would like to take this opportunity to first and foremost thank my mentor, Dr. Thomas Yankee. He brought a new life to my research career around four years ago during my transfer, the most difficult time I have had so far in my scientific career. His rigorous attitude and broad knowledge in science have inspired and encouraged me through my graduate studies in our department. It has been a GREAT pleasure to work in his lab and enjoy his mentoring. He has always granted me freedom in pursuing my research goals and emphasized developing the abilities I need to tackle scientific problems. He never gave me the direct answer when addressing a scientific question, but rather endeavored to lead me to find the right path myself. These “self-learning” processes actually cost him much more time but benefit me immensely. As far as I know, there are very few mentors who read every word of their trainees’ dissertations. Dr. Yankee did carefully go through every word of my dissertation a number of times and gave me a couple thousand comments and questions. By answering those comments and questions, I have learned a great deal during the logical thinking and writing processes and improved the quality of my dissertation. This revising process was definitely a precious opportunity to me. I deeply appreciate this and other solid training that Dr. Yankee has provided me. It has been my great honor to be the first graduate student of Dr. Yankee’s.

Next, I would like to sincerely appreciate the great efforts made by Drs. Stephen Benedict, Michael Parmely, Jianming Qiu and Charlotte Vines, who have served on both my comprehensive exam and dissertation committees. I deeply thank them for all the time, advice and patience they have put into my Ph.D. studies. I am especially grateful for their fantastic suggestions regarding my research projects and their challenges to the data I presented, aiming at stimulating deeper and more creative thinking in me.

Many thanks go to Brooks Parker for managing the mouse colony for my research projects. He helped me a lot take care of staining samples as well as withdraw mouse blood when I had time conflicts with multiple experiments. I truly appreciate the great support and help from him, as well as Dr. Aaron Yun Chen and Juan Xiong, during some of my huge experiments in the morphine project. Several times I had to “force” these three people to come to lab and begin experiments with me at 6 AM due to the heavy load of experiments at some critical time points. Without their help in harvesting various tissues I could not have finished the experiments smoothly and successfully.

I appreciate the help from Dr. Xiaochao Ma who taught me how to use the LC-MS/MS machine and the software to measure serum levels of morphine, which enriched our data sets. I also thank Dr. Joyce Slusser, Richard Hastings and Alicia Zeiger in the Flow Cytometry Core Laboratory for their assistance with sorting cells for a number of experiments. They also trusted me and gave me permission to use the flow cytometer to acquire data 24/7, which made my life much easier during extremely busy days with experiments. I also thank Dr. Leo LeFrançois from the University of Connecticut Health Center and Dr. Michael Bevan of the University of Washington for their generous gifts of the *listeria monocytogenes* strains which have largely facilitated our research. I would like to thank the people in the Benedict lab and Dr. Marci Chan for their helpful and detailed discussions about my data. I also thank Dr. Cheryl Rockwell for her assistance with statistical analysis in the morphine project. Special thanks to Julie Mitchell for her critical reviews and unreserved suggestions for my research work as well as those beautiful and tasty cheesecakes she has made for celebrating my accomplishments in my Ph.D. studies.

I also greatly appreciate the effort that Drs. Joe Lutkenhaus, Bang Shen, and Dorothy Knoll as well as Ms. Julia Shaw made in helping us during our transfer into our department. I sincerely thank Dr. Bao Ting Zhu for his direction in the first two years of my Ph.D. studies. Besides, I thank all the people in our Microbiology Department for their support and help.

I extend my appreciation to the support from Dr. Yankee's grants and a predoctoral award from the Biomedical Research Training Program (FY2011).

Words cannot express my appreciation to my husband, Dr. Aaron Yun Chen. We came to the US to pursue Ph.D. studies together, transferred twice together, joined our department together...we stick together through thick and thin. He always argues with me on scientific questions, which often turns out to enrich my logical thinking and knowledge base, as well as strongly helps and supports my research. More importantly, his encouragement and confidence in me have accompanied me through the whole journey.

Thanks to our two adorable boys, Ander and Anwen, 3- and 1-year young, respectively. Although they keep us much busier in balancing between research and family, they constantly provide us with great happiness and an extraordinary opportunity to train our ability in time-managing and multitasking.

I express my gratitude from the depth of my heart to my parents, Mr. Guirong Zhang and Mrs. Heying Zhang. They endeavored to culture me into a scientist probably since I was born. When I was a little girl, I already liked playing with experimental tools and observing experimental mice in the laboratories of the CDC in Nanjing, where my mother used to work. I have dreamt of being an excellent scientist since my childhood. Their efforts are absolutely indispensable not only in my physiological and psychological growth, but also in my research career as a scientist. I also greatly thank them as well as my parents-in law, Mr. Xiaoming Chen and Mrs. Huiru Yao, for their self-giving contribution and endless support to our young family so that we can devote more to research.

In a word, I truly thank all the people, including those I have not had a chance to list, who have cared about me and helped me during my Ph.D. studies. Thank you all very much!!!

Table of contents

List of Figures and Tables

List of Abbreviations

ACTH: adrenocorticotropic hormone

ADAP: adhesion and degranulation promoting adapter protein

Ag: antigen

AML: acute myeloid leukemia

APC: Antigen presenting cells

APL: altered peptide ligand

BCR: B cell receptor

CaM: calmodulin

CAM: Cell adhesion molecule

Cbl: Casitas B-lineage lymphoma

CDK: cyclin-dependent kinase

CFSE: carboxyfluorescein succinimidyl ester

CLP: common lymphoid progenitor

CMP: common myeloid progenitor

CN: calcineurin

CRH: corticotropin-releasing hormone

CTLA: Cytotoxic T-lymphocyte antigen

DAG: diacylglycerol

DAPI: 4',6-diamidino-2-phenylindole

DAPI: 4',6-diamidino-2-phenylindole

DC: dendritic cell

DN: double negative

DP: double positive

ECM: extracellular matrix

ERK: extracellular signal–regulated kinase

ESL: E-selectin ligand

FO: follicular

FTOC: Fetal thymic organ culture

Fyb: Fyn binding protein

Gab: Grb2-associated-binding

GC: Germinal center

GCIP: Grap2 cyclin-D interacting protein

GEF: guanine nucleotide exchange factors

GEM: glycolipid-enriched membrane microdomain

GPCR: G-protein coupled receptors

GPVI: glycoprotein VI

GR: glucocorticoid receptor

HPA: hypothalamic-pituitary-adrenal

HPK1: Hematopoietic Progenitor Kinase 1

HSC: hematopoietic stem cell

ICAM-1: intercellular adhesion molecule 1

IFN: interferon

IL: interleukin

IP3: 1,4,5-trisphosphate

IS: immunological synapse

ISP: immature single positive

ITAM: immunoreceptor tyrosine-based activation motif

Itk: IL-2-inducible T-cell kinase

LAT: linker of activated T cells

LC: liquid chromatography

LCK: lymphocyte-specific protein tyrosine kinase

LFA-1: lymphocyte function-associated antigen-1

LIME: Lck-interacting membrane protein

LM: *Listeria monocytogenes*

MFI: mean fluorescence intensity

MHC: major histocompatibility complex

MPEC: memory precursor effector cell

MS: mass spectroscopy

MZ: marginal zone

NF-AT: nuclear factor of activated T cells

NF-κB: nuclear factor κ-light-chain-enhancer of activated B cells

OT-I: ovalbumin-specific T cell receptor-major histocompatibility complex class I restricted

OVA: ovalbumin

PD: programmed death

pDC: plasmacytoid dendritic cell

PI: propidium iodide

PI3K: phosphoinositide 3-kinase

PIP2: phosphatidylinositol-4,5-bisphosphate

PKC: protein kinase C

PLC: phospholipase C

PMA: phorbol 12-myristate 13-acetate

PSGL: P-selectin glycoprotein ligand

pSMAC: peripheral supermolecular activation cluster

PTP: protein tyrosine phosphatases

PY: pyronin Y

RET: rearranged during transfection

rLM: recombinant *Listeria monocytogenes*

rLM-OVA: recombinant *Listeria monocytogenes* expressing ovalbumin

SAXS: small-angle x-ray scattering

SDF: stromal cell-derived factor

SHB: SH2 domain-containing adaptor protein B

SHP: SH2-containing protein tyrosine phosphatases

SLAP-130: SLP-76 associated phosphoprotein of 130 kDa

SLEC: short lived effector cell

SLP-76: SH2 domain-containing leukocyte protein of 76 kDa

SP: single positive

TCR: T cell receptor

TSP: transitional single positive

UTR: untranslated region

WT: wild type

ZAP-70: Zeta-chain-associated protein kinase of 70 kDa

Chapter I Introduction

General goals of this dissertation

The activation and function of $CD8^+$ T cells are critical in the treatment for tumors, bacterial or viral infections. The T cell receptors (TCRs) on T cells recognize pathogens or antigens presented by target cells. TCR ligation initiates signaling cascades, which are required for the activation and function of T cells. It is unknown how TCR ligation links to the activation of $CD8^+$ T cells. The major goal of our research is to define the TCR-proximal signaling events that regulate $CD8^+$ T cell-mediated immunity. I sought to accomplish the goal by investigating the role of Gads in $CD8^+$ T cell-mediated immunity. Why did I choose Gads in my dissertation? The adaptor protein Gads is critical for optimal TCR-mediated calcium mobilization, which is important for T cell activation and development. However, there was no documentation on the physiological relevance of Gads in peripheral $CD8^+$ T cells before our study. There is another reason why we looked at Gads first: $Gads^{-/-}$ mice have partial defect in T cell development so that there are peripheral $CD8^+$ T cells in $Gads^{-/-}$ mice, making the study on the role of Gads in peripheral $CD8^+$ T cells possible by comparing $Gads^{-/-}$ cells and $Gads^{+/+}$ cells. Based on the above reasons, I focused on the effect of Gads on $CD8^+$ T cell-mediated immunity in Chapter II to IV.

In addition to the results regarding the function of Gads in $CD8^+$ T cell-mediated immune responses, I worked on another important project in Chapter V. This study has enriched not only my knowledge in the field of Immunology but also the experimental experiences, and has expanded the scope of my research beyond peripheral $CD8^+$ T cells. Our goal was to determine the mechanisms through which the lymphocyte populations deplete and recover following morphine treatment. By addressing these mechanisms, we could better understand how

morphine affects immunity and it will help develop strategies to counteract the detrimental effects of morphine in clinical use or morphine abuse.

Immune system

The immune system is a versatile defense system within an organism to protect against invading pathogens and cancer. The immune system protects the host by identifying and killing pathogenic microorganisms (such as virus, bacteria) and tumor cells. It can also react against proteins, polysaccharides and other substances. In order to function properly, the immune system needs to distinguish the “non-self” from the “self”. The “self” part points to the organism’s own healthy cells and tissues. If the immune system targets the “self”, autoimmune diseases, such as type I diabetes and rheumatoid arthritis, might be induced.

Generally, the immune system can be divided into two categories: innate immunity and adaptive immunity. Innate immunity is available from birth and it provides the first line of immediate defense against pathogens by recognizing widely distributed “pathogen-associated molecular patterns”. Adaptive immunity is not available at birth but needs to be established gradually later on, so that it is also known as acquired immunity. The immune cells recognize and process the specific antigens, trigger a series of signaling events to produce antibodies and effector lymphocytes to specifically target and eliminate the antigen-bearing cells. More importantly, the adaptive immune system generates memory lymphocytes in response to the antigen so that it can carry out the recall immune responses in a much faster and stronger manner once encountering the same antigen again.

All immune cells are derived from the hematopoietic stem cells (HSCs). One classical model of hematopoiesis is that HSCs differentiate into common myeloid progenitors (CMPs) and

common lymphoid progenitors (CLPs). CLPs differentiate into B and T cell precursors, and develop into B cells in bone marrow and T cells in thymus, respectively. In Chapter V, I will talk about the effect of morphine administration on B cell development and T cell development.

The adaptive immune responses can be divided into humoral immune responses (mediated mainly by B lymphocytes, also known as B cells) and cell-mediated immune responses (primarily governed by T lymphocytes, T cells for short). B cells play the crucial role in humoral immune responses by producing antibodies against antigens. They get the name “B” from “bursa of Fabricius” where they mature in birds. In mammals, B cells develop in “bone marrow”. T cells, as well as other immune cells, such as macrophages and NK cells, are involved in the cell-mediated immune responses. Antigen presenting cells (APCs) present antigens to the T cell receptors (TCR) on the surface of T cells. The abbreviation “T” in “T cells” stands for thymus, which is the principal organ for T cell development. T cells can be divided into two major subsets: αβ T cells and γδ T cells. Most T cells in blood and lymphoid organs are αβ T cells. Their TCR consists of an α chain and a β chain, which form the α-β disulfide-linked heterodimeric glycoprotein. Less than 5% of T cells in blood and lymphoid organs and most T cells in skin and gut are γδ T cells. In γδ T cells, an alternative TCR heterodimer (γ-δ chains) is expressed. My research work focuses on αβ T cells (“T cells” is used in my dissertation to stand for αβ T cells except where indicated specifically).

According to the membrane glycoproteins (CD4 or CD8) on the surface of peripheral T cells, there are two well-defined subpopulations of T cells: $CD4^+$ T cells and $CD8^+$ T cells. $CD4^+$ T cells are mainly T helper (Th) cells and $CD8^+$ T cells are mainly T cytotoxic (Tc) cells. My primary research interest is on $CD8^+$ T cells. $CD8^+$ T cells are cytotoxic T cells as they recognize and kill target cells such as tumor cells and virus-infected cells. Target cells present antigen through major histocompatibility complex (MHC) class I molecule to the TCR complex on the surface of $CD8^+$ T cells. Upon TCR ligation, the naïve $CD8^+$ T cells become activated and

proliferate. There is an interesting question: How do the TCR-mediated signaling pathways affect $CD8^+$ T cells? To address this, I have focused on the role of Gads, a signaling protein downstream of the TCR, in $CD8^+$ T cell activation (Chapter II) and $CD8^+$ T cell-mediated immunity following infection with an intracellular pathogen (Chapter III). Furthermore, I investigate the homotypic interactions among $CD8^+$ T cells which can compensate for Gads deficiency in cell cycle progression (Chapter IV).

What is Gads?

Gads is an adaptor protein that plays an important role in TCR-mediated signaling. It was cloned by six different labs around the same time (1998-1999) using different strategies. Gads was also named as Mona, GrpL, Grap-2, Grf40, and GRID (1-6). Those analyses all revealed that Gads, which is around 37 kDa, belongs to the Grb2 protein family, which includes Grb2, Grap, and Gads and shares the SH3-SH2-SH3 structure (7). Different from Grb2 and Grap, there is a proline/glutamine-rich region between the SH2 domain and the C-terminal SH3 domain of Gads (1-6). Not like Grb2, which is ubiquitously expressed on mammalian cells (8), Gads is strictly expressed in hematopoietic cells (1-4, 6).

Gene level

Human Gads gene is located on chromosome 22q13.2 (Pubmed gene ID: 9402, updated on May-12-2011) and mouse Gads is located on chromosome 15E2 (Pubmed gene ID: 17444, updated on May-08-2011). In both human and mouse, the Gads gene is encoded by seven exons (4, 9).

Gads transcripts are relatively restricted to hematopoietic tissues, including lymph node, bone marrow, spleen, thymus, and peripheral blood leukocytes in adult mice and in day 11-17

mouse embryos, with the highest level of expressions in thymus. The level of Gads mRNA is low in testis, but not in stomach, thyroid, spinal cord, trachea, adrenal glands, prostate, ovary, small intestine or germinal center B cells in mice (3, 4, 6). Gads mRNA was also found in human thymus, spleen, lymph nodes and peripheral blood leukocytes (4, 5). In cell lines, Gads mRNA is expressed in chronic myelogenous and lymphoblastic leukemia cell lines, such as in the mature T-cell lines Jurkat and Molt-4, the pre-B cell line Nalm-6, the myeloid cell lines KG-1, KG-1a, and RC2A, and the K562 and HEL cell lines that exhibit megakaryocytic differentiation potential. No Gads mRNA expression could be detected in pre-B cell line Reh, the mature B-cell line Raji, the myelomonocytic cell line PLB-985, nor the monocytic cell line THP-1 (3, 4, 9). The distribution of Gads mRNA level suggests that Gads mRNA expression is highly regulated and restricted to subsets within hematopoietic lineages.

The Gads gene locus has been characterized to have two promoter segments (Gads-1A and Gads-1B) driving expression of alternate 5' untranslated exons, which were detected in a cell-lineage specific manner. T cells and immature myelomonocytic cell lines express transcripts containing 1A 5´- untranslated region (UTR), whereas Gads mRNA found in platelets and megakaryocytic cell lines contains 1B 5´-UTR (9, 10). In mouse Gads-1A promoter, the putative binding sites include IRF-2, myb, AML (acute myeloid leukemia)-1, Sp1, Sp3 and Spi-1 (11, 12). The AML-1 transcription factor has been implicated in transcriptional regulation of T cell and monocytic cell promoters (13). AML-1 regulates the expression of Gads in T cells and myeloid cells (11). The Gads-1B promoter, which exhibits typical features of megakaryocyte-specific promoters, has potential binding sites for Ikaros, Sp1, AP-1, Oct-1, NFAT, E12/E47, Bright, glucocorticoid receptor (GR), Myb, GATA, MEF2, CREB and Ets (10, 12). Garrett-Sinha *et. al.* (12) demonstrated that Spi-1and Spi-B bind to both Gads-1A and Gads-1B promoters but they transactivate the Gads-1B promoter only so as to regulate the expression of Gads on B cells. However, the inclusion of identical 3´-UTR of Gads gene is irrespective of the cell type (9).

Protein level

The human and murine Gads protein are highly conserved, sharing >90% identity in the SH3 and SH2 domains and 74% identity in proline-rich region (6). T cells have the highest expression level of Gads protein (14), but Gads expression was also detected in B cells, megakaryocytes, mast cells, NK cells, macrophages, plasmacytoid dendritic cells (pDCs), and platelets (9, 12, 14-16). Besides primary cells, Gads protein is expressed in various cell lines such as T cell lines (Jurkat, CTLL-2), monocyte/macrophage cell line (NFS-60/MAC, an M-CSF-dependent derivative of bipotential NFs-60 cells), NK and macrophage cell lines (1, 15). Interestingly, the expression of Gads changes after activation in cells of monocytic lineage or B cells: 1) Gads expression is induced during monocytic differentiation of NFS-60 cells (1); 2) Gads is expressed in mature naïve B cells. Upon BCR ligation, Gads expression is down-regulated. Germinal center (GC) B cells and memory B cells do not express Gads (14, 17).

Does the expression of Gads protein change through the B cell development? The first stage in which committed B cell precursors can be identified in the bone marrow is the pro-B cell stage ($B220^{+}IgM^{-}CD43^{+}$). Then the cells enter the pre-B cell stage ($B220^{+}IgM^{-}CD43^{-}$) and immature B cell stage ($B220^{lo}IgM^{+}$). Some immature B cells migrate to the spleen where they can be identified as transitional stage 1 (T1) B cells ($IgM^{+}IgD^{-}CD21^{-}CD23^{-}$). T1 cells differentiate into transitional stage 2 (T2) cells ($IgM^{+}IgD^{+}CD23^{+}$) and ultimately mature and become either follicular (FO) B cells ($IgM^{lo}IgD^{+}CD23^{+}$) or marginal zone (MZ) B cells ($IgM^{+}IgD^{-}CD21^{+}CD23^{-}$) (18, 19). Gads expression was not detected in pro-B cells or pre-B cells in bone marrow. However, Gads protein was expressed in T1B cells, T2B cells, FO B cells, and MZ B cells in splenocytes (16).

As the main focus of this dissertation is on the role of Gads in TCR-mediated T cell function, Let's look at the expression of Gads protein in T cell development. The T cell precursors in the

thymus have no expression of either CD4 or CD8 and are called $CD4^-CD8^-$ double negative (DN) stage. According to CD44 and CD25 expression, DN thymocytes can be divided into the DN1 ($CD44^{hi}CD25^-$), DN2 ($CD44^{hi}CD25^+$), DN3E ($CD44^{lo}CD25^{hi}$), DN3L ($CD44^{lo}CD25^{lo}$), and DN4 ($CD44^{lo}CD25^-$) subsets (20, 21). T cell lineage commitment is made and rearrangement of the genomic locus encoding TCR β chain or γδ chains begins in the DN1 and DN2 stages. In the thymus, Gads is expressed starting as early as in DN1 and DN2 stages (17).

The role of Gads in TCR signaling

TCR complex is composed of eight transmembrane proteins derived from six different genes (22-24): the α and β chains are responsible for recognition of antigen presented by MHC. The CD3 complex is composed of two heterodimers (γ-ε and δ-ε). The ζ chains in the TCR complex form a homodimer. The CD3 complex and the ζ chains are responsible for signal transduction (25, 26). TCR ligation by Ag-MHC complexes leads to the activation of Src family tyrosine kinases, such as Lck and Fyn. The activated Lck and Fyn phosphorylate the immunoreceptor tyrosine-based activation motifs (ITAMs) on the TCRζ chains and each chain of CD3 molecule (27, 28). After being phosphorylated, the tyrosine residues within ITAMs form docking sites for the protein tyrosine kinase Zeta-chain-associated protein kinase of 70 kDa (ZAP-70), which binds the phosphorylated ITAM sites and gets activated. In addition, Lck further activates ZAP-70. ZAP-70 phosphorylates the tyrosine residues of the transmembrane adaptor protein linker of activated T cells (LAT).

After TCR ligation, the SH2 domain-containing adaptor protein Gads binds the phosphotyrosine residues on LAT. Gads is constitutively in complex with SH2 domain-containing leukocyte protein of 76 kDa (SLP-76) (2, 6, 17, 29-31). Upon TCR ligation, LAT and Gads-SLP-76 achieve a relatively stable and specific complex LAT-Gads-SLP-76. Then, the

TCR signaling is further transduced. For example, after being brought to the signaling complex of LAT by Gads, SLP-76 can be phosphorylated directly by ZAP-70 to facilitate the activation (32). Phospholipase C (PLC)-γ1 binds to tyrosine-phosphorylated LAT [ref (33, 34) and reviewed in (35, 36)]. The activation of PLC-γ1 catalyzes the formation of the second messengers inositol 1,4,5-trisphosphate (IP3) and diacylglycerol (DAG) from the hydrolysis of phosphatidylinositol-4,5-bisphosphate (PIP2). IP3 triggers calcium signaling, which leads to the activation of nuclear factor of activated T cells (NF-AT) and nuclear factor κ-light-chain-enhancer of activated B cells (NF-κB) signaling pathways (37). DAG activates Ras-dependent signals (38, 39), such as the extracellular signal–regulated kinase (ERK) pathway, which are important for a number of cellular events, such as cytokine secretion and cell proliferation (40).

The LAT-Gads-SLP-76 signaling complex serves as the scaffold/platform for the recruitment of multiple signaling proteins as shown above. LAT becomes phosphorylated on multiple tyrosine residues (41-43). The interaction between LAT and Gads is via tyrosine-171 and tyrosine-191 residues of LAT and the SH2 domain of Gads upon TCR ligation (15, 41, 44-47). SLP-76 contains three domains: 1) The N-terminal acidic domain, which contains three tyrosines phosphorylation sites within consensus motifs for SH2 binding; 2) The proline-rich central region; 3) The C-terminal SH2 domain named P-I region. Via its R-X-X-K motif in the proline-rich region (amino acid 224-244), SLP-76 binds to C-terminal SH3 domain of Gads (2, 6, 15, 17, 29, 30, 48). They form a unique structure with high binding affinity, as described in “Structure” section below. Besides Gads, LAT also interacts with membrane-bound guanine nucleotide-binding protein Sos1, the E3 ubiquitin-protein ligase c-Casitas B-lineage lymphoma (c-Cbl) (49), the guanine nucleotide exchange factors (GEF) for the Rho family of GTP binding proteins Vav1, PLC-γ1 (44, 50), Grb2 (44), and SH2 domain-containing adapter protein B (Shb) (36, 50-52). SLP-76 also can interact with Vav1 (53-55), the adaptor protein Nck, which can regulate tyrosine kinase signaling (56, 57), the interleukin-2 (IL-2)-inducible tyrosine kinase (Itk)

(58-60), PLC-γ1(61), Lck (62), the adhesion and degranulation promoting adapter protein (ADAP) [formerly known as SLP-76 associated phosphoprotein of 130 kDa (SLAP-130), or Fyn binding protein (Fyb)] (63, 64), and the Ser/Thr kinase HPK1 (56, 65). By bridging LAT and SLP-76 upon TCR ligation, Gads brings many signaling proteins above into the signaling complex. Based on these evidences, the role of Gads in TCR signaling is important.

The Gads-binding domain of SLP-76 is required for the inducible association of SLP-76 with PLC-γ1(61, 66). Itk binds to SLP-76 while Lck phosphorylates and activates Itk, which then phosphorylates and activates PLC-γ1. Vav1 regulates PLC-γ1 phosphorylation and facilitates the interaction between Gads-SLP-76 and PLC-γ1. However, the adaptor protein complex LAT-Gads-SLP-76 is the center of all these signaling proteins. The adaptor proteins, also known as molecular scaffolds, lack any intrinsic enzymatic activity or transcription activation domains. Instead, they create a platform for other signaling molecules so as to facilitate coupling of antigen receptor as well as to trigger functional responses in lymphocytes (67, 68). The formation of LAT-Gads-SLP-76 is important for signal transduction in T cells (68).

The critical role of LAT-Gads-SLP-76 signaling complex in TCR signaling was supported by visualized microcluster results. T cell activation is initiated and sustained in TCR-containing microclusters generated at the initial contact sites and the periphery of the mature immunological synapse (IS) (69). By using imaging techniques, such as dynamic fluorescent and interference reflection microscopy, microclusters could be visualized. Upon TCR ligation, the TCR-rich microclusters are 200 to 500 nm in diameter. They are assembled within seconds of TCR-APC ligation (48, 69-73) and are the dominant locations where TCR-mediated tyrosine phosphorylation happens and tyrosine kinases and critical adaptor proteins co-accumulate (48, 49, 70, 74). Adaptor proteins including LAT, Gads, and SLP-76 co-cluster together with the TCR early and transiently in T cell activation (70). Gads enters persistent clusters in response to TCR ligation, colocalizing precisely with SLP-76. The recruitment of Gads to LAT requires SLP-76

and the recruitment of SLP-76 to LAT requires Gads (48). Mutation of various domains demonstrated that C-terminal domain of Gads plays a critical role in the persistence and movement of SLP-76-containing cluster, whereas the N-terminal SH3 and SH2 domains of Gads cooperate to recruit Gads into LAT-nucleated microclusters (48). Purbhoo *et. al.* (47) used multicolor, live-cell microscopy to visualize the protein organization. They also found during the activation of T cells, Gads always colocalized and co-migrated with microclusters of SLP-76. The trajectories of microclusters of Gads fully coincided with the ones of SLP-76. After TCR ligation, the LAT-Gads-SLP-76 signaling complex is localized in glycolipid-enriched membrane microdomains (GEMs), also known as lipid rafts (33, 34). Gads is inducibly recruited to GEMs while the SLP-76 mutant in which the Gads binding region was deleted Δ224-244 could not localize in GEMs after TCR ligation suggesting that Gads is essential for SLP-76 to localize to GEMs after TCR stimulation (75).

Gads plays an important role in the formation and function of the LAT-Gads-SLP-76 signaling complex. In activated Gads deficient thymocytes, SLP-76 was readily phosphorylated but failed to associate with LAT (76). By using a 50-amino acid polypeptide to block the binding between SLP-76 and Gads, Singer *et. al.* (56) found that it disrupted the proper localization of SLP-76 and SLP-76-dependent TCR signaling such as inhibiting TCR-induced integrin activity in Jurkat cells. It also significantly impaired SLP-76 recruitment as well as the activation marker expression upon TCR ligation. Single point mutations of the Gads-binding site on SLP-76 completely abrogated SLP-76 association with Gads *in vivo* and impaired SLP-76 function such as preventing its binding to Itk and Vav (30). In the thymocytes expressing the dominant-negative Gads mutant, Grf40-dSH2, the tyrosine phosphorylation of SLP-76 and phosphorylation levels of both PLC-γ1 and ERK1/2 were profoundly reduced (77). T cells from mice reconstituted with Gads-binding site Δ224-244 of SLP-76 mutant had defective ERK phosphorylation (78). Gads is very important in TCR-mediated calcium signaling as indicated in

the following evidences: 1) Gads$^{-/-}$ peripheral T cells had no detectable calcium influx upon TCR ligation (17, 76). 2) Blocking the binding between SLP-76 and Gads diminished the TCR-induced Ca^{2+} flux (56, 79). 3) T cells from SLP-76 mutant mice reconstituted with Gads-binding site Δ224-244 to block Gads-binding site had defective calcium mobilization and diminished proliferation upon TCR ligation (78). Calcium signaling is critical to NF-AT activation because calmodulin (CaM), a calcium sensor protein, activates the serine/threonine phosphatase calcineurin (CN) (80). The activated calcineurin dephosphorylates the NF-AT transcription factor, resulting in the nuclear localization of NF-AT (81, 82). Consistent with the model that calcium signaling regulates NF-AT activation, Gads regulates NF-AT activation as Gads-binding domain of SLP-76 is required NF-AT activation (48, 70). Furthermore, overexpression of Gads alone increased anti-CD3-induced NF-AT activation. An additive effect between Gads and SLP-76 on NF-AT activation was observed when both were overexpressed in Jurkat cells (6). Gads regulates the signaling threshold of the TCR as T cells are able to generate a small calcium response in the absence of Gads under the higher concentration of stimuli (17).

Structure of Gads

The low-resolution structure model of full-length Gads via using small-angle x-ray scattering (SAXS) also reveal that Gads remains monomeric in solution (83). Gads retains an overall compact structure though it possesses a long unstructured region. There are two structure models of Gads. One model is that the C-terminal SH3 domain is at one extreme of the molecular volume and the N-terminal SH3 domain is at the other extreme, whereas SH2 domain is in between, near the N-terminal SH3 domain. The alternative model is that

localization of N-terminal SH3 and SH2 domains is inverted, so that the SH2 domain is at the extreme of the molecular volume (83).

The C-terminal SH3 domain of Gads was observed to form a homodimer in solution and has the SH3 domain fold, formed from two antiparallel β-strands with a small 3_{10}-helix between β4 and β5 strands (29, 84, 85). The binding between C-terminal SH3 domain of Gads and SLP-76 is unique: Many SH3 domains bind classical proline-based P-X-X-P motif, often with moderate affinities. However, a subset of SH3 domains bind alternate peptide motif R-X-X-K with high affinity (86-88). For example, the Gads SH3 domain, bind ^{233}PSIDRSTKP^{241} in SLP-76 (85, 89, 90), which is necessary for optimal TCR signaling (2, 6, 15, 17, 29, 30). In addition, the peptide forms a unique structure characterized by a right-handed 3_{10} helix at the R-X-X-K locus, in contrast to the left-handed polyproline type II helix formed by canonical proline-rich SH3 ligands (84). It was further demonstrated that the 3_{10} helix formed by the central R-X-X-K motif inserts into a negatively charged double pocket on the ion (Zn^{2+})-dependent dimerization formed by C-terminal SH3 domain of Gads while several other residues complement binding through hydrophobic interactions, creating a short linear C-terminal SH3 binding epitope of uniquely high affinity (85). In addition, SLP-76 was demonstrated to promote and stabilize the Gads C-terminal SH3 homodimerization (90).

The proline/glutamine-rich linker region between SH2 and C-terminal SH3 domain is unstructured and disordered (83), which likely makes it difficult to get the high resolution of crystal structure of full-length Gads. Recently, it was discovered that the disordered regions are often functional. They could regulate transcription, translation, cellular signal transduction, protein phosphorylation. In addition, they could serve as storage of small molecules and facilitate the self-assembly of large multiprotein complexes (91, 92). The unstructured linker region of Gads might provide the flexibilities in steric configuration of the signaling complex LAT-Gads-SLP-76 to promote the formation of the TCR proximal multiprotein complex.

Function of Gads

Three groups generated Gads-deficient mice to study the function of Gads in T cell development. The Cheng group (76) used R1 ES cells and deleted the SH2 linker region and the C-terminal SH3 domain, but not the exon encoding the N terminal SH3 domain. By using this strategy, the binding sites of LAT and SLP-76 were depleted. The Sugamura laboratory (77) made a transgenic mouse expressing an SH2 mutant Gads in the dominant-negative form, Grf40-dSH2, to block the binding with LAT. The Clark laboratory (17) used C57BL/6 ES cells to generate mice deleted exons 1,2, and 3 of the *gads* gene, including the start ATG, to encode the N terminal SH3 domain, which was essentially equal to complete knock out of Gads. Although they used different strategies, the three groups reported the similar findings, for example, there was drastic decrease in the total thymocyte number and the T cell development has defect in mice with Gads deficiency (17, 76, 77). The role of Gads in each stage of T cell development is discussed as follows:

<u>Gads does not regulate the αβ/γδ T cell lineage commitment</u>

The T cell precursors in the thymus have no expression of either CD4 or CD8 and are in the $CD4^-CD8^-$ double negative (DN) stage. According to CD44 and CD25 expression, DN thymocytes can be divided into the DN1 ($CD44^{hi}CD25^-$), DN2 ($CD44^{hi}CD25^+$), DN3E ($CD44^{lo}CD25^{hi}$), DN3L ($CD44^{lo}CD25^{lo}$), and DN4 ($CD44^{lo}CD25^-$) subsets (20, 21). T cell lineage commitment is made and rearrangement of the genomic locus encoding TCR β chain or γδ chains begins in DN1 and DN2 stages. In the thymus, Gads is expressed starting as early as in DN1 and DN2 stages (17). TCRβ and TCRγδ protein can be first detected at the DN3E stage. Gads does not regulate αβ/γδ T cell lineage commitment as the absolute cell numbers of $TCR\beta^+$ DN3E and $TCR\gamma\delta^+$ DN3E thymocytes in $Gads^{-/-}$ mice are identical to those in $Gads^{+/+}$ mice (21).

Gads regulates β selection in T cell development

After expressed in DN3E stage, the TCRβ protein pairs with an invariant protein, pre-Tα, to form the pre-TCR (93). The expression of the pre-TCR complex provides the survival signal of DN3E thymocytes as well as promotes the proliferation and differentiation through the DN3L and DN4 stages. Gads plays a critical role in the DN3L to DN4 transition of T cell development as $Gads^{-/-}$ mice or Gads mutant mice have a block at DN3L stage (17, 21, 76, 77). Lower percentages of $Gads^{-/-}$ DN4 cells express TCRβ than $Gads^{+/+}$ DN4 cells while higher percentages of $Gads^{-/-}$ DN4 cells express TCRγδ than $Gads^{+/+}$ DN4 cells (21). Gads regulates the proliferation and survival and of DN thymocytes in DN3L and DN4 stages as there were lower percentages of $Gads^{-/-}$ $TCR\beta^{+}$ DN3L and DN4 thymocytes in S, G2, or M phases of cell cycle than $Gads^{+/+}$ thymocytes. In addition, Bcl-2 expression was dependent on Gads in $TCR\beta^{+}$ DN3L cells (21). IL-7 and its receptor CD127 are critical factors in T cell development (94), not only important in DN1, DN2, and DP stages (95), but also regulate the survival of thymocytes in DN3E, DN3L and DN4 stages between β selection and positive selection (unpublished data from our laboratory). Gads regulates CD127 expression in $TCR\beta^{+}$ DN3E and DN3L cells but not in TCR^{+} DN4 cells (21). We hypothesize that Gads and CD127-related signaling co-regulate the survival of DN3L cells via the expression of Bcl-2.

Gads regulates positive selection and negative selection in T cell development

After the DN4 stage, cells express CD8 and become immature single positive (ISP) $CD8^{+}$ T cells before expressing CD4 and becoming DP thymocytes. During the DP stage, cells rearrange the genomic locus encoding TCRα, express TCRα protein, and express a complete TCR complex. Once the TCR is expressed, positive and negative selection occur, the processes by which the T cell repertoire is selected. There are various models about positive

and negative selection in T cell development. The quantitative models relate response to the affinity, avidity or kinetics of TCR binding, whereas qualitative models require conformational or spatial changes in the TCR or associated molecules to modulate signal transduction (96). Currently, the affinity model has been widely accepted (97, 98): If there is no or very low binding affinity between TCR and self-peptides, which are presented on MHC, the thymocytes will be eliminated by "death by neglect" process. If the binding affinity between TCR and self-peptides on MHC is moderate, the thymocytes will be positively selected. If the binding affinity is high, the thymocytes will be developed into regulatory T cells. If there is very high binding affinity between TCR and self-peptides on MHC, the thymocytes will undergo negative selection.

Gads deficiency impairs positive selection. Gads is required for TCR upregulation in DP and SP thymocytes as lower percentages of DP, SP CD4, or SP CD8 thymocytes in $Gads^{-/-}$ mice were TCR^{hi} , as compared with those in $Gads^{+/+}$ mice (99). TCR-induced activation of ERK is significantly impaired in the thymocytes expressing dominant-negative Gads, Grf40-dSH2 (77). The usage of a 50-amino acid polypeptide to block the binding between SLP-76 and Gads diminished the positive selection (56, 79). The block in positive selection in $Gads^{-/-}$ mice was more severe when an MHC class II-restricted TCR was expressed than when an MHC class I-restricted TCR was expressed (99). So that the ratio of $CD4^+$ to $CD8^+$ thymocytes was skewed toward the SP $CD8^+$ population in $Gads^{-/-}$ mice (17, 76). CD3 and CD69 up-regulation in $CD4^+$ thymocytes is much more sensitive to Gads deficiency than in $CD8^+$ thymocytes (17). These data support the hypothesis that the development of $CD4^+$ thymocytes requires stronger signals than the development of $CD8^+$ thymocytes (100, 101). Some DP thymocytes down-regulate CD8 to become transitional single positive (TSP) $CD4^+$ thymocytes, which then mature into single positive (SP) $CD4^+$ and SP $CD8^+$ thymocytes (99, 102-104). So that during positive selection, the T cell lineage commitment to either $CD4^+$ or $CD8^+$ subsets is accomplished. Gads is not required for progression into the TSP $CD4^+$ stage of development (99).

Yoder *et. al.* (76) reported that both positive selection and negative selection were impaired in Gads$^{-/-}$ thymocyes. However, the question regarding how Gads regulates negative selection needs to be investigated extensively.

Gads is required more in CD4^{+} T cells than in CD8^{+} T cells

The function of Gads differs in CD4^{+} and CD8^{+} T cells (17). In periphery there are more defects of cell number and function in Gads$^{-/-}$ CD4^{+} T cells than in Gads$^{-/-}$ CD8^{+} T cells. For example, few peripheral CD4^{+} T cells were present in peripheral lymphoid tissues (spleen and lymph nodes) of Gads$^{-/-}$ mice. TCR-mediated proliferation is more impaired in CD4^{+} Gads$^{-/-}$ T cells than in CD8^{+} Gads$^{-/-}$ T cells. Furthermore, Gads$^{-/-}$ CD4^{+} T cells have an activated phenotype and a rapid turnover rate and produced cytokines in response to *in vitro* stimulation (17). When transferred into a wild-type host, Gads$^{-/-}$ CD4^{+} T cells proliferate at a higher rate than wild-type CD4^{+} T cells, demonstrating a defect in homeostatic proliferation in Gads$^{-/-}$ CD4^{+} T cells.

Gads is a substrate of caspases

Different groups reported that the cleavage of Gads is mediated by caspase 3: in Jurkat T cells, cell death triggered by activation of CD95, also known as Fas, results in the cleavage of Gads, which alters TCR-mediated signaling. Gads cleavage is mediated by caspase 3 and the cleavage site lies within the unique linker region of Gads (105-107). Besides that, Yankee *et. al.* (106) also reported that the cleavage removes the C-terminal SH3 domain of Gads to dissociate Gads from SLP-76 so that the truncated form of Gads inhibits TCR-mediated NF-AT signaling.

Oral administration of antigens can lead to systemic antigen-specific hyporesponsiveness, which is called oral tolerance (108, 109). Long term feeding of egg white diet to OVA23-3 mice of which the TCR recognize ovalbumin (OVA, antigen from egg white diet) induced oral

tolerance of peripheral T cells in which calcium/NF-AT signaling was impaired (110, 111). Furthermore, the caspase 3 was activated so as to cleave Gads and SLP-76 in the tolerized $CD4^+$ T cells (110). As a result, the cleavage of Gads and SLP-76 inhibits the associations between the two signaling proteins so as to impair TCR signaling in orally tolerized $CD4^+$ T cells (110, 112).

The function of Gads in cells other than T cells

Gads is important in signaling and function of immune cells other than T cells. Followings are some examples: In bone marrow-derived mast cells, the Gads binding domain together with N-terminal domain of SLP-76 are critical for FcεRI-mediated degranulation and IL-6 secretion (113). In addition, deletion of Gads-binding sites on LAT blocked the tyrosine phosphorylation of PLC-γ1 and PLC-γ2, calcium mobilization to affect the signaling in FcεRI-mediated mast cell activation (114). The Gads-binding site of SLP-76 is absolutely required for FcεRI-mediated mast cell degranulation or cytokine production (113, 115). These data suggested that the association of Gads with SLP-76 and LAT is required for FcεRI signaling in mast cells. Due to the defect in FcεRI signaling, $Gads^{-/-}$ mice had suppressed IgE-mediated allergic reaction, which is mediated by mast cells and basophils, with minimum adverse effects on both innate and acquired immune responses (116). In B cells, Gads regulates B cell receptor (BCR) signaling, as evidenced by $Gads^{-/-}$ B cells have increased calcium mobilization, but normal ERK and p38 MAPK phosphorylation (16). However, the exogenous expression of Gads in Gads-negative B cells enhancing phosphorylation of ERK and p38 MAPK (14) Further, the sera from the SLP-76 mutant mice reconstituted with Gads-binding site Δ224-244 had significant decreased level of OVA-specific IgE level (78), which demonstrated that Gads play an important role in the function of B cell. Macrophage generation is also modulated by Gads as overexpression of Gads in mouse bone marrow cells strongly decreases macrophage production *in vitro* (1). Cutaneous hypersensitivity responses, which are mediated by B cell, macrophages, and NK cells, in

addition to T cells (117), were significantly reduced in SLP-76 mutant mice reconstituted with Gads-binding site Δ224-244 (78).

Interactions involving Gads and their applications

Besides LAT and SLP-76, Gads can bind to a number of other proteins under different conditions in primary cells or cell lines.

HPK1

Hematopoietic Progenitor Kinase 1 (HPK1), also known as MAP4K1, is a hematopoietic-specific protein serine-threonine kinase and is a member of the MAP4K family of mammalian Ste20-related protein kinases (118-120). In DO11.10 murine T cell hybridoma cell line, HPK1 becomes tyrosine phosphorylated and inducibly associates with Gads upon TCR ligation. The interaction is mediated by the C-terminal SH3 domain of Gads and amino acid 467-471 in the fourth proline-rich region of HPK1. Deletion the Gads-binding site on HPK1 or a Gads SH2 mutant in T cells inhibits TCR-induced HPK1 tyrosine phosphorylation (121). Lewitzky *et. al.* (122) revealed that HPK1 has the consensus motif R-X-X-K and it is essential for the interaction between C-terminal SH3 domain of Gads and HPK1. HPK1 negatively regulates proximal TCR signaling involving LAT-Gads-SLP-76 complex; in $HPK1^{-/-}$ T cells, tyrosine phosphorylation of Gads-associated SLP-76 and LAT were higher than in $HPK1^{+/+}$ T cells (123).

Gab family

Proteins in the Gab family are Grb2-associated-binding proteins. Gab proteins regulate the signaling transduction triggered by activation of many different types of receptors, such as growth factor receptor, cytokine receptors (124). Gab1 and Gab2 are important mediators of branching tubulogenesis and play a central role in cellular growth response, transformation

and apoptosis (125). The extended P-X-X-X-R-containing motif, PX3RX2KPX7PL, found in Gab1 and Gab2, is the binding motif for the C-terminal SH3 domains of Gads or Grb2 protein (126). In the yeast two-hybrid system, Gads binds Gab1 (3). In 293T cells, Gab2 constitutively interacts with Gads or Grb2. Then Gab2 is recruited to the lipid raft to inhibit T cell activation (127). Gads interacts with both Gab2 and Gab3 *in vitro* but only with Gab3 in myeloid progenitor cells FDC-P1 cell line. C-terminal SH3 domain of Gads interacts with Gab3 via the atypical proline-rich domain of Gab3. During M-CSF-stimulated macrophage differentiation of mouse bone marrow cells, Gads and Gab3 expression is co-induced. In macrophage differentiation, the association of Gads and Gab3 is M-CSF dependent and the complex of Gads and Gab3 plays an important role in M-CSFR signaling (128). Gab family proteins modulate the activation of PI3K (125) and interact with PLC-γ1 (129, 130). They might play an important role in Gads-mediated TCR signaling.

CD28

The transmembrane protein CD28 contains the Y-M-N-M motif and two proline-rich P-X-X-P motifs in its cytoplasmic region (131, 132). The SH2 domain of Gads binds to the Y-M-N-M motif of CD28 upon phosphorylation at Tyr189 (131, 132). It was also documented that in Jurkat cells, following activation of CD28, the SH2 domain of Gads associates with CD28 via the phosphorylation of CD28 at tyrosine 173 (5). In mouse T cells, the interaction of Gads and CD28 requires the phosphorylation of CD28 at tyrosine 170 (133). The overall association of Gads and CD28, is stabilized by interactions between C-terminal SH3 domain of Gads and the P-X-X-P motifs in the CD28 cytoplasmic tail. The association between Gads and CD28 peaked at 1-4 min and declined thereafter (5). Besides Gads, CD28 has been shown to bind to several other intracellular proteins including PI3K, Grb2, and Itk (132, 134, 135). Gads is more efficiently involved in CD28-mediated IL-2 gene transcription than Grb2, and the maximal IL-2 promoter

activation by CD28 ligation may primarily require activation of NF- κB. The association between Gads and CD28 has a critical role in CD28-mediated activation of the NF-κB signaling pathway via PKCθ, CARMA1 and Bcl10 (131, 132).

SHP-2

The ubiquitously expressed SH2-containing protein tyrosine phosphatases (PTP), also known as SHPs, regulates numerous intracellular signaling cascades so as to control cell proliferation, differentiation, cell survival, migration, adhesion, and apoptosis (136). SHP-2 is a positive component of many receptor tyrosine kinase signaling pathways (137). In Jurkat cells, the SH2 domain of Gads interacts with SHP-2 (6). In addition, SHP-2 is recruited to the Gads-SLP-76 complex, but does not target SLP-76 itself as a substrate, and directly regulates the phosphorylation of key signaling proteins Vav1 and ADAP (138). SHP-2 functions as a facilitator of the Ras-Raf-MEK-ERK pathway through dephosphorylation of an unknown substrate (139, 140).

LIME

Lck-interacting membrane protein (LIME) is a raft-associated transmembrane adaptor protein, which regulates the T cell activation via association with Lck (141) and mediated by CD4 or CD8 coreceptor singlaing (142). Gads interacts with LIME in Jurkat T cells expressing CD8-LIME chimera (141). Moreover, phosphorylated LIME interacts with SH2 domain of Lck as its substrate (141). The recruitment and activation of Lck is a critical step in activating CD3-TCR complex and ZAP-70 (143). In addition to Gads, LIME also associates with some other SH2 domain–containing proteins: PI3K, Grb2, SHP-2 (141). It might indicate that the interaction among Gads, SHP-2 and LIME might play an indispensable role in TCR signaling. It needs to be investigated extensively.

GCIP

GCIP (Grap2 cyclin-D interacting protein) interacts with full-length and C-terminal proline-rich and SH3 domains of Gads in both yeast two-hybrid assays and co-transfection of Gads and GCIP in mammalian cell line COS-7. GCIP associates with cyclin D1 both *in vitro* and in COS-7 cell line (144). The roles of GCIP haven been demonstrated to inhibit the transcription activity of the cyclin D1 promoter, decrease the phosphorylation of the retinoblastoma (Rb) protein at Ser780, slow cell cycle progression, and decrease susceptibility to carcinogenesis (145, 146). GCIP also binds Rad (Ras associated with diabetes) and the latter translocates GCIP from the nucleus to the cytoplasm, thereby inhibiting the tumor suppressor activity of GCIP in nucleus. Besides that, in the presence of Rad, GCIP loses its ability to reduce Rb phosphorylation and inhibit cyclin D1 activity (147). Whether Gads is involved in these processes together with GCIP needs to be studied further.

RET

Gads is expressed in neuroendocrine tumors and cell lines known to bear mutated forms of rearranged during transfection (RET) (148). Activation of RET kinase activity is dependent on autophosphorylation of tyrosine residues located in the cytoplasmatic tail of RET. Constitutive ligand-independent activation of RET causes different forms of human thyroid cancer (149, 150). In 293T cell, Gads directly associates with RET and expression of activated RET relocates Gads to the plasma membrane. Overexpression of Gads inhibits RET-induced NF-κB activation. NF-κB inhibition mediated by Gads could be applied in a therapeutic strategy in neuroendocrine tumor cells transformed by oncogenic RET (148). The association between Gads and RET was also identified in human neuroendocrine cell lines LCC18 (colonic carcinoid), BON (pancreatic carcinoid), and TT (medullary thyroid carcinoma) cell line (148).

BLNK

In a yeast two-hybrid screen, Gads interacts with BLNK constitutively in a Syk (phosphotyrosine)-independent manner (65). In B cells, it was also found that Gads constitutively interacts with BLNK via C-terminal SH3 domain of Gads (14). BLNK (also known as SLP-65), CLNK and SLP-76 belong to the SLP-76 family (151). BLNK is expressed in B cells and macrophages. Following BCR stimulation, BLNK associates with Grb2, PLC-γ1, and Vav1 (152). Gads might regulate BCR signaling through interacting with BLNK.

Fms

In myeloid FDC-P1 cells, SH2 domain of Gads interacts with Fms (also called c-fms, M-CSFR, CSF-1R, CD115) via phosphorylated Tyr697 upon M-CSF stimulation (1, 153). Overexpression of Gads in the myeloid FDC-P1 cell line enhances ERK activity as indicated by phosphorylation of ERK in response to M-CSF (153). The inducible association between Fms and Gads might be important in the activation of myeloid progenitor cells.

Shc

It has been reported that in transfection of 293T cell line, Gads SH2 domain specifically binds to Shc via its phosphorylated Y239 or Y317 residues (154). It was also reported that in K562 cell line, through its SH2 domain, Gads binds to Shc. And the phosphorylation of Shc at Y240 was shown to inhibit the interaction of Shc and Gads (4). Phosphorylation of Shc at Y239/Y240 may lead to c-myc induction and suppression of apoptosis in BaF3 cells in a Ras-independent manner (154).

Others

In Jurkat cells, Gads binds Sos2 and Sam68 via the C-terminal SH3 domain of Gads (5). But it was reported by another group that isolated C-terminal, but not the full length of Gads,

binds to Sos, Sam68 and Cbl, suggesting the Gads C-terminal SH3 domain is covered with spatial orientation in the context of full length Gads protein (4).

In Jurkat cell line, Gads was found to associate with p55 Shb fusion protein independently of phosphotyrosine (155). Gads, but not Grb2 or Grap, associates with RACK-1 (receptor for activated protein kinase C-1) (5). In Jurkat cells and Daudi cells, after stimulation via the T or B cell receptor, respectively, membrane–associated adaptor protein, LAX (Linker for Activation of X cells), which is a negative regulator in lymphocyte signaling, interacts with Gads, Grb2, and the p85 subunit of PI3K (156).

The interactions involving Gads altered in cell types other than T cells. For example, in human B cell lines, Gads constitutively interacts with c-Cbl via the N-terminal SH3 domain of Gads (14), as compared to the fact that only the isolated C-terminal, but not the full length of Gads, binds to Cbl in Jurkat T cell line and 293T cell line (4).

The snake venom toxin convulxin activates platelets through the collagen receptor glycoprotein VI (GPVI). After stimulated with convulxin, besides SLP-76 and LAT, Gads associates with FcR-γ chain in platelets (157). In K562 cell line, through its SH2 domain, Gads binds to c-kit and Bcr-Abl oncoprotein (4).

Morphine and immune system

Opioids are very powerful and effective analgesic drugs frequently used in hospitals and abused by addicts. Morphine was first isolated in early 1800's (158) from opium, which is the dried latex derived from shallowly slicing the unripe seed capsule of opium poppy (*Papaver somniferum*) (159). Morphine is the prototypic and potent opioid commonly used for relieving

moderate to severe pain. However, the application of morphine has a variety of side effects, such as addiction, respiratory depression, constipation, anxiousness, and tolerance (160, 161).

Morphine and other opioids exert their pharmacological effects by binding to opioid receptors which belong to the family of G-protein coupled receptors (GPCR). The GPCRs are composed of an extracellular N-terminal domain, seven transmembrane guanine domains connected by three extracellular and three intracellular loops and an intracellular C-terminal tail (161, 162). There are three major types of opioid receptors: the μ-, κ-, and δ-opioid receptors which are distributed in various sites in the central nervous system. Besides that, opioid receptors are expressed on peripheral sensory neurons and non-neurologic tissues, such as heart, gastrointestinal tract (163-165).

Opioid receptors and a non-classic opioid-like binding receptor are present on cells of the immune system, including lymphocytes (166, 167). The modulatory effect of morphine on the immune system was discovered a long time ago. As early as in the late 19^{th} and early 20^{th} century, morphine was reported to have immunomodulatory effects. As Krueger *et. al.*, reviewed (168): In 1860, Laurence found that morphine had anti-inflammatory role for treating sclerotitis and iritis. In 1898, Cantacuzene reported that morphine regulates the level of chemotactic and phagocytic activity. In 1902, Cloetta showed chronic morphine injections resulted in leukopenia in rabbits. In 1901, Archard and Loeper described that leukopenia was detected among morphine addicts. Till now, morphine has been discovered to affect the cell numbers and functions of a variety of cell types in the immune system: natural killer (NK) cells, T cells, B cells, macrophages (169-172). However, it is still not clear that: 1) what are the direct and indirect effects of morphine on immune system and 2) what are the signaling events that mediate these effects from the interaction of the opioid receptors with their endogenous or exogenous ligands.

The effects of opioids on the immune system could be mediated through central (173) as well as peripheral mechanisms (158, 174). The central pathways include 1) the hypothalamic-pituitary-adrenal (HPA) axis, which is the major part of the neuroendocrine system and 2) the autonomic nervous system. Generally, the acute administration of morphine affects immune function primarily through the autonomic nervous system while chronic exposure to morphine alters immune system predominantly by activation of the HPA axis (158, 174, 175). Besides central pathway, the immunomodulatory function of morphine could also be fulfilled directly through the opioid receptors on immune cells in peripheral system without the involvement of central nervous systems, which is called peripheral pathways (158, 174) .

HPA axis: Activation of the HPA axis results in the production of a series of hormone and hormonal cascade from the hypothalamus, pituitary and adrenal glands. These hormones include corticotropin-releasing hormone (CRH), adrenocorticotropic hormone (ACTH), corticosteroids, and are released into the peripheral systems and affect immune system (172, 176, 177). The immunosuppressive effect of endogenous corticosteroids was found by the following two approaches. 1) Sepsis or stress-induced elevation of corticosteroids decreased the thymocyte numbers and accelerated thymic programmed cell death (178, 179). 2) Zinc-deficiency or restraint stress-induced thymic atrophy was attenuated by blocking the function of corticosteroids via one of the three strategies: surgical adrenalectomy, chemical adrenalectomy, and blocking of corticosteroid receptors (179, 180). What is the effect of exogenous corticosteroids on immune cells? *In vivo* treatment with corticosteroids caused a drastic loss of thymic weight and thymocyte numbers (181-183) as well as reduced peripheral lymphocyte numbers and their functions (184-186). These observations were consistent with the observations made when mice were treated with morphine (187-189). Furthermore, the administration of morphine stimulated the HPA axis by elevating the production of corticosteroid (176, 190-193). And the morphine-induced lymphopenia was abolished in adrenalectomized

animals (172). From those data, we believe that some immunomodulatory effects of morphine are mediated by activating HPA, specifically increased level of corticosteroids.

Autonomic nervous system: The sympathetic nervous system, the enteric system and parasympathetic system are three major parts of autonomic nervous system. Primary and secondary lymphoid organs are innervated by the sympathetic nervous system. Administration of morphine activated the sympathetic nervous system and increased the circulatory level of catecholamines, including epinephrine, norepinephrine, and dopamine (194, 195). Activation of the autonomic nervous system, such as elevated level of catecholamine, is responsible for some of the observed immunomodulatory effects following opioid administration. For example, the inhibitory effect of morphine on the proliferation of lymphocytes derived from blood was mediated through activation of the autonomic nervous system (196, 197).

Morphine could also modulate immune cells via peripheral pathways, in which the central nervous system is not involved. On one hand, immune cells can release endogenous opioids so as to modulate analgesia and immune responses such as inflammation. For example, Boue *et. al.* (198) demonstrated that analgesia was dependent on opioid release by Ag-primed $CD4^+$ T lymphocytes at the inflammatory site. On the other hand, as opioid receptors are expressed on the surface of immune cells (166, 167), the exogenous opioids might directly affect the immune cells. This has been demonstrated by a variety of *in vitro* experiments. For example, *in vitro* treatment of morphine has been reported to affect Th1/Th2 differentiation (199), antibody production(200), and chemotaxis (201, 202). Those data indicate that morphine alone has direct immunomodulatory effects. It was hypothesized that in the aspect of modulating immune system, opioids behave like cytokines. Their similarities include pleiotropy and synergy and the immunomodulatory effect of both cytokines and opioids involve complicated interactions with multiple cell types and unpredictable biologic effects (174).

We hypothesize that the immunomodulatory effects of morphine are through 1) the direct interaction with opioids receptors on immune cells and 2) stimulating HPA and increasing the blood level of corticosteroids. Furthermore, we asked two questions: 1) Which sub-populations of immune system are selectively targeted by morphine itself directly and which subsets are affected by the elevated corticosteroid level induced by the treatment of morphine? 2) What are the mechanisms by which morphine exerts its role on immune system through the opioid receptors on immune cells directly and through activating HPA, respectively? To address those questions and test our hypothesis, I did extensive studies with the focus on morphine-induced T and B lymphocyte depletion and recovery and described the detail in Chapter V.

Chapter II

Gads regulates the kinetics of $CD8^+$ T cell activation and proliferation

Abstract

The Gads adaptor protein is critical for T cell receptor (TCR)-mediated Ca^{2+} mobilization. We investigated the effect of Gads deficiency on the proliferation of the antigen-specific $CD8^+$ T cell population following stimulation with cognate antigen (SIINFEKL) *in vivo*. After stimulation, a lower percentage of $CD8^+$ T cells derived from $Gads^{-/-}$ donor mice proliferated than those from $Gads^{+/+}$ donor mice. Next, we stimulated $CD8^+$ T cells from $Gads^{+/+}$ OT-I and $Gads^{-/-}$ OT-I mice *in vitro* with SIINFEKL or altered peptide ligand (A2) and found that Gads regulated proliferation rather than survival of $CD8^+$ T cells. This defect was most evident at the early time points of proliferation and when low doses of antigen were used as stimuli. Cell cycle analysis revealed that $Gads^{-/-}$ $CD8^+$ T cells had impaired TCR-mediated exit from G0 phase of the cell cycle. Furthermore, $Gads^{-/-}$ $CD8^+$ T cells had delayed expression of c-myc and CD69 upon the stimulation with SIINFEKL. We conclude that Gads is required for the proliferation of $CD8^+$ T cells upon TCR ligation by regulating the signaling threshold of TCR and the kinetics of cell cycle entry and activation.

Introduction

$CD8^+$ T cells represent the branch of the adaptive immune system responsible for recognizing and killing target cells such as tumor cells, virus-infected cells with intracellular pathogens. For $CD8^+$ T cells to fulfill this function, the TCR on the $CD8^+$ T cells must recognize foreign peptides presented on MHC class I. When the TCR binds peptide-MHC complexes, signals are transmitted to the $CD8^+$ T cells that induce activation and proliferation. Thus, to fully understand the role of Gads in the function of $CD8^+$ T cells, we must first understand how proliferation is initiated.

The interaction of the TCR complex with a peptide-MHC complex leads to the recruitment and activation of Src- and Syk/ZAP-70 families of protein tyrosine kinases (35, 203). This kinase activity results in the phosphorylation of the membrane-bound adaptor protein LAT and the recruitment of the SLP-76 adaptor protein. Gads, a member of the Grb2 family of adaptor proteins, bridges LAT and SLP-76 enabling the recruitment of SLP-76 to LAT (1, 2, 4-6). The SH2 domain of Gads binds phosphorylated LAT and the C-terminal SH3 domain of Gads constitutively binds SLP-76. The formation of the LAT-Gads-SLP-76 complex leads to the activation of phospholipase C (PLC)-γ1 and calcium mobilization. Consistent with this model, TCR-mediated calcium influx in Gads-deficient T cells was markedly impaired (17, 76). However, when $Gads^{-/-}$ T cells were stimulated with high doses of anti-CD3ε, there was detectable calcium mobilization (17), suggesting that Gads might regulate the signaling threshold through the TCR.

To examine the function of Gads in T cells, Gads-deficient mouse lines were generated (17, 76). $Gads^{-/-}$ mice had defects in T cell development at stages that correspond to the expression of TCRβ and TCRα. During the $CD4^-CD8^-$ double negative (DN) stage of T cell development, Gads is required for the survival of thymocytes expressing TCRβ (21). Later, when TCRα is

expressed, Gads is required for positive and negative selection of $CD4^+CD8^+$ double positive (DP) thymocytes (99). While the locations of these blocks are consistent with a role for Gads in regulating TCR-mediated signal transduction, the fact that the blocks are not complete indicates that Gads expression is not an absolute requirement for TCR-mediated signal transduction. Rather, Gads may regulate a subset of signaling pathways or the intensity of signals through all pathways. Further, the function of Gads may change during T cell development and activation.

$Gads^{-/-}$ mice had few mature peripheral T cells (17). However, within the peripheral T cell population, $CD4^+$ T cells were more dependent on Gads expression for survival and homeostasis than $CD8^+$ T cells. This conclusion must be tempered by the observation that nearly all T cells in $Gads^{-/-}$ mice were of a memory-like phenotype. The signaling pathways required for the activation of memory T cells are different than those required for the activation of naïve T cells (204-206).

During our analysis of the function of Gads in T cell development, we found that crossing $Gads^{-/-}$ mice with mice expressing an MHC class I-restricted transgenic TCR could rescue the production of naïve $CD8^+$ T cells (99). These transgenic TCR-expressing $Gads^{-/-}$ mouse lines enable us to examine the function of Gads during the activation of naïve $CD8^+$ T cells. We present data from studies in which cells were stimulated with peptide antigen. We analyzed the kinetics of proliferation as well as cell cycle entry and expression of activation markers in this context.

Materials and Methods

Mice

C57BL/6 Gads$^{-/-}$ mice and Gads$^{-/-}$ OT-I mice were described previously (17, 99) and backcrossed onto the CD45.1^{+} C57BL/6 genetic background. All mice were housed under specific pathogen-free conditions and all experiments were performed in compliance with the University of Kansas Medical Center Institutional Animal Care and Use Committee (IACUC). Mice were used between the ages of six and eight weeks for the experiments.

Antibodies

Anti-CD8α-FITC, anti-CD8α-Alexa Fluor 647, anti-CD44-PE-Cy7, anti-CD44-Horizon V450, anti-CD45.1-PE, anti-CD45.1-allophycocyanin-Cy7, anti-CD45.2-PE-Cy5.5, anti-CD45.2-PE, anti-CD69-FITC, anti-CD62L-PE-Cy7, anti-CD122-PE, anti-TCRVα2-FITC, and anti-CD25-allophycocyanin-Cy7 were purchased from BD Biosciences (San Jose, CA), eBioscience, Inc. (San Diego, CA) or Biolegend, Inc. (San Diego, CA).

Cell labeling, and flow cytometry

Surface labeling of cells was performed as described previous (99). Briefly, single cell suspensions were prepared and labeled in staining buffer (PBS containing 2% FetalClone I bovine serum product (HyClone Laboratories, Inc., Logan, UT)) before fixing with 1% paraformaldehyde in PBS overnight or at least one hour at room temperature.

For carboxyfluorescein succinimidyl ester (CFSE) labeling, cells were labeled with CFSE as described in previously (17). Briefly, the cell concentration was adjusted to 2 x 10^7 cells/ml, and an equal volume of 10 μM CFSE (Invitrogen, Carlsbad, CA) was added. Cells were incubated for 10 min at 37°C and the reaction was quenched with cell culture media.

For 4',6-diamidino-2-phenylindole (DAPI) labeling, cells were harvested after stimulation, labeled with anti-CD8, and fixed in 1% paraformaldehyde. Then, cells were washed twice with staining buffer, incubated with 1ml of 1 μg/mL DAPI (Invitrogen, Carlsbad, CA) in 0.3% Tween-20 in staining buffer for 30 min at room temperature and analyzed immediately by flow cytometry.

For pyronin Y (PY) staining, cells were pelleted after DAPI staining and 850 μL of the supernatant were aspirated. Twenty μl of 25μg/mL PY (Polyscience, Inc., Warrington, PA) in staining buffer containing 0.3% Tween-20 were added into each tube. Cells were incubated for 10 min at room temperature and analyzed by flow cytometry.

Samples were analyzed using a BD LSRII (BD Biosciences, San Jose, CA). Data were analyzed using BD FACSDiva (BD Biosciences) and FlowJo (Tree Star, Inc., Ashland, OR).

Proliferation and activation assays

Splenocytes and lymphocytes were isolated from CD45.1$^+$ Gads$^{+/+}$ OT-I or CD45.1$^+$ Gads$^{-/-}$ OT-I mice and loaded with CFSE. The numbers of total splenocytes and lymphocytes were adjusted so that 2 x 10^6 CD8$^+$ T cells were injected i.v. into CD45.2$^+$ congenic mice. The next day, recipient mice were injected i.v. with SIINFEKL peptide (ProImmune Limited, Oxford, UK).

Three days later, lymphocytes were harvested, labeled with anti-CD45.1, anti-CD8, and anti-CD44 and analyzed by flow cytometry.

For *in vitro* assays, splenocytes from Gads$^{+/+}$ OT-I or Gads$^{-/-}$ OT-I mice were isolated, labeled with CFSE, and stimulated with varying doses of SIINFEKL or A2 peptide (ProImmune Limited, Oxford, UK) for the indicated amount of time. At harvest, cells were labeled with anti-CD8 and analyzed by flow cytometry.

For activation assays, splenocytes were isolated from Gads$^{+/+}$ OT-I or Gads$^{-/-}$ OT-I mice and were stimulated with SIINFEKL. At the indicated time points, splenocytes were labeled with anti-CD8, anti-CD69, anti-CD25 and analyzed by flow cytometry.

Cell death analysis

Splenocytes from Gads$^{+/+}$ OT-I mice or Gads$^{-/-}$ OT-I mice were stimulated with SIINFEKL. Two days later, the cells were labeled with anti-CD8, propidium iodide (PI) and Annexin V-Cy5 (BD Biosciences Pharmingen, San Jose, CA) at 4 °C for 30 min and analyzed by flow cytometry.

Immunoblot assay

Splenocytes from Gads$^{+/+}$ OT-I or Gads$^{-/-}$ OT-I mice were isolated and stimulated with 1 nM SIINFEKL. At various time points, CD8^{+} T cells were isolated using anti-mouse CD8α Magnetic Particles-DM (BD Biosciences Pharmingen) and positive selection. Lysates were prepared, separated by SDS-PAGE, and transferred to PVDF membrane. Membranes were probed with anti-c-myc, anti-cyclin D2, anti-p27^{kip1} and anti-β-actin (Cell Signaling Technology, Inc., Danvers, MA).

Statistics

All data are presented as mean ± SD and were analyzed using two-tailed Student's t tests.

Results

Most CD8$^+$ T cells in Gads$^{-/-}$ OT-I mice have a naïve phenotype

Our previous analysis of Gads$^{-/-}$ mice revealed that nearly all peripheral CD8$^+$ T cells in Gads$^{-/-}$ mice were of a memory-like phenotype (17), but crossing Gads$^{-/-}$ mice with mice expressing the MHC class I-restricted TCR OT-I partially restored T cell development (99). On average, spleens from Gads$^{+/+}$ OT-I mice contained 13 ± 2.5 x 10^6 CD8$^+$ cells and spleens from Gads$^{-/-}$ OT-I mice contained 2.2 ± 0.80 x 10^6 CD8$^+$ cells.

To characterize the peripheral CD8$^+$ T cells in Gads$^{+/+}$ OT-I and Gads$^{-/-}$ OT-I mice, we compared CD44, CD62L, CD122, and TCR expression in Gads$^{+/+}$, Gads$^{-/-}$, Gads$^{+/+}$ OT-I, and Gads$^{-/-}$ OT-I mice (Fig. 2-1). Despite the reduced numbers of CD8$^+$ T cells in Gads$^{-/-}$ OT-I mice, as compared to Gads$^{+/+}$ OT-I mice, most CD8$^+$ T cells in each mouse line were CD44^{hi}CD62L^{lo}CD122$^-$. On average, 78 $\pm$ 5.3% of Gads$^{-/-}$ OT-I CD8$^+$ cells were CD44^{lo}CD62L^{hi}, as compared to 90 $\pm$ 3.8 % of Gads$^{+/+}$ OT-I CD8$^+$ cells (p <0.001, n > 12 mice of each genotype). In addition, naïve CD8$^+$ T cells from Gads$^{+/+}$ OT-I and Gads$^{-/-}$ OT-I mice were CD122$^-$ (Fig. 2-1 B) and had comparable surface TCR levels (Fig. 2-1 C). Thus, while the number of naïve CD8$^+$ T cells in Gads$^{-/-}$ OT-I mice was lower than in Gads$^{+/+}$ OT-I mice, we are able to use this model to obtain a sufficient number of naïve T cells to examine the function of Gads in naïve CD8$^+$ T cells.

Fig. 2-1. OT-I expression in Gads$^{-/-}$ mice restores the production of naïve CD8^{+} T cells. Lymphocytes from Gads$^{+/+}$, Gads$^{-/-}$, Gads$^{+/+}$ OT-I, and Gads$^{-/-}$ OT-I mice were labeled with anti-CD8, anti-CD44, anti-CD62L, anti-CD122, and anti-TCRVα2. *A*) Expression of CD44 and CD62L was analyzed on CD8^{+} cells. Shown are the percentages of CD8^{+} cells that were CD44^{lo}CD62L^{hi}, CD44^{hi}CD62L^{hi}, and CD44^{hi}CD62^{lo}. *B*) CD44 and CD122 expression was analyzed on CD8^{+} cells. Shown are the percentages of CD8^{+}CD44^{lo} cells that expressed CD122. *C*) TCR expression on naïve CD8^{+} cells from Gads$^{+/+}$ OT-I (*shaded histogram*) and Gads$^{-/-}$ OT-I (*dark line*) mice is shown. The negative control is shown in the dotted line.

Figure 2-1

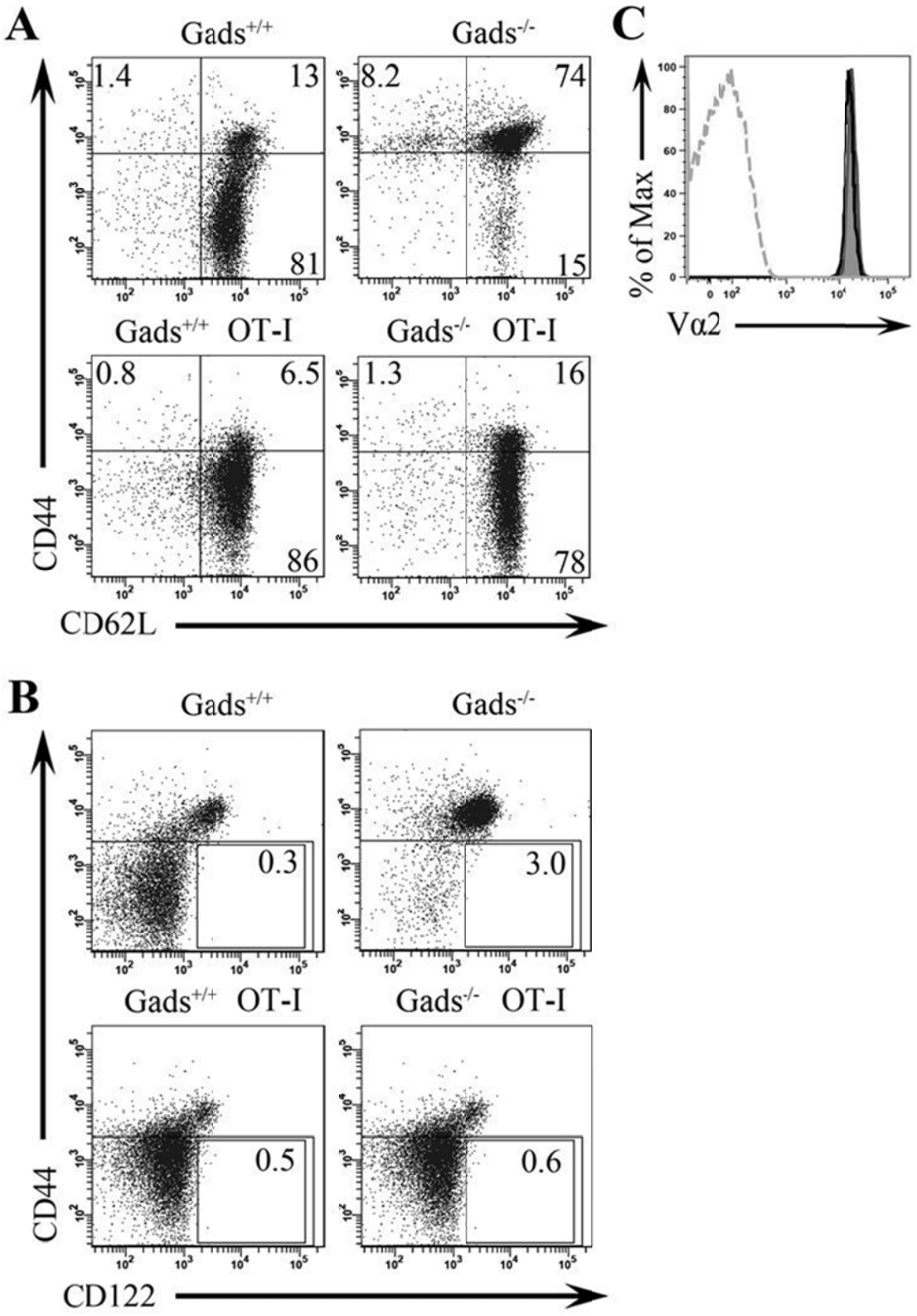
A
Gads+/+
Gads-/-
1.4
13
81
8.2
74
15
Gads+/+ OT-I
Gads-/- OT-I
0.8
6.5
86
1.3
16
78
CD44
CD62L
C
% of Max
Vα2
B
Gads+/+
Gads-/-
0.3
3.0
Gads+/+ OT-I
Gads-/- OT-I
0.5
0.6
CD44
CD122

Gads regulates proliferation of $CD8^+$ T cells

To test whether Gads could regulate proliferation of $CD8^+$ T cells, $CD8^+$ T cells from $Gads^{+/+}$ OT-I or $Gads^{-/-}$ OT-I mice were injected into congenic wild-type hosts. The following day, recipient mice were injected i.v. with SIINFEKL peptide. After three days, fewer $Gads^{-/-}$ cells divided than $Gads^{+/+}$ cells and $Gads^{-/-}$ cells that divided did not divide as extensively as $Gads^{+/+}$ cells (Fig. 2-2), suggesting that Gads regulates proliferation of $CD8^+$ T cells.

To examine the defect in proliferation more closely, we stimulated $Gads^{+/+}$ and $Gads^{-/-}$ $CD8^+$ T cells *in vitro* for three days with varying doses of SIINFEKL or the altered peptide ligand (APL) SAINFEKL, called A2. A2 binds the MHC and TCR with comparable affinity and kinetics as SIINFEKL (207, 208), but has been shown to be less efficient as SIINFEKL in inducing proliferation in an *in vitro* thymidine incorporation assay (209). Using a CFSE-based assay, we found that nearly all $Gads^{+/+}$ $CD8^+$ cells proliferated after stimulation with SIINFEKL or A2 (Fig. 2-3). There was little difference in the extent of proliferation of $Gads^{+/+}$ cells across the dose curve used. By contrast, $Gads^{-/-}$ cells only proliferated efficiently in response to the highest doses of SIINFEKL and A2 (Fig. 2-3). As the concentration of peptide was reduced, the percentage of $Gads^{-/-}$ cells that divided declined. This dose effect was more evident when cells were stimulated with A2 than SIINFEKL.

Regardless of the stimulating conditions, $Gads^{-/-}$ $CD8^+$ T cells failed to complete as many cell divisions as $Gads^{+/+}$ cells. When data were gated on those cells that divided more than five times, fewer $Gads^{-/-}$ cells were detected, even under conditions in which nearly all $Gads^{-/-}$ cells divided (Fig. 2-3).

Fig. 2-2. Gads regulates proliferation of $CD8^+$ T cells *in vivo*. CFSE-labeled splenocytes from $Gads^{+/+}$ OT-I and $Gads^{-/-}$ OT-I mice were adoptively transferred into congenic hosts. Then, mice were injected with the indicated quantity of SIINFEKL. Proliferation was measured by flow cytometry three days later. *A*) Shown are the percentages of $CD8^+$ cells that proliferated. *B*) Bar graph is summary of multiple experiments. Shown are the means ± SD of the percentages of $CD8^+$ cells that proliferated. $^{**}p < 0.01$, n = 4.

Figure 2-2

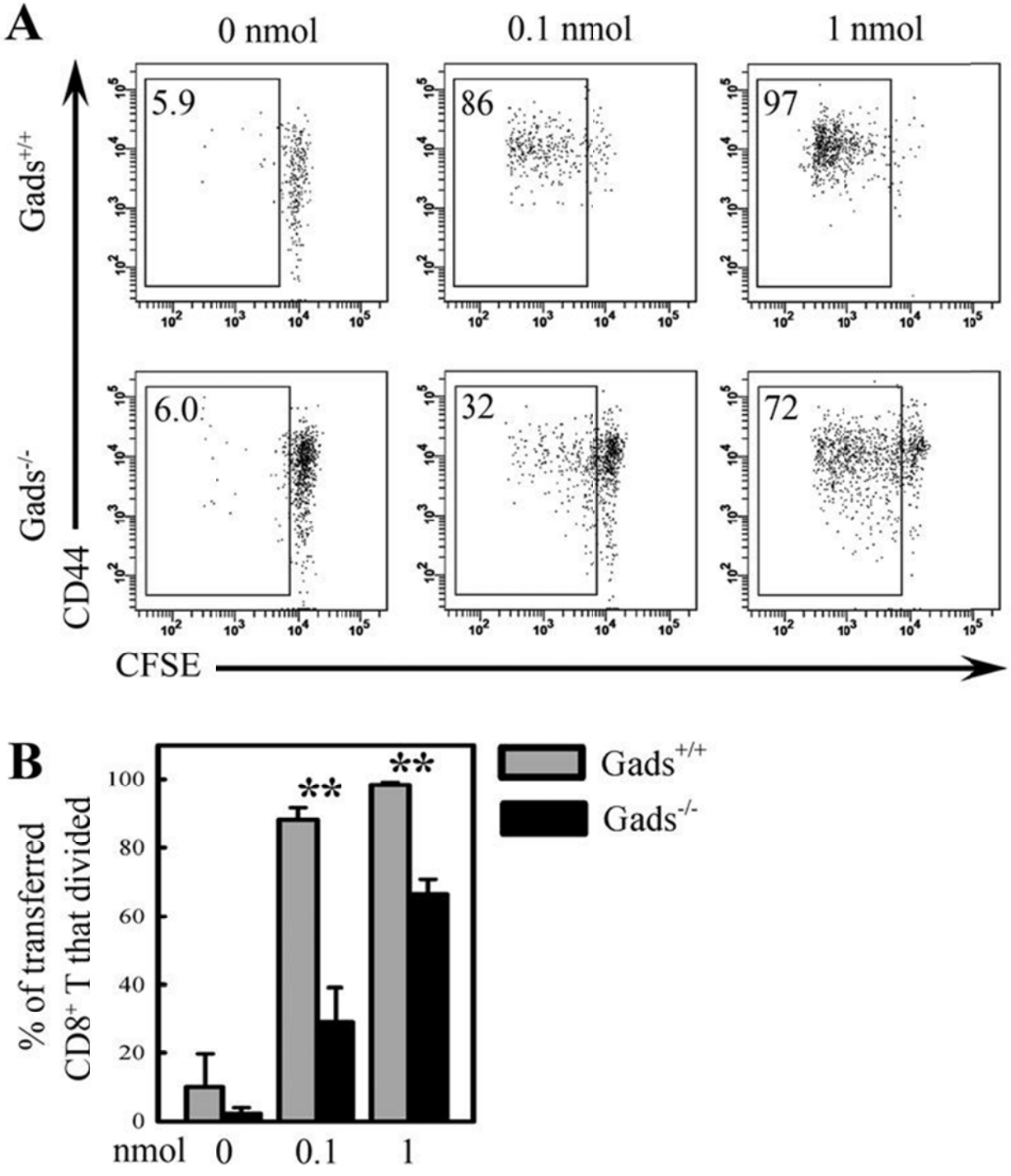
A
0 nmol
0.1 nmol
1 nmol
Gads+/+
Gads-/-
CD44
CFSE
5.9
86
97
6.0
32
72
B
% of transferred CD8+ T that divided
Gads+/+
Gads-/-
**
**
nmol 0 0.1 1

Fig. 2-3. Gads regulates proliferation of $CD8^+$ T cells *in vitro*. CFSE-labeled splenocytes from $Gads^{+/+}$ OT-I and $Gads^{-/-}$ OT-I mice were cultured for three days with the indicated concentrations of SIINFEKL or A2. *A*) Overlays show proliferation of $Gads^{+/+}$ $CD8^+$ T cells (*filled histograms*) and $Gads^{-/-}$ $CD8^+$ T cells (*open histograms*). *B*) *Left bar graph* – Shown are the means ± SD of the percentages of cells that proliferated. $^*p < 0.05$, $^{**}p < 0.01$, n = 3. *Right bar graph* – Shown are the means ± SD of the percentages of cells that completed more than five rounds of cell division. $^*p < 0.05$, $^{**}p < 0.01$, n = 3.

Figure 2-3

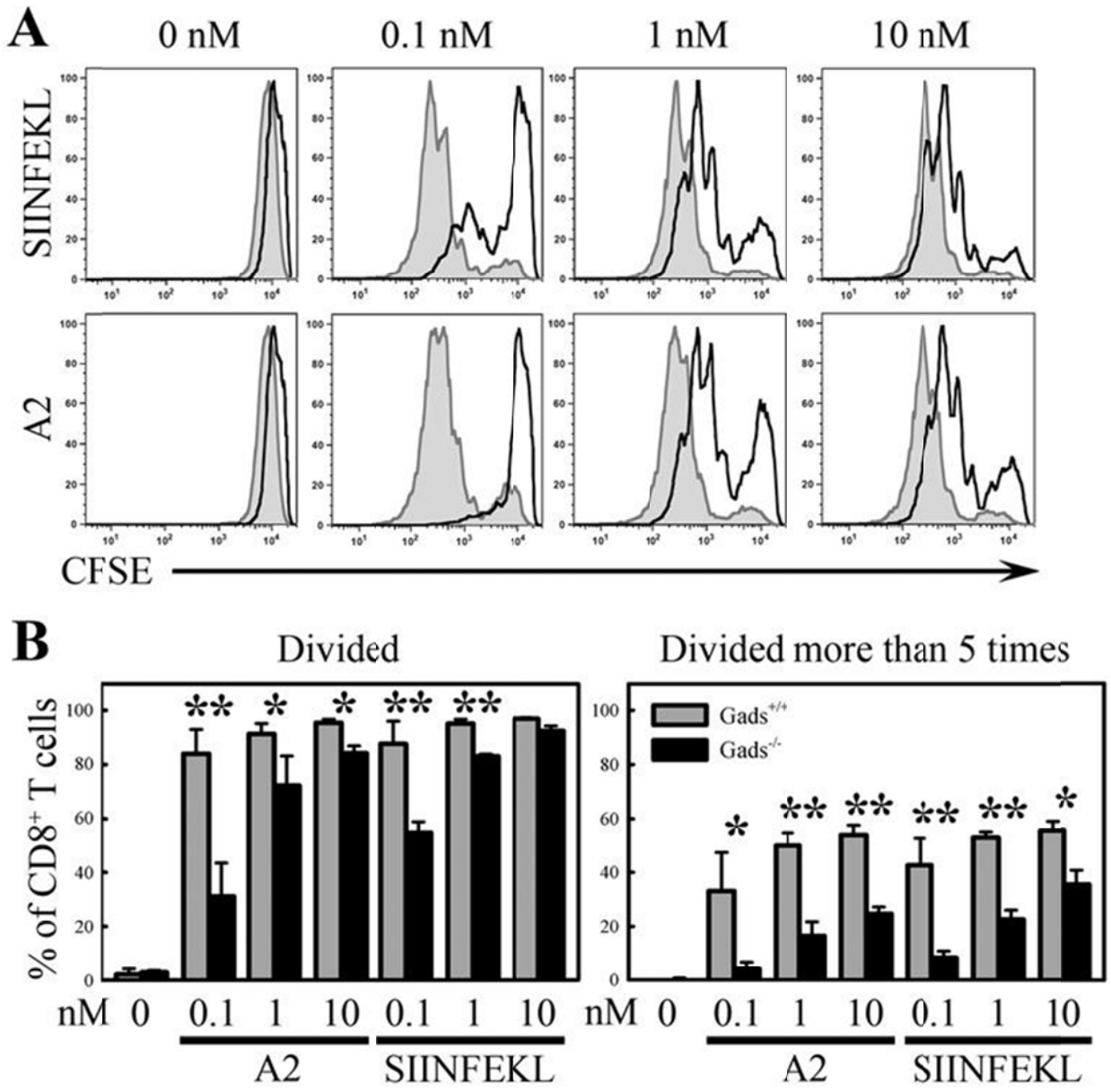
A
0 nM
0.1 nM
1 nM
10 nM
SIINFEKL
A2
CFSE
B
Divided
Divided more than 5 times
% of CD8+ T cells
Gads+/+
Gads-/-
nM 0 0.1 1 10 0.1 1 10
A2
SIINFEKL

These data suggest that Gads regulates the sensitivity of the TCR to ligand and regulates the kinetics of cell proliferation. However, these *in vitro* assays could reflect differences in antigen presentation. To test this possibility, we purified $CD8^+$ T cells from $Gads^{+/+}$ OT-I and $Gads^{-/-}$ OT-I mice and stimulated the cells with wild-type peritoneal macrophages loaded with peptide. This experiment resulted in data similar to that shown in Fig. 2-3 (data not shown).

Gads regulates cell cycle entry

To examine the function of Gads in regulating the onset of proliferation, we analyzed the progression through the S phase of the cell cycle and the completion of the first cell cycle after peptide stimulation. After 28 hours of stimulation with 1 nM SIINFEKL, $29 \pm 4.3\%$ of $Gads^{+/+}$ cells entered the S phase of the cell cycle, as compared to $9.7 \pm 3.2\%$ of $Gads^{-/-}$ cells ($p < 0.001$, n = 4) (Fig. 2-4 A). The percentage of $Gads^{-/-}$ cells entering S phase after stimulation with 1 nM SIINFEKL was statistically identical to the percentage of $Gads^{+/+}$ cells entering S phase after stimulation with 0.1 nM SIINFEKL ($9.7 \pm 3.2\%$ vs. $13 \pm 6.3\%$, $p = 0.34$, n = 4).

We also analyzed cells after 32 and 36 hours and found similar trends (Figs. 2-4 B and 2-4 C); fewer $Gads^{-/-}$ cells than $Gads^{+/+}$ cells entered the S phase of the cell cycle and the percentage of $Gads^{-/-}$ cells entering the cell cycle after stimulation with 1 nM SIINFEKL was comparable to the percentage of $Gads^{+/+}$ cells entering the cell cycle after stimulation with 0.1 nM SIINFEKL. These experiments were repeated using A2 peptide and identical trends were seen (Fig. 2-4).

These data suggest that Gads regulates the kinetics of cell cycle entry and the sensitivity of $CD8^+$ T cells to antigen. Alternatively, Gads could regulate survival of $CD8^+$ T cells. To test if Gads could regulate survival, $Gads^{+/+}$ and $Gads^{-/-}$ splenocytes were stimulated with varying

Fig. 2-4. Gads is required for entry into the S phase of the cell cycle. CFSE-labeled splenocytes from Gads$^{+/+}$ OT-I and Gads$^{-/-}$ OT-I mice were cultured with the indicated concentrations of SIINFEKL or A2 for 28 h (*A*), 32 h (*B*), or 36 h (*C*). At harvest, cells were permeabilized and labeled with DAPI. *Dot plots* – Shown are representative data from cells stimulated with SIINFEKL. The percentages of CD8$^+$ T cells in the S, G2, or M phase of the first cell cycle, G1 phase of the second cell cycle, and S, G2, or M phase of the second cycle are shown. *Bar graphs* – Shown are the means ± SD of the percentages of CD8$^+$ T cells that progressed beyond the G1 phase of the cell cycle. $^*p < 0.05$, $^{**}p < 0.01$, n = 4.

Figure 2-4

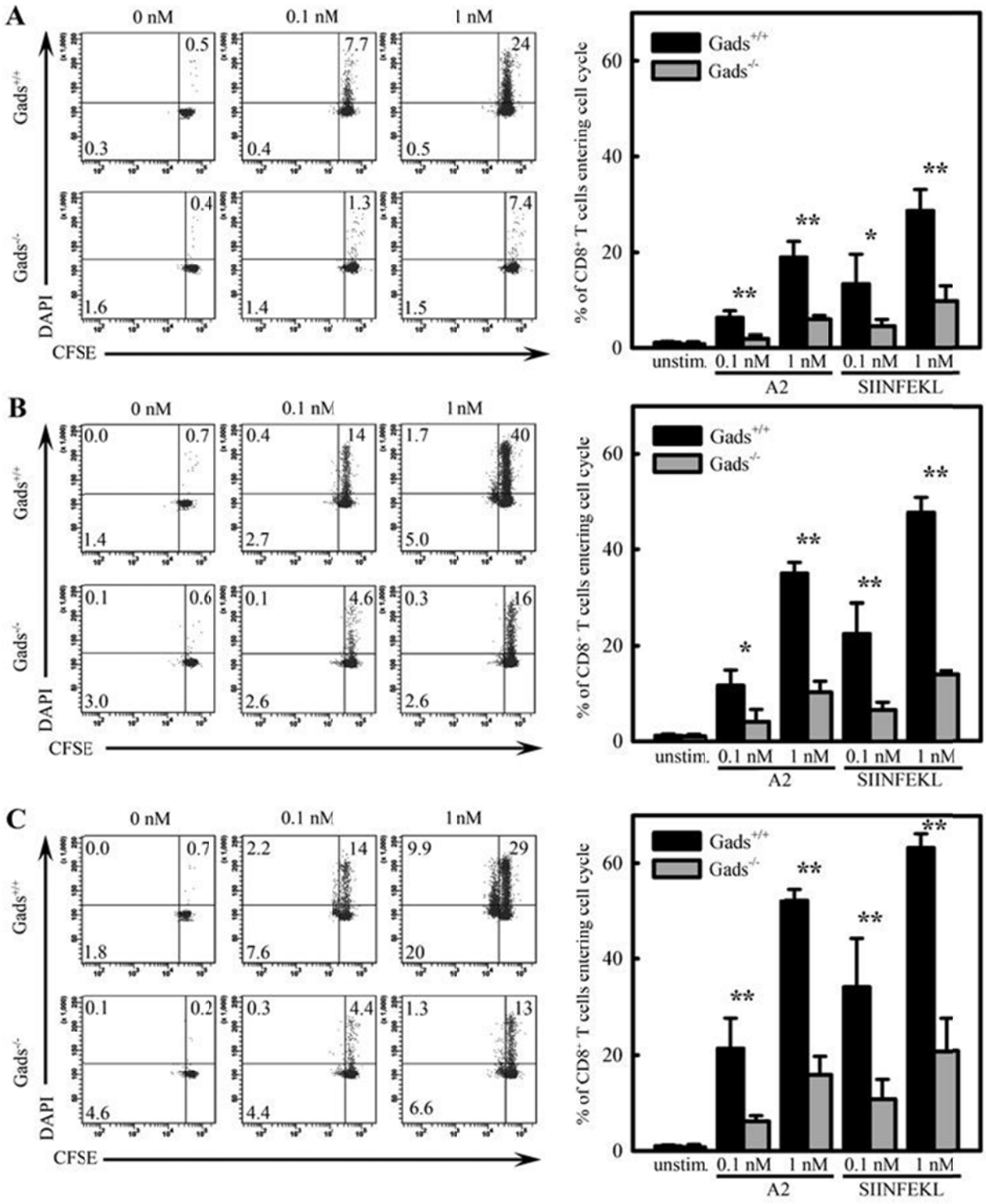
A
0 nM
0.1 nM
1 nM
Gads+/+
Gads-/-
DAPI
CFSE
0.5
7.7
24
0.3
0.4
0.5
0.4
1.3
7.4
1.6
1.4
1.5
% of CD8+ T cells entering cell cycle
Gads+/+
Gads-/-
unstim.
0.1 nM
1 nM
0.1 nM
1 nM
A2
SIINFEKL
B
0 nM
0.1 nM
1 nM
0.0
0.7
0.4
14
1.7
40
1.4
2.7
5.0
0.1
0.6
0.1
4.6
0.3
16
3.0
2.6
2.6
C
0 nM
0.1 nM
1 nM
0.0
0.7
2.2
14
9.9
29
1.8
7.6
20
0.1
0.2
0.3
4.4
1.3
13
4.6
4.4
6.6

doses of SIINFEKL for 48 hours. Cell death was assessed by Annexin V and propidium iodide staining (Fig. 2-5). No differences were observed in the survival of $Gads^{+/+}$ and $Gads^{-/-}$ cells, indicating that the primary function of Gads within the first two days of antigen stimulation is to regulate proliferation.

Gads regulates exit from G0 phase of cell cycle progression

To further define the stage of the cell cycle regulated by Gads, we stimulated splenocytes from $Gads^{+/+}$ OT-I and $Gads^{-/-}$ OT-I mice with varying doses of SIINFEKL and analyzed RNA content using PY and DNA content using DAPI (Fig. 2-6). After fifteen hours of stimulation with 1 nM SIINFEKL, 27 $\pm$ 5.4% of $Gads^{+/+}$ $CD8^+$ T cells had exited the G0 phase of the cell cycle, as compared to 6.7 $\pm$ 5.2% of $Gads^{-/-}$ cells ($p < 0.0001$, n = 6). As in the previous assay, a comparable percentage of $Gads^{-/-}$ cells stimulated with 1 nM SIINFEKL entered the cell cycle as $Gads^{+/+}$ cells stimulated with 0.1 nM SIINFEKL. By 21 hours after stimulation, some $Gads^{+/+}$ cells proceeded through the G1 phase and entered S phase, whereas most $Gads^{-/-}$ cells remained in the G0 phase of the cell cycle (Fig. 2-6 B). Because Gads is proposed to regulate PLCγ1 activity, we tested whether phorbol 12-myristate 13-acetate (PMA) 0.1 μg/ml and ionomycin 0.25 μg/ml could overcome the need for Gads. Indeed, cell cycle entry in $Gads^{-/-}$ cells was fully restored by PMA and ionomycin (Fig. 2-6). In fact, at the 15-hour time point, we noted a consistent increase in the percentage of $Gads^{-/-}$ cells that exited the G0 phase of the cell cycle, as compared to $Gads^{+/+}$ cells. This difference was not seen at the 21-hour time point. These data indicate that Gads regulates early signaling pathways that control the exit from the G0 phase of the cell cycle.

Fig. 2-5. Gads is not required for survival of CD8$^+$ T cells. Splenocytes from Gads$^{+/+}$ OT-I and Gads$^{-/-}$ OT-I mice were cultured with the indicated concentrations of SIINFEKL for two days. Cells were analyzed for Annexin V and propidium iodide (PI) staining. Shown are the percentages of cells that were Annexin V$^+$PI$^+$. Representative of three independent experiments.

Figure 2-5

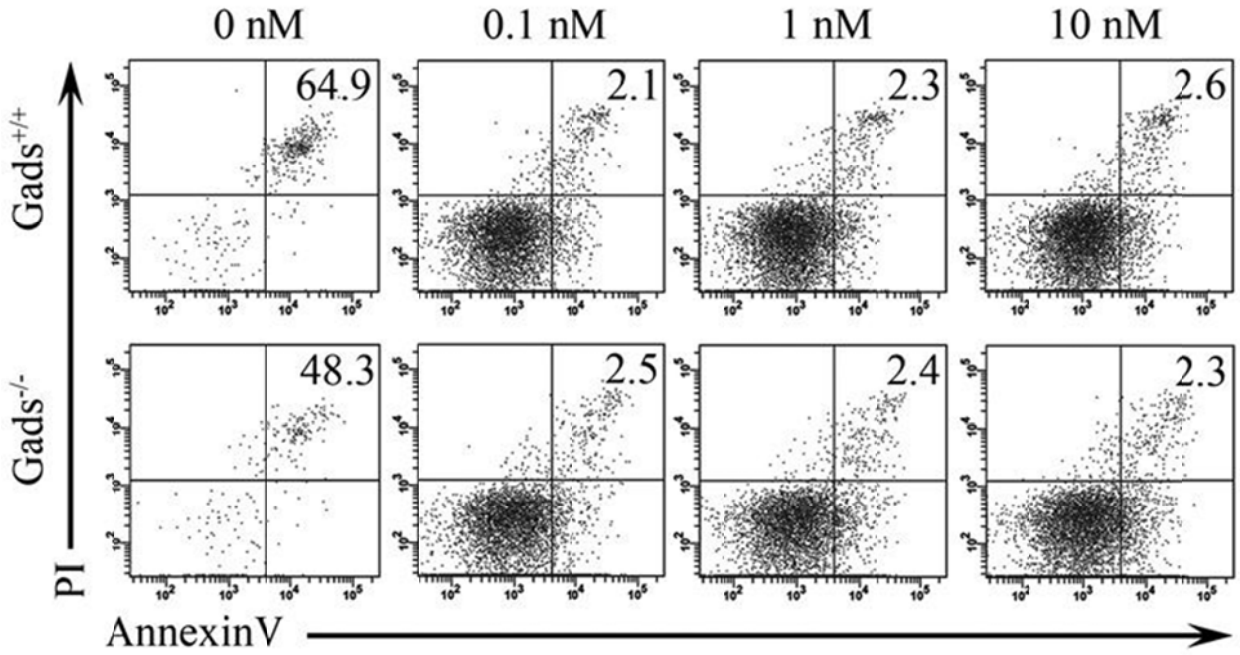
0 nM
0.1 nM
1 nM
10 nM
Gads+/+
Gads-/-
64.9
2.1
2.3
2.6
48.3
2.5
2.4
2.3
PI
AnnexinV

Fig. 2-6. Gads is required for entry into the G1 phase of the cell cycle. Splenocytes from Gads$^{+/+}$ OT-I and Gads$^{-/-}$ OT-I mice were cultured with the indicated concentrations of SIINFEKL, A2, or PMA and ionomycin for 15 h (*A*) or 21 h (*B*). At harvest, cells were labeled with DAPI and PY. *Dot plots* – Shown are representative data from cells stimulated with SIINFEKL and PMA and ionomycin. The percentages of cells in the G1 phase or the S, G2, or M phase of the cell cycle are shown. *Bar graphs* – Shown are the means ± SD of the percentages of CD8^{+} T cells that exited the G0 phase of the cell cycle. $^{*}p < 0.05$, $^{**}p < 0.01$, n ≥ three independent experiments for each sample.

Figure 2-6

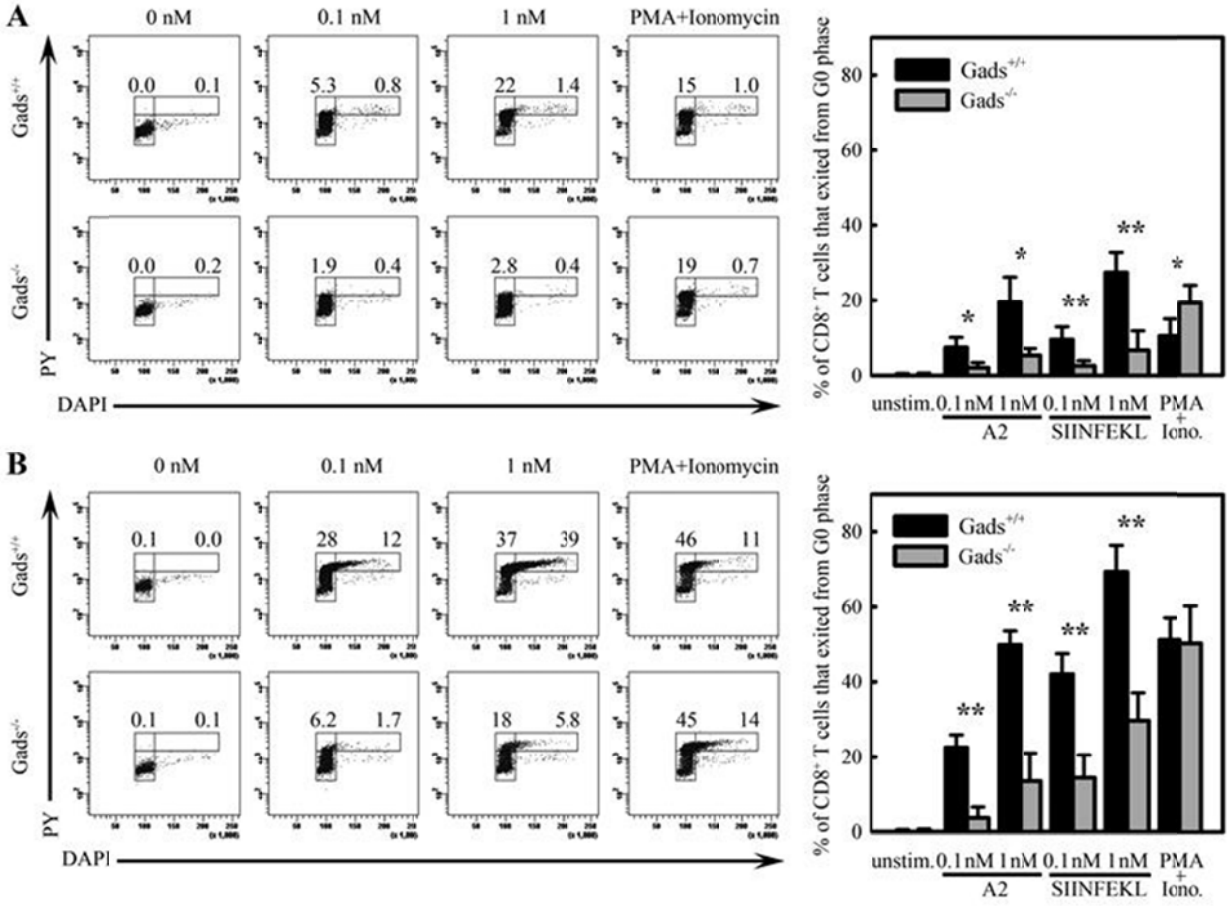
A
0 nM
0.1 nM
1 nM
PMA+Ionomycin
Gads+/+
Gads-/-
PY
DAPI
0.0 0.1
5.3 0.8
22 1.4
15 1.0
0.0 0.2
1.9 0.4
2.8 0.4
19 0.7
% of CD8+ T cells that exited from G0 phase
Gads+/+
Gads-/-
unstim.
0.1 nM
1 nM
0.1 nM
1 nM
PMA + Iono.
A2
SIINFEKL
B
0 nM
0.1 nM
1 nM
PMA+Ionomycin
0.1 0.0
28 12
37 39
46 11
0.1 0.1
6.2 1.7
18 5.8
45 14

To identify the mechanism by which Gads regulates cell cycle entry, we analyzed the expression of c-myc (Fig. 2-7), a regulator of quiescence in T cells (210-212). In $Gads^{+/+}$ cells, c-myc was expressed within one hour of stimulation and remained expressed throughout the duration of the experiment. By contrast, no c-myc expression was detected in $Gads^{-/-}$ cells until three hours after stimulation. Within 24 hours of stimulation, c-myc expression in $Gads^{+/+}$ and $Gads^{-/-}$ cells was comparable, consistent with our model that Gads regulates the onset of proliferation. Besides binding to cyclin-dependent kinases (CDK) 4/6 to regulate cell cycle progression, cyclin D, which is initially synthesized in G1 phase, plays a kinase independent role by sequestering cell cycle inhibitors $p27^{KIP1}$ and $p21^{CIP1}$ (213). We looked at the expression of cyclin D2, which is expressed in murine T cells, and $p27^{KIP1}$ at various time points, and found that at 1h, 3h and 24h after TCR ligation, there were lower expression of cyclin D2 and higher expression of $p27^{KIP1}$ in $Gads^{-/-}$ cells than in $Gads^{+/+}$ cells (Fig. 2-7).

Gads regulates the expression of early activation markers

Next, we tested whether Gads could regulate the kinetics of expression of the early activation marker CD69 (Fig. 2-8 A and B). Like c-myc expression, CD69 expression was reduced on $Gads^{-/-}$ cells at early time points, but nearly indistinguishable at later time points, as compared to $Gads^{+/+}$ cells. Upon TCR ligation, CD25 turns on later than CD69. Since six hours after stimulation, $Gads^{-/-}$ $CD8^+$ T cells had lower expression of CD25, compared with $Gads^{+/+}$ $CD8^+$ T cells (Fig. 2-8 C and D). These data indicate that Gads regulates the kinetics of activation and proliferation of $CD8^+$ T cells but is not required for the activation and proliferation of $CD8^+$ T cells.

Fig. 2-7. Gads regulates the expression of c-myc, cyclin D2, and $p27^{KIP1}$. Splenocytes from $Gads^{+/+}$ OT-I and $Gads^{-/-}$ OT-I mice were stimulated with SIINFEKL for the indicated lengths of time. After stimulation, $CD8^+$ T cells were isolated, lysed, and analyzed for c-myc, cyclin D2 and $p27^{KIP1}$ and β-actin expression by immunoblot. Representative of three independent experiments.

Figure 2-7

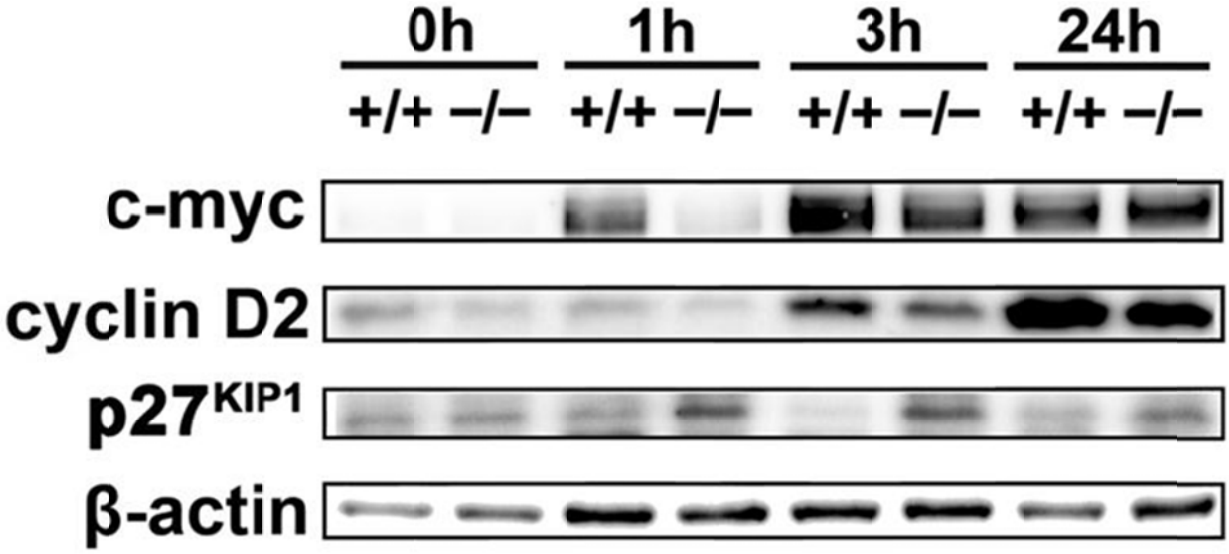

Fig. 2-8. Gads is required for the kinetics of CD69 and CD25 expression. Splenocytes from $Gads^{+/+}$ OT-I and $Gads^{-/-}$ OT-I mice were stimulated with SIINFEKL for the indicated lengths of time. *A*) and *B*), After stimulation, splenocytes were labeled with anti-CD8 and anti-CD69. *A*) Shown is CD69 expression on $Gads^{+/+}$ $CD8^+$ cells (*filled histograms*) and $Gads^{-/-}$ $CD8^+$ cells (*outlined histograms*). The upper number in each histogram represents the percentage of $Gads^{+/+}$ $CD8^+$ cells that expressed CD69 and the lower number represents the percentage of $Gads^{-/-}$ $CD8^+$ cells that expressed CD69. Representative of three independent experiments. *B*) Shown are the means ± SD of the percentages of $CD8^+$ T cells that that expressed CD69. *C*) and *D*), After stimulation, splenocytes were labeled with anti-CD8 and anti-CD25. *C*) Shown is CD25 expression on $Gads^{+/+}$ $CD8^+$ cells (*filled histograms*) and $Gads^{-/-}$ $CD8^+$ cells (*outlined histograms*). The upper number in each histogram represents the percentage of $Gads^{+/+}$ $CD8^+$ cells that expressed CD25 and the lower number represents the percentage of $Gads^{-/-}$ $CD8^+$ cells that expressed CD25. Representative of three independent experiments. *D*) Shown are the means ± SD of the percentages of $CD8^+$ T cells that that expressed CD25. In each time point, top asterisks indicate the *p* value between $Gads^{-/-}$ cells and $Gads^{+/+}$ cells, which were stimulated with SIINFEKL at 1nM; bottom asterisks represent the *p* value between $Gads^{-/-}$ cells and $Gads^{+/+}$ cells, which were stimulated with SIINFEKL at 0.1nM. $^{*}p < 0.05$, $^{**}p < 0.01$, n ≥ three independent experiments for each sample.

Figure 2-8

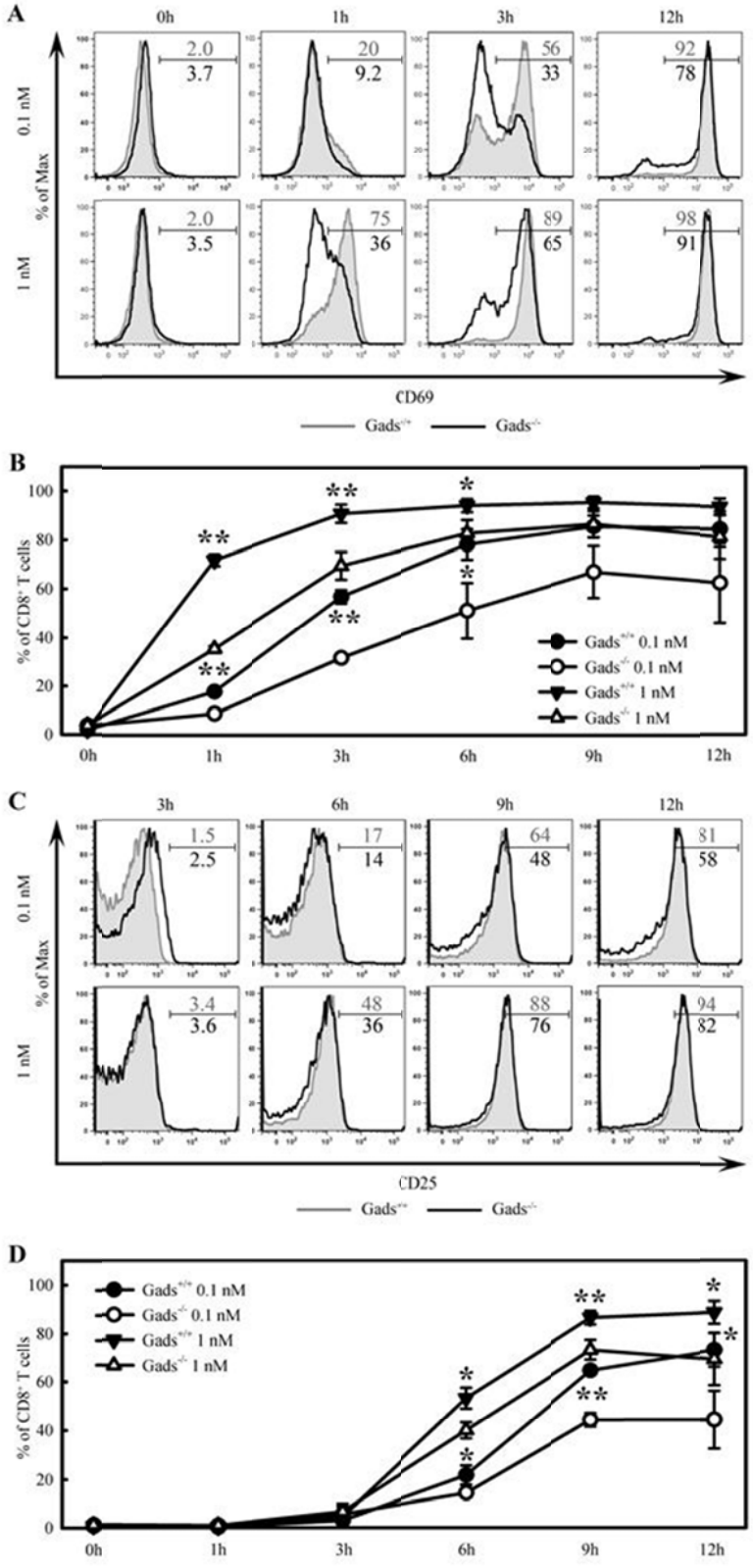
A
0h
1h
3h
12h
0.1 nM
1 nM
% of Max
2.0
3.7
20
9.2
56
33
92
78
2.0
3.5
75
36
89
65
98
91
CD69
Gads+/+
Gads-/-
B
% of CD8+ T cells
Gads+/+ 0.1 nM
Gads-/- 0.1 nM
Gads+/+ 1 nM
Gads-/- 1 nM
0h
1h
3h
6h
9h
12h
C
3h
6h
9h
12h
1.5
2.5
17
14
64
48
81
58
3.4
3.6
48
36
88
76
94
82
CD25
D

Discussion

We report the first analysis of the function of Gads in peripheral naïve $CD8^+$ T cells. We examined the activation and proliferation of T cells in response to cognate peptide antigen and found that Gads-dependent signaling pathways accelerate exit from the G0 phase of the cell cycle and enhance the sensitivity of $CD8^+$ T cells to antigen.

As we previously described, the $CD8^+$ T cells in $Gads^{-/-}$ mice were nearly exclusively of a memory phenotype (17), making a thorough analysis of the function of Gads in naïve $CD8^+$ T cells impossible. Also in our previous studies, we found that the single positive (SP) $CD8^+$ thymocytes in $Gads^{-/-}$ mice were of an unusual phenotype; nearly half the $Gads^{-/-}$ SP $CD8^+$ thymocytes expressed CD122 (99). This unusual phenotype within the SP thymocyte population was overcome by the expression of an MHC class I-restricted TCR. In Fig. 2-1, we demonstrate that many peripheral $CD8^+$ T cells in $Gads^{-/-}$ OT-I mice were naïve, as seen by the expression of CD44, CD62L, and CD122. These data indicate that the OT-I system provides us an opportunity to examine the effects of Gads deficiency on the proliferation and activation of naïve $CD8^+$ T cells.

We found that the major function of Gads is during the initiation of $CD8^+$ T cell activation and proliferation. Even when using high doses of SIINFEKL where nearly all $Gads^{-/-}$ $CD8^+$ T cells could proliferate, $Gads^{-/-}$ cells completed fewer rounds of cell division than $Gads^{+/+}$ cells (Fig. 2-4 B). Completion of fewer rounds of cell division was most likely caused by a delay in cell cycle entry.

Among proliferating cells several days after stimulation, the percentage of $Gads^{-/-}$ cells in the S, G2, or M phase of the cell cycle was comparable to that of $Gads^{+/+}$ cells and proliferating $Gads^{-/-}$ cells survived *in vitro* at the same rate as proliferating $Gads^{+/+}$ cells (data not shown).

This indicates that once Gads$^{-/-}$ CD8^{+} T cells begin proliferating, they progress through subsequent cycles normally.

A key event that is required for the onset of proliferation is the expression of c-myc (214, 215). Expression of c-myc is initiated within thirty minutes of TCR ligation and its expression precedes that of CD25 (216, 217). Analysis of c-myc expression during T cell development revealed that c-myc expression tightly correlates with stages of T cell development in which cells proliferate (212). The importance of c-myc in the proliferation of CD4^{-}CD8^{-} double negative thymocytes was seen when c-myc-deficient double negative thymocytes could not proliferate following pre-TCR expression (218). Further, loss of c-myc expression in CD4^{+} T cells resulted in a lack of TCR-induced proliferation, despite the up-regulation of the activation markers CD25 and CD44 (211). These observations illustrating the importance of c-myc during cell cycle progression were supported by studies showing that c-myc expression can regulate the exit from quiescence in T cells (210).

Because c-myc expression is critical for exit from quiescence and cell cycle entry, we examined c-myc expression following TCR ligation of Gads$^{+/+}$ and Gads$^{-/-}$ CD8^{+} T cells. In the absence of Gads, c-myc expression was delayed, as compared to Gads$^{+/+}$ cells (Fig. 2-7). In addition, expression of the early activation marker CD69 was also delayed in Gads$^{-/-}$ cells (Fig. 2-8 A and B), and the expression of CD25 was defective in Gads$^{-/-}$ cells (Fig. 2-8 C and D). These data indicate that the function of Gads is to regulate the kinetics of CD8^{+} T cell activation and proliferation.

Gads$^{-/-}$ cells were more sensitive to our decreasing the dose of SIINFEKL than Gads$^{+/+}$ cells. Despite the fact that TCR-peptide-MHC complexes with SIINFEKL and A2 have comparable dissociation constants and half-lives (207, 208), A2 is a less potent agonist for CD8^{+} T cell activation and proliferation than SIINFEKL (209, 219). So that we stimulated Gads$^{+/+}$ and Gads^{-}

$^{/-}$ $CD8^+$ T cells with the APL A2. When using $Gads^{+/+}$ cells, we noted little difference in proliferation and cell cycle entry between SIINFEKL and A2. However, proliferation of $Gads^{-/-}$ cells was more dramatically impaired when stimulated with varying concentrations of A2 than with SIINFEKL. This result is consistent with our model that Gads regulates the signaling threshold through the TCR as proliferation of $Gads^{-/-}$ cells in response to a weak agonist was more impaired than the proliferation in response to a strong agonist.

Like Gads-deficiency, APLs have been demonstrated to slow the kinetics of T cell activation (220-223). T cells stimulated with APLs have reduced phosphorylation of ζ chain and reduced recruitment of ZAP-70 to ζ chain than cells stimulated with cognate antigen (224, 225). The result of this decrease in ZAP-70 recruitment is less LAT and SLP-76 phosphorylation, reduced calcium mobilization, and reduced MAPK activation (221, 226). This decreased signaling when T cells are stimulated with APLs leads to reduced expression of activation markers and proliferation (223).

Similarly, $Gads^{-/-}$ $CD8^+$ T cells and delayed expression of activation markers and delayed cell cycle entry. Because of the defects in activation and proliferation seen when Gads-deficient $CD8^+$ T cells were stimulated with cognate antigens, $Gads^{-/-}$ cells were predicted to be more susceptible to reducing the potency of the antigen. Indeed, defects in cell cycle entry of $Gads^{-/-}$ $CD8^+$ T cells were more evident when the cells were stimulated with A2 peptide than SIINFEKL.

The biochemical function of Gads in TCR-mediated signal transduction that is most understood is to couple TCR ligation to calcium mobilization. The mechanism by which Gads fulfills this function is via the binding of the SH2 domain of Gads to the membrane-bound adaptor protein LAT. Following TCR ligation, LAT becomes phosphorylated on tyrosine providing the docking site for Gads. Gads constitutively interacts with the SLP-76 adaptor

protein and the formation of the LAT-Gads-SLP-76 complex is required for optimal calcium mobilization.

Analyses of T cell development in LAT$^{-/-}$, Gads$^{-/-}$, and SLP-76$^{-/-}$ mice support the model that these proteins regulate a common pathway (227-229); however, the pathway is not linear. LAT$^{-/-}$ mice and SLP-76$^{-/-}$ mice could not generate T cells beyond the double negative stage, while Gads$^{-/-}$ mice could generate mature T cells. In peripheral T cells from Gads$^{-/-}$ mice, we showed that calcium mobilization is dramatically impaired, but a calcium response could be detected when cells were stimulated with high doses of anti-CD3 (17).

The observations using Gads$^{-/-}$ mice indicate that Gads, unlike LAT and SLP-76, is not required for TCR-mediated calcium mobilization, but rather Gads enhances TCR signaling. The results presented here support this model. We observed that CD8^{+} T cells could become activated and proliferate without Gads, but Gads expression enhanced the rate at which CD8^{+} T cells become activated and entered the cell cycle. The most likely mechanism by which Gads fulfills this modulatory function is by stabilizing the LAT-centered signaling complex (48).

To test the effect of Gads deficiency on the proliferation of the antigen-specific CD8^{+} T cell population, we stimulated cells with cognate antigen and an APL. We found that Gads$^{-/-}$ cells could not expand in number to the same extent as Gads$^{+/+}$ cells (Fig. 2-3). This impairment could be caused by a failure of Gads$^{-/-}$ cells to initiate proliferation, sustain proliferation, or survive. In investigating these possibilities, we found that the major function of Gads in peptide-induced proliferation is during the initiation of CD8^{+} T cell activation and proliferation. Among proliferating cells several days after stimulation, the percentage of Gads$^{-/-}$ cells in the S, G2, or M phase of the cell cycle was comparable to that of Gads$^{+/+}$ cells and proliferating Gads$^{-/-}$ cells survived *in vitro* at the same rate as proliferating Gads$^{+/+}$ cells (data not shown). This indicates

that once Gads$^{-/-}$ CD8^{+} T cells begin proliferating, they progress through subsequent cell cycles normally.

A key event that is required for the onset of proliferation is expression of c-myc (214, 215). Expression of c-myc is initiated within thirty minutes of TCR ligation and its expression precedes that of CD25 (216, 217). Analysis of c-myc expression during T cell development revealed that levels of c-myc expression tightly correlate with stages of T cell development in which cells proliferate (212). The importance of c-myc in the proliferation of CD4^{-}CD8^{-} double negative thymocytes was seen when c-myc-deficient double negative thymocytes could not proliferate following pre-TCR expression (218). Further, loss of c-myc expression in CD4^{+} T cells resulted in a lack of TCR-induced proliferation, despite the up-regulation of the activation markers CD25 and CD44 (211). These observations illustrating the importance of c-myc during cell cycle progression were supported by studies showing that c-myc expression can regulate exit from quiescence in T cells (210).

Because c-myc expression is critical for exit from quiescence and cell cycle entry, we examined c-myc expression following TCR ligation of Gads$^{+/+}$ and Gads$^{-/-}$ CD8^{+} T cells. In the absence of Gads, c-myc expression was delayed, as compared to Gads$^{+/+}$ cells (Fig. 2-7). In addition, expression of the early activation marker CD69 was also delayed in Gads$^{-/-}$ cells (Fig. 2-8 A). Another activation marker CD25 was expressed in a significantly lower level in Gads$^{-/-}$ CD8^{+} T cells, as compared with that in Gads$^{+/+}$ CD8^{+} T cells. These data indicate that the function of Gads is to regulate the kinetics of CD8^{+} T cell activation and proliferation.

The impaired onset of proliferation seen in Gads$^{-/-}$ CD8^{+} T cells was most dramatic when the concentration of stimulating peptide was reduced or when a less potent peptide agonist, A2, was used (Fig. 2-3). Although TCR-SIINFEKL-MHC and TCR-A2-MHC complexes have comparable dissociation constants and half-lives (207, 208), A2 is a less potent agonist for

$CD8^+$ T cell activation and proliferation than SIINFEKL (209, 219). The more dramatic delay in cell cycle entry seen when $Gads^{-/-}$ cells were cultured with weaker stimuli is consistent with our model that Gads regulates the signaling threshold through the TCR.

Like Gads-deficiency, APLs have been demonstrated to slow the kinetics of T cell activation (220-223). T cells stimulated with APLs have reduced phosphorylation of ζ chain and reduced recruitment of ZAP-70 to ζ chain than cells stimulated with cognate antigen (224, 225). The result of this decrease in ZAP-70 recruitment is less LAT and SLP-76 phosphorylation, reduced calcium mobilization, and reduced MAPK activation (221, 226). This decreased signaling when T cells are stimulated with APLs leads to reduced expression of activation markers and proliferation (223), similar to our results with $Gads^{-/-}$ cells.

In conclusion, we demonstrate that Gads regulates the signaling threshold through the TCR by promoting cell cycle entry and expression of early activation markers of $CD8^+$ T cells following TCR ligation with a peptide agonist.

Chapter III

Gads regulates the expansion phase of $CD8^+$ T cell-mediated immunity

Abstract

The Gads adaptor protein is critical for TCR-mediated Ca^{2+} mobilization. We investigated how Gads regulates $CD8^+$ T cell-mediated immunity following infection with an intracellular pathogen. Naïve $CD8^+$ T cells from $Gads^{+/+}$ OT-I or $Gads^{-/-}$ OT-I mice were adoptively transferred into congenic wild-type mice that were subsequently infected with recombinant *Listeria monocytogenes* expressing ovalbumin or altered peptide ligand. After infection, expression of the activation markers CD69 and CD25 was impaired in $Gads^{-/-}$ cells. Our analysis of the kinetics of the immune response to infection indicates that Gads was not required for the onset of expansion of $CD8^+$ T cell population as at early time points, $Gads^{+/+}$ and $Gads^{-/-}$ $CD8^+$ T cells accumulated to a similar extent. However, Gads was required for the optimal expansion of the $CD8^+$ T cell populations as the peak response of $Gads^{-/-}$ cells was significantly lower than of $Gads^{+/+}$ cells. Restimulation of $Gads^{-/-}$ cells *in vitro* resulted in comparable Interferon-γ (IFN-γ) production as $Gads^{+/+}$ cells, suggesting $Gads^{-/-}$ cells were functional. We also found that $Gads^{-/-}$ cells persisted sixty days after infection, indicating that Gads was not required for the differentiation of naïve $CD8^+$ T cells into memory cells. However, $Gads^{-/-}$ memory cells did not expand as well as $Gads^{+/+}$ memory cells upon re-infection. We conclude that Gads regulates the expansion phase of $CD8^+$ T cell-mediated immune response upon infection as well as optimal recall responses but not the formation of memory $CD8^+$ T cells.

Introduction

$CD8^+$ T cells are cytotoxic T cells that recognize and kill cells infected with intracellular pathogens. For $CD8^+$ T cells to fulfill this function, the TCR on the $CD8^+$ T cells must recognize foreign peptides presented on MHC class I. When the TCR binds peptide-MHC complexes, signals are transmitted to the $CD8^+$ T cell that induce activation and proliferation, which precedes differentiation into effector or memory cells. Like with $CD4^+$ T cells (230), proliferation of $CD8^+$ T cells is required for the differentiation of $CD8^+$ T cells into effector and memory cells (231-236). In Chapter II, I demonstrated that Gads regulates the kinetics of cell cycle entry to affect the proliferation of $CD8^+$ T cells (237).

After primary encounter with a pathogen, the $CD8^+$ T cell-mediated immune responses can be divided into three distinct phases. 1) Expansion Phase (Days 0-8 p.i.): Naïve $CD8^+$ T cells are activated, undergo clonal expansion, and differentiate into effector cells and memory cells. 2) Contraction Phase (Days 8 to 30 p.i.): About 90% of the effector T cells are eliminated by apoptosis. Several groups (238-240) proposed the hypothesis that during expansion and contraction phases, effector $CD8^+$ T cells can be subdivided into two populations: short lived effector cells (SLECs) and memory precursor effector cells (MPECs). The majority of SLECs are considered terminally differentiated and destined for apoptosis while MPECs are not terminally differentiated, retaining the potential to survive and differentiate into memory $CD8^+$ T cells. 3) Memory Phase (>Days 30 p.i.): Upon the primary infection, a relatively stable number of pathogen-specific memory $CD8^+$ T cells is maintained indefinitely (238, 241). After encountering the same pathogen, memory $CD8^+$ T cells proliferate in a much faster and stronger manner in the secondary response, also called the recall response.

Listeria monocytogenes (LM) is gram positive bacterium discovered in 1926. Since then the epidemics have affected various species including rabbits, guinea pigs, and human (242, 243).

LM is recognized as a food borne pathogen which can be present in the gastro-intestinal tract of human. It can lead to severe diseases including septicemia, meningitis, meningo-encephalitis, and abortions, especially in immune-compromised individuals, such as newborn babies, the elderly, or pregnant women (244, 245). As LM is also a blood borne pathogen, many studies were performed by infecting mice with LM i.v. and studying the immune responses to the systemic infection (219, 246-249). In this model, the spleen is the main tissue for immune responses to LM infection to take place. The innate immune system can detect and restrict LM infection. However, leukocytes in the adaptive system, especially $CD8^+$ T cells, are the main force for clearance of LM and protection against future infection by memory cells (250, 251). We would like to know how Gads affects $CD8^+$ T cell- mediated immunity. In the previous chapter, we demonstrate that Gads regulates the kinetics of cell cycle entry as well as activation of $CD8^+$ T cells in *vitro*. In this chapter, the focus will be on the effect of Gads on the immune response of $CD8^+$ T cells to LM infection.

To examine the function of Gads in $CD8^+$ T cell mediated immune responses, we crossed $Gads^{-/-}$ mice with mice expressing the transgenic TCR OT-I. As we previously reported (99) and as shown in Chapter II (Fig. 2-1), expression of the OT-I TCR in $Gads^{-/-}$ mice could rescue T cell development so that $Gads^{-/-}$ OT-I mice have peripheral $CD8^+$ T cells. Thus, we are able to use $Gads^{-/-}$ OT-I mice to examine the function of Gads during $CD8^+$ T cell-mediated immune responses. I adoptively transferred the naïve $CD8^+$ T cells from $Gads^{+/+}$ OT-I mice and/or $Gads^{-/-}$ OT-I mice. We then examined how Gads regulates the expansion and memory phases of $CD8^+$ T cell-mediated immune responses against the live intracellular pathogen, recombinant LM expressing ovalbumin (rLM-OVA) or rLM expressing altered peptide ligand (rLM-APL).

Materials and Methods

Mice

C57BL/6 Gads$^{-/-}$ mice and Gads$^{-/-}$ OT-I mice were described previously (17, 99) and backcrossed onto the CD45.1^{+} C57BL/6 genetic background. To generate CD45.1^{+}CD45.2^{+} OT-I mice, CD45.1^{+} OT-I mice were bred with CD45.2^{+} wild-type C57BL/6 mice. All mice were housed under specific pathogen-free conditions and all experiments were performed in compliance with the University of Kansas Medical Center Institutional Animal Care and Use Committee (IACUC). Mice were used between the ages of six and ten weeks at the start of the experiments.

Antibodies, cell labeling, and flow cytometry

Anti-CD8α-FITC, anti-CD8α-Alexa Fluor 647, anti-CD45.1-PE, anti-CD45.1-allophycocyanin -Cy7, anti-CD45.2-PE-Cy5.5, anti-CD45.2-PE, anti-CD69-FITC, anti-CD25-allophycocyanin-Cy7, anti-CD127-allophycocyanin-e-Fluor® 780, and anti-KLRG1-PE were purchased from BD Biosciences (San Jose, CA), eBioscience, Inc. (San Diego, CA) or Biolegend, Inc. (San Diego, CA).

Surface labeling of cells was performed as described previous (99). Briefly, single cell suspensions were prepared and labeled in staining buffer (PBS containing 2% FetalClone I bovine serum product (HyClone Laboratories, Inc., Logan, UT)) before fixing with 1% paraformaldehyde in PBS overnight or at least one hour at room temperature.

For IFN-γ assays, splenocytes were re-stimulated in culture with SIINFEKL 1 nM in the presence of Brefeldin A. After fixation with 1% paraformaldehyde, cells were permeabilized with 0.3% Tween-20 and labeled with anti-CD8, anti-CD45.1, anti-CD45.2, and anti-IFN-γ.

Samples were analyzed using a BD LSRII (BD Biosciences, San Jose, CA). Data were analyzed using BD FACSDiva (BD Biosciences) and FlowJo (Tree Star, Inc., Ashland, OR).

Homing assays

Splenocytes and lymphocytes were isolated from CD45.1$^+$ Gads$^{+/+}$ OT-I or CD45.1$^+$ Gads$^{-/-}$ OT-I mice. The numbers of total splenocytes and lymphocytes were adjusted so that 2 x 10^6 CD8$^+$ T cells were injected i.v. into CD45.2$^+$ congenic mice. Four days later, splenocytes and lymphocytes were harvested, labeled with anti-CD45.1, anti-CD8 and analyzed by flow cytometry.

Recombinant *Listeria monocytogenes*-expressing OVA infections

Splenocytes were harvested from CD45.1$^+$CD45.2$^+$ Gads$^{+/+}$ OT-I or CD45.1$^+$ Gads$^{-/-}$ OT-I mice and naïve CD8$^+$ (CD8$^+$CD44^{lo}) T cells were FACS-purified using a BD FACSAria (BD Biosciences). 10^4 naïve CD8$^+$ T cells were adoptively transferred into CD45.2$^+$ congenic mice. For competition assays, 5 x 10^3 cells of each genotype were injected. rLM-OVA was a generous gift of Dr. Leo LeFrançois, University of Connecticut Health Center and rLM-APL (rLM-A2 and rLM-Q4) were kindly provided by Dr. Michael Bevan, University of Washington. rLMs were made by the LeFrançois lab and the Bevan lab as previously reported (219, 252). They were cultured in 5 mL brain heart infusion (BHI) broth containing 7.5 µg/ mL

chloramphenicol overnight and 1:10 diluted to 20 mL fresh BHI broth with same concentration of chloramphenicol. When they grew till the appropriate density according to the OD value (OD=0.8), they were centrifuged and re-suspended in 4 mL saline with the density of 5×10^8 CFU of rLM/100 µL. After diluted as 1:2.5×10^5, 2×10^3 CFU rLM-OVA, rLM-A2, or rLM-Q4 in 100 µL saline or vehicle control 100 µL saline was injected i.v. into each mouse. At the indicated time points, blood or splenocytes were harvested, labeled with anti-CD45.1, anti-CD45.2, anti-CD8, anti-KLRG1, and anti-CD127 and analyzed by flow cytometry. RBCs from blood samples were lysed with ACK lysis buffer prior to staining. For challenge assays, mice were re-infected i.v. sixty days post-infection with 10^4 CFU rLM-OVA. Blood and splenocytes were harvested and analyzed four days post-challenge.

For short-term activation assays, 2 x 10^6 $CD8^+$ T cells were positively selected from $Gads^{+/+}$ OT-I and $Gads^{-/-}$ OT-I mice using anti-CD8α Magnetic Particles-DM (BD Pharmingen) and injected into congenic wild-type mice. The following day, mice were infected with 2 x 10^3 CFU rLM-OVA, SIINFEKL or vehicle control. Twenty-four hours after infection, splenocytes were harvested and labeled with anti-CD8, anti-CD45.1, anti-CD45.2 and anti-CD69 and analyzed by flow cytometry.

Statistics

All data are presented as mean ± SD and were analyzed using two-tailed Student's t tests.

Results

Gads regulates the expansion phase of $CD8^+$ T cell-mediated immunity

To test how a delay in peptide-induced activation and proliferation could relate to an immune response against a live pathogen, we adoptively transferred naïve $CD8^+$ T cells from $Gads^{+/+}$ OT-I or $Gads^{-/-}$ OT-I mice into congenic wild-type mice, infected the recipients with rLM-OVA, and analyzed the $CD8^+$ T cells derived from the donor mice. For these experiments, we generated $CD45.1^+CD45.2^-$ $Gads^{-/-}$ OT-I mice and $CD45.1^+CD45.2^+$ $Gads^{+/+}$ OT-I mice, so we could test the expansion of $Gads^{+/+}$ and $Gads^{-/-}$ cells when the cells were injected into separate $CD45.2^+$ hosts as well as in a competition assay where the cells were mixed and injected into the same $CD45.2^+$ host. Regardless of whether the cells were injected separately or together, the expansion of $Gads^{+/+}$ and $Gads^{-/-}$ cells was statistically identical for the first five days after infection (Fig. 3-1 A and B). This similarity in expansion suggests that Gads did not regulate the onset of proliferation or homing of naïve $CD8^+$ T cells into lymphoid tissues. As another measure of homing, we injected $Gads^{+/+}$ and $Gads^{-/-}$ cells into congenic hosts and examined the percentages of $CD8^+$ T cells in the spleen and lymph nodes that were derived from the donor. In the absence of stimulation, identical percentages of $Gads^{+/+}$ and $Gads^{-/-}$ $CD8^+$ T cells were found (Fig. 3-2).

Despite not being required for expansion of the antigen-specific $CD8^+$ T cells early after infection, Gads was required to sustain the expansion of the naïve $CD8^+$ T cell population after infection with rLM-OVA. On day 7, 38 ± 3.2 % of $CD8^+$ T cells in infected mice were derived from $Gads^{+/+}$ mice and 11 ± 3.6 % were derived from $Gads^{-/-}$ mice ($p < 0.0001$, n = 10) (Fig. 3-1). This difference was exacerbated when $Gads^{+/+}$ and $Gads^{-/-}$ cells were mixed and injected into the same host; 8.5 ± 5.3-fold more $Gads^{+/+}$ $CD8^+$ T cells were recovered than $Gads^{-/-}$ cells.

Fig. 3-1. Gads regulates the expansion phase of $CD8^+$ T cell-mediated immunity following infection. Naïve $CD8^+$ T cells from $CD45.1^+$ $Gads^{-/-}$ OT-I mice, $CD45.1^+CD45.2^+$ $Gads^{+/+}$ OT-I mice, or both were adoptively transferred into separate $CD45.2^+$ wild-type mice or mixed and injected into the same $CD45.2^+$ wild-type mice before mice were injected i.v. with rLM-OVA. *A*) The percentages of $CD8^+$ T cells derived from the donor mice were calculated at the indicated time points. *B*) Shown are the means ± SD of the data from (*A*). *Left panel* - Shown are the means ± SD of the data from (*A*) in which $Gads^{+/+}$ and $Gads^{-/-}$ cells were injected into separate hosts. *Right panel* - Shown are the means ± SD of the data from (*A*) in which $Gads^{+/+}$ and $Gads^{-/-}$ cells were mixed and injected into the same hosts. $^{**}p < 0.01$, n = 4 in two independent experiments.

Figure 3-1

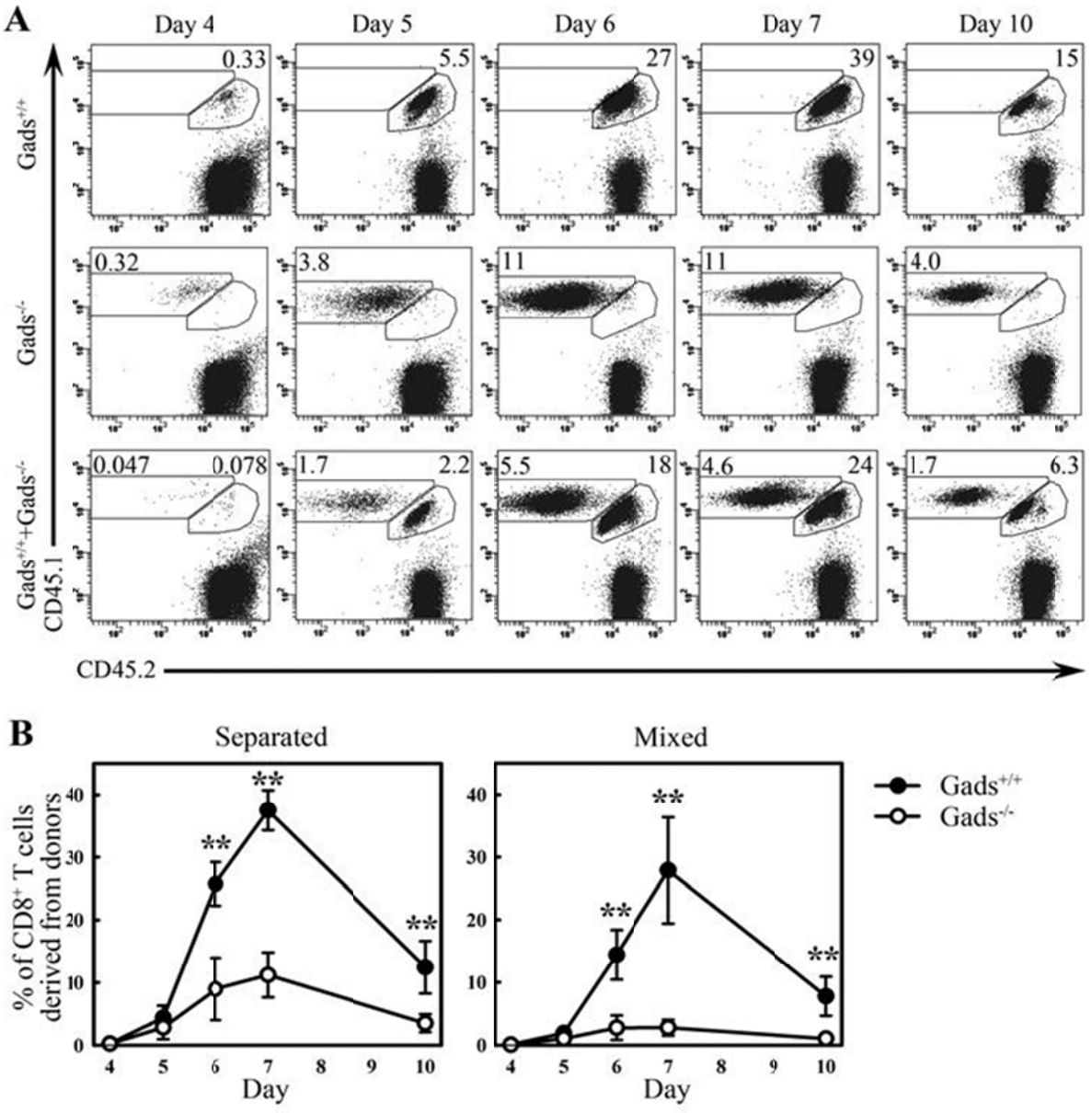
A
Day 4
Day 5
Day 6
Day 7
Day 10
Gads+/+
Gads-/-
Gads+/++Gads-/-
CD45.1
CD45.2
0.33
5.5
27
39
15
0.32
3.8
11
11
4.0
0.047
0.078
1.7
2.2
5.5
18
4.6
24
1.7
6.3
B
Separated
Mixed
% of CD8+ T cells derived from donors
Day
Gads+/+
Gads-/-
**

Fig. 3-2. Gads is not required for the homing of $CD8^+$ T cells in spleen and lymph nodes. Total splenocytes from $CD45.1^+$ $Gads^{+/+}$ OT-I or $Gads^{-/-}$ OT-I mice were injected into congenic hosts such that 2 x 10^6 $CD8^+$ T cells were injected. Lymphocytes from the spleens and lymph nodes were analyzed four days later. Shown are the percentages of $CD8^+$ T cells derived from $Gads^{+/+}$ and $Gads^{-/-}$ donors. Representative of three independent experiments.

Figure 3-2

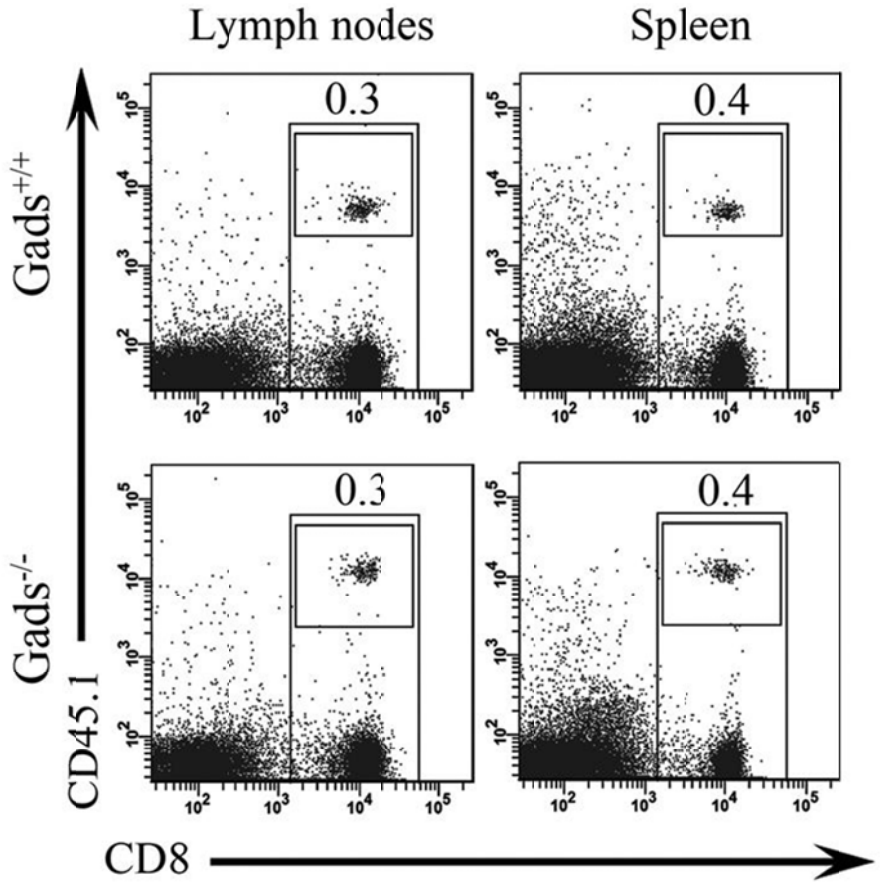

In Chapter II, we demonstrated that *in vitro* proliferation of Gads$^{-/-}$ cells stimulated with a weak agonist A2 was more impaired than cells stimulated with a strong agonist SIINFEKL. We would like to know whether this is true in the context of immune response to infection. We looked at the effect of Gads on the immune responses of CD8^{+} T cell upon infection with rLM-OVA or two of rLM-APLs with different potency. APLs for the OT-I TCR are peptide variants derived from the original antigenic OVA peptide SIINFEKL, with substitutions at particular residue(s) (208). SAINFEKL is called A2 as at the second amino acid position of SIINFEKL, alanine (A) replaces isoleucine (I). SIIQFEKL is named as Q4 because glutamine (Q) substitutes for asparagine (N) at the position of the forth amino acid of SIINFEKL. The rLM strains stably express secreted OVA containing either the native ligand SIINFEKL, or APL A2, or Q4 (219, 252). Among various strains of rLM-APLs (rLM-A2,Y3,Q4,T4,V4), infection with rLM-A2 could induce the strongest immune response of CD8^{+} T cells, although it was still slightly weaker, as compared with that induced by infection with rLM-OVA. Infection with rLM-Q4 yielded an expansion phase, which was markedly reduced, but was still readily detectable. (219). Therefore, we have chosen rLM-A2 and rLM-Q4, besides rLM-OVA in our studies. After the adoptive transfer of Gads$^{+/+}$ and Gads$^{-/-}$ CD8^{+} T cells into congenic hosts, the recipients were injected with rLM-OVA, rLM-A2, or rLM-Q4. Among these three strains of rLM, rLM-OVA is the strongest stimuli, rLM-A2 is the second and rLM-Q4 is the weakest one. At 5 days p.i. with rLM-OVA, there were similar percentages of CD8^{+} T cells derived from Gads$^{-/-}$ donor mice to that from Gads$^{+/+}$ donor mice in blood (Fig. 3-3 A), which were consistent with the results generated from spleen of mice infected by rLM-OVA (Fig 3-1). In contrast, from blood samples harvested at 5 days p.i. with rLM-A2 or rLM-Q4, lower percentages of CD8^{+} T cells were derived from Gads$^{-/-}$ donor mice than from Gads$^{+/+}$ donor mice (Fig. 3-3 A). However, at 7 days p.i. with any of the rLM strains, lower percentages of CD8^{+} T cells in blood were derived from Gads$^{-/-}$

Fig. 3-3. Gads regulates the expansion of $CD8^+$ T cell population following infection with rLM-APL. Naïve $CD8^+$ T cells from $CD45.1^+$ $Gads^{-/-}$ OT-I mice, $CD45.1^+CD45.2^+$ $Gads^{+/+}$ OT-I mice, or both were adoptively transferred into separate $CD45.2^+$ wild-type mice or mixed and injected into the same $CD45.2^+$ wild-type mice before mice were injected i.v. with rLM-OVA, rLM-A2, and rLM-Q4. *A*) Five days and *B*) seven days postinfection, the percentages of $CD8^+$ T cells derived from the donor mice in blood were calculated. Shown are the representative data from two mice.

Figure 3-3

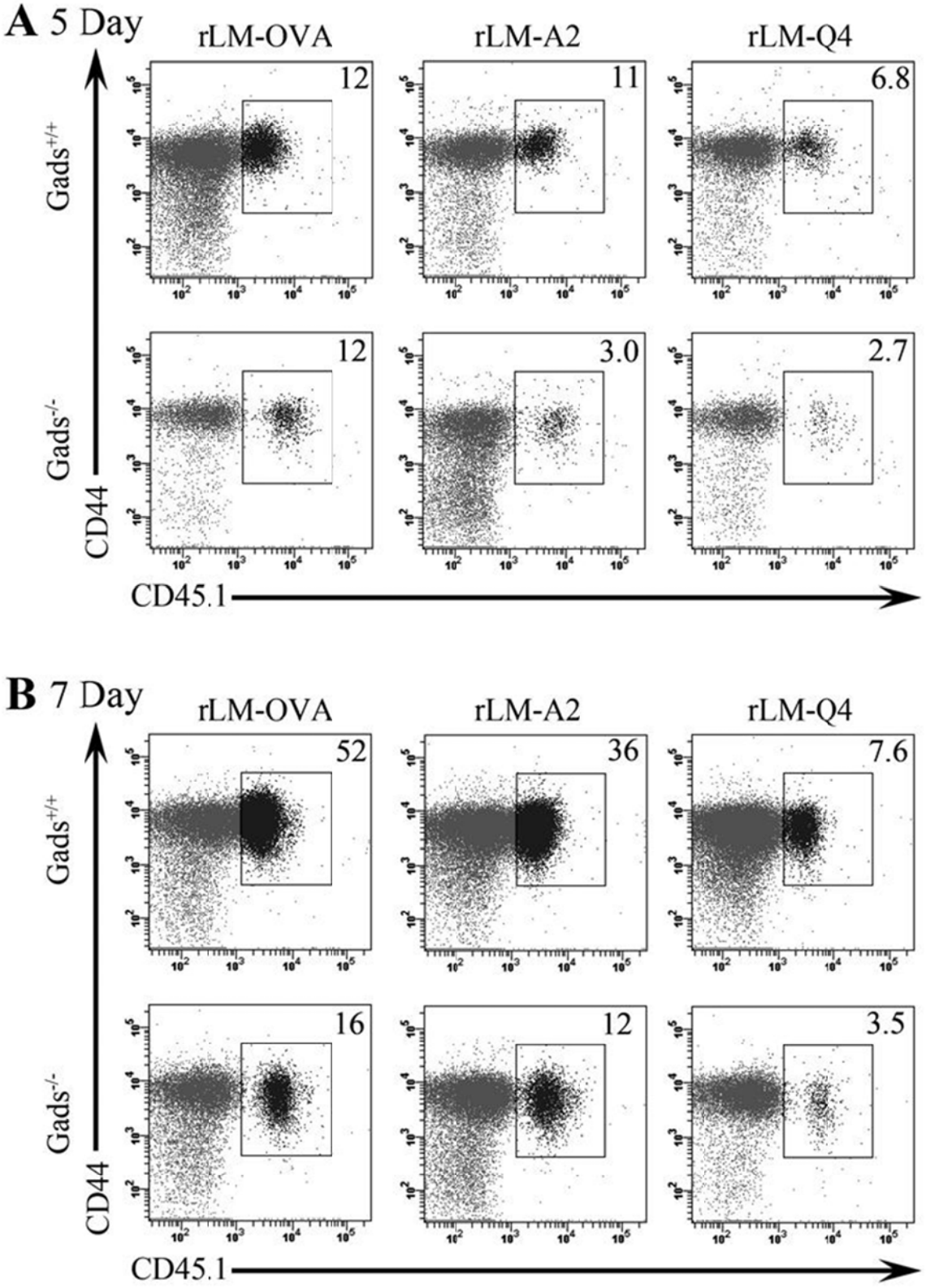
A 5 Day
rLM-OVA
rLM-A2
rLM-Q4
12
11
6.8
12
3.0
2.7
Gads+/+
Gads-/-
CD44
CD45.1
B 7 Day
rLM-OVA
rLM-A2
rLM-Q4
52
36
7.6
16
12
3.5
Gads+/+
Gads-/-
CD44
CD45.1

mice than from Gads$^{+/+}$ mice (Fig. 3-3 B). These data were consistent with the results in the spleen at 7 days p.i. with either of the rLM strains (Fig. 3-4 A).

In order to address the question whether the diminished accumulation of Gads$^{-/-}$ CD8^{+} T cell population is caused by a defect in proliferation of Gads$^{-/-}$ CD8^{+} T cells, we analyzed cell cycle progression of OVA-specific CD8^{+} T cells in spleen. At 7 days p.i. with either rLM-OVA or rLM-A2, there were comparable percentages of OVA-specific CD8^{+} T cells in the S, G2, or M phase of the cell cycle between mice receiving naïve Gads$^{-/-}$ CD8^{+} T cells and mice receiving naïve Gads$^{+/+}$ CD8^{+} T cells. When the recipient mice were infected with rLM-Q4, lower percentage of antigen-specific CD8^{+} T cells were in S, G2, or M phase of the cell cycle, as compared with mice infected with rLM-OVA or rLM-A2. However, there were comparable percentages of antigen-specific Gads$^{-/-}$ CD8^{+} T cells were in S, G2, or M phase of the cell cycle, as compared with antigen-specific Gads$^{+/+}$ CD8^{+} T cells in spleen at 7 days p.i. with rLM-Q4 (Fig. 3-4).

The above results demonstrated that Gads is not required for the onset of accumulation of antigen-specific CD8^{+} T cell but is required for the optimal expansion of the antigen-specific CD8^{+} T cell population upon infection with different strains of rLM.

Gads regulates the expression of early activation markers upon infection

We tested whether Gads could regulate the expression of the activation markers CD69 and CD25 *in vivo*. After the adoptive transfer of Gads$^{+/+}$ and Gads$^{-/-}$ CD8^{+} T cells into congenic hosts, the recipients were injected with SIINFEKL (Fig. 3-5 A) or rLM-OVA (Fig. 3-5 B and C). There were lower percentages of Gads$^{-/-}$ OVA-specific CD8^{+} T cells expressing CD69 or CD25 24 hours post stimulation with SIINFEKL *in vivo* or 24 hours and 5 days p.i. with rLM-OVA, as

Fig. 3-4. Gads regulates the expansion of $CD8^+$ T cell population upon infection with rLM-OVA, rLM-A2, or rLM-Q4. Naïve $CD8^+$ T cells from $CD45.1^+$ $Gads^{-/-}$ OT-I mice, $CD45.1^+CD45.2^+$ $Gads^{+/+}$ OT-I mice, or both were adoptively transferred into separate $CD45.2^+$ wild-type mice or mixed and injected into the same $CD45.2^+$ wild-type mice before mice were injected i.v. with rLM-OVA, rLM-A2, and rLM-Q4. *A*) The percentages of $CD8^+$ T cells derived from the donor mice in spleen were calculated at seven days postinfection and show are the representative data. *B*) Shown are the cell cycle status analyses of the $CD8^+$ T cells derived from donor mice.

Figure 3-4

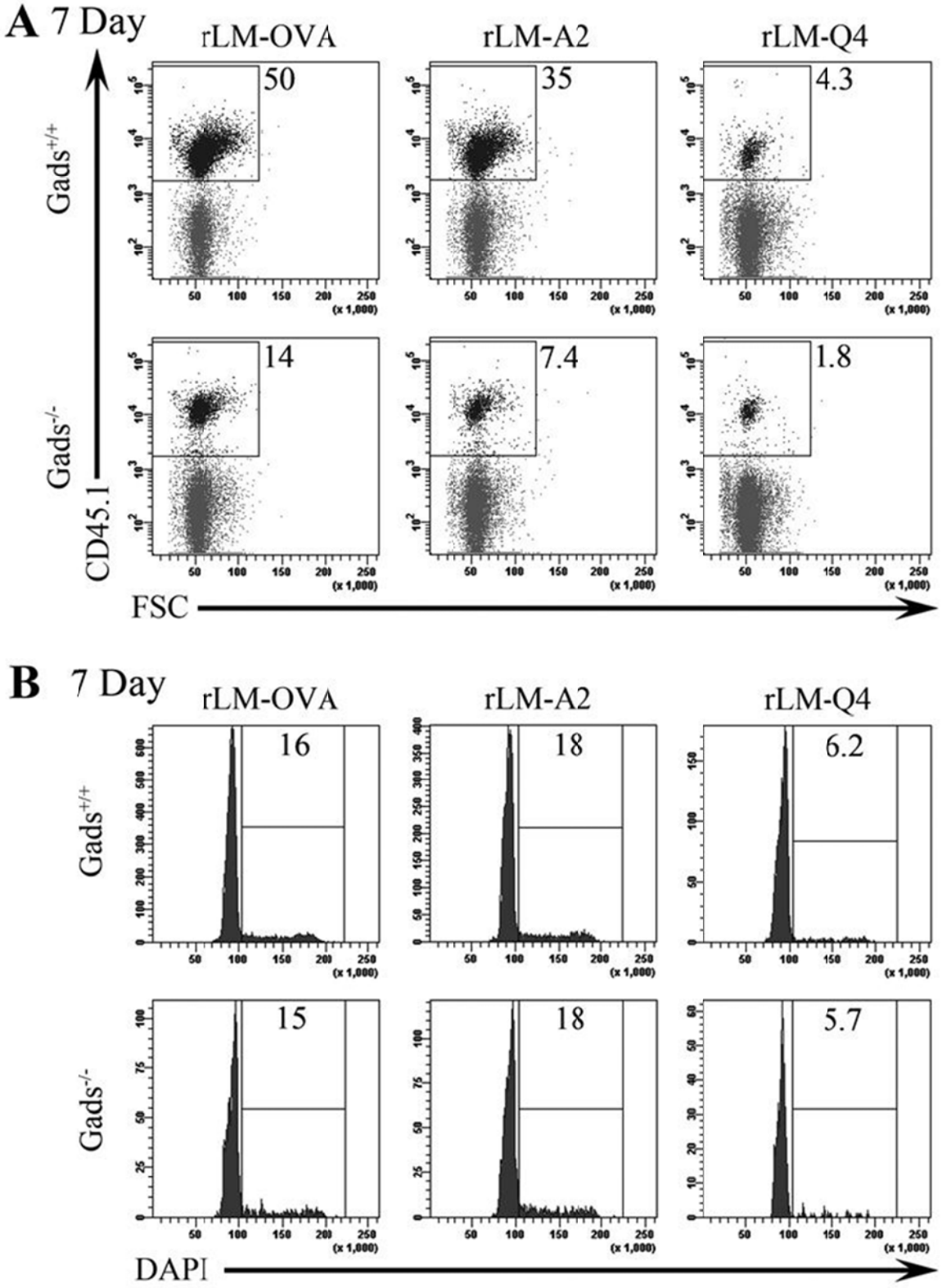
A 7 Day
rLM-OVA
rLM-A2
rLM-Q4
50
35
4.3
14
7.4
1.8
Gads+/+
Gads-/-
CD45.1
FSC
B 7 Day
rLM-OVA
rLM-A2
rLM-Q4
16
18
6.2
15
18
5.7
Gads+/+
Gads-/-
DAPI

Fig. 3-5. Gads regulates the expression of CD69 and CD25 on $CD8^+$ T cells *in vivo*. $CD8^+$ T cells from $CD45.1^+$ $Gads^{-/-}$ OT-I mice, $CD45.1^+CD45.2^+$ $Gads^{+/+}$ OT-I mice, or both were adoptively transferred into $CD45.2^+$ wild-type mice. Mice were injected i.v. with SIINFEKL (*A*) or rLM-OVA (*B* and *C*). *A* and *B*) Splenocytes were analyzed 24 hours post-stimulation. *C*) Cells were analyzed five days post-infection. *Dot plots* are representative data showing the percentages of donor-derived $CD8^+$ T cells that were $CD69^+$, $CD25^+$, or $CD69^+CD25^+$. *Bar graphs* – Shown are the means ± SD of the percentages of donor-derived $CD8^+$ T cells from *A* and *B* expressing CD69 and CD25. $^*p < 0.05$, $^{**}p < 0.01$, when comparing stimulated $Gads^{+/+}$ and $Gads^{-/-}$ cells, n = 5 from two independent experiments.

Figure 3-5

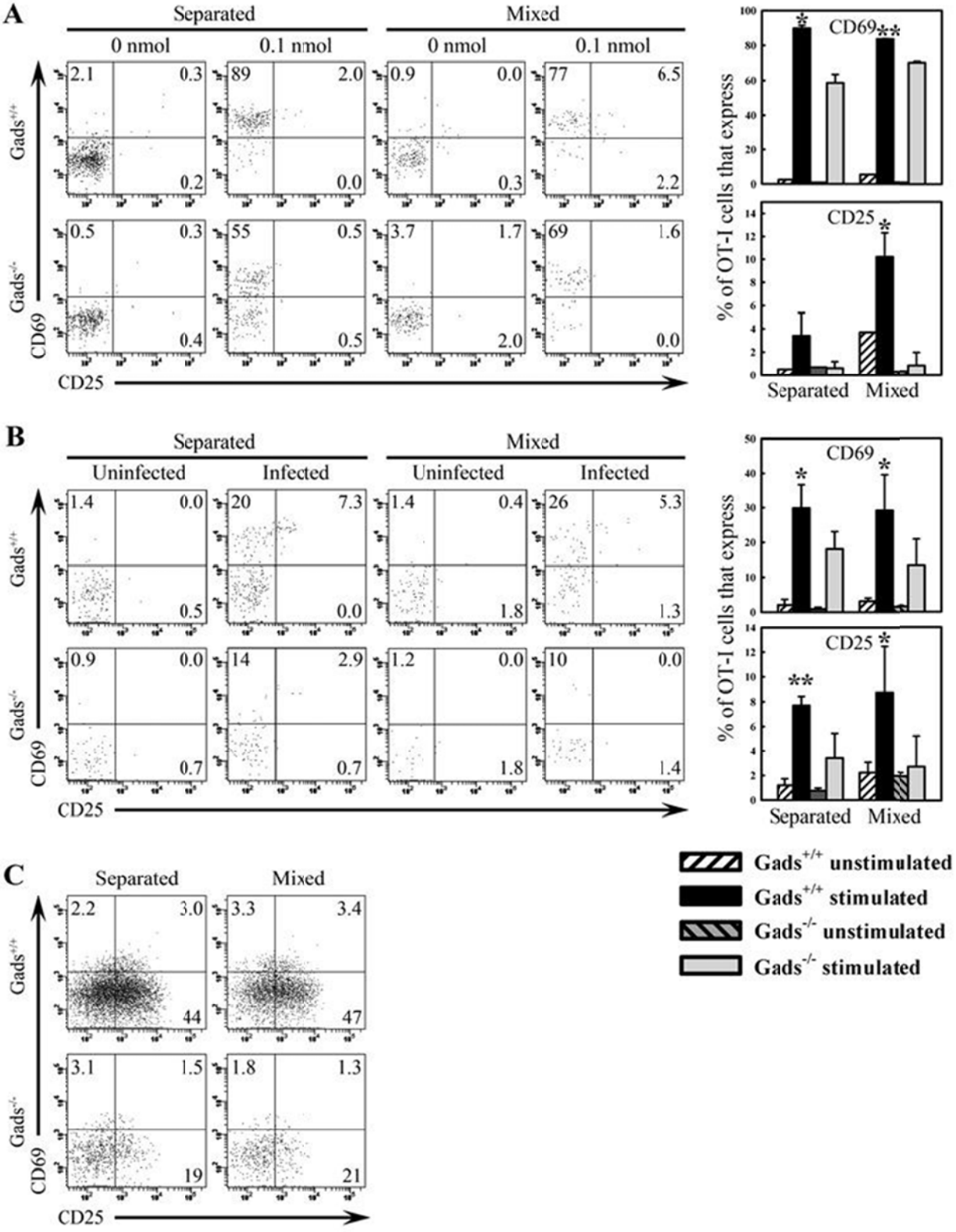
A
Separated
Mixed
0 nmol
0.1 nmol
0 nmol
0.1 nmol
Gads+/+
Gads-/-
CD69
CD25
2.1
0.3
0.2
89
2.0
0.0
0.9
0.0
0.3
77
6.5
2.2
0.5
0.3
0.4
55
0.5
0.5
3.7
1.7
2.0
69
1.6
0.0
CD69
CD25
% of OT-I cells that express
Separated
Mixed
B
Separated
Mixed
Uninfected
Infected
Uninfected
Infected
1.4
0.0
0.5
20
7.3
0.0
1.4
0.4
1.8
26
5.3
1.3
0.9
0.0
0.7
14
2.9
0.7
1.2
0.0
1.8
10
0.0
1.4
C
Separated
Mixed
2.2
3.0
44
3.3
3.4
47
3.1
1.5
19
1.8
1.3
21
Gads+/+ unstimulated
Gads+/+ stimulated
Gads-/- unstimulated
Gads-/- stimulated

compared with Gads$^{+/+}$ OVA-specific CD8^{+} T cells. These data indicate that Gads is required for CD69 and CD25 expression *in vivo*. It was consistent with our results *in vitro* that Gads regulates the expression of CD69 and CD25 on CD8^{+} T cells at early time points after stimulation with SIINFEKL (Fig. 2-8). Gads$^{-/-}$ CD8^{+} T cells have a defect in turning on the expression of early activation markers as early as Gads$^{+/+}$ CD8^{+} T cells but without Gads, the antigen-specific CD8^{+} T cells have a normal start in expanding their population *in vivo* following infection. This suggests that there are different pathways to control the expression of activation markers and to regulate the initiation of accumulation of CD8^{+} T cells upon infection.

Gads is not required for the secretion of IFN-γ after infection

Gads regulates sustained expansion and the expression of activation markers. How is the function of Gads$^{-/-}$ CD8^{+} T cells upon infection? To address this question, we investigated the ability of Gads$^{-/-}$ CD8^{+} T cells to produce IFN-γ after infection. We re-stimulated the splenocytes harvested from infected mice with SIINFEKL and examined IFN-γ expression. As controls, the endogenous CD8^{+} T did not produce IFN-γ under the stimulation of SIINFEKL (data not shown). In addition, the OVA-specific CD8^{+} T cells, that were derived from donor OT-I mice did not produce IFN-γ either, if the re-stimulation with SIINFEKL *in vitro* was not provided (Fig. 3-6). Those data in control groups indicated that the detected IFN-γ production was OVA-specific. Like Gads$^{+/+}$ cells, Gads$^{-/-}$ CD8^{+} T cells recovered from mice at indicated days post-infection were able to produce IFN-γ. Despite impaired expansion and expression of activation markers, Gads$^{-/-}$ CD8^{+} T cells are capable of secreting IFN-γ upon infection (Fig. 3-6). Interestingly, a higher percentage of OVA-specific CD8^{+} T cells could produce IFN-γ in Gads$^{-/-}$ CD8^{+} T cells, as compared with Gads$^{+/+}$ CD8^{+} T cells at 5 days p.i. with rLM-OVA. Gads$^{-/-}$ CD8^{+} T cells actually

Fig. 3-6. Gads is not required for IFN-γ production. Mice were adoptively transferred with naïve $CD8^+$ T cells from $Gads^{+/+}$ OT-I mice or $Gads^{-/-}$ OT-I mice. Five, seven, and ten days postinfection, splenocytes were stimulated *in vitro* with SIINFEKL (open histogram) or vehicle (shaded histogram). Shown are the representative data indicating the percentages of donor-derived $CD8^+$ T cells that expressed IFN-γ after re-stimulation.

Figure 3-6

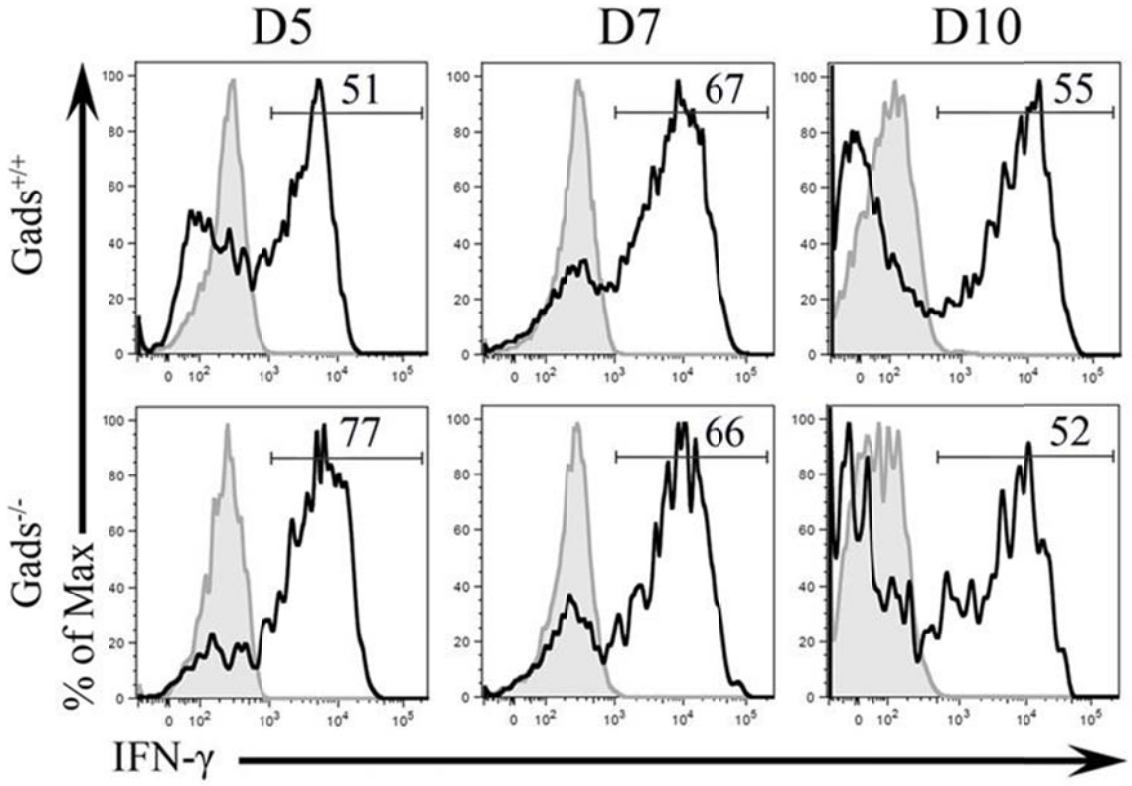

have the ability to secrete more IFN-γ than Gads$^{+/+}$ CD8^{+} T cells at 5 days but not 7 days p.i. (Fig. 3-6). This suggested in the early time points p.i., Gads$^{-/-}$ CD8^{+} T cells exert the effector function better than Gads$^{+/+}$ CD8^{+} T cells.

Gads is not required for the differentiation of naïve CD8^{+} T cells into memory cells, but is required for an optimal recall response

To determine whether Gads was required for the differentiation of naïve CD8^{+} T cells into memory cells, naïve CD8^{+} T cells from Gads$^{+/+}$ OT-I and Gads$^{-/-}$ OT-I mice were adoptively transferred into separate congenic hosts or mixed and injected into the same host. Mice were infected with rLM-OVA and the percentage of CD8^{+} T cells in the blood derived from donor mice was tracked over time (Fig. 3-7 A). As shown in the previous experiment (Fig. 3-1), Gads was necessary for optimal expansion of the CD8^{+} T cell population. However, both Gads$^{+/+}$ and Gads$^{-/-}$ cells persisted sixty days after infection, indicating that Gads$^{-/-}$ cells could differentiate into memory cells. When Gads$^{+/+}$ and Gads$^{-/-}$ cells were injected into separate mice, the percentages of CD8^{+} T cells derived from the donor mice were identical after three weeks. When in direct competition, the percentages of donor-derived CD8^{+} T cells that were Gads$^{+/+}$ cells were 2.4 ± 0.46-fold greater than the percentages of donor-derived CD8^{+} T cells that were Gads$^{-/-}$ cells. Because Gads$^{-/-}$ cells were readily detectable 60 days post-infection, we concluded that Gads$^{-/-}$ cells could differentiate into memory cells.

As an additional indicator of whether Gads is required for memory T cell development, we analyzed CD127 and KLRG1 expression, markers that can identify the short-lived effector cells (KLRG1^{+}CD127^{-}) and memory precursor effector cells (CD127^{+}KLRG1^{-}) (239, 253-256). There were no statistically significant differences in the percentages of Gads$^{+/+}$ and Gads$^{-/-}$ CD8^{+} T cells that were SLECs and MPECs (Fig. 3-7 B). However, more Gads$^{-/-}$ cells were

Fig. 3-7. Gads is not required for the memory T cell development. Mice were injected with naïve $CD8^+$ T cells from $Gads^{+/+}$ OT-I mice, $Gads^{-/-}$ OT-I mice, or both and infected with rLM-OVA, as described in Fig. 3-1. *A*) The percentages of $CD8^+$ T cells in the blood of recipient mice that were derived from each donor are shown (mean ± SD) *Upper panel* – recipient mice were injected with either $Gads^{+/+}$ or $Gads^{-/-}$ cells. *Lower panel* – recipient mice were injected with a mixture of $Gads^{+/+}$ and $Gads^{-/-}$ cells. *B*) On day 7 post-infection, donor-derived $CD8^+$ T cells in the spleen were analyzed for KLRG1 and CD127 expression. $^{*}p < 0.05$, $^{**}p < 0.01$, n > 7, from three independent experiments.

Figure 3-7

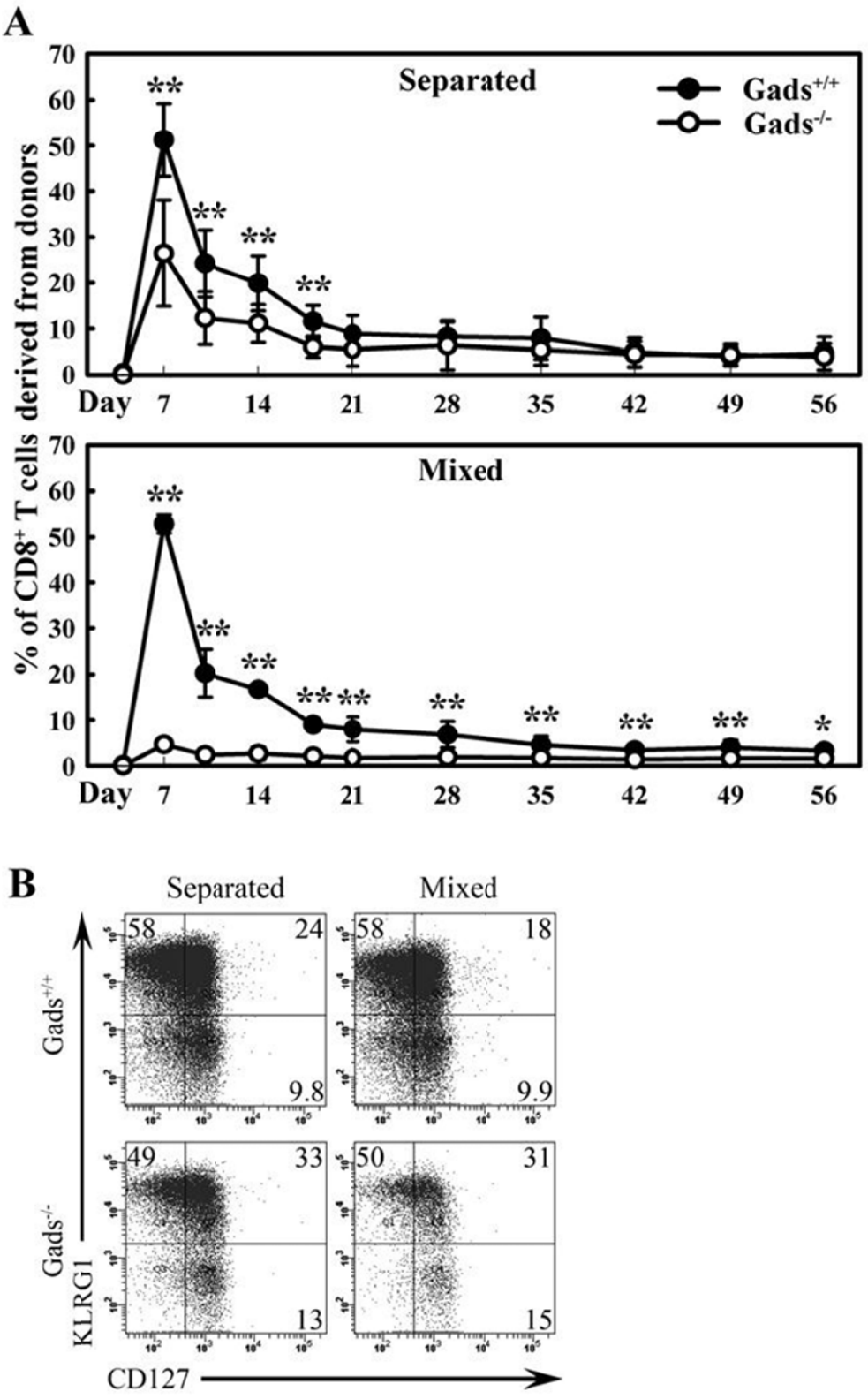
A
Separated
Gads+/+
Gads-/-
% of CD8+ T cells derived from donors
Day 7 14 21 28 35 42 49 56
Mixed
B
Separated
Mixed
Gads+/+
Gads-/-
KLRG1
CD127
58
24
9.8
58
18
9.9
49
33
13
50
31
15

$CD127^{+}KLRG1^{+}$ than $Gads^{+/+}$ cells. These data are consistent with a model in which Gads is not required for the differentiation of naïve $CD8^{+}$ T cells into memory T cells.

We next tested whether $Gads^{-/-}$ memory $CD8^{+}$ T cells could expand in number in response to re-infection with rLM-OVA. More $Gads^{-/-}$ cells were found four days post-challenge than pre-challenge, indicating that $Gads^{-/-}$ cells had differentiated into memory cells and could proliferate in response to challenge (Fig. 3-8). However, $Gads^{-/-}$ cells did not expand in number as robustly as $Gads^{+/+}$ cells, suggesting that, like in the primary immune response, Gads is required for optimal expansion of $CD8^{+}$ T cells in a secondary immune response. Also, as with the primary immune response, the defect with $Gads^{-/-}$ cells was more apparent when $Gads^{+/+}$ and $Gads^{-/-}$ cells were in direct competition.

Fig. 3-8. Gads is required for the expansion phase of the secondary immune response. Mice were injected with naïve $CD8^+$ T cells from $Gads^{+/+}$ OT-I mice, $Gads^{-/-}$ OT-I mice, or both and infected with rLM-OVA, as described in Fig. 4-1. Sixty days post-infection, mice were challenged with rLM-OVA. *A*) *Dot plots* – Shown are representative data indicating the percentage of $CD8^+$ T cells in the blood and spleen before and after challenge. *B*) *Bar graphs* - Shown are the means ± SD of the percentages of $CD8^+$ T cells derived from $Gads^{+/+}$ (black bars) and $Gads^{-/-}$ (grey bars) donors. $^{*}p < 0.05$, $^{**}p < 0.01$, n > 7, from three independent experiments.

Figure 3-8

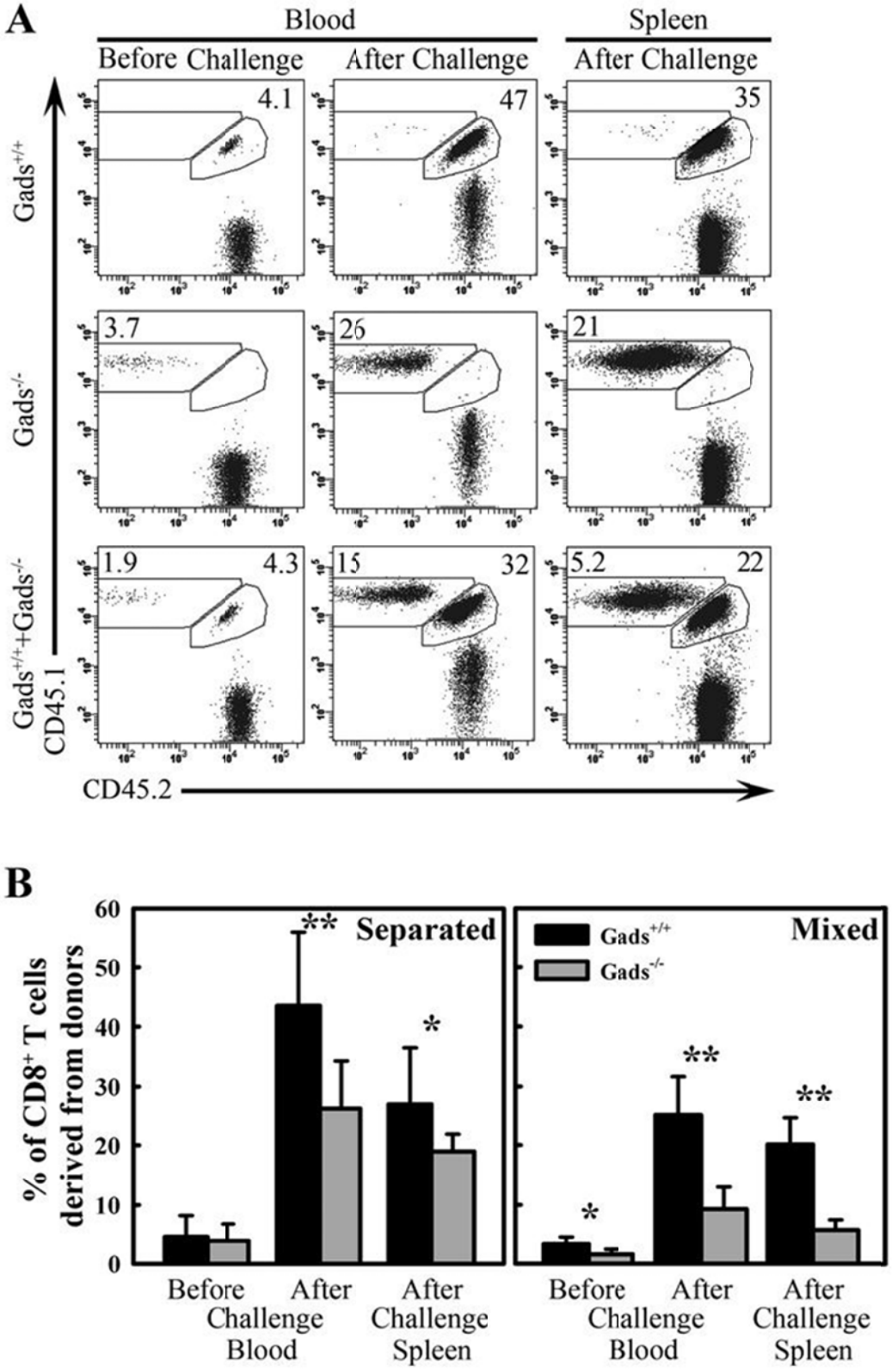
A
Blood
Spleen
Before Challenge
After Challenge
After Challenge
4.1
47
35
3.7
26
21
1.9
4.3
15
32
5.2
22
Gads+/+
Gads-/-
Gads+/++Gads-/-
CD45.1
CD45.2
B
% of CD8+ T cells derived from donors
Separated
Mixed
Gads+/+
Gads-/-
Before Challenge Blood
After Challenge Blood
After Challenge Spleen
Before Challenge Blood
After Challenge Blood
After Challenge Spleen

Discussion

We used the rLM-OVA infection model to demonstrate how Gads regulates the $CD8^+$ T cell-mediated immune response against a live pathogen. In contrast to peptide-induced proliferation, there was no apparent defect in $Gads^{-/-}$ cells during the initial stages of $CD8^+$ T cell expansion following infection (Fig. 3-1). This discrepancy between peptide-induced proliferation and infection-induced proliferation is consistent with cells stimulated with APLs. As described in Chapter III, $CD8^+$ T cells stimulated with APLs *in vitro* have reduced proliferation and expression of activation markers. However, $CD8^+$ T cells responding to rLM-APLs proliferated at a similar rate as cells responding to rLM-OVA, during the first few days post-infection (219).

Our data showed that at 5 days p.i. with rLM-OVA, the percentage of $Gads^{-/-}$ $CD8^+$ T cells that were derived from donors were identical to that of $Gads^{+/+}$ $CD8^+$ T cells. In contrast, at 5 days p.i. with rLM-A2, and rLM-Q4, which are weaker stimuli than rLM-OVA, there were significantly lower percentages of $CD8^+$ T cells derived from $Gads^{-/-}$ donors than $Gads^{+/+}$ donors. Why did Gads have different effects on the expansion of antigen-specific $CD8^+$ T cell population upon infection with different rLM strains? We demonstrated that Gads is required for optimization, but not onset, of the expansion of antigen-specific $CD8^+$ T cell population (Fig. 3-1). By analyzing $CD8^+$ T cell expansion at multiple time points following infection with different rLM-APL strains, Zehn *et. al.* (219) revealed that the weaker the ligand, the earlier the antigen-specific $CD8^+$ T cells reached their peak level of expansion and began to contract. Upon infection with rLM-OVA, the expansion of $CD8^+$ T cell population peaked at 7 days p.i. (Fig. 3-1); while the peak of expansion of $CD8^+$ T cell population upon infection with rLM-A2 or rLM-Q4 was expected to be prior to 7 days p.i. Gads regulates the accumulation of antigen-specific $CD8^+$ T cells upon infection with rLM-A2 or rLM-Q4 at 5 days p.i., as the time point was around the time of expansion peak. However, at 7 days p.i. with rLM-OVA, rLM-A2, or rLM-Q4, there were much lower percentages of $Gads^{-/-}$ $CD8^+$ T cells derived from donors, as compared with

Gads$^{+/+}$ cells (Fig. 3-3). In order to get the more direct and convincing conclusion, detailed kinetics studies with rLM-A2 or rLM-Q4 need to be performed.

Why could Gads$^{-/-}$ CD8^{+} T cells in spleen secrete more IFN-γ than Gads$^{+/+}$ CD8^{+} T cells at 5 days p.i. but similar percentages of OVA-specific CD8^{+} T cells derived from Gads$^{-/-}$ and Gads$^{+/+}$ mice could secrete IFN-γ at 7 and 10 days p.i.? It was consistent with the data showing percentages of OVA-specific CD8^{+} T cells which were SLECs (KLRG1^{+}CD127^{-}), which is related to the effector function (238, 239, 254, 257). There was higher percentage of Gads$^{-/-}$ OVA-specific CD8^{+} T cells which were SLECs at 5 days p.i. than Gads$^{+/+}$ cells. However, at 7 and 10 days p.i., the percentages of OVA-specific CD8^{+} T cells that were SLECs were similar between Gads$^{-/-}$ cells and Gads$^{+/+}$ cells. The difference in SLECs population between Gads$^{-/-}$ and Gads$^{+/+}$ cells at 5 days p.i. might be caused by the same reason by which Gads is not required for the accumulation of OVA-specific CD8^{+} T cells at 4 and 5 days p.i.. This possibility will be discussed in Chapter VI.

Despite normal expansion of the CD8^{+} T cells within the first few days of infection, Gads$^{-/-}$ cells could not sustain the accumulation of CD8^{+} T cell population necessary for an optimal peak response. One possible explanation is that, after 5 days p.i., Gads$^{-/-}$ CD8^{+} T cells have a defect in proliferation. For example, Gads$^{-/-}$ CD8^{+} T cells slow or stop their proliferation though they have a normal start. Another possibility is that Gads$^{-/-}$ CD8^{+} T cells fail to survive as well as Gads$^{+/+}$ CD8^{+} T cells. The analysis of cell cycle progression (Fig. 3-4) supported a model in which Gads promotes the CD8^{+} T cell survival after the initiation stage of the expansion phase upon infection. When we compared the percentages of OVA-specific CD8^{+} T cells that were in S, G2, M phases of the cell cycle, there were no differences between Gads$^{-/-}$ CD8^{+} T cells and Gads$^{+/+}$ CD8^{+} T cells at the peak of the expansion (Fig. 3-4) or 5 days p.i., when the expansion were still the same between Gads$^{-/-}$ CD8^{+} T cells and Gads$^{+/+}$ CD8^{+} T cells (data not shown). The infection with rLM-Q4 induced the lower percentages of antigen-specific CD8^{+} T cells were

in S, G2, or M phase of the cell cycle at 7 days p.i., as compared with infection with rLM-OVA or rLM-A2. The difference might be caused by the following reason. Seven days p.i. is the time around the peak response for infection with rLM-OVA and rLM-A2, in which the OVA peptide or A2 peptide, which has been presented by rLM, are relatively stronger stimuli for OVA-specifc $CD8^+$ T cells. For infection with rLM-Q4, which is the weakest stimuli among the three strains of rLM, 7 days p.i. falls within the contraction phase of the immune response so that the proliferation of antigen-specific $CD8^+$ T cells may have already slowed down in this case, as compared with the proliferation at peak expansion. However, it will be more convincing to look at the cell death of the OVA-specific $CD8^+$ T cells upon infection directly.

Why could not $Gads^{-/-}$ $CD8^+$ cells sustain the expansion of the population? This phenomenon may be related to the reduced level of CD25 expression observed in $Gads^{-/-}$ cells (Fig. 3-3). The function of IL-2 and CD25 in $CD8^+$ T cells is controversial. In the context of infection with LM, IL-2 is required for sustained expansion of antigen-specific T cells (258). This is consistent with an *in vitro* role for IL-2 in driving sustained proliferation of $CD8^+$ T cells after the removal of antigen (234), but in contrast to studies using LCMV infection, where IL-2 did not contribute to the expansion phase of the primary immune response (259-262). These observations suggest that the reduced CD25 expression seen in $Gads^{-/-}$ cells may result in reduced responsiveness to IL-2 and a lower peak of the expansion phase.

Consistent with a role for CD25 in $Gads^{-/-}$ cells, when $CD8^+$ T cells were stimulated with low doses of IL-2, more cells express CD127 than when cells were stimulated with high concentrations of IL-2 (261). In our studies, more $Gads^{-/-}$ cells than $Gads^{+/+}$ cells expressed CD127 after rLM-OVA infection (Fig. 3-5 B). CD127 is a marker typically associated with memory precursors (253, 263). Among CD127-expressing $Gads^{-/-}$ cells, many also expressed KLRG1, a marker typically associated with short-lived effector cells (239, 254, 255). The

function of these $CD127^{+}KLRG1^{+}$ cells is unknown, but these cells may represent a transition point in the differentiation between effector and central memory cells (264).

The increased percentage of $Gads^{-/-}$ $CD8^{+}$ T cells expressing CD127 seen at the peak of the primary immune response suggested that Gads may not be required for the differentiation of naïve $CD8^{+}$ T cells into memory T cells. Indeed, when $Gads^{+/+}$ and $Gads^{-/-}$ cells were injected into separate hosts, the percentage of $CD8^{+}$ T cells that derived from donor in the blood was identical during the memory phase of the immune response, even though the peak response was lower with $Gads^{-/-}$ cells (Fig. 3-5). This is in contrast to data from experiments using APL-expressing rLM, where the number of memory cells produced was proportional to the peak primary response (219). The increase in CD127 expression and persistence of memory T cells seen with $Gads^{-/-}$ cells was similar to that reported for mice expressing tyrosine phosphorylation mutants of SLP-76 (257), supporting the biochemical model of TCR signaling in which Gads is upstream of SLP-76 phosphorylation.

While $Gads^{-/-}$ $CD8^{+}$ T cells could differentiate into memory cells, they could only produce normal numbers of memory cells when injected into mice where the number of competing OVA-specific $CD8^{+}$ T cells was quite small. When $Gads^{+/+}$ and $Gads^{-/-}$ cells were in direct competition with each other, the expansion of $Gads^{-/-}$ cells and the number of $Gads^{-/-}$ memory cells produced was more dramatically impaired than when $Gads^{+/+}$ and $Gads^{-/-}$ cells were injected into separate mice. These data suggest that multiple factors influence the expansion of antigen-specific T cells and the number of memory cells that differentiated from a T cell population. While strength of signaling intensity may be a component, another important factor is the nature of the other T cell populations in the mouse responding to the infection. If there are competing cells with higher affinity for the antigen or cells more capable of efficient signal transduction, then these competing populations are more likely to dominant the effector and memory T cell pools. The mechanisms by which some populations dominate the immune response are unclear, but

subdominant cells may cease proliferating and undergo apoptosis earlier in the immune response than dominant cells.

In conclusion, we demonstrate in the context of infection, the initial expansion of the antigen-specific $CD8^+$ T cell population is independent of Gads. However, Gads is necessary to sustain the expansion phase. The differentiation of naïve $CD8^+$ T cells into memory T cells is independent of Gads. In addition, Gads is required for the optimal expansion of $CD8^+$ T cell population in both primary and recall responses.

Chapter IV

Homotypic interactions can compensate for Gads deficiency in promoting cell cycle progression of $CD8^+$ T cells

Abstract

In this chapter, I have examined the effect of homotypic interactions among $CD8^+$ T cells on cell cycle progression. Analyses of cell cycle progression and the related cellular events were made between $Gads^{-/-}$ $CD8^+$ T cells and $Gads^{+/+}$ $CD8^+$ T cells when total splenocytes or purified $CD8^+$ T cells were stimulated. The defect of Gads deficiency in cell cycle progression of $CD8^+$ T cells when total splenocytes were stimulated could be overcome by stimulating the purified $CD8^+$ T cells. The homotypic interactions altered the TCR-mediated signals in a Gads-dependent manner. These observations suggested that the signals mediated by adhesion molecules on the surface of $Gads^{-/-}$ $CD8^+$ T cells are more activated than those of $Gads^{+/+}$ $CD8^+$ T cells. Expression of an important adhesion integrin, LFA-1, was higher in $Gads^{-/-}$ $CD8^+$ T cells than $Gads^{+/+}$ $CD8^+$ T cells. In addition, we found that more $Gads^{-/-}$ $CD8^+$ T cells were in the lung than $Gads^{+/+}$ cells. Furthermore, we demonstrated that the formation of more and bigger cell clusters observed in purified $Gads^{-/-}$ $CD8^+$ T cells, as compared with that in $Gads^{+/+}$ $CD8^+$ T cells was mediated by LFA-1. However, the cell cycle progression of $CD8^+$ T cells, which were stimulated in the context of total splenocytes but not purified $CD8^+$ T cells, was mediated by LFA-1. Furthermore, Gads regulates the conjugation between $CD8^+$ T cells and EL-4 cells. We conclude that the activation of adhesion molecules on the surface of $CD8^+$ T cells regulates the interactions involving $CD8^+$ T cells. The homotypic interactions among $CD8^+$ T cells can compensate for Gads deficiency in cell clustering and cell cycle progression.

Introduction

In vitro culture of lymphocytes has been performed extensively and widely to mimic the *in vivo* situation in biomedical studies. When splenocytes from OT-I mice are stimulated with SIINFEKL *in vitro*, the $CD8^+$ T cells need to interact with APCs which have MHC class I on their surface. The cell-cell interactions promote TCR-mediated signaling and also the cellular events triggered by TCR ligation. The adhesion molecules mediate cell-cell interactions to ensure the TCR-MHC binding can occur. Furthermore, the adhesion molecules, such as LFA-1 and intercellular adhesion molecule 1 (ICAM-1), could deliver signals that promote the activation and proliferation as well as influence the differentiation of T cells (265-270). When T cells interact with APCs, the stable regions of contact between the cells are called immunological synapses (IS); adhesion molecules in the peripheral supermolecular activation cluster (pSMAC) stabilize the IS (271, 272).

Cell adhesion molecules (CAMs) are proteins located on the cell surface that regulate the binding with other cells or with the extracellular matrix (ECM) in the process called cell adhesion. There are four protein families in CAMs: immunoglobulin superfamily (IgSF), integrins, cadherins, and selectins (273). Integrins are a large family of proteins that function as adhesion molecules as well as signaling molecules. They are transmembrane heterodimers, consisting of one α-subunit and one β-subunit. There are 18 α-subunits and 8 β-subunits that have been identified so far. The β2 class of integrins, which are selectively expressed on hematopoietic cells, mediates leukocyte-leukocyte and leukocyte-endothelial cell interactions (272, 274-276). This β2 integrin family has 4 αβ combinations. They share a common β2 chain (CD18) and associate with one of four α subunits: αLβ2 (CD11a), αMβ2 (CD11b), αXβ2 (CD11c), and αDβ2 (CD11d). Among them, αLβ2 integrin, also known as lymphocyte function-associated antigen-1 (LFA-1), is primarily expressed on T cells. The αL chain is also called CD11a.

There are two major roles of LFA-1 in T cell activation. Firstly, in lymphocytes, activated LFA-1 regulates the formation of transient attachments to the vasculature and causes leukocytes to slow down the movement in circulation. Ultimately, activated LFA-1 leads to the firm adhesion and transmigration of leukocytes into the lymphoid tissues, such as lymph nodes and spleens, or injury sites. Secondly, when T cells interact with ICAM-expressing and Ag-bearing APCs to form an IS, the pSMAC is mainly composed of LFA-1 and its ligand ICAM-1 (277). The strength of this contact reduces the amount of antigen required for T cell activation as Wang *et. al.* (278) revealed that LFA-1 decreases the strength of TCR signal for T cell activation *in vivo* as well as *in vitro*.

The activity of LFA-1 is controlled by signaling through other membrane receptors. The intracellular signaling, which converts LFA-1 from an inactive to an active conformation, is called "inside-out" signaling (279). The signaling pathways of LFA-1 activation have been studied using three different modes of stimulation: 1) Chemokine signaling through activation of G protein-coupled receptors (GPCRs); 2) TCR ligation and 3) Selectin binding to the ligands P-selectin glycoprotein ligand 1 (PSGL1), CD44 and E-selectin ligand 1 (ESL1) on neutrophils (280). We investigate the role of LFA-1 in $CD8^+$ T cell activity in this chapter, so let's look at the TCR-mediated LFA-1 activation. TCR ligation activates LFA-1 by increasing the binding affinity of LFA-1 to its ligand ICAM-1(279, 281). The TCR proximal signaling is important for LFA-1 activation. We would like to investigate how the TCR signaling regulates LFA-1 activation. The modulating role of some key proteins of TCR proximal signaling in LFA-1 activation has been revealed: Baker *et. al.* (282) reported that SLP-76 is a key component of transmitting TCR signaling to LFA-1 signaling such as in SLP-76 deficient T cells, LFA-1 failed to bind ICAM-1. In addition, upon TCR ligation, the SLP-76–ADAP complex is recruited to LFA-1-initiated microclusters (282). Finkelstein *et. al.* demonstrated that the Tec kinase ITK is required for TCR-mediated up-regulation of adhesion via the LFA-1 (283). However, little is known about the

role of Gads is in transmitting TCR proximal signaling to LFA-1 signaling. That is what we are going to test in this chapter.

As a signaling receptor, activated LFA-1 transduces the intracellular signal. This process is called “outside-in” signaling (279, 284). The “outside-in” signaling can lead to adhesion strengthening and the final stage of LFA-1 activation. The LFA-1-mediated signaling can modulate T cell activation (265, 267, 285), proliferation (266), survival (286) and differentiation (267). Baker *et. al.* (282) reported that SLP-76 relocalizes to LFA-1-initiated signaling complexes and mediates “outside-in” signaling of LFA-1. Although SLP-76 and Gads constitutively interact with each other (2, 6, 17, 29-31), there is no report on the role of Gads in LFA-1-mediated signaling. In order to investigate the role of Gads in LFA-1-mediated signaling, one of the objectives of this chapter is to identify whether and how LFA-1 mediated signaling is involved in the regulation of Gads in $CD8^+$ T cell activation.

As cell-cell contact is critical in T cell activation, we initiated our studies on the effect of homotypic interactions among $CD8^+$ T cells on TCR-mediated cellular events such as cell cycle progression. It is of note that $CD8^+$ T cells express both LFA-1 and its ligand ICAM-1, which regulate cell-cell contact, so that the role of LFA-1 in homotypic interactions as well as interactions between $CD8^+$ T cells and other cells are also included in this chapter.

Materials and Methods

Mice

C57BL/6 Gads$^{-/-}$ mice and Gads$^{-/-}$ OT-I mice were described previously (17, 99). All mice were housed under specific pathogen-free conditions and all experiments were performed in compliance with the University of Kansas Medical Center Institutional Animal Care and Use Committee (IACUC). Mice were used between the ages of six and eight weeks for the experiments.

Antibodies

Anti-CD8α-Alexa Fluor 647, anti-CD44-Horizon V450, anti-CD11c-PE-Cy7, anti-CD11a-PE, anti-TCRVα2-FITC, anti-TCRVβ5-PE, and purified anti-CD11a were purchased from BD Biosciences (San Jose, CA), eBioscience (San Diego, CA) or Biolegend (San Diego, CA).

Cell labeling, and flow cytometry

Single cell suspensions of splenocytes and lymphocytes were collected by gently disrupting the tissue using a wire mesh and a syringe plunger. Blood samples were withdrawn in the presence of heparin and the red blood cells were lysed using ACK lysis buffer. Lungs were isolated and then homogenized. Cells were filtered through a 100 μm nylon mesh. Surface labeling of cells was performed as described previously (99). Briefly, single cell suspensions were prepared and labeled in staining buffer (PBS containing 2% FetalClone I bovine serum

product (HyClone Laboratories, Inc., Logan, UT)) before fixing with 1% paraformaldehyde in PBS overnight or at least one hour at room temperature.

For DAPI labeling, cells were harvested after stimulation, labeled with anti-CD8, and fixed in 1% paraformaldehyde. Then, cells were washed twice with staining buffer, incubated with 1ml of 1 μg/mL DAPI (Invitrogen, Carlsbad, CA) in 0.3% Tween-20 in staining buffer for 30 min at room temperature and analyzed immediately by flow cytometry.

For pyronin Y (PY) staining, cells were pelleted after DAPI staining and 850 μL of the supernatant were aspirated. Twenty μl of 25μg/mL PY (Polyscience, Inc., Warrington, PA) in staining buffer containing 0.3% Tween-20 were added into each tube. Cells were incubated for 10 min at room temperature and analyzed by flow cytometry.

Samples were analyzed using a BD LSRII (BD Biosciences, San Jose, CA). Data were analyzed using BD FACSDiva (BD Biosciences) and FlowJo (Tree Star, Inc., Ashland, OR).

Cell clustering assay

Splenocytes were isolated from Gads+/+ OT-I or Gads-/- OT-I mice and CD8+ T cells were isolated by positive selection using anti-mouse CD8α Magnetic Particles-DM (BD Biosciences Pharmingen). Total splenocytes or purified CD8+ T cells were stimulated with 1 μg/mL plate-bound anti-CD3 and 0.25 μg/mL plate-bound anti-CD28 or 1 μM SIINFEKL (ProImmune Limited, Oxford, UK) in the absence or presence of anti-LFA-1 or anti-CD48 at 1 μg/mL, respectively. At indicated time points, pictures of cell morphology were taken using a Nikon Ti inverted microscope (Nikon Instruments Inc., Melville, NY) or scanned by Celigo cytometer (Cyntellect Inc., San Diego, CA).

Cell conjugation assay

Splenocytes were isolated from Gads$^{+/+}$ OT-I or Gads$^{-/-}$ OT-I mice and CD8^{+} T cells were isolated by using anti-mouse CD8α Magnetic Particles-DM (BD Biosciences Pharmingen) and positive selection. EL-4 cells were loaded with CFSE as described previously (17). Briefly, the cell concentration was adjusted to 2 x 10^7 cells/ml, and an equal volume of 10 μM CFSE (Invitrogen, Carlsbad, CA) was added. Cells were incubated for 10 min at 37°C and the reaction was quenched with cell culture media. Then CFSE-labeled EL-4 cells were pulsed with SIINFEKL at different concentrations for 60 min. Then, cells were washed to remove peptide and the EL-4 cells were incubated with purified CD8^{+} T cells for indicated time. After gentle vortexing (1 sec per sample), the cell conjugates were fixed with 1% paraformaldehyde in PBS for 30 min and then stained for anti-CD8 before fixing again. Those CD8 cells, that are interacting with EL-4 cells would appear large and CFSE^{+} by flow cytometry. Samples were analyzed using a BD LSRII (BD Biosciences, San Jose, CA). Data were analyzed using BD FACSDiva (BD Biosciences).

Immunoblot assay

Stimulation of total splenocytes for longer time than 1 hour: Splenocytes from Gads$^{+/+}$ OT-I or Gads$^{-/-}$ OT-I mice were isolated and stimulated with 1 nM SIINFEKL. At various time points, CD8^{+} T cells were isolated using anti-mouse CD8α Magnetic Particles-DM (BD Biosciences Pharmingen) and positive selection.

Stimulation of purified CD8^{+} T cells for shorter time within 1 hour: CD8^{+} T cells were purified by positive selection with anti-mouse CD8α Magnetic Particles. After resting in serum free media for 30 min, the cells were incubated biotinylated anti-CD3 and biotinylated anti-CD28 in

50 μL RPMI 1640 media for 30min at 4°C and then cross-linked by adding 50 μL pre-warmed avidin in RPMI 1640 at 37°C 25ug/mL for indicated time. The final concentrations of biotinylated anti-CD3, biotinylated anti-CD28, and avidin were 10, 10, and 25 μg/mL respectively. Twenty-five μL of 5X lysis buffer was added to quench the stimulation.

Lysates were prepared, separated by SDS-PAGE, and transferred to PVDF membrane. Membranes were probed with anti-c-myc (Cat. No. 9402), anti-PKCθ (Cat. No. 2059), anti-phopspho-PKCθ (Cat. No. 9377), anti-phospho-AKT (Cat. No. 4060), anti-phospho-ERK (Cat. No. 9101), and anti-β-actin (Antibodies are all from Cell Signaling Technology, Inc., Danvers, MA).

Statistics

All data are presented as mean ± SD and were analyzed using two-tailed Student's t tests.

Results

Homotypic interactions among $CD8^+$ T cells rescue the defect of $Gads^{-/-}$ $CD8^+$ T cells in TCR-mediated cell cycle progression

Firstly, we compared the role of Gads in TCR-mediated cell cycle progression in different stimulation contexts: total splenocytes or purified $CD8^+$ T cells. My previous results in Chapter III showed that Gads is required in cell cycle progression of $CD8^+$ T cells. The cell cycle analysis revealed that there was delayed cell cycle entry of $Gads^{-/-}$ $CD8^+$ T cells, compared with $Gads^{+/+}$ $CD8^+$ T cells, when total splenocytes were stimulated with SIINFEKL (Fig. 4-1 A). However, when purified $CD8^+$ T cells were stimulated with 1 nM SIINFEKL, which was the same concentration to stimulate the splenocytes, there were similar percentages of $CD8^+$ T cells that were in S, G2, or M phase of cell cycle between $Gads^{-/-}$ $CD8^+$ T cells and $Gads^{+/+}$ $CD8^+$ T cells (Fig. 4-1 B).

As PKCθ-mediated expression of c-myc is critical for T cell growth during G1 phase of cell cycle (287), we investigated the expression of c-myc and the activation of PKCθ of $Gads^{+/+}$ $CD8^+$ T cells and $Gads^{-/-}$ $CD8^+$ T cells upon TCR ligation in two different contexts: total splenocytes or purified $CD8^+$ T cells. We first looked at c-myc expression. Our results revealed that Gads regulates the kinetics of c-myc expression when splenocytes were stimulated. The expression of c-myc was turned on in $Gads^{+/+}$ $CD8^+$ T cells but not in $Gads^{-/-}$ $CD8^+$ T cells after 1 hour of stimulation. But 24 hours after stimulation, there were comparable levels of c-myc expression in $Gads^{+/+}$ cells and $Gads^{-/-}$ cells (Fig. 4-2 A). When purified $CD8^+$ T cells were stimulated, within the first 60 min, purified $Gads^{+/+}$ $CD8^+$ T cells had stronger expression of c-myc than $Gads^{-/-}$ $CD8^+$ T cells. This result was consistent with the results when splenocytes were stimulated. In contrast, 24 hours after TCR ligation, purified $CD8^+$ T cells from either $Gads^{+/+}$ or $Gads^{-/-}$ mouse had drastically elevated expression of c-myc, as compared with the

Fig. 4-1. Homotypic interactions among $CD8^+$ T cells overcome the defect of $Gads^{-/-}$ $CD8^+$ T cells in cell cycle progression. *A*) Splenocytes from $Gads^{+/+}$ OT-I and $Gads^{-/-}$ OT-I mice were cultured with 1μM SIINFEKL for 21h and were labeled with anti-CD8, DAPI and PY. Cells were analyzed by flow cytometry. Shown are the percentages of cells in the S, G2, or M phase of the cell cycle. *n* = 5 in five independent experiments. *B*) Purified $CD8^+$ T cells from $Gads^{+/+}$ OT-I mice or $Gads^{-/-}$ OT-I mice were stimulated with SIINFEKL at 1μM for 21h. At harvest, cells were labeled with DAPI. Shown are the percentages of cells in the S, G2, or M phase of the cell cycle. *n* = 2 in two independent experiments.

Figure 4-1

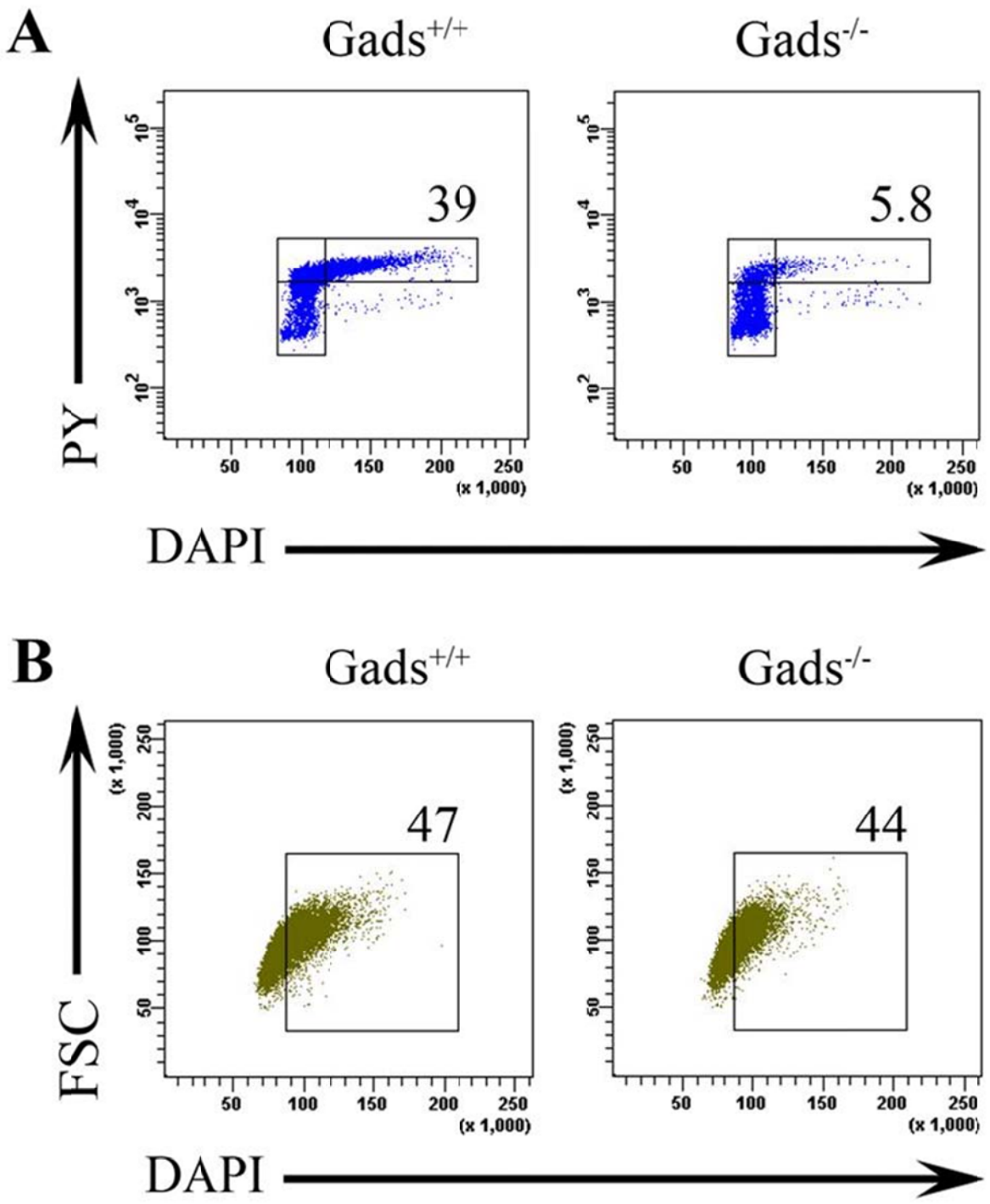

Fig. 4-2. Homotypic interactions among $CD8^+$ T cells alter TCR-mediated signals in both $Gads^{-/-}$ $CD8^+$ T cells and $Gads^{+/+}$ $CD8^+$ T cells. *A*) Splenocytes from $Gads^{+/+}$ OT-I and $Gads^{-/-}$ OT-I mice were stimulated with SIINFEKL for the indicated lengths of time. After stimulation, $CD8^+$ T cells were isolated, lysed, and analyzed for phospho-PKCθ, PKCθ, c-myc, and β-actin protein expression by immunoblot. *n* = 1. *B*) Splenocytes from $Gads^{+/+}$ OT-I and $Gads^{-/-}$ OT-I mice were harvested, $CD8^+$ T cells were isolated, and cells were stimulated with anti-CD3 and anti-CD28 for the indicated lengths of time. The cell lysates were analyzed for phospho-PKCθ, PKCθ, phospho-AKT, phospho-ERK, c-myc, and β-actin protein expression by immunoblot. *n* = 1.

Figure 4-2

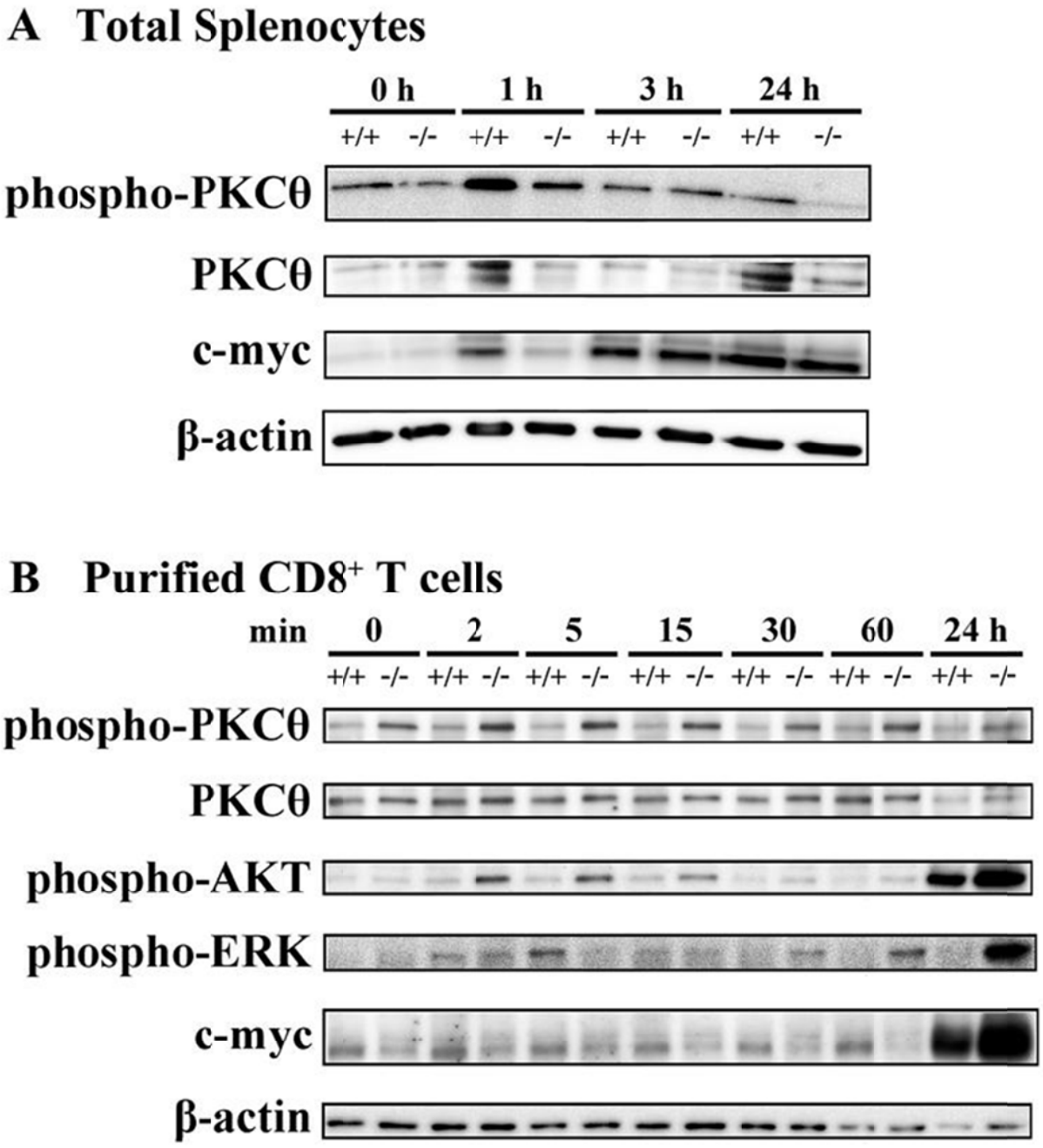
A Total Splenocytes
0 h
1 h
3 h
24 h
+/+ -/- +/+ -/- +/+ -/- +/+ -/-
phospho-PKCθ
PKCθ
c-myc
β-actin
B Purified CD8+ T cells
min
0
2
5
15
30
60
24 h
+/+ -/- +/+ -/- +/+ -/- +/+ -/- +/+ -/- +/+ -/- +/+ -/-
phospho-PKCθ
PKCθ
phospho-AKT
phospho-ERK
c-myc
β-actin

expression of c-myc within 1 hour of stimulation. In addition, purified Gads$^{-/-}$ CD8^{+} T cells had much stronger c-myc expression than Gads$^{+/+}$ CD8^{+} T cells at 24 hours (Fig. 4-2 B).

Then, we examined the expression and phosphorylation of PKCθ. When splenocytes were stimulated and analyzed for PKCθ in CD8^{+} T cells, the expression of PKCθ increased and peaked at 1 hour, went down to a level slightly above baseline within 3 hours and increased again at 24 hours in Gads$^{+/+}$ CD8^{+} T cells (Fig. 4-2 A). PKCθ expression of Gads$^{-/-}$ CD8^{+} T cells stayed almost the same as unstimulated cells, except a slight increase at 24 hours. When we looked at the phosphorylation level of PKCθ, there was increased phosphorylation of PKCθ in Gads$^{+/+}$ cells at 1 hour, compared with other time points tested. In Gads$^{-/-}$ CD8^{+} T cells, the phosphorylation of PKCθ increased slightly at 1 hour and decreased drastically at 24 hours after stimulation. At 1 and 24 hours, there was slightly reduced PKCθ phosphorylation in Gads$^{-/-}$ cells, as compared to Gads$^{+/+}$ cells. Except these two time points, phosphorylation of PKCθ was comparable between Gads$^{+/+}$ cells and Gads$^{-/-}$ cells. In striking contrast to the results when splenocytes were stimulated, PKCθ expression of purified CD8^{+} T cells remained constant for both Gads$^{+/+}$ CD8^{+} T cells and Gads$^{-/-}$ CD8^{+} T cells throughout the experiment. In addition, stronger phosphorylation of PKCθ was detected in Gads$^{-/-}$ CD8^{+} T cells at each time point tested (Fig. 4-2 B).

The Altman group and the Bault group reported that Phosphoinositide 3-kinase (PI3K) activities are required for the membrane recruitment and phosphorylation of PKCθ in T cells (288, 289). In addition, Gads and PI3K are linked by CD28 (131, 132, 135) or LIME (141). In order to investigate the effect of Gads on PI3K activity, we compared the phosphorylation of AKT, which is a substrate of PI3K, between Gads$^{-/-}$ CD8^{+} T cells and Gads$^{+/+}$ CD8^{+} T cells. The phosphorylation of AKT was slightly elevated in purified Gads$^{+/+}$ CD8^{+} cells at 2 min and the signal declined to baseline within 30 min. Starting 2 min after TCR ligation, Gads$^{-/-}$ CD8^{+} T cells had higher phosphorylation of AKT than Gads$^{+/+}$ CD8^{+} T cells. The phosphorylation of AKT

gradually decreased after 5min of TCR ligation in Gads$^{-/-}$ CD8^{+} T cells, but was still higher than in Gads$^{+/+}$ CD8^{+} T cells. The increased phosphorylation of AKT in Gads$^{-/-}$ cells than in Gads$^{+/+}$ cells was also observed at 24 hour after stimulation, when both Gads$^{+/+}$ and Gads$^{-/-}$ CD8^{+} T cells had elevated phosphorylation of AKT (Fig. 4-2 B).

Unpublished data from our lab demonstrated that Gads can regulate ERK phosphorylation in thymocytes. In addition, inhibition of ERK dramatically decreased c-myc expression level in a number of human cancer cell lines (290). So we tested the role of Gads in phosphorylation of ERK when purified CD8^{+} T cells were stimulated. Within the first hour after TCR ligation, Gads$^{-/-}$ cells and Gads$^{+/+}$ cells had similar intensity in the peak of ERK phosphorylation. However, purified CD8^{+} T cells from Gads$^{+/+}$ mice and Gads$^{-/-}$ cells showed different kinetics in ERK phosphorylation. In Gads$^{+/+}$ CD8^{+} T cells, the peak of ERK phosphorylation occurred at 5 min, but for Gads$^{-/-}$ CD8^{+} T cells, the peak appeared at 60 min. The results indicate that Gads$^{-/-}$ CD8^{+} T cells had a delayed phosphorylation of ERK, as compared with Gads$^{+/+}$ CD8^{+} T cells. In addition, there was drastically stronger phosphorylation of ERK in purified Gads$^{-/-}$ CD8^{+} cells 24 hours after stimulation, than in Gads$^{+/+}$ CD8^{+} T cells (Fig. 4-2 B).

These data indicated that the delayed cell cycle entry observed in Gads$^{-/-}$ CD8^{+} T cells, as compared with Gads$^{+/+}$ CD8^{+} T cells, upon TCR ligation observed in the context of total splenocytes could be rescued by stimulating purified CD8^{+} T cells. Changing the stimulation context from total splenocytes to purified CD8^{+} T cells also resulted in altered TCR-mediated signaling. Homotypic interactions among CD8^{+} T cells might account for these observations.

Gads negatively regulates the expression of LFA-1 protein on $CD8^+$ T cells.

In order to study the mechanisms by which homotypic interactions among $CD8^+$ T cells rescue the impaired cell cycle entry and TCR signaling in Gads deficiency, we first targeted one β2 integrin molecule, LFA-1, which largely expresses on T cells. LFA-1 is an important molecule in the integrin family to mediate cell adhesion. In order to function properly, LFA-1 needs to be expressed and activated on the surface of $CD8^+$ T cells. We examined the role of Gads in LFA-1 expression by flow cytometry. Higher percentages of $Gads^{-/-}$ $CD8^+$ T cells were LFA-1^{hi}, as compared with $Gads^{+/+}$ $CD8^+$ T cells. This finding was also observed in the naïve $CD8^+$ T cells ($CD44^{lo}CD8^+$) and memory $CD8^+$ T cells ($CD44^{hi}CD8^+$) (Fig. 4-3). Besides percentages, the mean fluorescence intensity (MFI) was also checked on these populations of $CD8^+$ T cells. $Gads^{-/-}$ $CD8^+$ T cells had higher MFI than $Gads^{+/+}$ $CD8^+$ T cells. This observation was also true for naïve $CD8^+$ T cells and memory $CD8^+$ T cells (Fig. 4-3).

Gads regulates the distribution of $CD8^+$ T cells in a tissue-dependent manner.

The ability of leukocytes to penetrate into tissues and to make contacts with other cells depends mainly on LFA-1 (272). As $Gads^{-/-}$ $CD8^+$ T cells had higher expression of LFA-1 protein than $Gads^{+/+}$ cells, $CD8^+$ T cells might have a different distribution pattern between $Gads^{+/+}$ and $Gads^{-/-}$ mice. The comparisons were made in lymphoid tissues such as lymph nodes and spleen and non-lymphoid tissues such as blood and lung. In lymph nodes (Fig. 4-4 A) and spleens (Fig. 4-4 B), there were lower percentages of lymphocytes expressing CD8 in $Gads^{-/-}$ OT-I mice than in $Gads^{+/+}$ OT-I mice. The frequency of $CD8^+$ T cells in blood was also lower in $Gads^{-/-}$ OT-I mice than in $Gads^{+/+}$ OT-I mice (Fig. 4-4 C). In contrast, higher percentages of lymphocytes were $CD8^+$ T cells in the lungs of $Gads^{-/-}$ mice, as compared with $Gads^{+/+}$ mice (Fig. 4-4 D). In all the tissue tested, there were lower percentages of $Gads^{-/-}$ $CD8^+$ T cells that express the OT-I TCR,

Fig. 4-3. Gads$^{-/-}$ CD8^{+} T cells have higher expression of LFA-1 than Gads$^{+/+}$ CD8^{+} T cells. Splenocytes from Gads$^{+/+}$ OT-I and Gads$^{-/-}$ OT-I mice were stained with anti-CD8, anti-CD44 and anti-CD11a. Inside the histogram – Shown are the percentages of CD8^{+} T cells that were CD11a^{hi}. Above the histogram – Shown are the mean fluorescence intensity (MFI) of LFA-1 on total CD8^{+} T cells, naïve CD8^{+} T cells, and memory CD8^{+} T cells). Representative of 2 mice in two independent experiments.

Figure 4-3

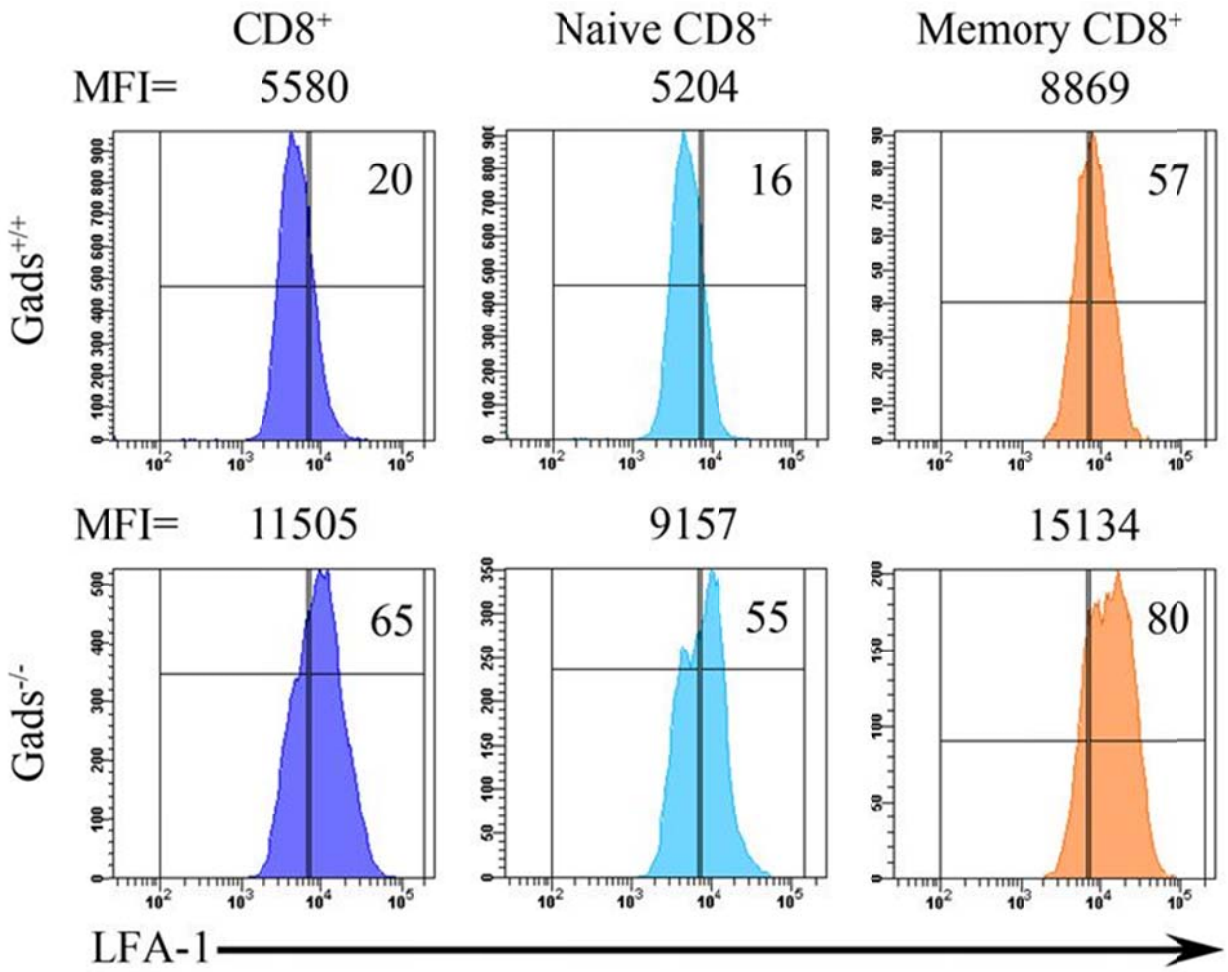
CD8+
Naive CD8+
Memory CD8+
MFI=
5580
5204
8869
20
16
57
Gads+/+
MFI=
11505
9157
15134
65
55
80
Gads-/-
LFA-1

Fig. 4-4. A comparison of the distribution of $CD8^+$ T cells in lymphoid tissues and lungs in $Gads^{-/-}$ OT-I mice and in $Gads^{+/+}$ OT-I mice. Lymphocytes were harvested from the axillary and inguinal lymph nodes (*A*), spleens (*B*), blood (*C*), and lung (*D*) from $Gads^{+/+}$ OT-I or $Gads^{-/-}$ OT-I mice. Shown are the representative data indicating the percentages of lymphocytes that were $CD8^+$. *E*) Bar graph summarizes data from multiple experiments. $^{*}p < 0.05$, $^{**}p < 0.01$, n ≥ 4 from at least two independent experiments.

Figure 4-4

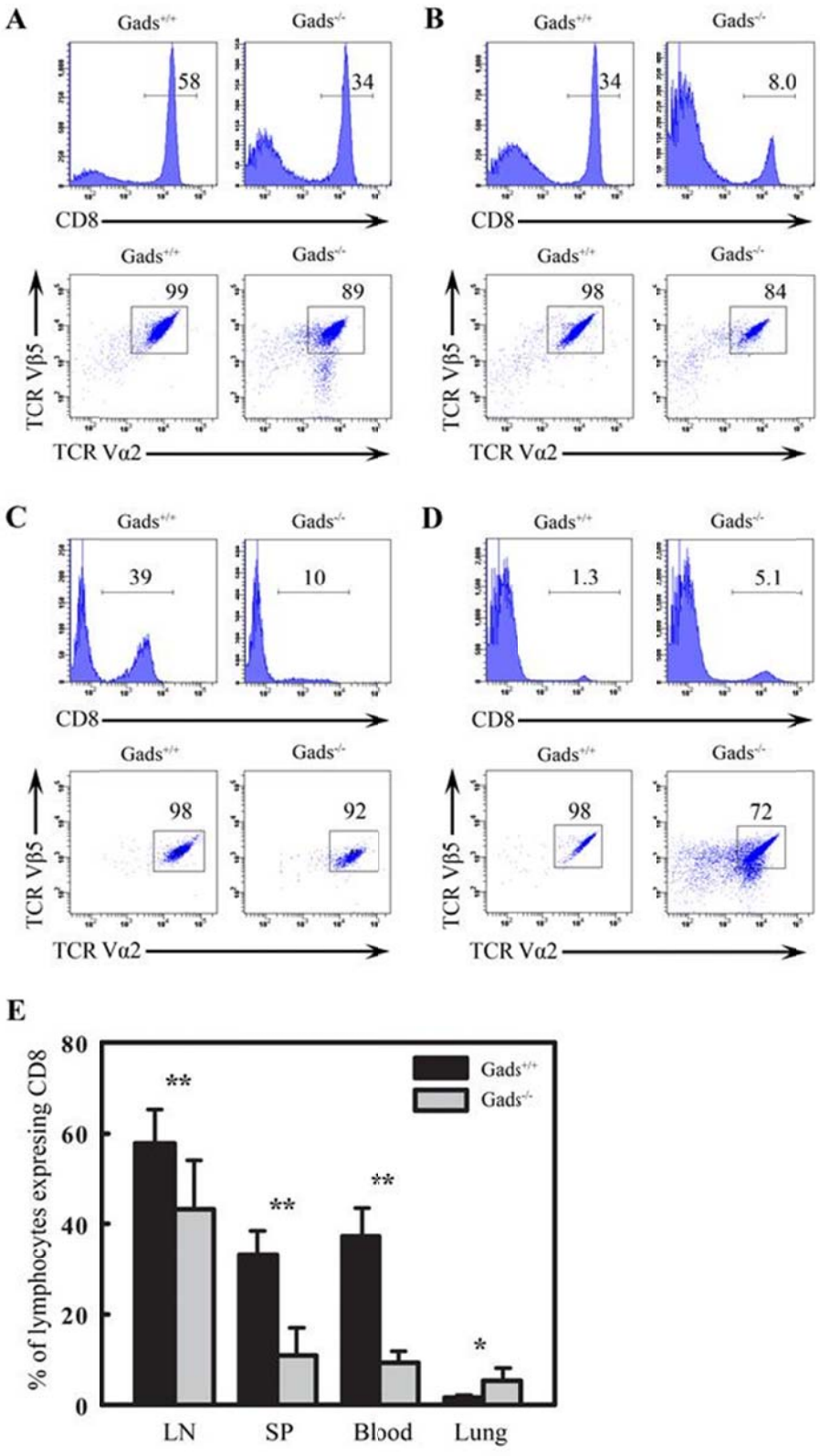
A
Gads+/+
Gads-/-
58
34
CD8
99
89
TCR Vβ5
TCR Vα2
B
34
8.0
98
84
C
39
10
98
92
D
1.3
5.1
98
72
E
% of lymphocytes expresing CD8
80
60
40
20
0
**
**
**
*
LN
SP
Blood
Lung

than Gads$^{+/+}$ CD8^{+} T cells, especially the expression of TCR Vα2 was turned down in some Gads$^{-/-}$ CD8^{+} T cells. The phenomenon might be caused by allelic exclusion of TCR α-chain (291, 292). Results from multiple experiments revealed that significantly lower percentages of lymphocytes, splenocytes, and blood leukocytes, that express CD8^{+} T cell are in Gads$^{-/-}$ mice than in Gads$^{+/+}$ mice (Fig. 4-4 E). In contrast, the lung from Gads$^{-/-}$ mice has significantly higher percentage of lymphocytes expressing CD8^{+} T cells, as compared with Gads$^{+/+}$ mice. These data suggested that Gads negatively regulates the penetration of CD8^{+} T cells into lung.

Increased quantity and size of cell clusters in purified Gads$^{-/-}$ CD8^{+} T cells than Gads$^{+/+}$ CD8^{+} T cells were mediated by LFA-1.

In order to examine whether the homotypic interactions among CD8^{+} T cells are mediated by LFA-1, an *in vitro* culture assay was performed to analyze the formation of cell clusters in the absence and presence of a neutralizing antibody, soluble anti-LFA-1 (Fig. 4-5 A and C) or soluble anti-CD48 (Fig. 4-5 C).

Total splenocytes (Column 1 and 3) formed small clusters when stimulated with SIINFEKL, but not when stimulated with anti-CD3 and anti-CD28 at 21 hours. In addition, more cell clusters in wells containing Gads$^{+/+}$ total splenocytes were observed than Gads$^{-/-}$ cells. Anti-LFA-1 seemed to have little effect on clustering of total splenocytes.

In contrast to total splenocytes, purified CD8^{+} T cells (Column 2 and 4) showed significant amount of cell clustering regardless of stimuli. The cell clusters even could be observed in unstimulated purified CD8^{+} T cells. Gads$^{-/-}$ CD8^{+} T cells consistently formed more and bigger clusters than Gads$^{+/+}$ CD8^{+} T cells, under all three experimental conditions: unstimulated, stimulated with anti-CD3+anti-CD28, or stimulated with SIINFEKL. Interestingly, cells stimulated

Fig. 4-5. More cell clusters are present in purified $CD8^+$ T cells from $Gads^{-/-}$ OT-I mice than from $Gads^{+/+}$ OT-I mice in an LFA-1 dependent manner. Splenocytes were harvested from $Gads^{+/+}$ OT-I or $Gads^{-/-}$ OT-I mice and red blood cells were lysed. *A*) Total splenocytes (column 1 and 3) and purified $CD8^+$ T cells (column 2 and 4) were stimulated with plate-bound anti-CD3 and anti-CD28 (row 3-4), SIINFEKL (row 5-6) or left unstimulated (row 1-2). 0.2 X 10^6 cells were cultured in each well of 96-w plate in the absence (column 1-2) or presence (column 3-4) of soluble anti-LFA-1. $Gads^{+/+}$ cells are shown in the row 1, 3, and 5, while $Gads^{-/-}$ cells are shown in the row 2, 4, and 6. Twenty-one hours after cultured *in vitro*, the cells were observed under microscope and pictures were taken to display the cell clustering. Magnification: 100 X. *n* = 2 from two independent experiments. *B*) FACS-purified naïve $CD8^+$ T cells ($CD44^{lo}CD8^+$) from $Gads^{+/+}$ OT-I mice or $Gads^{-/-}$ OT-I mice were stimulated with SIINFEKL at 1μM for 21h (1 X 10^6 per well in 24-w plate). Shown are the pictures of the cell clustering from duplicate samples. Samples 1 and 2 were the representatives to show the cell clusters from $Gads^{+/+}$ naïve $CD8^+$ T cells. Samples 3 and 4 were from $Gads^{-/-}$ naïve $CD8^+$ T cells. Sample 3 was focused on the center area of the huge bulk of cell clusters and sample 4 showed the edge of the huge bulk of cell clusters. Magnification: 200 X. *n* = 1. *A*) Total splenocytes (column 1, 3 and 5) and purified $CD8^+$ T cells (column 2, 4 and 6) were stimulated with plate-bound anti-CD3 and anti-CD28 (row 3-4), SIINFEKL (row 5-6) or left unstimulated (row 1-2). 0.2 X 10^6 cells were cultured in each well of 96-w plate in the absence (column 1-2) or presence of soluble anti-LFA-1 (column 3-4) or soluble anti-CD48 (column 5-6). $Gads^{+/+}$ cells are shown in the row 1, 3, and 5, while $Gads^{-/-}$ cells are shown in the row 2, 4, and 6. Twenty-one hours after cultured *in vitro*, the plate was scanned by Celigo. *n* = 1.

Figure 4-5

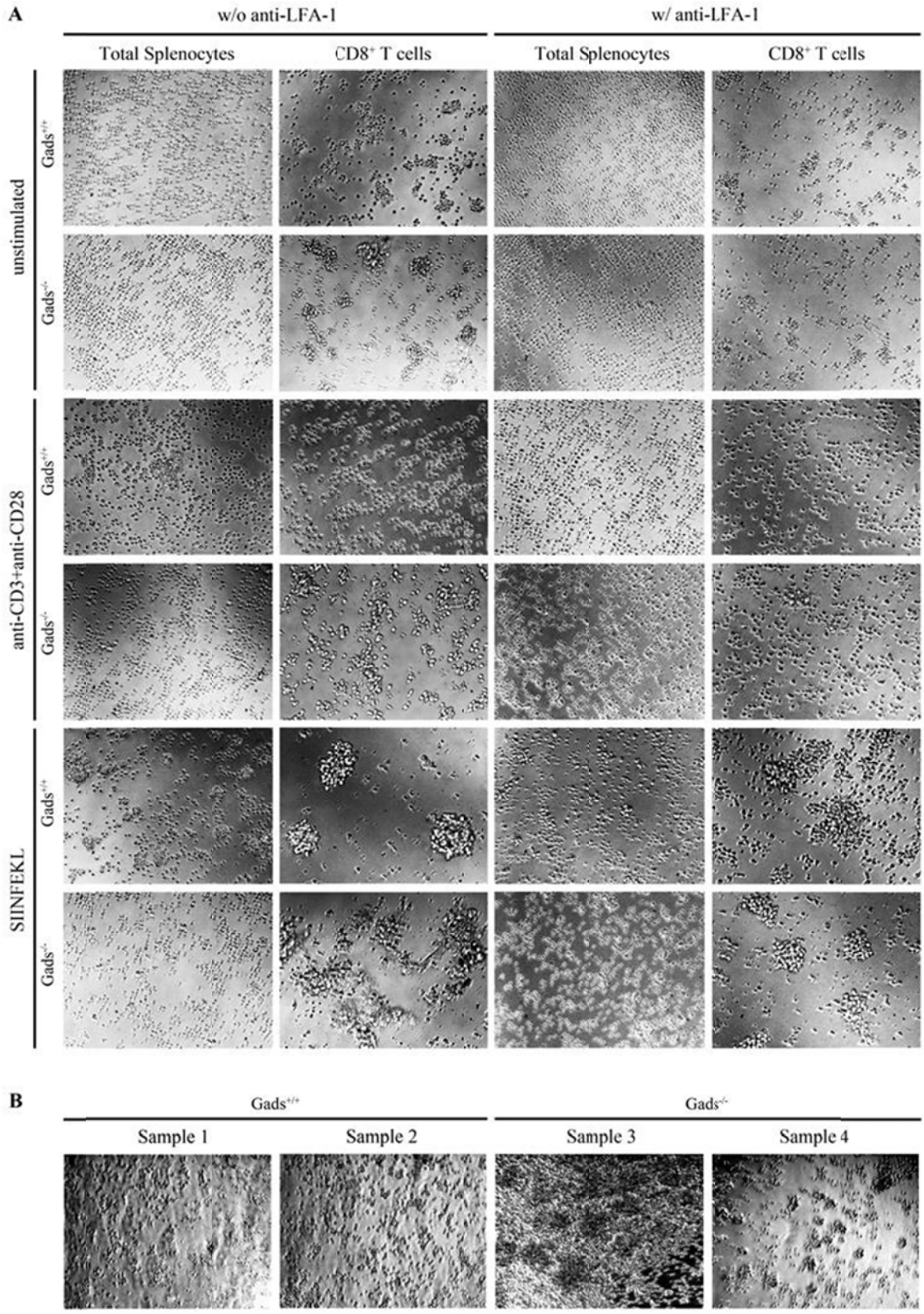
A
w/o anti-LFA-1
w/ anti-LFA-1
Total Splenocytes
CD8+ T cells
Total Splenocytes
CD8+ T cells
unstimulated
anti-CD3+anti-CD28
SIINFEKL
Gads+/+
Gads-/-
B
Gads+/+
Gads-/-
Sample 1
Sample 2
Sample 3
Sample 4

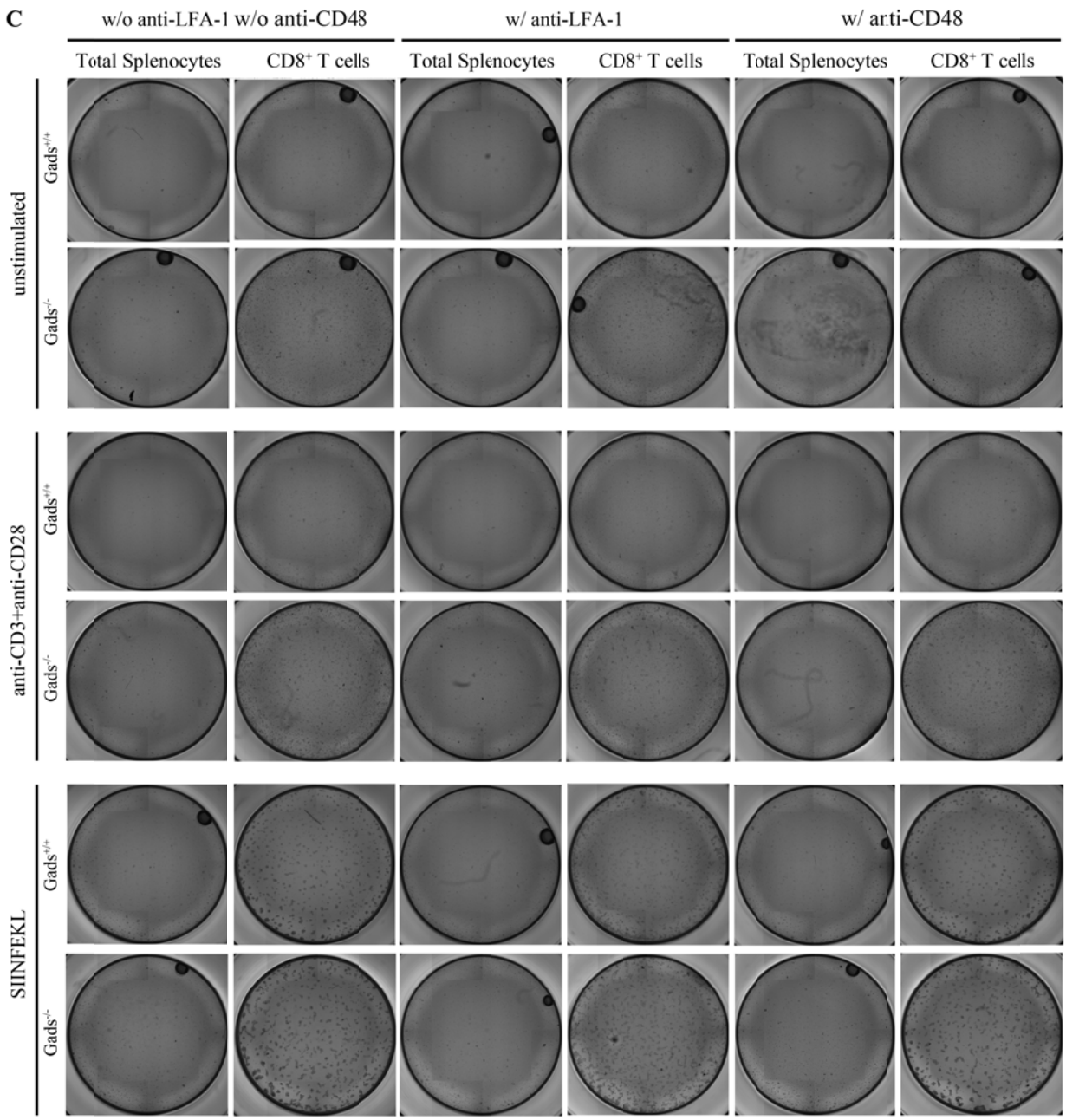
C
w/o anti-LFA-1 w/o anti-CD48
w/ anti-LFA-1
w/ anti-CD48
Total Splenocytes
CD8+ T cells
Total Splenocytes
CD8+ T cells
Total Splenocytes
CD8+ T cells
unstimulated
anti-CD3+anti-CD28
SIINFEKL
Gads+/+
Gads-/-

with SIINFEKL formed bigger clusters than those stimulated by anti-CD3 and anti-CD28. This observation is probably caused by the nature of the stimuli as plate bound anti-CD3 and anti-CD28 cross-linked cells in a relatively immobilized manner while the peptide SIINFEKL allowed more $CD8^+$ T cells to aggregate freely. The addition of anti-LFA-1 into the cell culture media significantly decreased the size and numbers of cell clusters seen with purified $Gads^{-/-}$ $CD8^+$ T cells. The effect of anti-LFA-1 on formation of cell clusters was also obvious in purified $Gads^{+/+}$ $CD8^+$ T cells, but not as dramatic as in $Gads^{-/-}$ $CD8^+$ T cells. The differences in the formation of cell clusters between $Gads^{-/-}$ $CD8^+$ T cells and $Gads^{+/+}$ $CD8^+$ T cells was reduced by anti-LFA-1 treatment. As a result, when anti-LFA-1 was present, the cell cluster pattern in the two groups looked similar under same culture condition (Fig. 4-5 A and C Column 4). The role of anti-CD48 in the formation of cell cluster was not obvious (Fig. 4-5 C).

We compared the cell clustering formed by purified total $CD8^+$ T cells (Fig. 4-5 A Column 2, Row 5 and 6) and purified naïve $CD8^+$ T cells (Fig. 4-5 B) after stimulation with SIINFEKL for 21 hours. $Gads^{+/+}$ naïve $CD8^+$ T cells formed fewer and smaller cell clusters than $Gads^{+/+}$ total $CD8^+$ T cells. In contrast, $Gads^{-/-}$ naïve $CD8^+$ T cells formed much bigger cell clusters than $Gads^{-/-}$ total $CD8^+$ T cells. When we compared the cell clusters formed from $Gads^{-/-}$ naïve $CD8^+$ T cells and $Gads^{+/+}$ naïve $CD8^+$ T cells, drastically bigger cell cluster were observed in $Gads^{-/-}$ cells than in $Gads^{+/+}$ cells.

Collectively, these data indicated that purified $CD8^+$ T cells form more and bigger cell clusters upon TCR ligation than total splenocytes. In addition, as compared with purified $Gads^{+/+}$ $CD8^+$ T cells, $Gads^{-/-}$ $CD8^+$ T cells have higher level of cell clustering, which is mediated by LFA-1. Furthermore, purified naïve $CD8^+$ T cells and purified total $CD8^+$ T cells behave differently in cell clustering. The level of cell clustering is: $Gads^{-/-}$ naïve $CD8^+$ T cells > $Gads^{-/-}$ total $CD8^+$ T cells > $Gads^{+/+}$ total $CD8^+$ T cells > $Gads^{+/+}$ naïve $CD8^+$ T cells.

Homotypic interactions partially rescued the defect of cell cycle entry in Gads$^{-/-}$ CD8^{+} T cells in a LFA-1-independent manner.

Previous data showed that Gads$^{-/-}$ CD8^{+} T cells have delayed antigen-induced cell cycle entry, when compared with Gads$^{+/+}$ CD8^{+} T cells (Fig. 2-6). Here, in total splenocytes (Column 1), the defect in cell cycle entry was observed not only in Gads$^{-/-}$ CD8^{+} T cells stimulated with SIINFEKL (Row 5 and 6), but also in Gads$^{-/-}$ CD8^{+} T cells stimulated with anti-CD3 and anti-CD28 (Row 3 and 4); upon TCR ligation, there were lower percentages of Gads$^{-/-}$ CD8^{+} T cells in G1 phase of cell cycle, as compared with Gads$^{+/+}$ CD8^{+} T cells. Overall, cells stimulated with SIINFEKL had better cell cycle progression than those stimulated with anti-CD3 and anti-CD28. After the stimulation with SIINFEKL, lower percentages of Gads$^{-/-}$ CD8^{+} T cells exited from G0 phase of the cell cycle, as compared with Gads$^{+/+}$ CD8^{+} T cells (Fig. 4-6). The purified CD8^{+} T cells (Column 2) underwent a faster cell cycle progression than total splenocytes, even though they were cultured with the same stimuli. This applied to both Gads$^{+/+}$ and Gads$^{-/-}$ cells. The defect of cell cycle entry was largely rescued by culturing purified CD8^{+} T cells instead of splenocytes under the stimulations of either anti-CD3 and anti-CD28 or SIINFEKL. Although the purified CD8^{+} T cells stimulated with SIINFEKL had lower percentage of cells in G1 phase of cell cycle in Gads$^{-/-}$ CD8^{+} T cells, as compared with Gads$^{+/+}$ CD8^{+} T cells, the percentages of CD8^{+} T cells in S, G2, and M phase of cell cycle were similar between Gads$^{+/+}$ and Gads$^{-/-}$ cells (Fig. 4-6). This suggests that homotypic interactions among CD8^{+} T cells overcome the need for Gads in promoting cell cycle entry.

LFA-1 can regulate T cell activation (265, 267, 285) and proliferation (266). In order to investigate the effect of LFA-1 on cell cycle entry of CD8^{+} T cells, soluble anti-LFA-1 was added to the cell culture media to block the interaction between LFA-1 and its ligand (Column 3 and 4). When total splenocytes were stimulated with either stimuli, anti-LFA-1 inhibited the cell cycle entry in both Gads$^{+/+}$ cells and Gads$^{-/-}$ cells. However, for purified CD8^{+} T cells stimulated with

Fig. 4-6. Gads promotes cell cycle progression of $CD8^+$ T cells when stimulating total splenocytes but does not when stimulating the purified $CD8^+$ T cells. Splenocytes were harvested from $Gads^{+/+}$ OT-I or $Gads^{-/-}$ OT-I mice and red blood cells were lysed. Total splenocytes (column 1 and 3) and purified $CD8^+$ T cells (column 2 and 4) were stimulated with plate-bound anti-CD3 and anti-CD28 (row 3-4), SIINFEKL (row 5-6) or left unstimulated as control (row 1-2). Cells were cultured in the absence (column 1-2) or presence (column 3-4) of soluble anti-LFA-1. $Gads^{+/+}$ cells are shown in the row 1, 3, and 5, while $Gads^{-/-}$ cells are shown in the row 2, 4, and 6. Twenty-one hours after cultured *in vitro*, the cells were harvested, labeled with anti-CD8, DAPI and PY. Shown are the percentages of cells, which were gated on $CD8^+$ population, in the G1 phase (top left gates) as well as in the S, G2, or M phase (top right gates) of the cell cycle. n = 1.

Figure 4-6

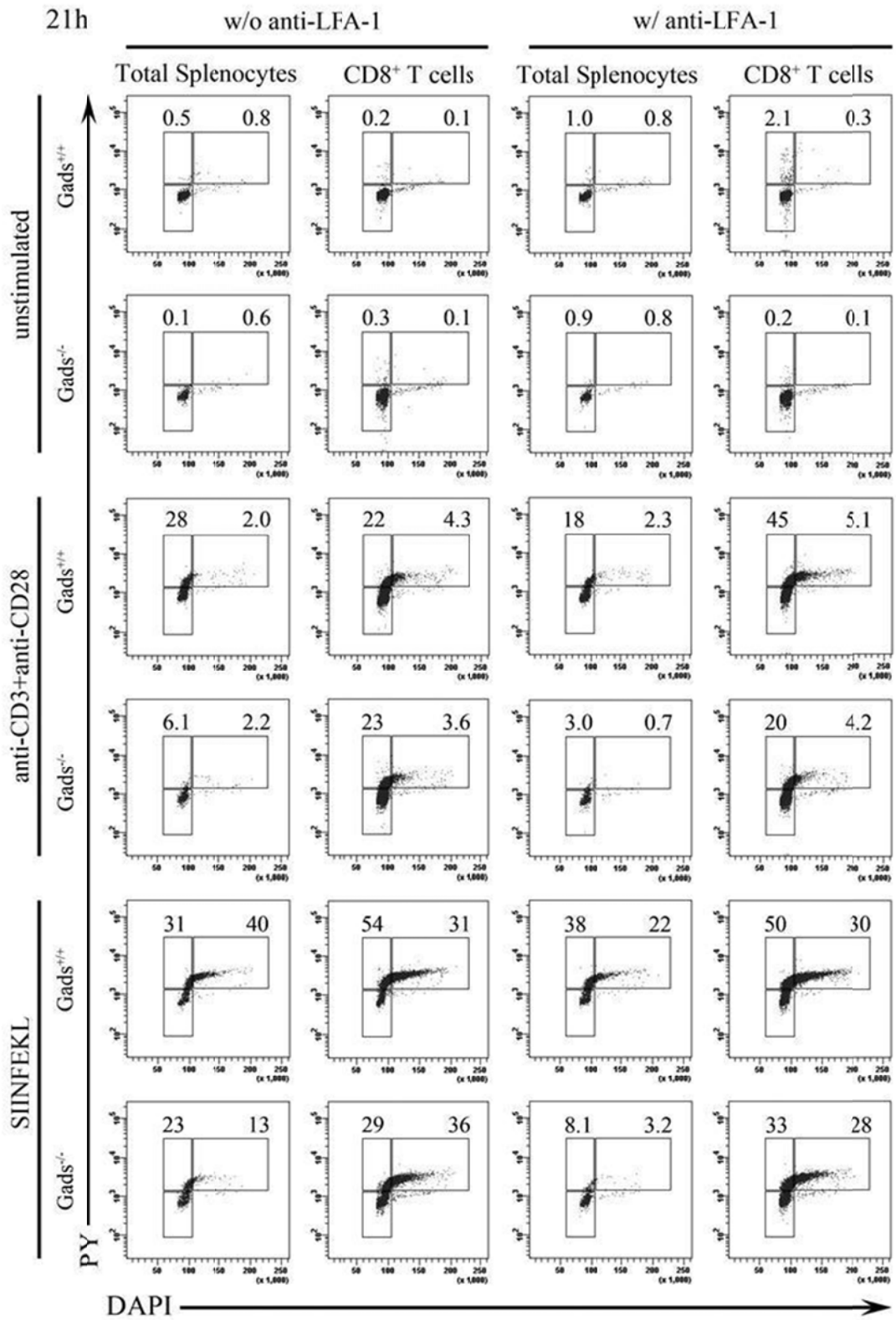
21h
w/o anti-LFA-1
w/ anti-LFA-1
Total Splenocytes
CD8+ T cells
Total Splenocytes
CD8+ T cells
unstimulated
anti-CD3+anti-CD28
SIINFEKL
Gads+/+
Gads-/-
0.5 0.8
0.2 0.1
1.0 0.8
2.1 0.3
0.1 0.6
0.3 0.1
0.9 0.8
0.2 0.1
28 2.0
22 4.3
18 2.3
45 5.1
6.1 2.2
23 3.6
3.0 0.7
20 4.2
31 40
54 31
38 22
50 30
23 13
29 36
8.1 3.2
33 28
PY
DAPI

anti-CD3 and anti-CD28, adding anti-LFA-1 promoted the cell cycle entry in Gads$^{+/+}$ CD8^{+} T cells while it did not affect the cell cycle entry in Gads$^{-/-}$ CD8^{+} T cells. When stimulated with SIINFEKL, both purified Gads$^{+/+}$ CD8^{+} T cells and Gads$^{-/-}$ CD8^{+} T cells were not affected in terms of cell cycle pattern by adding anti-LFA-1 (Fig. 4-6). These data indicated that LFA-1 promotes cell cycle entry when CD8^{+} T cells are stimulated in the context of total splenocytes. However, LFA-1 is not required for the cell cycle entry when purified CD8^{+} T cells are stimulated.

Gads regulates the conjugation of CD8^{+} T cells and EL-4 cells.

Homotypic interactions among CD8^{+} T cells, which can rescue the defect of Gads deficiency of cell cycle progression upon TCR ligation, is likely mediated by adhesion molecules, such as integrins, on the surface of CD8^{+} T cells. In the cell culture of splenocytes including T cells, B cells, DCs, and microphages, the adhesion molecules can stabilize the interactions between T cells and APCs to facilitate the formation of TCR-Ag-MHC complex. Next, we looked at the interaction between CD8^{+} T cells and APCs (EL-4 cells) to identify the role of Gads in the formation of CD8^{+} T cell-EL-4 cell conjugates.

Percentages of CD8^{+} T cells that were CFSE^{+}, indicating the percentages of CD8^{+} T cells that were conjugated with EL-4 cells, were displayed to compare the conjugation ability between Gads$^{-/-}$ CD8^{+} T cells and Gads$^{+/+}$ CD8^{+} T cells (Fig. 4-7 A). Higher percentages of Gads$^{-/-}$ CD8^{+} T cells than Gads$^{+/+}$ CD8^{+} T cells formed conjugates with antigen-pulsed EL-4 cells after co-incubation for 90 min (Fig. 4-7 B). Then, we tested varying the concentration of SIINFEKL, ranging from 0.1 pM to 10 μM. Within the range from 10 pM to 10 μM, the highest concentration of SIINFEKL tested, more Gads$^{-/-}$ CD8^{+} T cells than Gads$^{+/+}$ CD8^{+} T cells formed conjugates with EL-4 cells. In both Gads$^{+/+}$ and Gads$^{-/-}$ group, at the doses of 1 μM and 10 μM, decreased percentages of CD8^{+} T cells were observed in conjugation with EL-4 cells, as compared with the

Fig. 4-7. Higher percentages of Gads$^{-/-}$ CD8^{+} T cells than Gads$^{+/+}$ CD8^{+} T cells are conjugated with EL-4 cells. CD8^{+} T cells were purified from Gads$^{+/+}$ OT-I or Gads$^{-/-}$ OT-I splenocytes and incubated with EL-4 cells that had been loaded with CFSE and pulsed with SIINFEKL for indicated time. *A*) Shown is the gating strategy: the CD8^{+} population was gated first. Within the CD8^{+} gate, CFSE positive cells were the CD8^{+} T cells that were conjugated with EL-4 cells. The percentages of CD8^{+} T cells that were CFSE positive were calculated. *B*) EL-4 cells were pulsed with 100nM of SIINFEKL and incubated with CD8^{+} T cells for 90 min. Shown are the representative data indicating the percentages of CD8^{+} T cells that were conjugated with EL-4 cells. *C*) *Top* –EL-4 cells were incubated with CD8^{+} T cells for 90 min after pulsed with the indicated concentrations of SIINFEKL. Shown are the percentages of CD8^{+} T cells that were conjugated EL-4 cells, which have been pulsed with various concentrations of SIINFEKL. n = 1. *Middle* –EL-4 cells were pulsed with 100 nM SIINFEKL and then incubated with CD8^{+} T cells for indicated time points. Shown are the percentages of CD8^{+} T cells that were conjugated EL-4 cells after co-incubation for various time points. n = 1. *Bottom* – Bar graph indicates the statistical analysis of the conjugation results when EL-4 cells were pulsed with SIINFEKL at 0 and 100 nM for 90min. $^{*}p < 0.05$, n = 3 from three independent experiments.

Figure 4-7

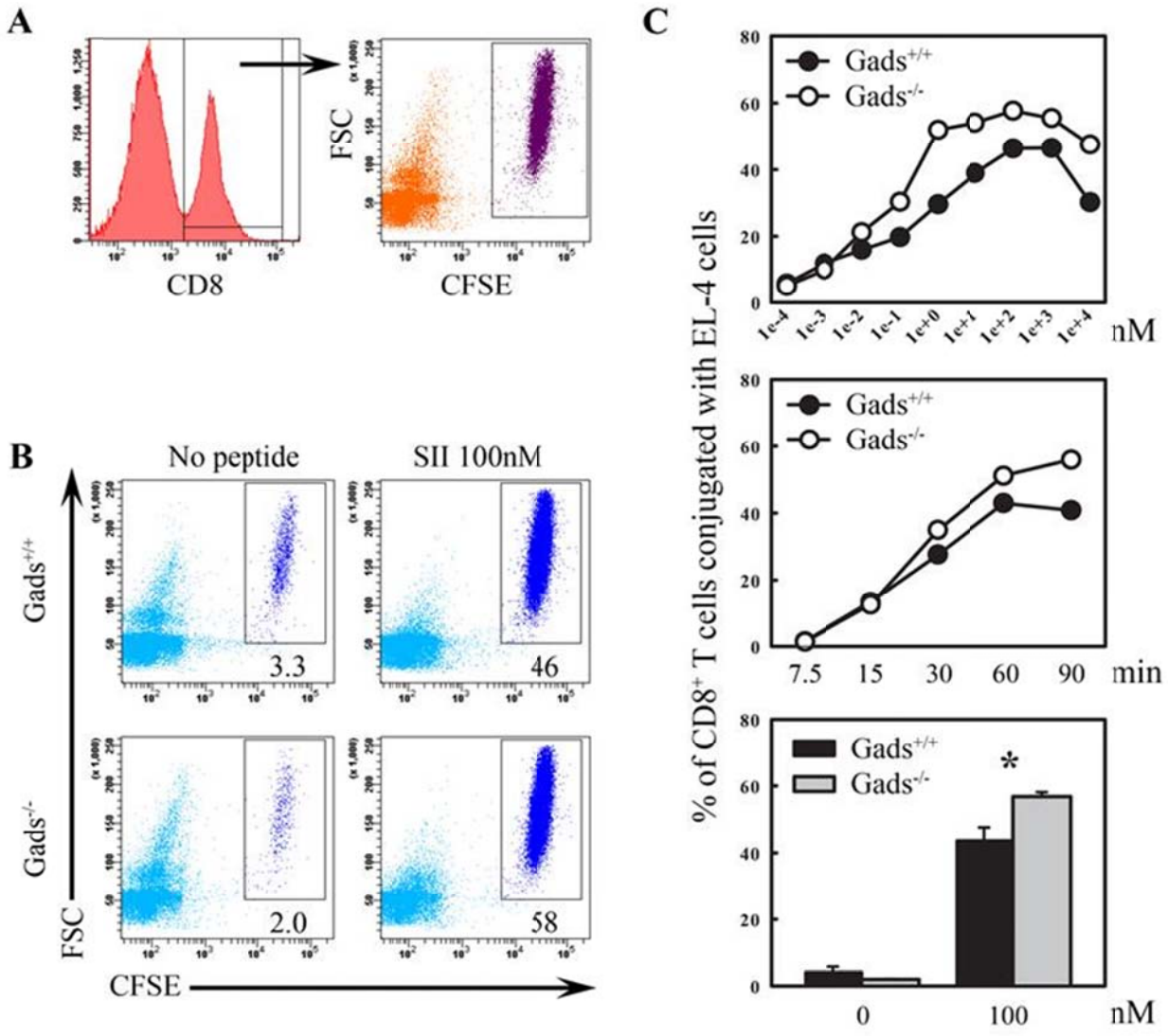
A
CD8
FSC
CFSE
B
No peptide
SII 100nM
Gads+/+
Gads-/-
3.3
46
2.0
58
FSC
CFSE
C
Gads+/+
Gads-/-
% of CD8+ T cells conjugated with EL-4 cells
nM
7.5
15
30
60
90
min
*
0
100
nM

lower doses (Fig. 4-7 C). Then the dose of 100 nM was used to pulse EL-4 cells for determining the time course of incubation between EL-4 cells and $CD8^+$ T cells. At 30 min, 60 min, and 90 min of incubation, more $Gads^{-/-}$ $CD8^+$ T cells than $Gads^{+/+}$ $CD8^+$ T cells were conjugated with EL-4 cells (Fig. 4-7 D). Data from multiple experiments revealed that significantly more $Gads^{-/-}$ $CD8^+$ T cells than $Gads^{-/-}$ $CD8^+$ T cells formed conjugates with EL-4 cells, which were pulsed with 100nM SIINFEKL before incubated with $CD8^+$ T cells for 90 min (Fig. 4-7 E).

These results indicate that Gads expression in $CD8^+$ T cells inhibits the conjugation between $CD8^+$ T cells and EL-4 cells, suggesting that the signaling mediated by adhesion molecules is more activated in $Gads^{-/-}$ $CD8^+$ T cells than $Gads^{+/+}$ $CD8^+$ T cells.

Discussion

In this chapter, we raise the model that homotypic interactions among $CD8^+$ T cells could trigger the optimal signaling mediated by the adhesion molecules to promote the TCR signaling. We stimulated the $CD8^+$ T cells in two different contexts: total splenocytes and purified $CD8^+$ T cells from $Gads^{+/+}$ OT-I mice and $Gads^{-/-}$ OT-I mice. $CD8^+$ T cells behaved differently in both cell clustering and cell cycle progression when stimulated in different contexts, regardless of in the presence or absence of Gads. Furthermore, upon TCR ligation, signals triggered in the context of purified $CD8^+$ T cells compensated the defect of Gads deficiency in cell cycle progression observed when total splenocytes were stimulated. In addition, the model was supported by the results indicating that adhesion molecules, such as LFA-1, regulate the formation of cell clusters.

Our model of signaling pathways linking Gads to c-myc can be enriched by involving homotypic interactions and the mediator: adhesion molecules, such as LFA-1 (Fig. 4-8). I propose that Gads regulates the activation of PKCθ via PI3K to trigger LFA-1-mediated signaling of $CD8^+$ T cells, when they interact with APCs. However, during the homotypic interactions among $CD8^+$ T cells, Gads inhibits the expression and function of LFA-1. The activated LFA-1 can regulate the expression of c-myc via PKCθ and PI3K.

To test this model, we first examined the activation of PKCθ and AKT, which is the readout of the PI3K activity. Based on the published data demonstrating that Gads regulates PI3K and PKCθ in Jurkat cell (131, 132), we examined the role of Gads in phosphorylation of PKCθ and AKT in $CD8^+$ T cells, especially when the homotypic interactions among $CD8^+$ T cells occurred. In purified $CD8^+$ T cells, shortly (2-15 min) after TCR ligation, $Gads^{-/-}$ $CD8^+$ T cells had much elevated phosphorylation level of AKT while $Gads^{+/+}$ $CD8^+$ T cells almost stayed at the baseline level. The phosphorylation of AKT was consistent with phosphorylation of PKCθ, suggesting that PI3K activity might be also regulated by LFA-1 in homotypic interactions among $CD8^+$ T cells.

Fig. 4-8. A model of TCR-mediated, LFA-1-dependent signaling pathways linking Gads to c-myc in $CD8^+$ T cells.

Figure 4-8

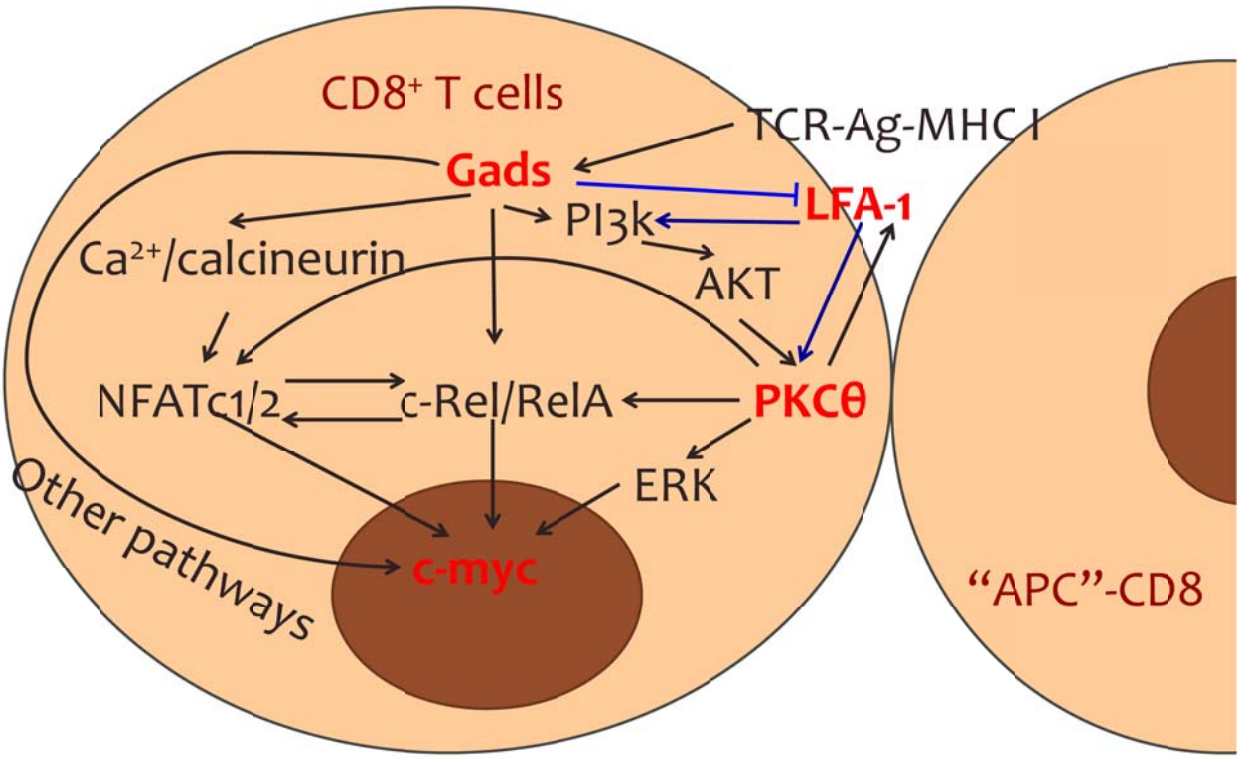
CD8+ T cells
TCR-Ag-MHC I
Gads
LFA-1
PI3k
Ca2+/calcineurin
AKT
NFATc1/2
c-Rel/RelA
PKCθ
ERK
Other pathways
c-myc
"APC"-CD8

We also extend the investigation of the signaling pathways from the other side, c-myc to the upstream proteins. Marampon *et. al.* (290) showed that c-myc expression was largely decreased by inhibition of ERK in human cancer cell lines, suggesting that c-myc is a target of ERK signal. So we also examined the phosphorylation of ERK in purified Gads$^{+/+}$ CD8^{+} T cells as well as in Gads$^{-/-}$ CD8^{+} T cells. ERK did not show the stronger phosphorylation in purified Gads$^{-/-}$ CD8^{+} T cells than Gads$^{+/+}$ CD8^{+} T cells until 30 min after TCR ligation. The earlier time, 5 min after TCR ligation, purified Gads$^{-/-}$ CD8^{+} T cells had obviously lower phosphorylation of ERK, as compared with Gads$^{+/+}$ CD8^{+} T cells. Another group reported that a delayed and longer lasting CD8-TCR interaction induced by weaker agonists (APLs) resulted in the delayed phosphorylation of ERK recruitment to the synapse, as compared to the one induced by SIINFEKL (208). This result was consistent with our previous observations in Chapter II and III that Gads$^{-/-}$ cells stimulated with SIINFEKL mimic Gads$^{+/+}$ cells stimulated with APL in cell cycle progression (Fig. 2-4 and 2-6) and accumulation of CD8^{+} T cells upon infection [Fig. 3-3, 3-4 and ref (219)]. In addition, unpublished data from our lab showed a similar pattern of ERK phosphorylation in Gads$^{-/-}$ thymocytes when stimulated with anti-CD3 and anti-CD28. These data were consistent with the pattern of ERK phosphorylation seen in our purified Gads$^{-/-}$ CD8^{+} T cells. However, these results seem to contradict with our previously published data that 2-10 min after stimulation, CD8^{+} T cells from conventional Gads$^{-/-}$ mice and wild type (WT) mice showed comparable level of phosphorylation of ERK (17). It might be due to the fact that nearly all peripheral CD8^{+} T cells from conventional Gads$^{-/-}$ mice were of a memory-like phenotype. In contrast, most of the peripheral CD8^{+} T cells from WT mice were naïve cells [Fig. 2-1 and ref (17)]. CD8^{+} T cells in ref (17) were isolated from conventional Gads$^{-/-}$ mice and WT mice before we crossing Gads- mice with OT-I mice. However, comparable frequencies of peripheral CD8^{+} T cells from both Gads$^{+/+}$ OT-I mice and Gads$^{-/-}$ OT-I mice were naïve cells (Fig. 2-1). So I used the OT-I system in my dissertation work.

The expression of c-myc in purified Gads$^{-/-}$ CD8^{+} T cells caught up with and exceeded purified Gads$^{+/+}$ CD8^{+} T cells later than 60 min after TCR ligation. Our data in mouse T cells support the model that c-myc is downstream of ERK (290). The adhesion molecule(s)-mediated signaling pathway have cross-talk with the other TCR-mediated signaling pathways. It is of note that the expression of c-myc is the overall result of various pathways. Though within the first 60 min, purified Gads$^{-/-}$ CD8^{+} T cells had lower expression of c-myc than Gads$^{+/+}$ CD8^{+} T cells, 24 hours after TCR ligation, purified Gads$^{-/-}$ CD8^{+} T cells indeed had much stronger c-myc expression (Fig. 4-3). I suspect that at longer stimulation, in purified CD8^{+} T cells, LFA-1-PKCθ-mediated signaling overwhelms signals generated from other pathways. In order to test the LFA-1- PKCθ-mediated signaling pathway in this model, we will carry out a series of similar but more extended experiments as done in Fig 4-2. We will 1) stimulate the splenocytes followed by purification of CD8^{+} T cells or 2) purify CD8^{+} T cells from splenocytes before stimulation. Firstly, we will incubate the cells in the presence or absence of anti-LFA-1 to see the effect of LFA-1 on a series of signaling events such as the activation of AKT, PKCθ, ERK and expression of c-myc. Then, we will compare the expression and activation of those proteins after stimulation with: anti-CD3 alone, anti-CD3 and anti-CD28, anti-CD28 alone, anti-LFA-1 alone, or anti-CD3+anti-LFA-1. We will do these comparisons as LFA-1 is a co-stimulatory molecule on T cells and anti-CD3 and anti-CD28 has been used as standard stimulation for crosslinking TCR and coreceptors.

LFA-1 is usually in an inactive form until it receives stimulation signals from other receptors through “inside-out” signaling. There are three distinct conformations of LFA-1, which exist in equilibrium on the cell membrane. In the low affinity form of LFA-1, the extracellular regions of the α- and β-subunits are in the bent and compact shape and the subunits are closely packed and held together by outer and inner “membrane clasp”. The high affinity form of LFA-1 is extended and when fully activated, the globular headpiece opens and the β-subunit hybrid

domain and the rest of the LFA-1 “leg” swing out. In the intermediate affinity form of LFA-1, the inner membrane clasp is disrupted and in the high-affinity LFA-1 conformation, both inner and outer clasps are disrupted (271). It will be important to determine the expression of high-affinity LFA-1 in both Gads$^{+/+}$ and Gads$^{-/-}$ CD8^{+} T cells upon TCR ligation. Thus far, we have tested the expression of total LFA-1, including all three conformations by targeting other common epitopes (Fig. 4-3). Gads$^{-/-}$ CD8^{+} T cells have higher expression of LFA-1^{+} population than Gads$^{+/+}$ CD8^{+} T cells without stimulation. It is possible that Gads$^{-/-}$ CD8^{+} T cells have the constitutively activated LFA-1. Following are some data to support the model that LFA-1 is more activated in Gads$^{-/-}$ CD8^{+} T cells.

Firstly, LFA-1 regulates leukocyte distribution by mediating the process of rolling on vascular surfaces to recruit circulating leukocytes to specific organs or to sites of infection or injury (280). In peripheral lymphoid tissues (lymph nodes and spleens) and blood, there are fewer CD8^{+} T cells in Gads$^{-/-}$ OT-I mice than Gads$^{+/+}$ OT-I mice. By contrast, Gads$^{-/-}$ OT-I mice have more CD8^{+} T cells in the lungs than Gads$^{+/+}$ OT-I mice. This phenomenon supports the model that LFA-1-mediated signal is more activated in Gads$^{-/-}$ CD8^{+} T cells than Gads$^{+/+}$ CD8^{+} T cells. LFA-1 and other integrin family proteins mediate the arrest and rolling of T cells (280) so as to regulate the attachment between T cells and the vasculature as well as migration of T cells into lymphoid and non-lymphoid tissues (272). Higher expression and more elevated activation of LFA-1 in Gads$^{-/-}$ CD8^{+} T cells might cause more Gads$^{-/-}$ CD8^{+} T cells than Gads$^{+/+}$ CD8^{+} T cells to migrate to non-lymphoid tissues. Besides lung, are there any other non-lymphoid tissues where the activated LFA-1 signal drives Gads$^{-/-}$ CD8^{+} T cell accumulation? In order to answer the above question, extensive studies need to be performed regarding the distribution of CD8^{+} T cell in various organs between Gads$^{-/-}$ OT-1 mice and Gads$^{+/+}$ OT-I mice.

Secondly, we noticed that the resting purified CD8^{+} T cells spontaneously formed cell clusters and Gads$^{-/-}$ CD8^{+} T cells had more and bigger cell clusters than Gads$^{+/+}$ CD8^{+} T cells

(Fig. 4-5 A). The clustering of cells happened within a couple of hours after purification. These observations support the hypothesis that Gads$^{-/-}$ CD8^{+} T cells have the constitutively activated LFA-1.

We raised the possibility that homotypic interactions among CD8^{+} T cells compensate for Gads deficiency in promoting cell cycle progression by activating the signals mediated by adhesion proteins on the surface of CD8^{+} T cells. Besides this explanation, there are other possibilities to explain our data showing the different behaviors of CD8^{+} T cells in different contexts of stimulation. For example, the interaction between CD8^{+} T cells and other cells in splenocytes might inhibit cell cycle progression more in Gads$^{-/-}$ splenocytes, as compared with Gads$^{+/+}$ splenocytes. In detail, the signal mediated by co-receptors on CD8^{+} T cells can inhibit T cell activation, and Gads$^{-/-}$ CD8^{+} T cells are affected more by this inhibitory signaling than Gads$^{+/+}$ CD8^{+} T cells. So that after disturbing the inhibitory signal in splenocytes by removing other cells that express ligands of the inhibitory molecules, purified Gads$^{-/-}$ CD8^{+} T cells behave similar to Gads$^{+/+}$ CD8^{+} T cells in homotypic interactions. Cytotoxic T-lymphocyte antigen (CTLA)-4 and Programmed Death (PD)-1 on the surface of T cells act as negative regulators of T cell activation (293-295). These two proteins are structurally similar to CD28 and all the three proteins bind the B7 family proteins on APCs (294, 296). CD28 and CTLA-4 can bind CD80 (B7-1) and CD86 (B7-2), while the ligands of PD-1 are PD-L1 (B7-DC) and PD-L2 (B7-H1) (297-299). In contrast to the inhibitory proteins CTLA-4 and PD-1, the costimulatory protein CD28 can promote TCR signaling (300). Upon stimulation, CD28 directly binds Gads (5, 131, 132). Gads could be associated with CTLA-4 or PD-1, which are similar to CD28 in terms of structure, to block the inhibitory signal to T cell activation.

We noticed the difference in cell clustering between stimulating purified total CD8^{+} T cells and naïve CD8^{+} T cells. When stimulated, naïve Gads$^{-/-}$ CD8^{+} T cells (FACS-purified) formed much bigger and more cell clumps than naïve Gads$^{+/+}$ CD8^{+} T cells, or purified Gads$^{-/-}$ total

$CD8^+$ T cells (positively selected using magnetic beads). Thummler *et. al.* (301) demonstrated that homotypic interactions between naïve and memory $CD4^+$ T cells could generate suppressor T cells. It is possible that in magnetic bead-purified $CD8^+$ T cells, the interactions between naïve $CD8^+$ T cells and memory $CD8^+$ T cells suppressed the signaling induced by homotypic interactions among naïve $CD8^+$ T cells, like the suppression among $CD4^+$ T cells (301). So that compared to naïve $CD8^+$ T cells, culturing total $CD8^+$ T cells reduced the level of cell clusters.

In summary, homotypic interactions among $CD8^+$ T cells overcome the defect of $Gads^{-/-}$ $CD8^+$ T cells in cell cycle entry and alters the TCR-mediated signals in a Gads-dependent way. In addition, $Gads^{-/-}$ $CD8^+$ T cells, as compared with $Gads^{+/+}$ $CD8^+$ T cells, have higher expression of LFA-1, which might account for the accumulation of $Gads^{-/-}$ $CD8^+$ T cells in lung. Furthermore, the results indicated that the homotypic interactions among $CD8^+$ T cells, in terms of the formations of cell clusters are mediated by LFA-1. However, LFA-1 regulates the cell cycle progression of $CD8^+$ T cells under the stimulation context of total splenocytes not purified $CD8^+$ T cells. Gads negatively regulates the formation of conjugates between $CD8^+$ cells and EL-4 cells. Does Gads regulate the conjugation among $CD8^+$ T cells? What is the role of LFA-1 in the conjugations among $CD8^+$ T cells? I talk about the experiments including possible results and interpretation in detail in Chapter VI.

Chapter V

Depletion and recovery of lymphoid subsets following morphine administration

Abstract

Opioid use and abuse has been linked to significant immunosuppression, which has been attributed, in part, to drug-induced depletion of lymphocytes. We sought to define the mechanisms by which lymphocyte populations are depleted and recover following morphine treatment in mice. Mice were implanted with morphine pellets and B and T cell subsets in the bone marrow, thymus, spleen, and lymph nodes were analyzed at various time points. We also examined the effects of morphine on T cell development using an *ex vivo* assay. The lymphocyte populations most susceptible to morphine-induced depletion were the precursor cells undergoing selection. The mechanism by which lymphocyte precursors were depleted could be due to the cytotoxic effects of corticosteroids released following morphine treatment. As the lymphocytes recovered, more lymphocyte precursors proliferated in morphine-treated mice than in control mice. In addition, peripheral T cells in morphine-treated mice displayed evidence that they had undergone homeostatic proliferation during the recovery phase of the experiments. The recovery of lymphocytes following morphine-induced depletion occurred in the presence of morphine and via increased proliferation of lymphoid precursors and homeostatic proliferation of T cells.

Introduction

Opioid use and abuse renders individuals susceptible to infection (302, 303) and a variety of mechanisms have been proposed to explain how opioids suppress the immune system. These mechanisms include effects on both the innate and adaptive branches of the immune system. Within the adaptive immune system, morphine treatment in mice has been demonstrated to induce profound loss in thymic and splenic mass, but the lymphoid tissues recover over time (304-307). In addition to inducing lymphocyte depletion, morphine can also alter lymphocyte function (158). Our goal here is to determine the mechanisms by which the lymphocyte populations recover after depletion and whether this recovery can occur while serum morphine levels remain at physiologically significant levels. By understanding these mechanisms, we will be able to understand how morphine affects immunity and develop strategies to avoid the detrimental effects of morphine.

To determine the mechanisms of recovery, one must first characterize the B and T cell populations that remain after morphine treatment. Although it is known that morphine treatment can deplete total B and T cells, the subpopulations of lymphocytes that remain after morphine treatment are not defined, especially for B cells.

Lymphoid development is characterized by an ordered set of steps that result in fully functional mature B and T cell subsets. For B cell development, the first stage in which committed B cell precursors can be identified in the bone marrow is the pro-B cell stage (18). During this stage, rearrangements in the μ heavy chain genomic locus begin. Upon expression of μ, the cells enter the pre-B cell stage. Then, cells rearrange the light chain genomic loci and become immature B cells. Some immature B cells migrate to the spleen where they can be identified as transitional stage 1 (T1) B cells (19). T1 cells differentiate into transitional stage 2

(T2) cells and ultimately become either follicular (FO) B cells or marginal zone (MZ) B cells. The effects of morphine treatment on these B cell subsets have not been defined.

Like B cell development, T cell development proceeds in an ordered manner. The earliest T cell precursors identified within the thymus lack CD4 and CD8 expression and are called $CD4^-$ $CD8^-$ double negative (DN) stage. DN thymocytes can be divided into the DN1 ($CD44^{hi}CD25^-$), DN2 ($CD44^{hi}CD25^+$), DN3E ($CD44^{lo}CD25^{hi}$), DN3L ($CD44^{lo}CD25^{lo}$), and DN4 ($CD44^{lo}CD25^-$) subsets (20, 21). During the DN1 and DN2 stages, cells receive signals that induce commitment to the T cell lineage and begin rearrangement of the genomic locus that encodes T cell receptor (TCR) β chain. TCRβ protein can be first detected at the DN3E stage of development; approximately 20% of DN3E thymocytes express TCRβ protein. Upon expression of TCRβ, DN thymocytes proliferate and differentiate through the DN3L and DN4 stages. After the DN4 stage, cells express CD8 and become immature single positive (ISP) $CD8^+$ T cells before expressing CD4 and becoming DP thymocytes. During the DP stage, cells rearrange the genomic locus encoding TCRα, express TCRα protein, and express a complete TCR complex. Once the TCR is expressed, positive selection and negative selection occur, the processes by which the T cell repertoire is selected. Some DP thymocytes down-regulate CD8 to become transitional single positive (TSP) $CD4^+$ thymocytes, which then mature into single positive (SP) $CD4^+$ and SP $CD8^+$ thymocytes (99, 102-104). Previous analyses of the thymocyte populations in morphine-treated mice demonstrated that DP thymocytes are highly susceptible to morphine treatment (306, 307). However, the effects of morphine on the DN and SP subsets have not been investigated.

In this chapter, we define the B and T cell subsets that remain when mice are treated with morphine and examine the mechanisms by which B and T cells repopulate the primary and secondary lymphoid organs. In particular, we examine the production of lymphocytes in primary

lymphoid organs and homeostatic proliferation of cells in secondary lymphoid organs. We demonstrate that morphine-induced corticosteroid production is the most likely cause of depletion of immature lymphocytes. After depletion, B and T cell subsets recover via a combination of increased proliferation of lymphoid precursors and homeostatic proliferation of mature T cells.

Materials and Methods

Mice

Male C57BL/6 mice were housed and bred under specific pathogen-free conditions and all experiments were performed in compliance with the University of Kansas Medical Center Institutional Animal Care and Use Committee. At the onset of the experiments, mice were between the ages of 8 and 12 weeks.

Pellet implantation

Mice were anesthetized with ketamine (75 mg/kg) and xylazine (7.5 mg/kg) and pellets were implanted subcutaneously. Morphine 75 mg, naltrexone 30 mg, and placebo pellets were obtained through the NIH AIDS Research and Reference Program, Division of AIDS, NIAID, NIH. Tissues were harvested on days 7, 14, and 21 post-implantation.

Antibodies

Anti-CD3-PE-Cy7, anti-CD8α-Alexa Fluor 647, anti-CD4-FITC, anti-CD44-PE-Cy7, anti-CD44-Horizon V450, anti-CD25-allophycocyanin-Cy7, anti-CD24-PE-Cy7, anti-TCRβ-PE, anti-B220-PE, anti-IgM-FITC, anti-CD34-Alexa Fluor 647, anti-IgD-Alexa Fluor 647, anti-CD21-PE-Cy7, anti-CD23-Pacific blue, and anti-CD62L-PE-Cy7 were purchased from BD Biosciences (San Jose, CA), eBioscience (San Diego, CA) or Biolegend (San Diego, CA).

Cell labeling and flow cytometry

Single cell suspensions of thymocytes, splenocytes, and lymphocytes were collected by gently disrupting the tissue using a wire mesh and a syringe plunger. Bone marrow cells were collected by flushing one femur with PBS using a 27-gauge needle. Cells were filtered through a 100 μm nylon mesh. Surface, intracellular staining, and DNA staining were performed as described (21). Briefly, cells were surface labeled by incubating cells with antibodies for 30 min on ice in staining buffer [PBS containing 2% Fetal Clone I (HyClone Laboratories, Inc., Logan, UT)]. After washing, cells were fixed in 1% paraformaldehyde. For intracellular staining, fixed cells were permeabilized and labeled in permeabilization buffer (0.3% Tween-20 in PBS with 2% Fetal Clone I). For DNA staining, fixed cells were incubated with 1 μg/ml 4',6-diamidino-2-phenylindole (DAPI) in permeabilization buffer for 30 min and analyzed immediately. For cell cycle analysis, single flow cytometric events were defined using DAPI-Area versus DAPI-Height and cells in the S, G2, or M phase of the cell cycles were defined as those cells that contained greater than 2N DNA. Samples were analyzed using a BD LSRII (BD Biosciences, San Jose, CA). Data were analyzed using BD FACSDiva (BD Biosciences) or FlowJo (TreeStar, Inc., Ashland, OR).

Serum morphine concentrations

To 10 μl serum, the internal standard, d3-morphine, was added. Protein was removed by extracting the morphine into acetonitrile. The concentration of morphine was determined by liquid chromatography (LC)-mass spectroscopy (MS)/MS using a Waters ACQUITY ultra performance LC system, a Waters Quattro Premier XE triple quadrupole instrument with an ESI source (Waters, Milford, MA), and MassLynx 4.1 software. Morphine was separated using an ACQUITY UPLC C18 column (1.7 μm, 100 mm × 2.1 mm internal diameter) equipped with an

ACQUITY UPLC C18 guard column (Waters, Milford, MA). The flow rate through the column at ambient temperature was 0.30 ml/min with 80% acetonitrile and 20% H_2O containing 0.1% formic acid. The MS was operated in a positive mode with electrospray ionization. Source and desolvation temperatures were 120°C and 350°C, respectively. Nitrogen was applied as the cone gas (10 liters/h) and desolvation gas (700 liters/h) and argon as the collision gas. Detection and quantification were performed using the multiple reactions monitoring mode with m/z 286/152 for morphine and 289/152 for d3-morphine.

Serum corticosterone concentrations

Corticosterone concentrations in sera were determined using the Corticosterone EIA Kit (Cayman, Ann Arbor, MI). Briefly, 50 μl sera or standard, tracer, and anti-corticosterone antiserum were added into the pre-coated plate. The plate was then incubated at room temperature with gentle shaking. After washing, the substrate reagent (Ellman's) was added into each well, incubated for 40 min, and analyzed using Synergy HT Microplate Reader (BioTek, Winooski, VT).

Fetal thymic organ culture

Fetal thymic organ culture (FTOC) was performed as described (308, 309). Briefly, thymic lobes were isolated from E15.5 fetus and placed on the surface of membrane filters (0.8 μm, Millipore, Billerica, MA), which were supported by surgical gelfoam (Pfizer Inc, NY, NY) soaked in DMEM-10 media. Thymic lobes were cultured for 7 days, minced, and analyzed by flow cytometry.

Statistics

All data are presented as mean ± SD. For day 7 analyses, 13 mice were implanted with morphine pellets and 7 mice each were implanted with placebo, naltrexone, or morphine and naltrexone pellets. Data were analyzed using a one-way ANOVA and a multiple comparisons post-hoc analysis (Dunnett's method) between the morphine group and the control groups. For other time points, statistics were based on three to ten mice for each parameter. All data included represent at least three independent experiments and were analyzed using two-tailed Student's t tests. For the FTOC experiments, data were analyzed using a one-way ANOVA and a multiple comparisons versus a control group post-hoc analysis (Dunnett's method).

Results

Morphine induces the depletion of peripheral lymphocytes

Previous studies showed that morphine pellet implantation induces loss of thymic and splenic tissue weight and depletion of lymphocytes and then cells recover over time. We initiated our studies on day 7 after morphine pellet implantation, a time point at which the spleen has recovered most of its mass (187) and after the thymocyte numbers reached their nadir (306, 307), and examined the lymphocyte populations. The total number of B cells, $CD4^+$ T cells, and $CD8^+$ T cells in the spleens and lymph nodes of morphine-treated animals remained significantly lower than placebo-treated mice (Table 5-1). Naltrexone treatment prevented the morphine-induced lymphocyte depletion, although variability within groups prevented some differences between the morphine and morphine plus naltrexone groups from being statistically different. It is feasible that the duration of morphine administration exceeded that of naltrexone in some mice, accounting for this variability. Few differences were noted between mice treated with placebo, naltrexone, or morphine plus naltrexone.

Morphine induces depletion of immature B cells

To determine which subsets of splenic B cells were most susceptible to morphine treatment, we analyzed IgM and IgD expression on $B220^+$ cells, which allowed us to distinguish among follicular (FO) B cells (IgD^+IgM^{lo}), transitional stage 2 (T2) B cells (IgD^+IgM^+), and transitional stage 1 (T1)/marginal zone (MZ) B cells (IgM^+IgD^-). The percentages of $B220^+$ splenocytes that were in the T1/MZ B cell populations were dramatically decreased in morphine-treated mice, as compared to the other groups (Fig. 5-1 A). In morphine-treated mice, 1.5 ± 0.53% of the splenic B cells were T1 or MZ B cells. Using CD21 to differentiate between T1 ($CD21^-CD23^-$) and MZ

Table 5-1. Spleen, lymph node, bone marrow, and thymus cell numbers in morphine-treated and control groups.[a]

		Morphine	Mor + Nal	Naltrexone	Placebo
	n =	13	7	7	7
Spleen	B cells	6.9 ± 7.2	14 ± 7.7	14 ± 7.2[b]	18 ± 15[b]
	$CD4^+$ cells	2.3 ± 1.1	6.1 ± 1.8[b]	6.2 ± 2.0[b]	6.0 ± 3.5[b]
	$CD8^+$ cells	2.1 ± 0.91	3.9 ± 0.85[b]	3.8 ± 1.1[b]	5.7 ± 4.3[b]
Lymph nodes	B cells	1.2 ± 0.96	7.5 ± 3.1	2.7 ± 1.4	2.4 ± 1.5[b]
	$CD4^+$ cells	0.95 ± 0.50	3.1 ± 1.3[b]	2.4 ± 0.44[b]	2.8 ±0.46[b]
	$CD8^+$ cells	0.90 ± 0.49	2.0 ± 1.3	1.2 ± 0.46	3.1 ± 2.7[b]
Bone marrow		14 ± 3.2	15 ± 1.1	14 ± 2.2	15 ± 2.9
Thymus		2.6 ± 2.2	32 ± 9.3[b]	41 ± 25[b]	46 ± 29[b]

[a]Absolute number of cells (x 10^6) in the indicated tissues (mean ± S.D) in morphine-treated, morphine+naltrexone-treated, naltrexone-treated, and placebo-treated mice.

[b]$p < 0.05$, as compared to morphine-treated group

Fig. 5-1. Morphine treatment depletes immature B cells in spleen. Mice were treated with morphine (M), morphine and naltrexone (M+N), naltrexone (N), or placebo (P) and analyzed seven days later. *A*) Splenocytes were gated on $B220^+$ cells and analyzed for IgM and IgD expression. The percentages of B cells in each gate are shown. *B*) $B220^+IgM^+IgD^-$ cells from (*A*) were analyzed for CD21 and CD23 expression. The percentages of gated cells that were T1 ($CD21^-$) and MZ ($CD21^+$) B cells are shown. *C*) $B220^+IgM^+IgD^-$ cells (*shaded histogram*), $B220^+IgM^+IgD^+$ cells (*grey line*), and $B220^+IgM^{lo}IgD^+$ cells (*black line*) from (*A*) were analyzed for CD23 expression.

Figure 5-1

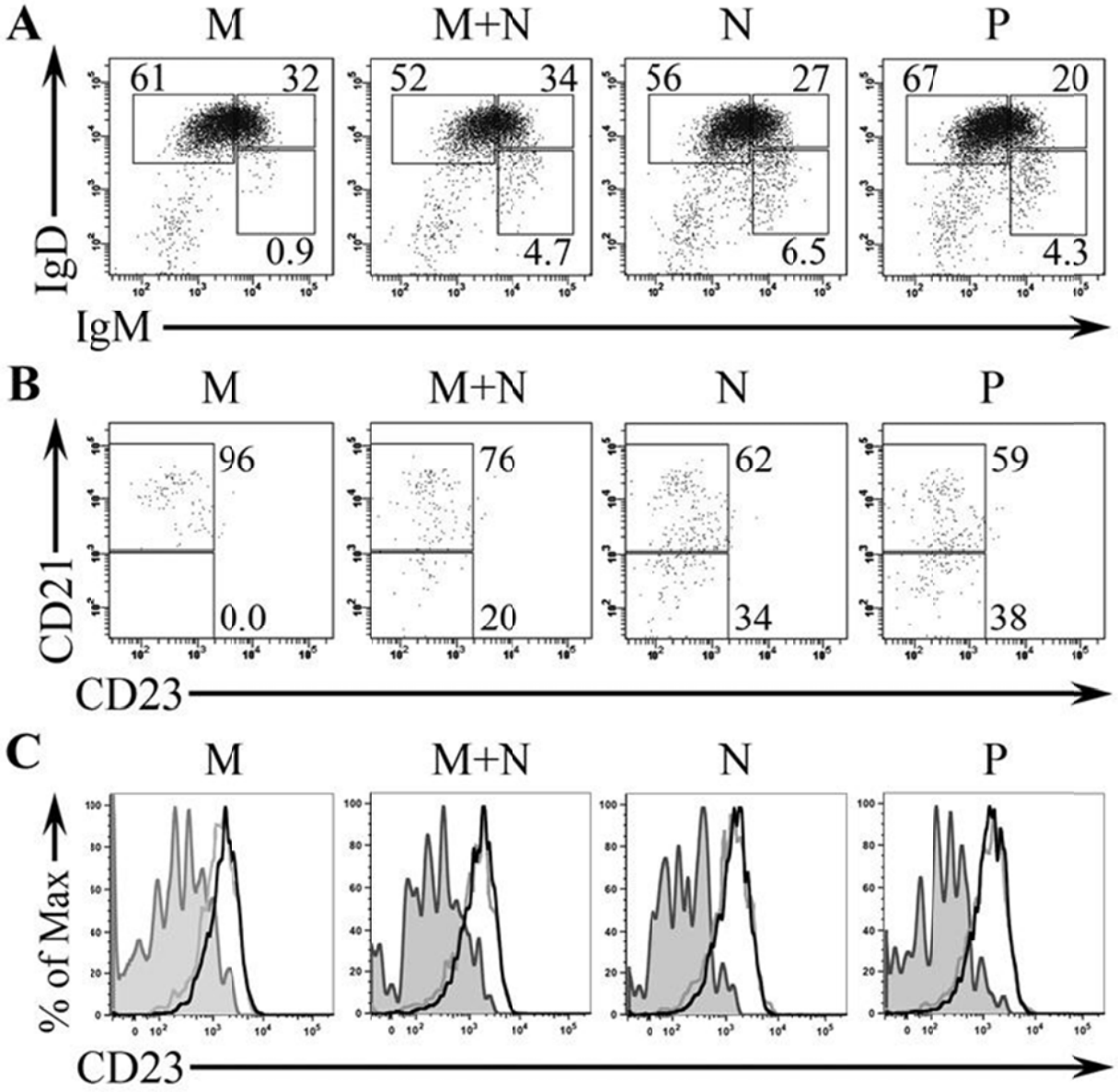
A
M
M+N
N
P
61
32
0.9
52
34
4.7
56
27
6.5
67
20
4.3
IgD
IgM
B
M
M+N
N
P
96
0.0
76
20
62
34
59
38
CD21
CD23
C
M
M+N
N
P
% of Max
CD23

($CD21^+CD23^-$) B cells revealed that nearly all of the IgM^+IgD^- cells in morphine-treated mice were MZ B cells in morphine-treated mice (Fig. 5-1 B). By contrast, 4.4 ± 0.60% of splenic B cells in placebo-treated mice were T1 or MZ B cells ($p < 0.001$) and 2.4 ± 0.40% of B cells were MZ B cells ($p = 0.015$). To further demonstrate that the IgM^+IgD^- cells lacked CD23 expression and were indeed T1 or MZ B cells, we analyzed CD23 expression on the IgM^+IgD^-, IgM^+IgD^+, and $IgM^{lo}IgD^+$ populations (Fig. 5-1 C). As previously reported (310), T2 and FO B cells expressed higher levels of CD23 than T1 and MZ B cells, supporting our conclusion that the IgM^+IgD^- gate contained only T1 and MZ B cells. These data indicated that the T1 B cells were most sensitive to morphine treatment and suggested that B cell development could be impaired by morphine treatment. In addition, the MZ B cells were more sensitive to morphine treatment than T2 and FO B cells, as the percentage of B cells that were MZ B cells declined after morphine treatment.

We traced B cell development to the bone marrow and analyzed the B cell precursor populations. The absolute numbers of bone marrow cells in each group were nearly identical across treatment groups (Table 5-1). Further, the percentage of bone marrow cells expressing CD34 was similar across groups (Fig. 5-2 A). These data indicated that morphine did not induce the depletion of all hematopoietic precursors. In contrast to the $CD34^+$ population, the percentage of bone marrow cells that expressed B220 was reduced in morphine-treated mice (Fig. 5-2 B). In particular, pro-B/pre-B ($B220^+IgM^-$) cells and immature B ($B220^{lo}IgM^+$) cells were markedly decreased in morphine-treated mice, as compared to the control groups. In morphine-treated mice, 0.74 ± 0.35% of the bone marrow cells were pro-B/pre-B cells while 5.0 ± 2.4% of the bone marrow cells in placebo-treated mice were pro-B/pre-B cells ($p < 0.001$). These data indicated that morphine treatment in mice impairs B cell development by inducing the deletion of B cell precursors.

Fig. 5-2. Morphine treatment selectively depletes immature B cells in bone marrow.

A) The percentages of bone marrow cells that expressed CD34 are shown. *B*) Bone marrow cells were analyzed for B220 and IgM expression. The percentages of cells in each gate are shown. Data shown represent one mouse from each group.

Figure 5-2

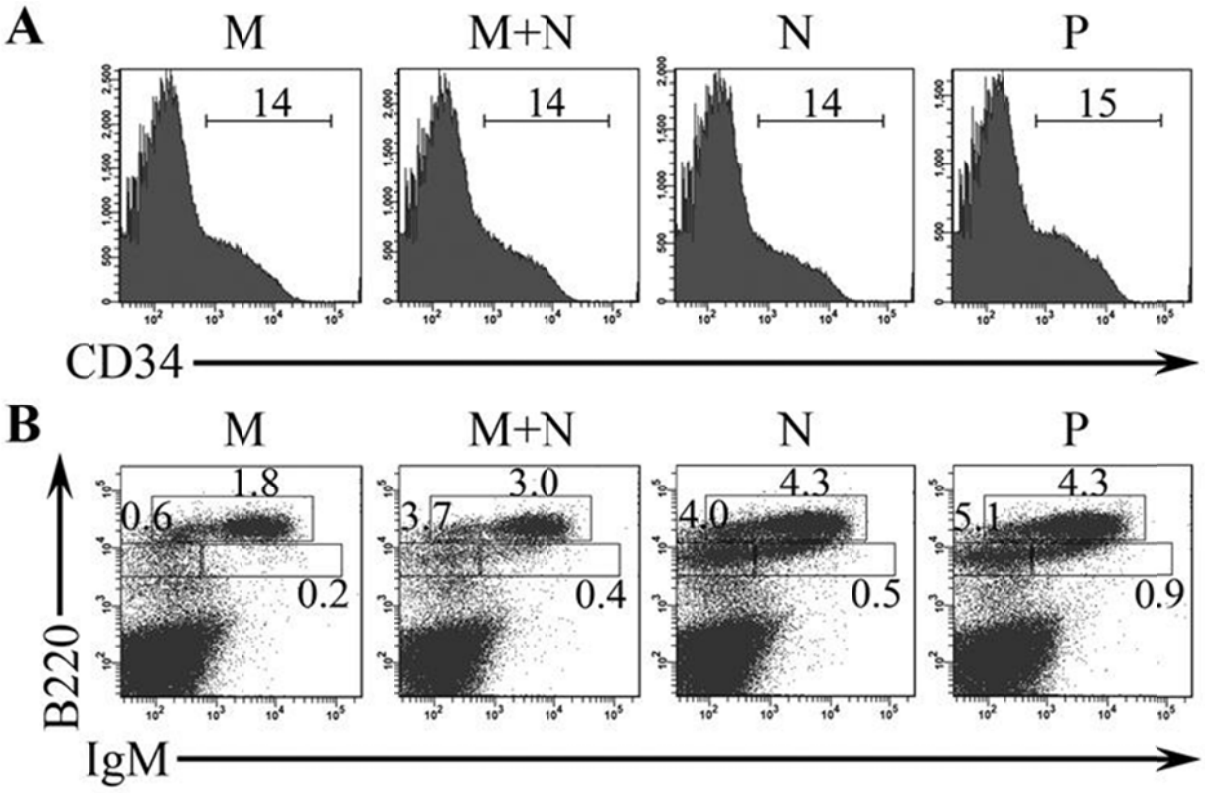
A
M
M+N
N
P
14
14
14
15
CD34
B
M
M+N
N
P
1.8
0.6
0.2
3.0
3.7
0.4
4.3
4.0
0.5
4.3
5.1
0.9
B220
IgM

B cells recover from morphine-induced depletion via proliferation of B cell precursors

By day 21 of the experiment, the number of B cells in the spleen recovered to levels that were nearly identical to that of placebo-treated mice (Fig. 5-3 A). Because there were few differences between the three groups of control mice (placebo, naltrexone, and morphine plus naltrexone) at day 7, we used the placebo-treated mice as controls for the latter time points. We also compared the data throughout the experiment to a control group of untreated mice. We tested whether peripheral B cells might proliferate as a mechanism by which splenic B cells recover in number. Less than 2% of splenic B cells were in the S, G2, or M phase of the cell cycle in any of the groups (Fig. 5-3 B), indicating that B cell recovery did not occur via proliferation of the remaining cells.

Like splenic B cells, the B cell precursors in the bone marrow also recovered during the course of the experiment (Fig. 5-3 C). The percentage of bone marrow cells that were $B220^+$ cells were decreased in all groups seven days after pellet implantation, but the morphine-treated mice had the largest decrease. By day 14, the percentage of bone marrow cells that were pro-B/pre-B cells in morphine-treated mice, placebo-treated mice, and untreated mice were comparable. The immature B cells and mature B cells recovered more slowly in the morphine-treated mice than placebo-treated mice.

A possible mechanism by which bone marrow B cell precursors could recover in number is through increased proliferation. The most dramatic increase in the percentage of cells in the cell cycle were found in the immature B cell subset at day 14 (Fig. 5-3 D); 28 ± 11% of immature B cells in morphine-treated mice were in the S, G2, or M phase of the cell cycle, as compared to 7.1 ± 3.1% of immature B cells in placebo-treated mice ($p < 0.001$). In addition, more mature B cells in the bone marrow were in the S, G2, or M phase in morphine-treated mice than placebo-treated mice at day 21.

Fig. 5-3. Recovery of B cells after morphine treatment is due to proliferation of B cell precursors. Mice were treated with morphine (*closed circles*) or placebo (*open circles*) for 7, 14, or 21 days. Untreated control mice are shown as a dashed line. *A*) The absolute numbers of splenic B cells are shown. *B*) The percentage of splenic B cells in the S, G2, or M phase of the cell cycle are shown. *C*) Bone marrow cells were analyzed for B220 and IgM expression and the percentages of cells in each gate are shown. *D*) Cells were gated as in (*C*) and analyzed for DNA content. The percentages of cells in each gate that were in the S, G2, or M phase of the cell cycle are shown. $^{*}p < 0.05$, $^{**}p < 0.01$, comparing morphine-treated mice and placebo-treated mice.

Figure 5-3

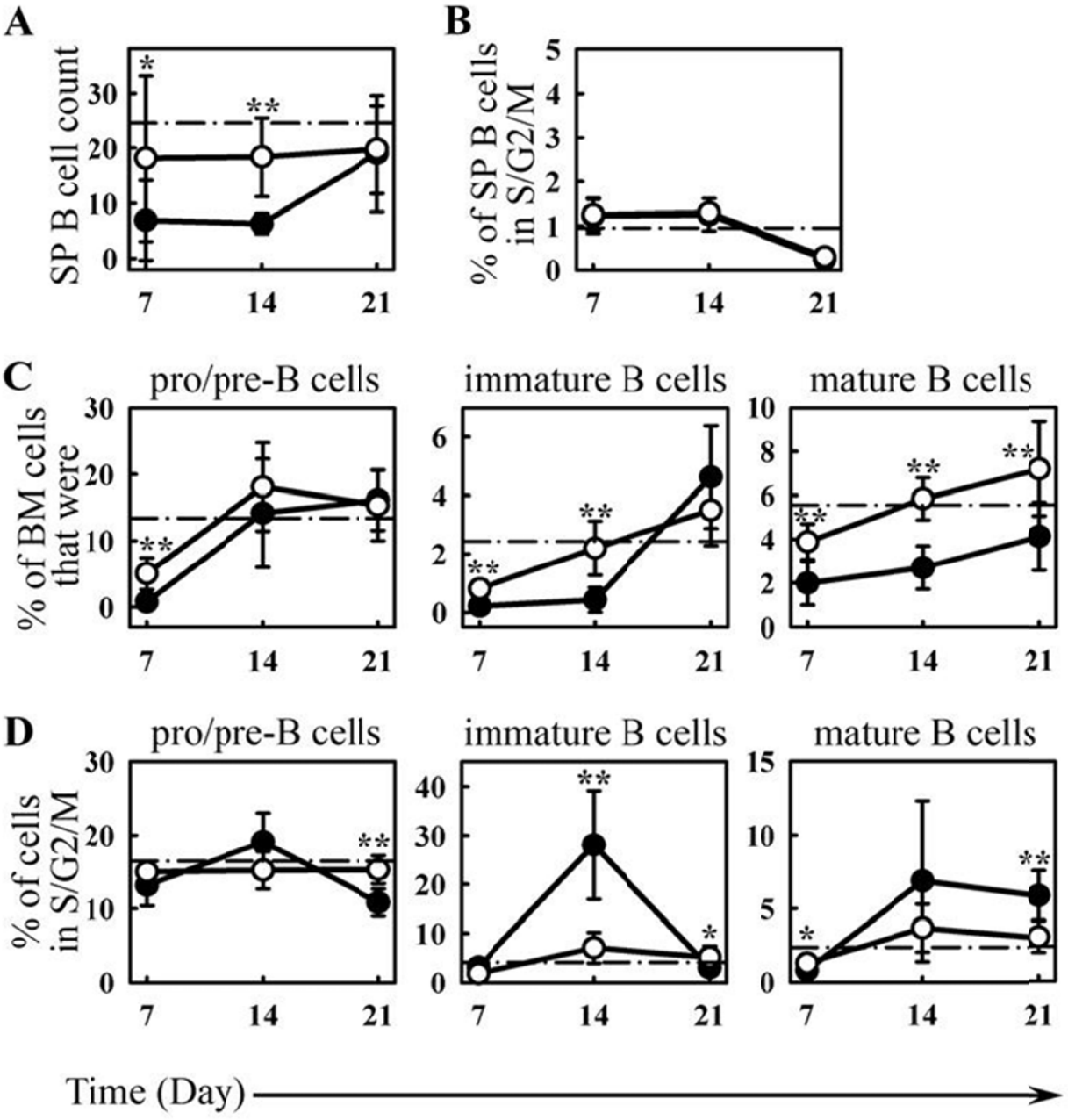
A
SP B cell count
B
% of SP B cells in S/G2/M
C
pro/pre-B cells
immature B cells
mature B cells
% of BM cells that were
D
pro/pre-B cells
immature B cells
mature B cells
% of cells in S/G2/M
Time (Day)

Collectively, these data suggest that the mechanism by which the B cells recover is primarily through increased proliferation of B cell precursor populations. While splenic B cells did not display elevated percentages of cells in the S, G2, or M phase of the cell cycle, $B220^{hi}$ bone marrow B cells in morphine-treated mice did increase their proliferation. This suggests that different populations of B cells may recover from depletion using different mechanisms.

Morphine treatment induces depletion of naïve and memory T cell subsets

Morphine also induced the depletion of $CD4^+$ and $CD8^+$ T cells in the spleens and lymph nodes (Table 5-1). To determine whether some T cell subsets were more susceptible to the effects of morphine than others, we analyzed whether naïve, central memory, or effector memory subsets were preferentially depleted by morphine treatment. There were no differences across groups of mice between the percentages of $CD4^+$ or $CD8^+$ T cells that were naïve ($CD44^{lo}CD62L^{hi}$), central memory ($CD44^{hi}CD62L^{hi}$), or effector memory ($CD44^{hi}CD62L^{lo}$) in the spleen (Fig. 5-4) or in the lymph node (data not shown), indicating that the major peripheral T cell subsets were depleted by morphine to the same extent.

Morphine treatment induces depletion of thymocytes undergoing selection

As shown in Table 5-1, the number of thymocytes per mouse was greatly reduced in morphine-treated mice, as compared to other groups. However, not all thymocyte subsets were depleted to a comparable extent. The population of cells most dramatically depleted by morphine treatment was the DP subset (Fig. 5-5 A), consistent with previous reports (306, 307). Within the DN population, DN3L and DN4 cells were most susceptible to depletion by morphine treatment (Fig. 5-5 B).

Fig. 5-4. Morphine treatment does not affect the percentages of T cells that are naïve, central memory, and effector memory. Splenocytes were labeled with anti-CD4, anti-CD8, anti-CD44, and anti-CD62L seven days after pellet implantation. The percentages of $CD4^+$ cells (*A*) and $CD8^+$ (*B*) in each gate are shown. Data shown represent one mouse from each group.

Figure 5-4

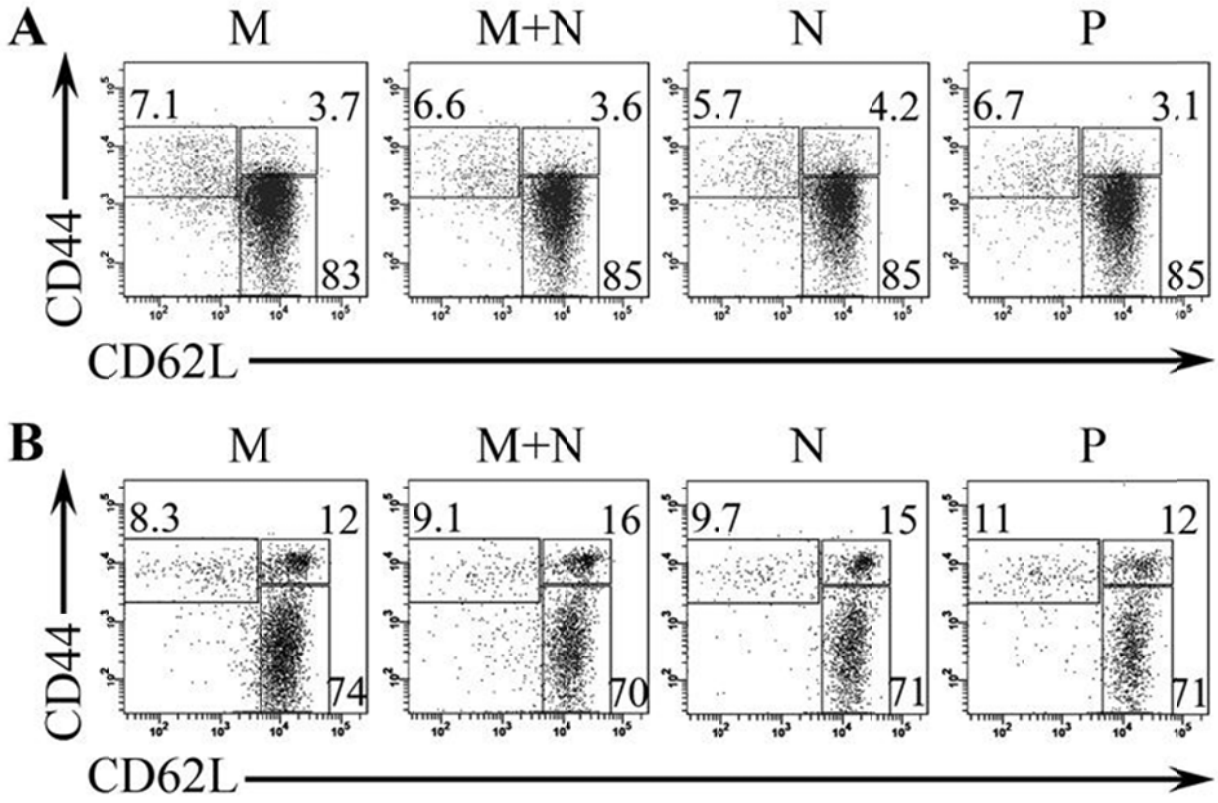
A
M
M+N
N
P
7.1
3.7
83
6.6
3.6
85
5.7
4.2
85
6.7
3.1
85
CD44
CD62L
B
M
M+N
N
P
8.3
12
74
9.1
16
70
9.7
15
71
11
12
71
CD44
CD62L

Fig. 5-5. Morphine treatment depletes thymocytes in DN3L and DN4 subsets. Mice were treated with morphine (M), morphine and naltrexone (M+N), naltrexone (N), or placebo (P) and analyzed seven days later. Thymocytes were analyzed for surface expression of CD4, CD8, CD44, and CD25 and intracellular expression of TCRβ. (*A*-*C*) Data shown represent one mouse from each group. *A*) The percentages of thymocytes that were DN, DP, SP $CD4^+$, and SP $CD8^+$ cells are shown. *B*) Thymocytes were gated on the DN population and analyzed for CD44 and CD25 expression. Shown are the percentages of DN cells that were DN1, DN2, DN3E, DN3L, and DN4.

Figure 5-5

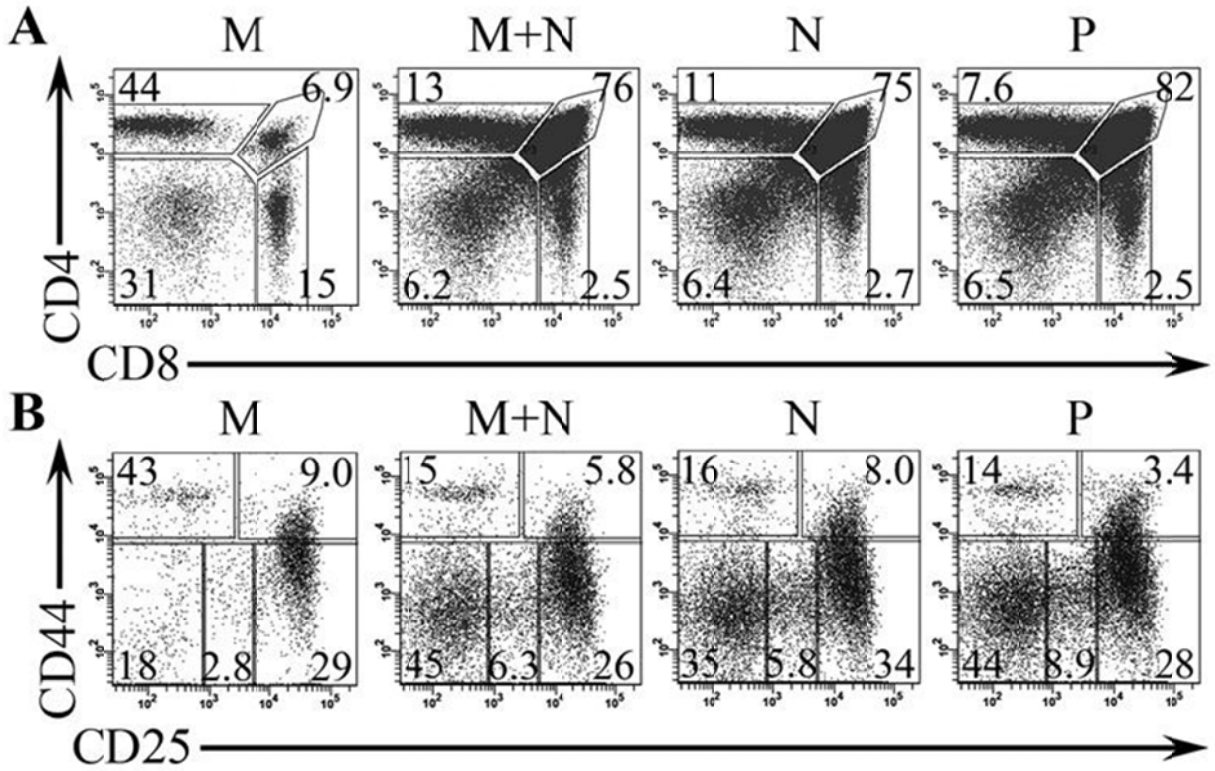
A
M
M+N
N
P
44
6.9
31
15
13
76
6.2
2.5
11
75
6.4
2.7
7.6
82
6.5
2.5
CD4
CD8
B
M
M+N
N
P
43
9.0
18
2.8
29
15
5.8
45
6.3
26
16
8.0
35
5.8
34
14
3.4
44
8.9
28
CD44
CD25

Consistent with our previous report in untreated mice (21), more than 80% of DN3L and DN4 thymocytes in control mice expressed TCRβ (Fig. 5-6 A) and many of these cells were in the S, G2, or M phase of the cell cycle (Fig. 5-6 B). Following morphine-treatment, the percentage of DN3L and DN4 thymocytes that expressed TCRβ was reduced, as compared to control groups. In morphine-treated mice, 31 ± 18% of DN3L cells expressed TCRβ and 40 ± 27% of DN4 cells expressed TCRβ ($p \leq 0.001$, as compared to placebo-treated mice). In addition, fewer $TCR\beta^+$ DN3E, $TCR\beta^+$ DN3L, and $TCR\beta^+$ DN4 thymocytes were in the S, G2, or M phase of the cell cycle in morphine-treated mice than placebo-treated mice (Fig. 5-6 B), although only in the DN4 population did this difference reach statistical significance. These data indicate that morphine treatment blocks cell cycle progression and induces the depletion of $TCR\beta^+$ DN thymocytes.

The stage of T cell development following the DN4 stage is the immature single positive (ISP) $CD8^+$ thymocyte stage, defined as $CD8^+CD4^-CD24^{hi}TCR^{lo}$. ISP $CD8^+$ thymocytes were nearly absent in morphine-treated mice, whereas they represent approximately half of SP $CD8^+$ thymocytes in control mice (Fig. 5-7 A). Following the ISP $CD8^+$ stage, cells become DP thymocytes and then down-regulate CD8 to become transitional single positive (TSP) $CD4^+$ thymocytes, a population defined as $CD4^+CD8^{-/lo}CD24^{hi}$. Like ISP $CD8^+$ and DP thymocytes, TSP $CD4^+$ thymocytes were also nearly completely depleted in morphine-treated mice; nearly all SP $CD4^+$ thymocytes in morphine-treated mice were $CD24^{lo}$, indicating that the cells were mature (Fig. 5-7 B). These data suggest that cells in the developmental stages immediately following the β selection and positive selection steps are most susceptible to morphine-induced depletion.

Fig. 5-6. Morphine treatment depletes thymocytes undergoing β selection. Mice were treated with morphine (M), morphine and naltrexone (M+N), naltrexone (N), or placebo (P) and analyzed seven days later. *A*) Thymocytes were gated on DN3E, DN3L, and DN4 thymocytes and analyzed for intracellular TCRβ expression. Shown are the percentages of DN3E, DN3L, and DN4 thymocytes that expressed TCRβ. *B*) $TCR\beta^+$ DN3E, $TCR\beta^+$ DN3L, and $TCR\beta^+$ DN4 thymocytes were analyzed for their cell cycle status. The percentages of cells that were in the S, G2, or M phase of the cell cycle are shown. $^{*}p < 0.05$, $^{**}p < 0.01$, as compared to morphine-treated mice.

Figure 5-6

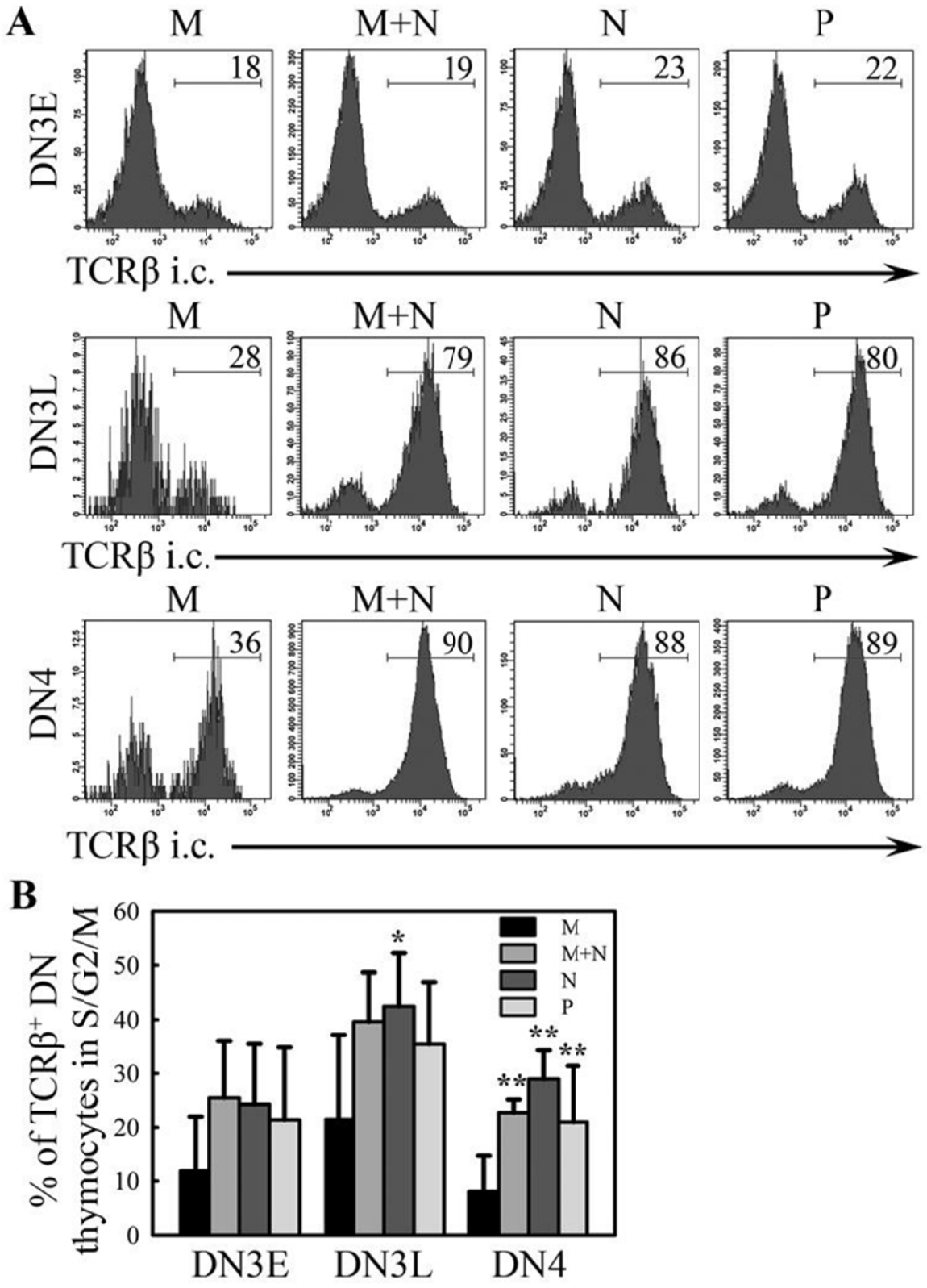
A
M
M+N
N
P
DN3E
18
19
23
22
TCRβ i.c.
DN3L
28
79
86
80
DN4
36
90
88
89
B
% of TCRβ+ DN thymocytes in S/G2/M
M
M+N
N
P
DN3E
DN3L
DN4

Fig. 5-7. Morphine treatment induces depletion of ISP $CD8^+$ and TSP $CD4^+$ thymocytes. Mice were treated with morphine (M), morphine and naltrexone (M+N), naltrexone (N), or placebo (P) and analyzed seven days later. Thymocytes were surface labeled with anti-CD4, anti-CD8, anti-CD24, and anti-TCRβ. Cells were gated on SP $CD8^+$ (*A*) or SP $CD4^+$ (*B*) thymocytes and analyzed for CD24 and TCRβ expression. The percentages of SP $CD8^+$ or SP $CD4^+$ thymocytes in each gate are shown. Data shown represent one mouse from each group.

Figure 5-7

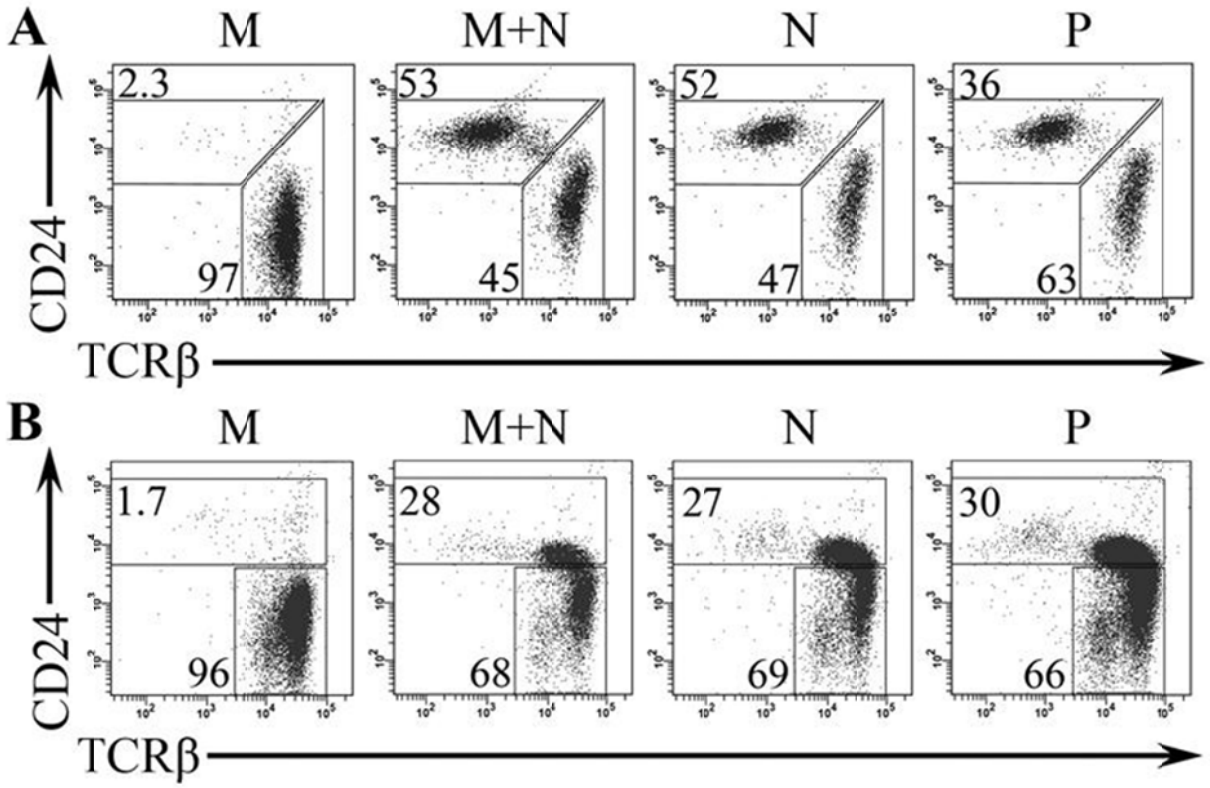
A
M
M+N
N
P
2.3
53
52
36
97
45
47
63
CD24
TCRβ
B
M
M+N
N
P
1.7
28
27
30
96
68
69
66
CD24
TCRβ

Peripheral T cell subsets recover via homeostatic proliferation

Unlike splenic B cells, peripheral T cells failed to completely restore their numbers to that of placebo-treated mice over the course of the experiment (Fig. 5-8 A). Although the amount of recovery in the peripheral T cells was subtle and not statistically significant within the time frame of the experiment, we examined the peripheral T cells for signs of homeostatic proliferation, the process by which lymphocytes expand in number in response to a lymphopenic environment. Seven days after pellet implantation, more $CD4^+$ and $CD8^+$ T cells in the lymph node were in the S, G2, or M phase of the cell cycle than in placebo-treated mice ($p < 0.10$) (Fig. 5-8 B). In the spleen, more $CD4^+$ T cells were in the S, G2, or M phase of the cell cycle 14 days after morphine treatment than placebo treatment ($p < 0.10$) (Fig. 5-8 B).

As a further test of whether T cells underwent homeostatic proliferation, we examined whether the T cells converted to a memory-like phenotype during the study (Fig. 5-9). T cells undergoing homeostatic proliferation convert to a memory-like phenotype (311-315). Greater percentages of $CD4^+$ T cells in the spleens and lymph nodes on days 14 and 21 of the experiment displayed central memory and effector memory phenotypes in morphine-treated mice than placebo-treated mice. Likewise, more $CD8^+$ T cells in morphine-treated mice had a central memory phenotype than in placebo-treated mice.

In summary, the analysis of peripheral T cells suggested that the T cells in morphine-treated mice underwent homeostatic proliferation. However, homeostatic proliferation is likely a minor component of the recovery of T cells following morphine treatment, as the T cells failed to recover to normal numbers during the experiment.

Fig. 5-8. Peripheral T cells from morphine-treated mice proliferate more than placebo-treated mice in the recovery from morphine-induced depletion. Mice were treated with morphine (*closed circles*) or placebo (*open circles*) for 7, 14, or 21 days. Untreated control mice are shown as a dashed line. *A*) The absolute number of splenic (SP) and lymph node (LN) T cells are shown. *B*) The percentages of SP and LN $CD4^+$ and $CD8^+$ cells that were in the S, G2, or M phase of the cell cycle are shown.

Figure 5-8

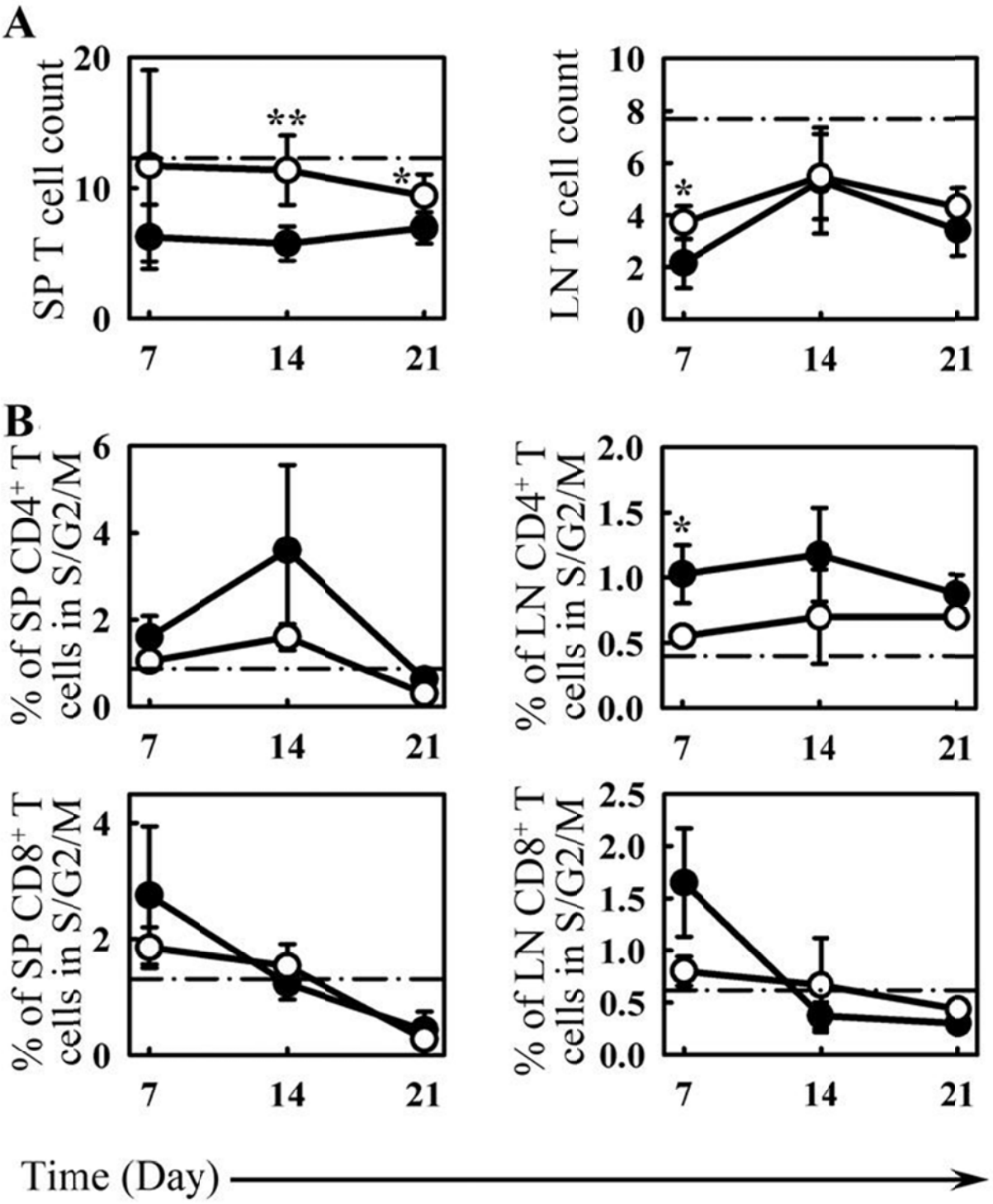
A
SP T cell count
20
10
0
**
*
7
14
21
LN T cell count
10
8
6
4
2
0
*
7
14
21
B
% of SP CD4+ T cells in S/G2/M
6
4
2
0
7
14
21
% of LN CD4+ T cells in S/G2/M
2.0
1.5
1.0
0.5
0.0
*
7
14
21
% of SP CD8+ T cells in S/G2/M
4
2
0
7
14
21
% of LN CD8+ T cells in S/G2/M
2.5
2.0
1.5
1.0
0.5
0.0
7
14
21
Time (Day)

Fig. 5-9. Peripheral T cells from morphine-treated mice proliferate more than placebo-treated mice in the recovery from morphine-induced depletion. Splenocytes were labeled with anti-CD4, anti-CD8, anti-CD44, and anti-CD62L 7, 14 or 21 days after pellet implantation. $CD4^+$ cells were gated and analyzed in *A*) and $CD8^+$ cells were gated and analyzed in *B*). The percentages of cells that were central memory or effector memory are shown. $^*p < 0.05$, $^{**}p < 0.01$.

Figure 5-9

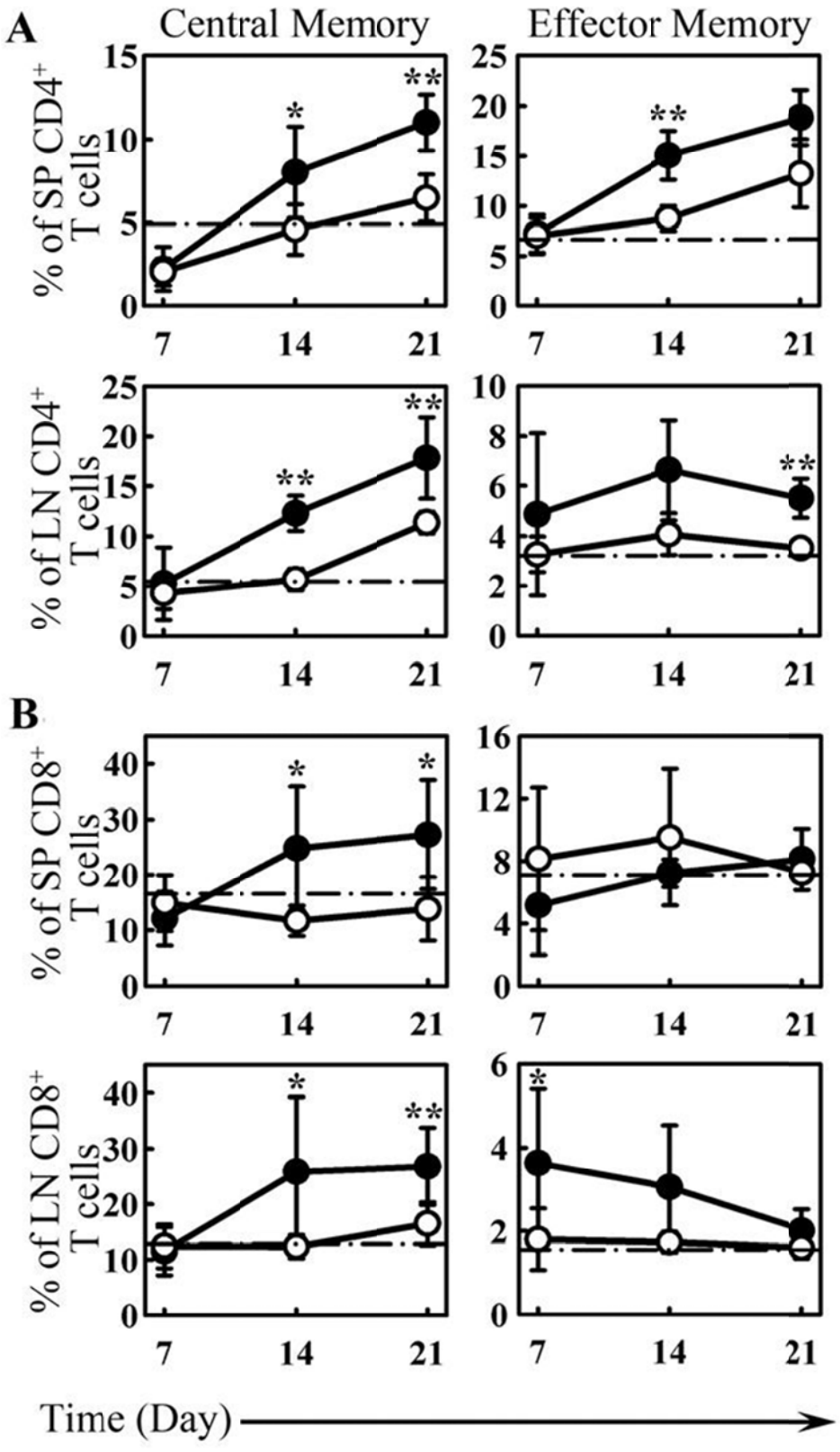
A
Central Memory
Effector Memory
% of SP CD4+ T cells
% of LN CD4+ T cells
B
% of SP CD8+ T cells
% of LN CD8+ T cells
Time (Day)

T cells recover from morphine via increased proliferation of precursor cells

In the weeks following morphine pellet implantation, the number of thymocytes returned to nearly normal numbers (Fig. 5-10 A). In addition, the distribution of thymocytes into the DN, DP, SP $CD4^+$, and SP $CD8^+$ populations was fully restored within three weeks of morphine pellet implantation (Fig. 5-10 B). After two weeks of morphine treatment, the percentage of thymocytes that were DP slightly exceeded that of placebo-treated mice. The percentages of DN thymocytes that were DN1, DN2, DN3E, DN3L, and DN4 returned to nearly normal levels within three weeks (Fig. 5-10 C). Also, the percentage of SP $CD8^+$ thymocytes that were ISP $CD8^+$ cells and the percentage of SP $CD4^+$ thymocytes that were TSP $CD4^+$ cells returned to normal levels (Fig. 5-10 D).

Because we observed a decrease in the percentage of DN3L and DN4 thymocytes that expressed TCRβ after seven days of morphine treatment (Fig. 5-6 A), we examined these populations over time. The percentage of $TCR\beta^+$ DN3E thymocytes in mice treated with morphine for 14 days exceeded that of placebo-treated mice (Fig. 5-10 E), suggesting that increased production of $TCR\beta^+$ DN3E thymocytes could contribute to the restoration of the T cell populations. We next examined mechanisms by which this rebound in the $TCR\beta^+$ DN3E population could occur. We found that a greater percentage of DN1, DN2, and $TCR\beta^+$ DN3E thymocytes were in the S, G2, or M phase of the cell cycle in morphine-treated mice than placebo-treated mice (Fig. 5-10 F). The percentage of $TCR\beta^+$ DN3L and $TCR\beta^+$ DN4 thymocytes in the S, G2, or M phase of the cell cycle did not differ between the groups of mice on days 14 and 21 of the experiment (data not shown). However, more DP thymocytes were in the S, G2, or M phase of the cell cycle seven days after pellet implantation in morphine-treated mice than placebo-treated mice (Fig. 5-10 F).

Fig. 5-10. Recovery of T cells via increased proliferation of precursor cells. Mice were treated with morphine (*closed circles*) or placebo (*open circles*) for 7, 14, or 21 days. Untreated control mice are shown as a dashed line. Thymocytes were analyzed as described in Figs. 5-5, 5-6 and 5-7. *A*) The absolute number of thymocytes are shown. *B*) The percentages of thymocytes that were DN, DP , SP $CD4^+$, and SP $CD8^+$ thymocytes and shown. *C*) The percentages of DN thymocytes that were DN1, DN2, DN3E, DN3L, and DN4 thymocytes are shown. *D*) The percentages of SP $CD8^+$ and SP $CD4^+$ thymocytes that were ISP $CD8^+$ and TSP $CD4^+$ thymocytes, respectively, are shown. *E*) The percentages of DN3E, DN3L, and DN4 thymocytes that expressed TCRβ are shown. *F*) The percentages of DN1, DN2, $TCR\beta^+$ DN3E, and DP thymocytes that were in the S, G2, or M phase of the cell cycle are shown. $^*p < 0.05$, $^{**}p < 0.01$.

Figure 5-10

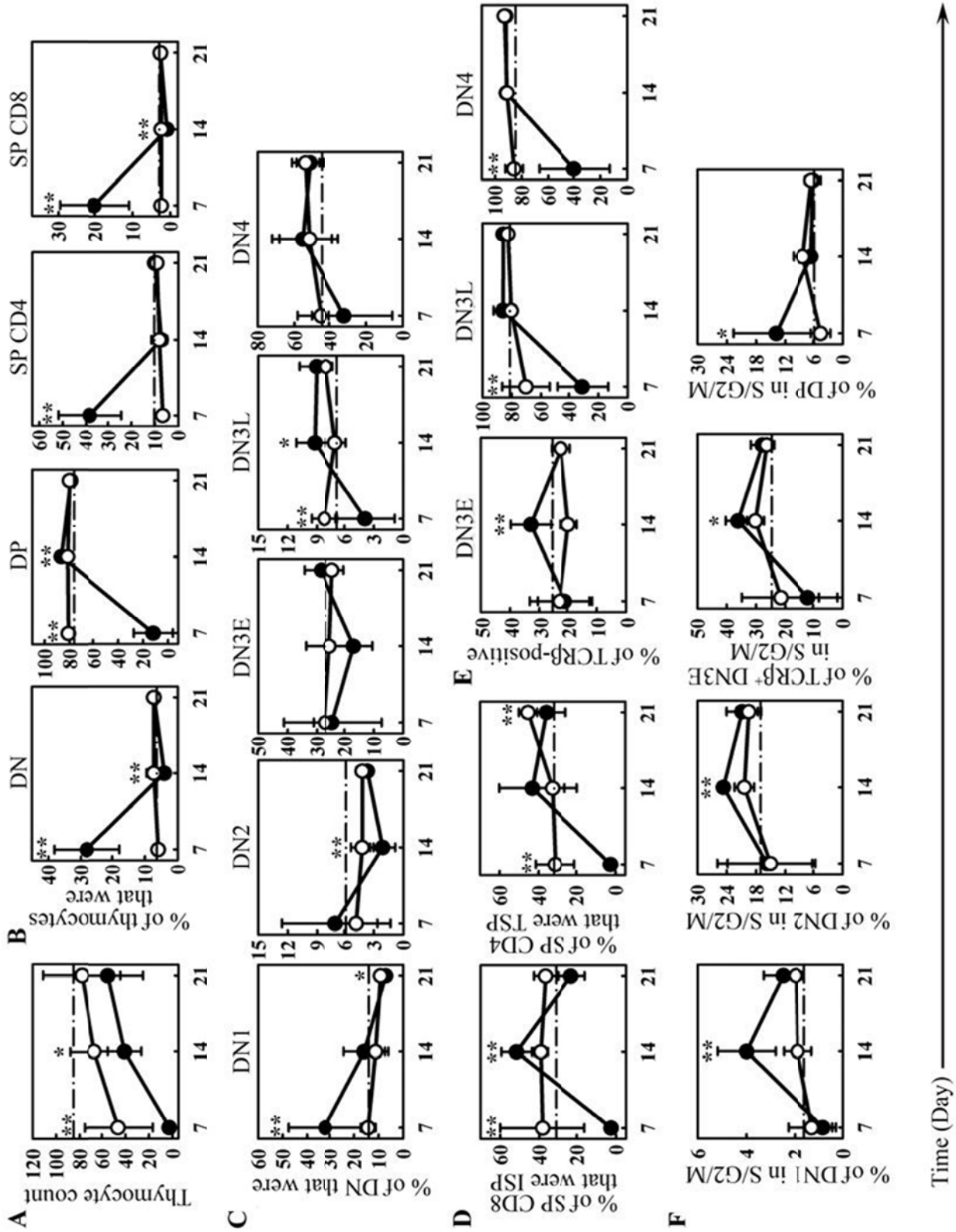
A
Thymocyte count
B
% of thymocytes that were
DN
DP
SP CD4
SP CD8
C
% of DN that were
DN1
DN2
DN3E
DN3L
DN4
D
% of SP CD8 that were ISP
% of SP CD4 that were TSP
E
% of TCRβ-positive
DN3E
DN3L
DN4
F
% of DN1 in S/G2/M
% of DN2 in S/G2/M
% of TCRβ+ DN3E in S/G2/M
% of DP in S/G2/M
Time (Day)

In summary, these data suggest that thymocyte populations recover following morphine treatment via increased proliferation of DN1, DN2, TCRβ^+ DN3E, and DP thymocytes. This proliferation seen in morphine-treated mice may cause the percentage of thymocytes that were TCRβ^+ DN3L, ISP CD8$^+$, and DP cells to transiently exceed that of placebo-treated mice.

Morphine pellet implantation results in sustained plasma morphine levels and a transient increase in corticosterone levels

Previous reports suggested that morphine treatment in mice could induce elevated corticosteroid production (173, 176, 192, 193, 306). To test whether this occurred during our experiments, we examined serum morphine and corticosterone levels in mice from each group. Serum concentrations of free, unconjugated morphine reached an average of 4.3 ± 0.56 μM within six hours of implantation, decayed to 1.3 ± 0.61 μM within seven days, and was 0.22 ± 0.11 μM on day 21 (Fig. 5-11 A). Within six hours of morphine pellet implantation, corticosterone levels reached levels that were 5.3 ± 1.6-fold greater than pre-implantation levels (Fig. 5-11 B). Mice receiving placebo, naltrexone, and morphine plus naltrexone had corticosterone levels six hours after implantation that were approximately two-fold greater than pre-surgery levels.

These data indicated that lymphocyte populations were depleted while corticosterone levels were elevated and recovered when corticosterone levels returned to nearly baseline levels. In addition, lymphocyte recovery occurred while morphine levels remained at physiologically significant levels.

Fig. 5-11. Morphine pellet implantation leads to sustained serum morphine levels and a transient increase in serum corticosterone levels. Mice were implanted with pellets containing morphine (M), morphine and naltrexone (M+N), naltrexone (N), or placebo (P) and blood was collected at the indicated time points. The concentrations of morphine (*A*) and corticosterone (*B*) in sera of mice treated for the indicated lengths of time are shown. Untreated control mice (C) were also analyzed (*B*).

Figure 5-11

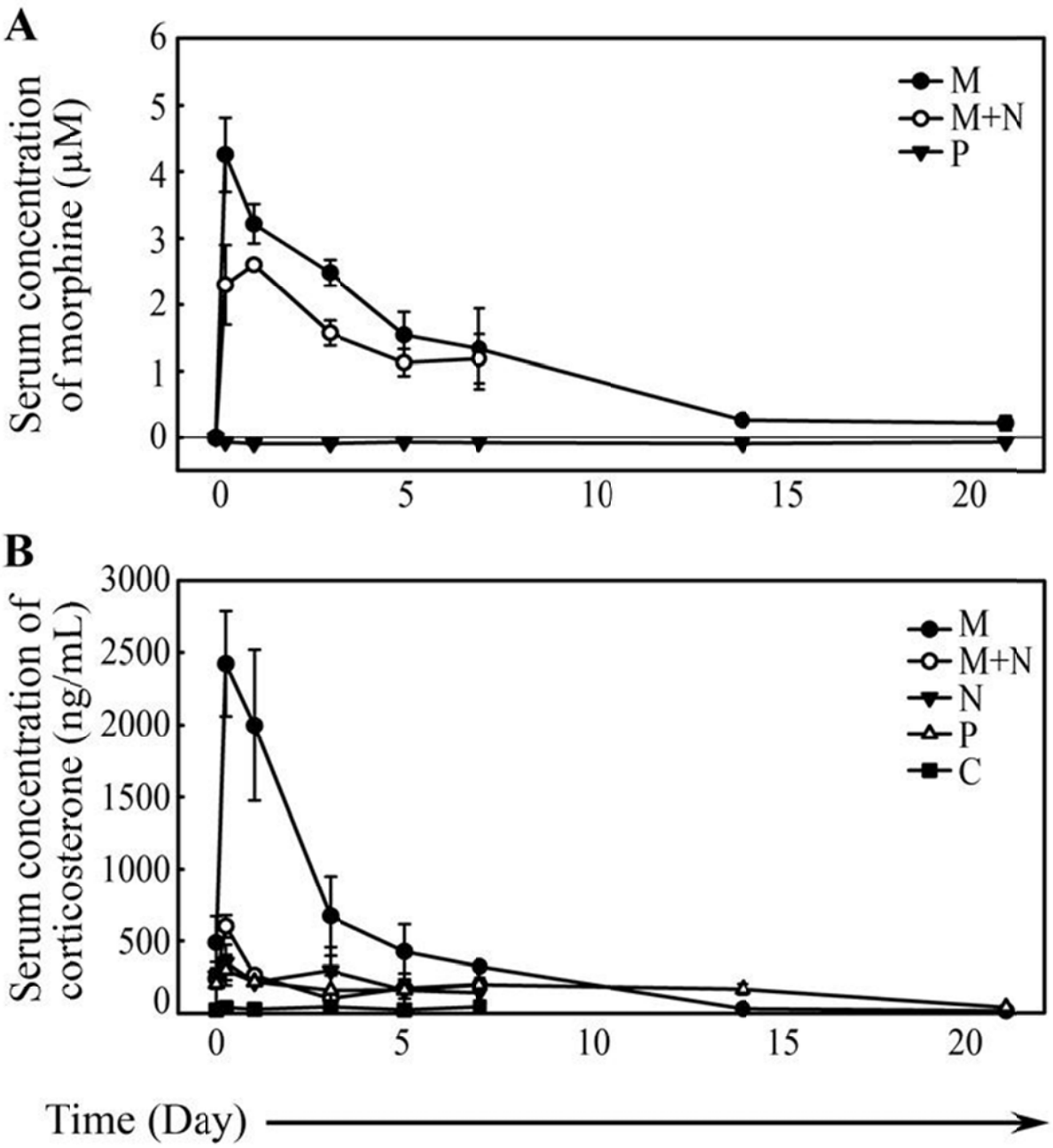
A
Serum concentration of morphine (μM)
6
5
4
3
2
1
0
0
5
10
15
20
M
M+N
P
B
Serum concentration of corticosterone (ng/mL)
3000
2500
2000
1500
1000
500
0
0
5
10
15
20
M
M+N
N
P
C
Time (Day)

Morphine does not directly impair T cell development

We tested whether morphine could directly impair T cell development using fetal thymic organ culture (FTOC). Thymi were collected from day E15.5 fetuses and cultured in the presence of morphine, morphine plus naltrexone, or no drug. The higher dose of morphine used in this experiment was based on the peak concentration of morphine in sera of morphine-treated mice. The lower dose of morphine used resembled the concentration of morphine in sera of mice treated with morphine for seven days. In addition, dexamethasone was added to some samples to mimic the effects of increased corticosteroid production *in vivo*. The concentration of dexamethasone used in this assay was approximately one-tenth the concentration of corticosterone observed *in vivo*. Because dexamethasone is approximately 10-fold more potent at inducing apoptosis of thymocytes than corticosterone (316), the relative activity of dexamethasone in our assay is comparable to the activity of corticosterone seen *in vivo*.

Similar numbers of thymocytes were recovered from thymi cultured with morphine, morphine plus naltrexone, and no drug (Fig. 5-12 A). Further, the distributions of DN, DP, SP $CD4^+$, and SP $CD8^+$ thymocytes were similar between morphine-treated samples and the control samples (Fig. 5-12 B). To ensure that morphine was not rapidly degraded in culture, we analyzed the concentration of morphine in a separate tissue culture experiment and found that the concentration remained stable for at least ten days (data not shown).

In contrast to morphine-treated samples, few thymocytes were harvested from dexamethasone-treated samples and most thymocytes recovered were DN thymocytes (Fig. 5-12). These data suggested that morphine does not directly induce loss of thymocyte populations. Rather, the depletion of thymocytes observed *in vivo* was most likely due to the surge in corticosterone levels.

Fig. 5-12. Morphine does not directly impair thymic development. FTOC was performed as described in *Methods* in the presence of 6 μM (M(H)) or 1 μM (M(L)) morphine, 6 μM morphine plus 6 μM naltrexone (M+N), 1 μM dexamethasone (D), or media (C). *A*) The absolute numbers of thymocytes recovered after seven days of culture are shown. *B*) Thymocytes were analyzed for CD4 and CD8 expression. The percentages of cells that were DN, DP, SP $CD4^+$, and SP $CD8^+$ thymocytes are shown. Dot plots represent one mouse from each group.

Figure 5-12

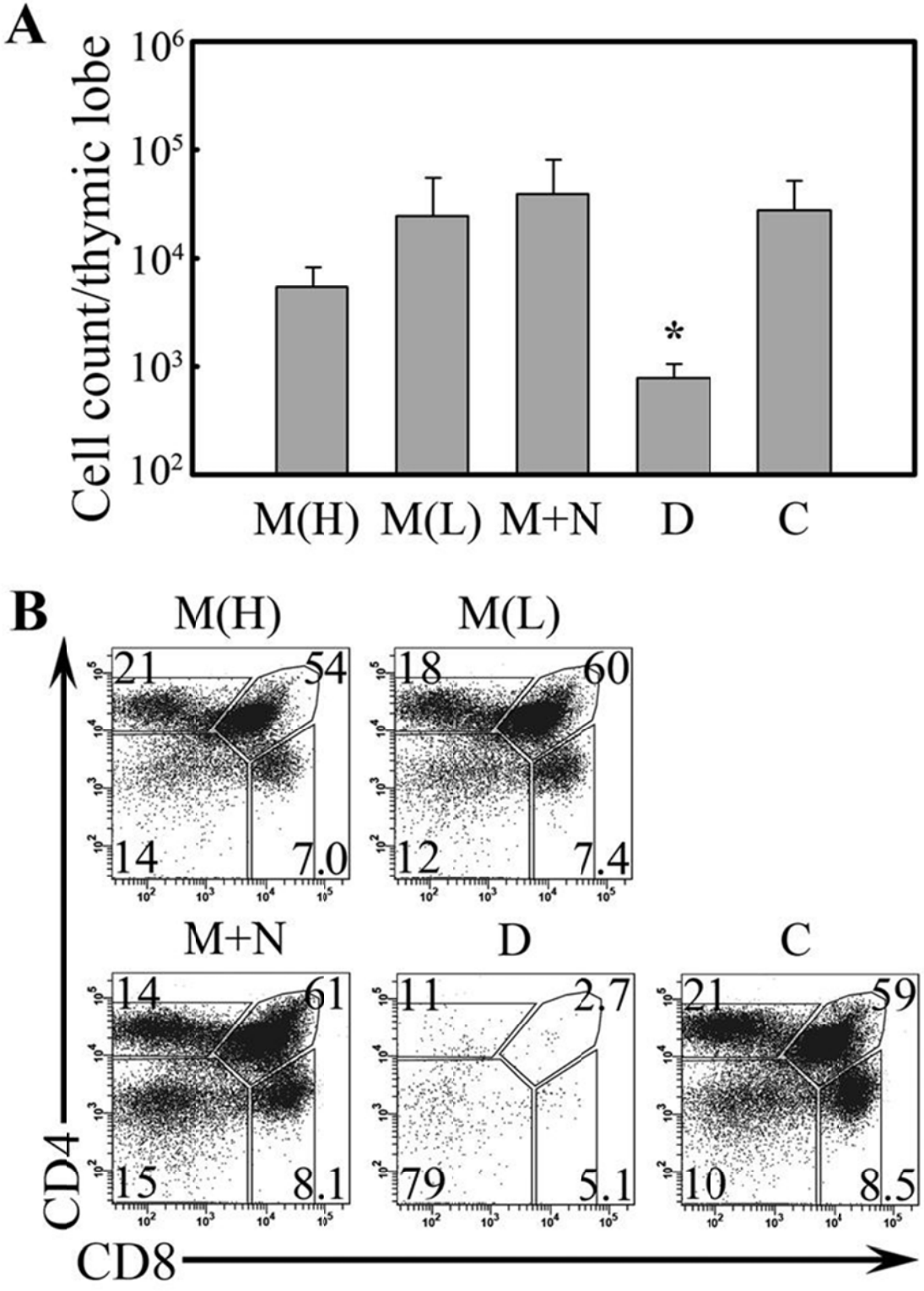
A
Cell count/thymic lobe
10^6
10^5
10^4
10^3
10^2
*
M(H) M(L) M+N D C
B
M(H)
M(L)
M+N
D
C
21 54 14 7.0
18 60 12 7.4
14 61 15 8.1
11 2.7 79 5.1
21 59 10 8.5
CD4
CD8

Discussion

In this report, we provide the most detailed analysis of B and T cell populations that remain after morphine treatment in mice. This level of description directed us toward discovering the mechanisms by which lymphocytes recover following morphine-induced depletion. We found that the mechanisms of recovery included a combination of accelerated B and T cell development and homeostatic proliferation of peripheral T cells. Understanding these mechanisms will enable us to comprehend the immunologic changes observed in patients using or abusing opioids.

The populations of lymphocyte precursors that were most susceptible to morphine-induced depletion were generally the populations that normally undergo positive selection. For example, the pro-B/pre-B cell, immature B cell, and T1 B cell subsets were dramatically depleted in morphine-treated mice (Fig. 5-1). The pre-B and immature B cell subsets are the populations in which rearrangements of the immunoglobulin genetic loci occur and the cells are under selection pressure to respond to pre-BCR and BCR signals. The T1 stage of B cell development is a transient stage that is also subjected to selection pressure (19). T1 cells also undergo a high degree of turnover (16). Although it is not clear whether MZ B cells continuously receive selection signals, MZ B cells proliferate and are eliminated at a higher rate than T2 and FO B cells (16). MZ B cells are also susceptible to morphine-induced depletion (Fig. 5-1), suggesting that cells that undergo high rates of turnover are particularly sensitive to morphine-induced depletion.

T cell precursors undergoing selection were also depleted following morphine treatment. Namely, TCRβ^+ DN thymocytes, ISP, and DP thymocyte subsets include cells that recently completed genomic rearrangements at the TCRβ and TCRα loci and receive signals from the pre-TCR or TCR to undergo positive selection. These populations were also highly sensitive to

morphine-induced depletion (Fig. 5-6). The TSP $CD4^+$ thymocyte population, which was depleted in morphine-treated mice, consists primarily of cells that completed positive selection (99) and receive signals that determine whether the cells become mature SP $CD4^+$ or mature SP $CD8^+$ cells (102-104). In our studies, we could not determine whether TSP $CD4^+$ thymocytes were direct targets of the effects of morphine or whether this population was depleted because of the dramatic losses in the cell populations that precede the TSP $CD4^+$ stage.

The stages of early T cell development that were most resistant to morphine treatment were the DN1 and DN2 stages (Fig. 5-5 A). These stages of T cell development are unique in that they are highly dependent upon Notch signaling for their survival (317, 318). After cells express TCRβ and cells proceed through the DN3L, DN4, ISP, and DP stages, Notch1 expression declines and the cells no longer respond to Notch ligands (319, 320). Thus, cells that respond to Notch ligands were relatively resistant to morphine-induced cell depletion. This observation is similar to previous studies that demonstrated that Notch signaling could render thymocytes resistant to corticosteroid-induced cell death (321), implying that corticosteroids, not morphine, are responsible for the thymocyte depletion observed in our studies. Indeed, we observed a large increase in serum corticosterone levels following morphine pellet implantation (Fig. 5-11 B), consistent with previous reports (322, 323).

We tested whether morphine could directly impair T cell development using FTOC. In this system, developing T cells are provided the stroma required for T cell development *in vivo*. Cells are able to survive, proliferate, and undergo positive and negative selection using FTOC. Further, because T cell development is a lifelong process, the FTOC system likely mimics T cell development at all stages of life. Morphine had no effect on the expansion and differentiation of thymocytes (Fig. 5-12). By contrast, few thymocytes were recovered from dexamethasone-

treated cultures. These observations were consistent with previous reports showing that morphine-induced thymic hypoplasia did not occur in adrenalectomized mice (306). These data indicate that morphine does not directly impair T cell development. Rather, the corticosterone production that resulted from morphine treatment likely prevented thymocyte expansion and differentiation.

The toxic effects of corticosteroids in the FTOC experiment are consistent with previous reports showing that corticosteroids induce apoptosis of developing B and T cells. *In vivo* administration of corticosterone resulted in a dramatic loss of thymic weight (180, 184, 185). Further, the immature T cell populations were most susceptible to corticosteroid treatment (178, 179, 181, 182). Like developing T cells, immature B cells were also susceptible to corticosterone-induced apoptosis, while other bone marrow cell types were resistant to corticosteroids (183-186, 324). The selective loss of lymphoid precursors in corticosterone-treated mice was similar to morphine-induced depletion of lymphocyte precursors.

Like immature lymphocytes, mature B and T cells were also susceptible to the depleting effects of morphine (Table 5-1), consistent with previous reports (187-189). While depletion of immature lymphocyte was most likely due to the effects of corticosteroids, depletion of mature lymphocytes was likely due to the interplay between corticosteroids and the μ opioid receptor. Stress responses, which lead to elevated corticosteroid levels, can trigger lymphocyte apoptosis in a manner dependent on elevated CD95/Fas expression and expression of the μ opioid receptor on splenocytes (325-327). Consistent with a role of corticosteroids in the depletion of splenocytes, the total number of splenocytes in mice decreased within two days of systemic prednisolone treatment (328, 329). *In vitro* experiments showed that prednisolone could induce apoptosis of mature lymphocytes (330-332). In our studies, we provided exogenous morphine and induced a corticosteroid response. Thus, cell depletion in our studies is likely due to the

direct effects of morphine as well as the indirect effect of corticosteroids influencing endogenous opioid production.

We observed a slight increase in serum corticosterone levels in all mice undergoing pellet implantation, although the increase was significantly greater in morphine-treated mice than control mice (Fig. 5-11 B). This transient increase in corticosterone levels likely accounts for the fact that the placebo pellets also affected some parameters analyzed within the B and T cell populations (Figs. 5-3, 5-8, 5-9 and 5-10).

The serum concentrations of morphine observed in our studies resembled physiologically relevant levels. While many opioid addicts have sustained serum morphine concentrations less that 0.1 μM (333), chronic morphine use can result in levels greater than 4 μM (334). This indicates that, while the levels of morphine observed in our studies are high, they are achievable in humans.

At least two mechanisms contributed to the recovery of peripheral B cell and T cells following morphine-induced depletion: increased lymphocyte production and homeostatic proliferation. For both B and T cells, there was an increase in the production of progenitor populations. Immature B cells and DN1, DN2, TCRβ^+ DN3E, and DP thymocytes proliferated more extensively two weeks after morphine pellet implantation than in control mice (Fig. 2D and Fig. 5-10 F). This proliferation would create a larger pool of cells to be released from the primary lymphoid organs into the secondary lymphoid organs.

These data are consistent with experiments in which dexamethasone was injected into mice and elevated serum levels of IL-7 and stromal cell-derived factor (SDF)-1α were observed (335). These cytokines are critical for B and T cell development (94, 336, 337). The primary function of IL-7 in T cell development is to promote the survival and proliferation of DN1 and DN2 thymocytes. In B cells, IL-7 promotes differentiation beyond the pre-B cell stage. Thus, IL-7

levels are likely elevated in morphine-treated mice and IL-7 would likely induce the increased proliferation of lymphoid precursors seen in this study.

In secondary lymphoid organs, B cells recovered to nearly normal levels in the three weeks after morphine pellet implantation while T cell numbers lagged. During the recovery, we did not observe an increase in the percentage of B cells that were in the S, G2, or M phase of the cell cycle (Fig. 5-3 B), suggesting that homeostatic proliferation was unlikely to be a mechanism by which peripheral B cell numbers recovered. By contrast, peripheral T cells displayed evidence of homeostatic proliferation, yet failed to restore their numbers to normal levels (Fig. 5-8 and 5-9). The consequence of this homeostatic proliferation is that an increased percentage of T cells had a memory phenotype and function. Memory T cells can be activated by a lower concentration or affinity of antigen than naïve cells and memory cells do not have a strict requirement for co-stimulation. This increase in memory cells is similar to what is observed in elderly patients, who are at increased risk for autoimmune disease (338, 339). This increase in memory cells also resembles that observed in patients undergoing therapy that causes lymphocyte depletion, such as cancer chemotherapy or anti-T cell therapy. In these patients, the conversion to memory cells is associated with autoimmune disease and transplant rejection (340, 341). Thus, it is possible that depletion and recovery of the T cell population may render patients susceptible to autoimmune disease.

In summary, we determined the mechanisms by which morphine administration to mice caused depletion of the B and T cell populations. We found that morphine had no direct effect on thymocyte populations and the profound depletion of thymocytes seen *in vivo* was most likely caused by an increase in the serum corticosterone levels. For mature lymphocyte subsets, depletion was most likely caused by a combination of corticosteroids and the direct effects of morphine. Once the corticosterone levels returned to control levels, the lymphocytes recovered even though morphine was still present at significant levels. This recovery was due to a

combination of increased B and T cell production and homeostatic proliferation. Homeostatic proliferation was most evident among T cells and not detected in B cells, indicating that different populations of lymphocytes have different propensities to undergo homeostatic proliferation in morphine-treated mice.

Chapter VI

Discussion and Conclusions

The studies presented in my PhD dissertation can be divided into two sub-topics. Firstly, in Chapters II-IV, I emphasize the studies on peripheral $CD8^+$ T cells, which represent my primary research interest, and the role of Gads in $CD8^+$ T cell-mediated immune responses. In Chapter II, I address the role of Gads in proliferation and cell cycle entry of $CD8^+$ T cells upon TCR ligation *in vitro*. The focus of Chapter III is placed on the effect of Gads on $CD8^+$ T cell-mediated immune responses upon infection with an intracellular pathogen, rLM. In Chapter IV, I investigate the homotypic interactions among $CD8^+$ T cells and the role of Gads in the interactions. Then, the process of morphine-induced lymphocyte depletion and recovery is studied in Chapter V with focus on the mechanisms by which T and B lymphocyte populations are depleted and recovered following morphine treatment in mice. Here, I will summarize the findings of the research projects for my dissertation, integrate the experimental results from Chapter II to IV, and propose a model which is supported by the data from Chapter II to Chapter IV. In addition, I will discuss future directions for the “Gads-CD8” project.

The “discrepancy” between *in vitro* cell cycle data in Chapter II and *in vivo* infection data in Chapter III

In Chapter II, I demonstrate that Gads regulates the kinetics of cell cycle entry of $CD8^+$ T cells, as $Gads^{-/-}$ $CD8^+$ T cells had impaired TCR-dependent exit from G0 phase of the cell cycle. However, in Chapter III, regarding the immune response to infection, I showed that Gads is not required for the onset of accumulation $CD8^+$ T cells, as for the first 5 days p.i., $Gads^{+/+}$ and $Gads^{-/-}$ $CD8^+$ T cells accumulated to a similar extent. How do we explain these apparently contradictory results? A possibility is that rLM-OVA infection results in the production and

presentation of a large quantity of high affinity antigen that can overcome Gads deficiency. As we showed in Chapter II, stimulating Gads$^{-/-}$ cells with a high concentration of SIINFEKL largely rescued the defect in proliferation *in vitro* (Fig 2-3). However, analyses of results in Chapter IV revealed a more likely interpretation: the homotypic interactions among CD8^{+} T cells might facilitate the TCR signaling so as to compensate for Gads deficiency in promoting cell cycle entry and proliferation. In addition, we acknowledge that the potential influence of inflammatory mediators induced by the infection might also contribute to overcoming the need for Gads.

In Chapter II, total splenocytes, including CD8^{+} T cells, B cells, DCs, and macrophages, were stimulated with SIINFEKL. Most likely, antigen presenting cells (APCs) (mainly B cells in this context) serve as the major resources to present antigen and provide ligands for the adhesion molecules and other co-receptors on CD8^{+} T cells. In the following text, "conventional APCs" will be used to stand for these APCs, which express MHC class I and are non-CD8^{+} T cells. When total splenocytes were stimulated, the defect of Gads$^{-/-}$ CD8^{+} T cells in cell cycle entry and proliferation is so obvious that it affects proliferation later on (Fig 2-3). In Chapter III, Gads does not regulate the initiation stage of proliferation of antigen-specific CD8^{+} T cells in the context of infection. However, Gads regulates the optimal expansion of the CD8^{+} T cell population. In Chapter IV, the homotypic interactions among CD8^{+} T cells and the interactions between CD8^{+} T cells and conventional APCs were compared to reveal their role in TCR-mediated signaling. Based on the previous results, I hypothesize that adhesion molecule-dependent signaling regulates the expansion phase of CD8^{+} T cell-mediated immune responses induced by infection with rLM, in a stage (early and later stage)-dependent manner. During the early stage of the expansion phase, after DCs present antigen to CD8^{+} T cells, homotypic interactions among CD8^{+} T cells promote the accumulation of antigen-specific CD8^{+} T cells, while the association between CD8^{+} T cells and conventional APCs sustains the expansion phase later on. Both the homotypic interactions among CD8^{+} T cells during the early stage and

the interactions between $CD8^+$ T cells and conventional APCs during the later stage are regulated by either different adhesion molecules or same adhesion molecules via different mechanisms. Gads regulates the interactions between $CD8^+$ T cells and conventional APCs at later stage rather than the homotypic interaction among $CD8^+$ T cells at early stage of expansion phase in the immune responses.

The experimental systems were different between *in vitro* proliferation of $CD8^+$ T cells where total splenocytes were stimulated with peptides in Chapter II and the *in vivo* accumulation of $CD8^+$ T cells triggered by rLM infection in Chapter III. *In vivo* infection system is much more complicated than *in vitro* culture system as infection triggers the responses from the entire immune system rather than several types of immune cells *in vitro*. For example, pathogen-induced inflammatory cytokines, such as type I interferons (IFN-αβ), type II interferon (IFN-γ) and IL-12, act directly on the responding $CD8^+$ T cells to regulate the expansion and differentiation of pathogen-specific $CD8^+$ T cells (342-345). IL-15 and IL-7 have been reported to promote the survival of SLECs and MPECs, individually (346, 347). In addition, IL-2, IL-15 and IL-21 regulate the fate decision of memory precursors into either central memory or effector memory populations (347, 348).

In order to avoid involving the differences of experimental systems, I stimulated $CD8^+$ T cells *in vitro* with SIINFEKL or anti-CD3 and anti-CD28 and then checked the formation of cell clusters and the cell cycle entry. The only difference was that either total splenocytes or purified $CD8^+$ T cells were stimulated. By stimulating purified $CD8^+$ T cells instead of the total splenocytes, $CD8^+$ T cells had much bigger cell clusters accompanied with advanced cell cycle progression. This observation was true for both $Gads^{+/+}$ cells and $Gads^{-/-}$ cells (Fig. 4-5 A). As compared with $Gads^{+/+}$ $CD8^+$ T cells, $Gads^{-/-}$ $CD8^+$ T cells behaved similarly or better in terms of cell cluster formation. In addition, the defect of cell cycle progression in $Gads^{-/-}$ $CD8^+$ T cells was largely rescued. These data support my model that the homotypic interactions among $CD8^+$ T

cells overcome the need for Gads in the accumulation of OVA-specific $CD8^+$ T cells at early stage of infection with rLM-OVA.

In order to test the hypothesis using infection model, we would like to see the interactions involving antigen-specific $CD8^+$ T cells after infection. Recently, in situ imaging using multiphoton microscopy (349) and dynamic imaging of live tissue using intravital microscopy (249) were applied to the study of the immune response to LM infection. Both studies revealed that after activation, antigen-specific $CD8^+$ T cells aggregate together in spleen during the expansion phase of the immune response.

The above experimental results from others and us suggest that the homotypic interactions between $CD8^+$ T cells *in vivo* might play a critical role in TCR-mediated cell cycle entry so as to overcome the need for Gads in the initiation stage of $CD8^+$ T cell-mediated immune responses upon infection with rLM-OVA.

We raise the concept that T cells can serve as APCs to present Ag to other T cells as well as provide costimulatory signals through adhesion molecules so as to activate T cells. The homotypic interactions was described as “in the absence of APCs” by several groups (301, 350). Are APCs really absent? In those T cell clusters, we believe, T cells themselves serve as APCs. Let’s take an example in the experimental system using purified $CD8^+$ T cells, which were from OT-I mice, stimulated with SIINFEKL. The MHC class I molecules on the surface of $CD8^+$ T cells present SIINFEKL to other $CD8^+$ T cells. The binding of ligands and receptors, which are adhesion molecules, regulates the homotypic interactions and facilitate the TCR signaling. However, we have no solid data to reveal whether the MHC class I molecules and ligands of coreceptors have to come from a different $CD8^+$ T cells or could be from the stimulated $CD8^+$ T cell itself. In other words, can a $CD8^+$ T cell serve as APC to itself? It is possible that the self-presenting and self-costimulation as well as regular antigen presentation and costimulation between different $CD8^+$ T cells happen simultaneously. This possibility needs to be tested.

Then, we ask whether homotypic interactions can stimulate $CD8^+$ T cells without antigen. The results in chapter IV indicate that homotypic interactions among $CD8^+$ T cells could induce the formation of cell clusters (Fig. 4-5 A) but could not initiate cell cycle progression in unstimulated samples, as almost all the $CD8^+$ T cells were in G0 phase of the cell cycle (Fig. 4-6). So that we conclude that homotypic interactions among $CD8^+$ T cells can facilitate TCR signaling only when antigen is present to initiate the TCR signaling. Is antigen still required after the initiation stage? In the case of immune response of $CD8^+$ T cells upon infection with LM, the answer is “no”. The Pamer group demonstrated that generation of Ag-specific $CD8^+$ T cell population could occur when Ag exposure was transient upon infection with rLM (351, 352). Prlic *et. al.* (353) further reported that upon infection with LM, shortening antigen exposure time significantly reduced the primary immune response but not recall response of $CD8^+$ T cells. In primary response to LM infection, there were less antigen-specific $CD8^+$ T cells accumulated with reduced proliferating rate by shortening antigen exposure time. In contrast, the antigen exposure time does not affect $CD8^+$ T cell functionality in terms of IFN-γ secretion in both primary and recall response. These results indicate that the expansion and differentiation of $CD8^+$ T cells can take place without persistent exposure to antigen. Is antigen required all the time for homotypic interactions among $CD8^+$ T cells in the context of infection? In order to address this question, we could perform the experiment based on what we did in Chapter III. In addition, at 1-2 days p.i., antibiotics will be administered to infected mice to eliminate the antigen. Then we could visualize the effect of antigen removal on interactions involving antigen-specific $CD8^+$ T cells: interactions with conventional APCs as well as homotypic interactions among $CD8^+$ T cells, using microscopic techniques.

The role of LFA-1-mediated signaling in Gads-dependent homotypic interactions and its application

In order to identify the adhesion molecules on the surface of $CD8^+$ T cells to mediate the homotypic interactions, we looked at the first candidate: LFA-1. We found that Gads negatively regulates the expression level of LFA-1 protein (Fig. 4-3), which was further supported by the fact that the peripheral tissues, such as lung, from $Gads^{-/-}$ mice have higher percentages and larger quantities of $CD8^+$ T cells than $Gads^{+/+}$ mice (Fig. 4-4). Anti-LFA-1 (anti-CD11a) binds the α chain of the LFA-1 molecule so that the application of the antibody *in vitro* or *in vivo* could reduce LFA-1-mediated functions, such as cell-cell adhesion, T cell-mediated cytotoxicity, and the severity of graft-versus-host reactions (354-358). In order to test whether LFA-1 regulates interactions between $CD8^+$ T cells and conventional APCs and the homotypic interactions among $CD8^+$ T cells, soluble anti-LFA-1 was added into the cell culture media to block LFA-1-mediated signaling. In total splenocytes, LFA-1 not only regulates the formation of cell clusters, but also regulates cell cycle entry; in purified $CD8^+$ T cells, LFA-1 does facilitate the formation of cell clusters, but not cell cycle entry. These observations indicate that LFA-1 mediates homotypic interactions among $CD8^+$ T cells, but not their cell cycle progression.

How did anti-LFA-1, however, decrease the degree of cell cluster formation in purified $CD8^+$ T cells 21 hours after TCR ligation but not cell cycle entry? One possibility is that some of the anti-LFA-1 stuck to the bottom of the plate and became plate-bound anti-LFA-1 during the 21-hour incubation, resulting in the functional change from blocking LFA-1 signaling earlier to stimulat later on. During the first several hours, the added anti-LFA-1 mainly functions as a blocker. If we shorten the duration the incubation time to several hours, it might give us a direct answer to whether LFA-1 can regulate the homotypic interactions to promote cell cycle progression of $CD8^+$ T cells. We might measure the increasing RNA content in purified $CD8^+$ T cells in the first several hours, to look at the early stage of cell cycle entry.

In the conjugation assay, during which anti-LFA-1 was present for a relatively short time, anti-LFA-1 inhibited the formation of $CD8^+$ T cell-EL-4 cell conjugates (data not shown). It supported the conclusion that LFA-1 mediates the interaction between $CD8^+$ T cells and other cells (EL-4 cells here). To address the question whether Gads and LFA-1 can regulate the homotypic interactions among $CD8^+$ T cells, we could perform the conjugation assay among $CD8^+$ T cells. $CD8^+$ T cells will be purified from $Gads^{-/-}$ OT-I and $Gads^{+/+}$ OT-I mice. Then an aliquot of the $CD8^+$ T cells, which play the role as APCs, will be pulsed with peptide ligand SIINFEKL, A2 or G4 after CFSE loading. After removing the free peptide in solution by centrifugation, the peptide-pulsed $Gads^{+/+}$ or $Gads^{-/-}$ $CD8^+$ T cells (I will call them "APC"-CD8 for short in the following text) will be incubated with non-CFSE loaded, non-pulsed $Gads^{+/+}$ or $Gads^{-/-}$ $CD8^+$ T cells in the presence or absence of anti-LFA-1. The analyses will be based on comparisons of the percentages of $CD8^+$ T cells which will have been conjugated with "APC"-CD8 between different samples. Samples will include:

① $Gads^{-/-}$ $CD8^+$ T cells incubated with SIINFEKL-pulsed $Gads^{-/-}$ "APC"-CD8, w/ anti-LFA-1;

② $Gads^{-/-}$ $CD8^+$ T cells incubated with SIINFEKL-pulsed $Gads^{+/+}$ "APC"-CD8, w/ anti-LFA-1;

③ $Gads^{+/+}$ $CD8^+$ T cells incubated with SIINFEKL-pulsed $Gads^{-/-}$ "APC"-CD8, w/ anti-LFA-1;

④ $Gads^{+/+}$ $CD8^+$ T cells incubated with SIINFEKL-pulsed $Gads^{+/+}$ "APC"-CD8, w/ anti-LFA-1;

⑤ $Gads^{-/-}$ $CD8^+$ T cells incubated with SIINFEKL-pulsed $Gads^{-/-}$ "APC"-CD8, w/o anti-LFA-1;

⑥ $Gads^{-/-}$ $CD8^+$ T cells incubated with SIINFEKL-pulsed $Gads^{+/+}$ "APC"-CD8, w/o anti-LFA-1;

⑦ $Gads^{+/+}$ $CD8^+$ T cells incubated with SIINFEKL-pulsed $Gads^{-/-}$ "APC"-CD8, w/o anti-LFA-1;

⑧ $Gads^{+/+}$ $CD8^+$ T cells incubated with SIINFEKL-pulsed $Gads^{+/+}$ "APC"-CD8, w/o anti-LFA-1.

There will be another set of the above samples for un-pulsed group as control. If anti-LFA-1 reduces the conjugation level among $CD8^+$ T cells, it would suggest that LFA-1 indeed plays a role in the homotypic interactions among $CD8^+$ T cells. Besides this important conclusion, we might also get other information from this experiment. For example, does Gads regulate the

conjugation among $CD8^+$ T cells? Is the role of Gads in the formation of conjugates on the side of $CD8^+$ T cells or on the side of "APC"-CD8 or both? Possible results and explanations are listed here (Table 6-1).

LFA-$1^{-/-}$, also known as $CD11a^{-/-}$ mice, were generated by deletion of CD11a gene (359, 360). Using LFA-$1^{-/-}$ mice, recently, the effect of LFA-1 on $CD8^+$ T cell-mediated immune response to infection with LM was reported (361). After infection with LM, compared with wild type mice, LFA-$1^{-/-}$ mice generated blunted primary $CD8^+$ T cell responses after infection. In detail, in the absence of LFA-1, there was decreased immune response of $CD8^+$ T cells, together with the reduced differentiation of the SLEC subset. However, LFA-$1^{-/-}$ $CD8^+$ T cells had similar level of cytokine secretion, when compared with LFA-$1^{+/+}$ $CD8^+$ T cells during primary responses. Generally, the $CD8^+$ T cell-mediated primary immune responses against LM infection had a lot of similarities between LFA-$1^{-/-}$ mice and our $Gads^{-/-}$ mice. In Chapter IV, our data showed, however, $Gads^{-/-}$ $CD8^+$ T cells had higher expression of LFA-1 than $Gads^{+/+}$ $CD8^+$ T cells (Fig. 4-3). Thus, the relationship between Gads and LFA-1 in TCR-dependent immune responses could be complicated.

At the early stage of the immune response: in the absence of LFA-1, antigen-specific $CD8^+$ T cells had diminished expansion of the population from the beginning of the immune response. It was consistent with our data and hypothesis that LFA-1 is a critical regulator for the formation of cell conjugates among $CD8^+$ T cells in the spleen after infection so as to promote proliferation of antigen-specific $CD8^+$ T cells. With the regulation of LFA-1, $Gads^{-/-}$ $CD8^+$ T cells had normal beginning of immune responses.

There is one possibility that LFA-1 regulates the interaction between $CD8^+$ T cells and APCs and the homotypic interactions among $CD8^+$ T cells via binding different ligands. ICAM regulates the memory phase of immune response of $CD8^+$ T cells, as $ICAM^{-/-}$ mice have

Table 6-1. Possible results of the conjugation experiments among $CD8^+$ T cells.	
Compare conjugation level among samples	Interpretation
① < ⑤, ② < ⑥, ③ < ⑦, ④ < ⑧.	LFA-1 promotes homotypic interactions among $CD8^+$ T cells.
① = ⑤, ② = ⑥, ③ = ⑦,④ = ⑧.	LFA-1 does not promote homotypic interactions among $CD8^+$ T cells.
① > ⑤, ② > ⑥, ③ > ⑦,④ > ⑧.	LFA-1 inhibits homotypic interactions among $CD8^+$ T cells.
① > ②, ③ > ④, ⑤ > ⑥,⑦ > ⑧.	Gads inhibits homotypic interactions among $CD8^+$ T cells on “APC”-CD8 side.
① = ②, ③ = ④, ⑤ = ⑥,⑦ = ⑧.	Gads does not regulate homotypic interactions among $CD8^+$ T cells on “APC”-CD8 side.
① < ②, ③ < ④, ⑤ < ⑥,⑦ < ⑧.	Gads promotes homotypic interactions among $CD8^+$ T cells on “APC”-CD8 side.
① > ③, ② > ④, ⑤ > ⑦,⑥ > ⑧.	Gads inhibits homotypic interactions among $CD8^+$ T cells on $CD8^+$ T cell side.
① = ③, ② = ④, ⑤ = ⑦,⑥ = ⑧.	Gads does not regulate homotypic interactions among $CD8^+$ T cells on $CD8^+$ T cell side.
① < ③, ② < ④, ⑤ < ⑦,⑥ < ⑧.	Gads promotes homotypic interactions among $CD8^+$ T cells on $CD8^+$ T cell side.
① > ②, ① > ③, ① > ④, ⑤ > ⑥, ⑤ > ⑦, ⑤ > ⑧.	Gads inhibits homotypic interactions among $CD8^+$ T cells on both “APC”-CD8 side and $CD8^+$ T cell side.
① = ② = ③ = ④, ⑤ = ⑥ = ⑦ = ⑧.	Gads does regulate homotypic interactions among $CD8^+$ T cells.
①<②,①<③,①<④, ⑤<⑥,⑤<⑦,⑤<⑧.	Gads promots homotypic interactions among $CD8^+$ T cells on both “APC”-CD8 side and $CD8^+$ T cell side.

reduced memory $CD8^+$ T cell activity (362). In contrast, LFA-1 not only regulates the survival ofmemory $CD8^+$ T cells in memory phase, but also the survival of effector $CD8^+$ T cells in the expansion and contraction phases (286). These findings support the model that LFA-1 has a ligand other than ICAM-1 to regulate TCR singling in $CD8^+$ T cells. Besides ICAM-1, ligands of LFA-1 include ICAM-2, ICAM-3, and JAM-1 (363, 364). In addition, Scholer *et. al.* (362) reported that ICAM-1 on mature DCs is critical for long-lasting contacts with $CD8^+$ T cells but is dispensable for short-lived antigen-specific interactions. So that during the $CD8^+$ T cell-mediated immune responses, such as those upon LM infection, the signaling mediated via homotypic interactions among $CD8^+$ T cells might mainly regulate the onset of the response; and interaction between DCs and $CD8^+$ T cells plays a major role later on. I hypothesize the role of LFA-1 in $CD8^+$ T cell-mediated immune response is dependent on the stages of the response. In detail, the signaling, which is not mediated by the interaction between LFA-1 and ICAM-1, regulates the homotypic interactions among $CD8^+$ T cells in the initiation stage. In contrast, the association between LFA-1 on $CD8^+$ T cells and ICAM-1 on “conventional APCs” sustains the expansion phase later on. Gads is required for the optimal expansion of $CD8^+$ T cell population (Fig. 3-1). Furthermore, homotypic interactions among $CD8^+$ T cells, which can compensate for Gads deficiency in the formation of cell clusters, are mediated by LFA-1 (Fig. 4-5). The modulatory effect of Gads in the later stage of expansion of $CD8^+$ T cell population in primary response to infection might be mediated through LFA-1.

In addition, other evidences suggest that the role of Gads in the secondary immune responses of $CD8^+$ T cells is not mediated by LFA-1. Gads is required for the secondary responses of $CD8^+$ T cells (Fig. 3-8) to LM infection, while LFA-1 is dispensable, as the antigen-specific memory CD8 T cells in LFA-$1^{-/-}$ mice responded robustly (361).

Other thoughts about LM infection

The classic rLM infection model has been widely used to study $CD8^+$ T cells (219, 243, 252). Many studies, including ours, were performed by adoptively transferring $CD8^+$ T cells from TCR transgenic (such as OT-I) mice into recipient mice and then infecting with the strain of bacteria expressing the antigen recognized by the transgenic TCR (such as rLM-OVA). However, these models involving the exogenous TCR transgenic T cells might not mimic very well the authentic immune responses upon infection. Firstly, by administrating the transgenic T cells, the model brings a lot of complexities. For example, the number of exogenous TCR transgenic $CD8^+$ T cells affects immune responses including the formation and proliferation of memory cells. The more $CD8^+$ T cell adoptively transferred, the more central memory cells formed and the faster the memory $CD8^+$ T cells proliferated (365). In addition, TCR transgenic T cells, which are adoptively transferred, exhibits distinct physiological characteristics from endogenous congenic wild type $CD8^+$ T cells. The characteristics include different survival and lymphopenia-driven proliferation requirements (366). Secondly, the endogenous $CD8^+$ T cells also respond to LM infection, so the immune responses mediated by endogenous and exogenous $CD8^+$ T cells might affect each other such as secreting cytokines or competing with “space” for expanding their own populations. It would be better to avoid using the adoptive transfer the OT-I cells by infecting mice with LM and using GYKDGNEYI MHC class I Pentamer to identify the antigen-specific $CD8^+$ T cell response to LM infection (367, 368). LM secretes, listeriolysin O (LLO), which is pore-forming cytolysin, into the cytosol of infected host cells (369, 370). The peptide GYKDGNEYI is the amino acid 91-99 of LLO, a known immunodominant epitopes of LM (371). GYKDGNEYI MHC class I Pentamer comprises five MHC class I-peptide complexes assembled through a coiled-coil domain. All five MHC class I-peptide complexes in the Pentamer bind to TCR of LLO specific-$CD8^+$ T cells. A drawback of this method is, in peripheral lymphoid tissues, most of the $CD8^+$ T cells in conventional $Gads^{-/-}$ mice are memory $CD8^+$ T cells, while most of

them in wild type C57BL/6 mice are naïve $CD8^+$ T cells (Fig. 2-1). Memory T cells are more responsive to antigen than naive T cells, and there is increased TCR-mediated signaling in memory T cells than naïve T cells (204). So if the study is performed by infecting conventional $Gads^{-/-}$ mice and wild type mice without adoptive transferring OT-I cells, it is not fair to compare naïve $Gads^{+/+}$ $CD8^+$ T cells and memory-like $Gads^{-/-}$ $CD8^+$ T cells in respond to LM infection. Based on the above information regarding different method, at present, the method we used in my dissertation probably is a better way to study the effect of Gads on $CD8^+$ T cell-mediated immune response upon infection. Meanwhile, we also acknowledge that both methods have their own advantages and limitations.

We reveal the role of Gads in different phases of $CD8^+$ T cell-mediated immune responses here in my dissertation. However, we did not directly show the effect of Gads on the clearance of LM. In the future, we might isolate spleen and liver and analyze the CFU of LM at different times (at 4 to 7 days p.i.) and compare whether $Gads^{+/+}$ $CD8^+$ T cells and $Gads^{-/-}$ $CD8^+$ T cells have different ability to mediate killing LM. Alternatively, we could perform a cytotoxic T lymphocyte assay *in vitro* and *in vivo*. To measure cytotoxicity *in vitro*, a chromium-release assay could be performed. Briefly, OVA-specific $Gads^{-/-}$ or $Gads^{+/+}$ $CD8^+$ T cells, which are effector cells, will be FACS-purified from infected mice. EL-4 cells, which are target cells, will be incubated with radioactive chromium (^{51}Cr) and pulsed with SIINFEKL. After washing to remove the extra peptide and ^{51}Cr, target cells will be mixed with effector cells at different ratios. ^{51}Cr, which have been absorbed by target cells during incubation, will be released into supernatant when the cells die. We will have spontaneous lysis control by measuring ^{51}Cr release from target cells in the absence of effector cells. Maximum lysis control will be measured when detergent (Triton X-100), but not effector cells, is added. Radioactivity of the supernatants is measured using scintillation counter. The amount of radioactivity measured in the supernatant is a proxy for the number of cells that have been killed by effector cells (372). The difference of

released chromium between samples containing Gads$^{-/-}$ cells or Gads$^{+/+}$ will be compared. To measure cytotoxicity *in vivo*, splenocytes from CD90.1 C57BL/6 are harvested and split into two aliquots. One aliquot is labeled with a high concentration of CFSE, while the other aliquot is labeled with a low concentration of CFSE. Then, the CFSE^{hi} splenocytes are pulsed with SIINFEKL while the CFSE^{lo} splenocytes are pulsed with an irrelevant peptide to serve as an internal control. After washing to get rid of the extra peptides, the two populations are mixed at a 1:1 ratio. Then, the mixture of cells are injected i.v. into the recipient mice, which will have been adoptively transferred with CD8^{+} T cells from Gads$^{-/-}$ or Gads$^{+/+}$ OT-I mice 7 days ago and infected with rLM-OVA 6 days ago as what we have done in Chapter IV. The next day, splenocytes of recipient mice are isolated and the ratio CFSE^{hi} cells to CFSE^{lo} cells will be analyzed by flow cytometry as evidence of *in vivo* killing. SIINFEKL-pulsed CD90.1 cells will be recognized by OVA-specific CD8^{+} T cells in the recipient, resulting in the destruction of target cells. The “killing” ability of OVA-specific CD8^{+} T cells will be determined by the decreased percentages of CFSE^{hi} cells, which have been pulsed with SIINFEKL, as compared with CFSE^{lo} cells, which have not been pulsed with SIINFEKL. The effect of Gads on cytotoxicity of CD8^{+} T cells will be evaluated by the results of the above three experiments comparing the killing activities between Gads$^{-/-}$ CD8^{+} T cells and Gads$^{+/+}$ CD8^{+} T cells. The differences of between the percentages of CFSE^{hi} cells targeted by Gads$^{-/-}$ CD8^{+} T cells and Gads$^{+/+}$ CD8^{+} T cells.

Upon infection with blood borne pathogens, such as LM, immune responses mainly occur in spleen. DCs in the MZ and red pulp of spleen encounter LM from blood and present the antigen from LM to T CD8^{+} T cells to initiate the immune responses to infection (246-248). Although the innate immune system can restrict LM infection to certain extent, CD8^{+} T cells are required for sterilizing immunity (251). Driven by the inflammatory signals, which start to be generated in the innate immune responses, chemokines and chemokine receptors regulate the migration of CD8^{+} T cells and may also facilitate the cell clustering among them. So that, besides adhesion

molecules, such as integrin family proteins on the surface of $CD8^+$ T cells, chemokines and chemokine receptors might also contribute to the homotypic interactions among $CD8^+$ T cells.

Other evidence supporting that Gads regulates adhesion signaling

ADAP, is also known as FYN binding protein (FYB-120/130), FYB, and SLAP-130 (SLP-76 associated phosphoprotein of 130 kDa). ADAP is necessary for optimal T cell responses and activation of integrins (373, 374). For example, ADAP is required for TCR-induced clustering of LFA-1 and the associated changes in the adhesion of antigen-stimulated T cells (375). The interaction of ADAP with SLP-76 is required for TCR-induced, LFA-1-mediated cell clustering (376). Upon TCR ligation, Gads associates with ADAP via SLP-76 (138). Gads constitutively interacts with SLP-76 (2, 6, 15, 17, 29, 30, 48). From these evidences, Gads might regulate TCR-induced cell clustering through ADAP.

TCR microclusters, which are formed after TCR ligation, provide an actin-dependent scaffold for signal amplification (71). Cytoskeletal changes are required for lymphocyte movement, and they accompany and control adhesive interactions to regulate cell-cell interactions (377). A number of TCR signaling-dependent proteins including WASP and ADAP, have been found to regulate actin polymerization (378-380). Those proteins have been detected directly or indirectly associated with Gads. In addition, Gads associates with Ezrin, which belongs to the ERM (Ezrin-Radixin-Moesin) protein family. The above results suggest that Gads might closely regulate cytoskeletal movement. More research needs to be performed to investigate whether and how Gads regulates actin remodeling in T cells.

Conclusions and implications

The primary goal of my dissertation is to investigate the role of Gads in CD8+ T cell-mediated immunity. In Chapter II, I have addressed in detail how Gads regulates the activation and proliferation of $CD8^+$ T cells following stimulation with peptide agonists. Then in Chapter III, The results indicated that Gads regulates the expansion phase of $CD8^+$ T cell-mediated immune response upon infection with an intracellular pathogen as well as optimal recall responses but not the formation of memory $CD8^+$ T cells. Next in Chapter IV, Our recent data showed that the homotypic interactions among $CD8^+$ T cells could overcome the need for Gads in promoting cell cycle progression. To conclude, the research in my dissertation demonstrates that the role of Gads in TCR-mediated activation of $CD8^+$ T cells is dependent on the interaction of $CD8^+$ T cells and their partners. Interestingly, if $CD8^+$ T cells interact with conventional APCs, Gads promotes the interaction and regulate the kinetics of cell cycle entry; if $CD8^+$ T cells interact with other $CD8^+$ T cells, however, Gads inhibits the homotypic interactions and Gads is dispensable for cell cycle entry of $CD8^+$ T cells. Potentially, this knowledge can be applied to the therapies such as increasing the activation of $CD8^+$ T cells in the treatment for tumors and bacterial or viral infections and inactivating $CD8^+$ T cells in the treatment for autoimmune diseases.

References

1. Bourette, R. P., S. Arnaud, G. M. Myles, J. P. Blanchet, L. R. Rohrschneider, and G. Mouchiroud. 1998. Mona, a novel hematopoietic-specific adaptor interacting with the macrophage colony-stimulating factor receptor, is implicated in monocyte/macrophage development. *EMBO J* 17:7273-7281.

2. Asada, H., N. Ishii, Y. Sasaki, K. Endo, H. Kasai, N. Tanaka, T. Takeshita, S. Tsuchiya, T. Konno, and K. Sugamura. 1999. Grf40, A novel Grb2 family member, is involved in T cell signaling through interaction with SLP-76 and LAT. *J Exp Med* 189:1383-1390.

3. Qiu, M., S. Hua, M. Agrawal, G. Li, J. Cai, E. Chan, H. Zhou, Y. Luo, and M. Liu. 1998. Molecular cloning and expression of human grap-2, a novel leukocyte-specific SH2- and SH3-containing adaptor-like protein that binds to gab-1. *Biochem Biophys Res Commun* 253:443-447.

4. Liu, S. K., and C. J. McGlade. 1998. Gads is a novel SH2 and SH3 domain-containing adaptor protein that binds to tyrosine-phosphorylated Shc. *Oncogene* 17:3073-3082.

5. Ellis, J. H., C. Ashman, M. N. Burden, K. E. Kilpatrick, M. A. Morse, and P. A. Hamblin. 2000. GRID: a novel Grb-2-related adapter protein that interacts with the activated T cell costimulatory receptor CD28. *J Immunol* 164:5805-5814.

6. Law, C. L., M. K. Ewings, P. M. Chaudhary, S. A. Solow, T. J. Yun, A. J. Marshall, L. Hood, and E. A. Clark. 1999. GrpL, a Grb2-related adaptor protein, interacts with SLP-76 to regulate nuclear factor of activated T cell activation. *J Exp Med* 189:1243-1253.

7. Cheng, A. M., T. M. Saxton, R. Sakai, S. Kulkarni, G. Mbamalu, W. Vogel, C. G. Tortorice, R. D. Cardiff, J. C. Cross, W. J. Muller, and T. Pawson. 1998. Mammalian

Grb2 regulates multiple steps in embryonic development and malignant transformation. *Cell* 95:793-803.

8. Lowenstein, E. J., R. J. Daly, A. G. Batzer, W. Li, B. Margolis, R. Lammers, A. Ullrich, E. Y. Skolnik, D. Bar-Sagi, and J. Schlessinger. 1992. The SH2 and SH3 domain-containing protein GRB2 links receptor tyrosine kinases to ras signaling. *Cell* 70:431-442.

9. Guyot, B., S. Arnaud, P. Phothirath, R. P. Bourette, M. F. Grasset, D. Rigal, and G. Mouchiroud. 2002. Genomic organization and restricted expression of the human Mona/Gads gene suggests regulation by two specific promoters. *Gene* 290:173-179.

10. Guyot, B., and G. Mouchiroud. 2002. Characterization of the promoter controlling Mona/Gads expression in the megakaryocytic lineage. *Gene* 296:151-159.

11. Guyot, B., and G. Mouchiroud. 2003. Characterization of promoter elements directing Mona/Gads molecular adapter expression in T and myelomonocytic cells: involvement of the AML-1 transcription factor. *J Leukoc Biol* 73:263-272.

12. Garrett-Sinha, L. A., P. Hou, D. Wang, B. Grabiner, E. Araujo, S. Rao, T. J. Yun, E. A. Clark, M. C. Simon, and M. R. Clark. 2005. Spi-1 and Spi-B control the expression of the Grap2 gene in B cells. *Gene* 353:134-146.

13. Licht, J. D. 2001. AML1 and the AML1-ETO fusion protein in the pathogenesis of t(8;21) AML. *Oncogene* 20:5660-5679.

14. Yankee, T. M., S. A. Solow, K. D. Draves, and E. A. Clark. 2003. Expression of the Grb2-related protein of the lymphoid system in B cell subsets enhances B cell antigen receptor signaling through mitogen-activated protein kinase pathways. *J Immunol* 170:349-355.

15. Liu, S. K., N. Fang, G. A. Koretzky, and C. J. McGlade. 1999. The hematopoietic-specific adaptor protein gads functions in T-cell signaling via interactions with the SLP-76 and LAT adaptors. *Curr Biol* 9:67-75.

16. Yankee, T. M., K. E. Draves, and E. A. Clark. 2005. Expression and function of the adaptor protein Gads in murine B cells. *Eur J Immunol* 35:1184-1192.

17. Yankee, T. M., T. J. Yun, K. E. Draves, K. Ganesh, M. J. Bevan, K. Murali-Krishna, and E. A. Clark. 2004. The Gads (GrpL) adaptor protein regulates T cell homeostasis. *J Immunol* 173:1711-1720.

18. Hardy, R. R., and K. Hayakawa. 2001. B cell development pathways. *Annu Rev Immunol* 19:595-621.

19. Chung, J. B., M. Silverman, and J. G. Monroe. 2003. Transitional B cells: step by step towards immune competence. *Trends Immunol* 24:343-349.

20. Godfrey, D. I., J. Kennedy, T. Suda, and A. Zlotnik. 1993. A developmental pathway involving four phenotypically and functionally distinct subsets of CD3-CD4-CD8- triple-negative adult mouse thymocytes defined by CD44 and CD25 expression. *J Immunol* 150:4244-4252.

21. Zeng, L., S. L. Dalheimer, and T. M. Yankee. 2007. Gads-/- mice reveal functionally distinct subsets of TCRbeta+ CD4-CD8- double-negative thymocytes. *J Immunol* 179:1013-1021.

22. Ashwell, J. D., and R. D. Klusner. 1990. Genetic and mutational analysis of the T-cell antigen receptor. *Annu Rev Immunol* 8:139-167.

23. Clevers, H., B. Alarcon, T. Wileman, and C. Terhorst. 1988. The T cell receptor/CD3 complex: a dynamic protein ensemble. *Annu Rev Immunol* 6:629-662.

24. Weiss, A. 1990. Structure and function of the T cell antigen receptor. *J Clin Invest* 86:1015-1022.

25. Weiss, A. 1991. Molecular and genetic insights into T cell antigen receptor structure and function. *Annu Rev Genet* 25:487-510.

26. Weiss, A. 1993. T cell antigen receptor signal transduction: a tale of tails and cytoplasmic protein-tyrosine kinases. *Cell* 73:209-212.

27. Chan, A. C., and A. S. Shaw. 1996. Regulation of antigen receptor signal transduction by protein tyrosine kinases. *Curr Opin Immunol* 8:394-401.

28. Gobel, T. W., and L. Bolliger. 2000. Evolution of the T cell receptor signal transduction units. *Curr Top Microbiol Immunol* 248:303-320.

29. Seet, B. T., D. M. Berry, J. S. Maltzman, J. Shabason, M. Raina, G. A. Koretzky, C. J. McGlade, and T. Pawson. 2007. Efficient T-cell receptor signaling requires a high-affinity interaction between the Gads C-SH3 domain and the SLP-76 RxxK motif. *EMBO J* 26:678-689.

30. Berry, D. M., P. Nash, S. K. Liu, T. Pawson, and C. J. McGlade. 2002. A high-affinity Arg-X-X-Lys SH3 binding motif confers specificity for the interaction between Gads and SLP-76 in T cell signaling. *Curr Biol* 12:1336-1341.

31. Swamy, M., Y. Kulathu, S. Ernst, M. Reth, and W. W. Schamel. 2006. Two dimensional Blue Native-/SDS-PAGE analysis of SLP family adaptor protein complexes. *Immunol Lett* 104:131-137.

32. Bubeck Wardenburg, J., C. Fu, J. K. Jackman, H. Flotow, S. E. Wilkinson, D. H. Williams, R. Johnson, G. Kong, A. C. Chan, and P. R. Findell. 1996. Phosphorylation of SLP-76 by the ZAP-70 protein-tyrosine kinase is required for T-cell receptor function. *J Biol Chem* 271:19641-19644.

33. Zhang, W., R. P. Trible, and L. E. Samelson. 1998. LAT palmitoylation: its essential role in membrane microdomain targeting and tyrosine phosphorylation during T cell activation. *Immunity* 9:239-246.

34. Lin, J., A. Weiss, and T. S. Finco. 1999. Localization of LAT in glycolipid-enriched microdomains is required for T cell activation. *J Biol Chem* 274:28861-28864.

35. Jordan, M. S., A. L. Singer, and G. A. Koretzky. 2003. Adaptors as central mediators of signal transduction in immune cells. *Nat Immunol* 4:110-116.

36. Wange, R. L. 2000. LAT, the linker for activation of T cells: a bridge between T cell-specific and general signaling pathways. *Sci STKE* 2000:re1.

37. Qi, Q., and A. August. 2007. Keeping the (kinase) party going: SLP-76 and ITK dance to the beat. *Sci STKE* 2007:pe39.

38. Roose, J. P., M. Mollenauer, V. A. Gupta, J. Stone, and A. Weiss. 2005. A diacylglycerol-protein kinase C-RasGRP1 pathway directs Ras activation upon antigen receptor stimulation of T cells. *Mol Cell Biol* 25:4426-4441.

39. Ebinu, J. O., S. L. Stang, C. Teixeira, D. A. Bottorff, J. Hooton, P. M. Blumberg, M. Barry, R. C. Bleakley, H. L. Ostergaard, and J. C. Stone. 2000. RasGRP links T-cell receptor signaling to Ras. *Blood* 95:3199-3203.

40. Tsukamoto, H., A. Irie, and Y. Nishimura. 2004. B-Raf contributes to sustained extracellular signal-regulated kinase activation associated with interleukin-2 production stimulated through the T cell receptor. *J Biol Chem* 279:48457-48465.

41. Zhu, M., E. Janssen, and W. Zhang. 2003. Minimal requirement of tyrosine residues of linker for activation of T cells in TCR signaling and thymocyte development. *J Immunol* 170:325-333.

42. Perez-Villar, J. J., G. S. Whitney, M. T. Sitnick, R. J. Dunn, S. Venkatesan, K. O'Day, G. L. Schieven, T. A. Lin, and S. B. Kanner. 2002. Phosphorylation of the linker for activation of T-cells by Itk promotes recruitment of Vav. *Biochemistry* 41:10732-10740.

43. Sommers, C. L., R. K. Menon, A. Grinberg, W. Zhang, L. E. Samelson, and P. E. Love. 2001. Knock-in mutation of the distal four tyrosines of linker for activation of T cells blocks murine T cell development. *J Exp Med* 194:135-142.

44. Zhang, W., R. P. Trible, M. Zhu, S. K. Liu, C. J. McGlade, and L. E. Samelson. 2000. Association of Grb2, Gads, and phospholipase C-gamma 1 with phosphorylated LAT tyrosine residues. Effect of LAT tyrosine mutations on T cell angigen receptor-mediated signaling. *J Biol Chem* 275:23355-23361.

45. Lin, J., and A. Weiss. 2001. Identification of the minimal tyrosine residues required for linker for activation of T cell function. *J Biol Chem* 276:29588-29595.

46. Cho, S., C. A. Velikovsky, C. P. Swaminathan, J. C. Houtman, L. E. Samelson, and R. A. Mariuzza. 2004. Structural basis for differential recognition of tyrosine-phosphorylated sites in the linker for activation of T cells (LAT) by the adaptor Gads. *EMBO J* 23:1441-1451.

47. Purbhoo, M. A., H. Liu, S. Oddos, D. M. Owen, M. A. Neil, S. V. Pageon, P. M. French, C. E. Rudd, and D. M. Davis. 2010. Dynamics of subsynaptic vesicles and surface microclusters at the immunological synapse. *Sci Signal* 3:ra36.

48. Bunnell, S. C., A. L. Singer, D. I. Hong, B. H. Jacque, M. S. Jordan, M. C. Seminario, V. A. Barr, G. A. Koretzky, and L. E. Samelson. 2006. Persistence of cooperatively stabilized signaling clusters drives T-cell activation. *Mol Cell Biol* 26:7155-7166.

49. Braiman, A., M. Barda-Saad, C. L. Sommers, and L. E. Samelson. 2006. Recruitment and activation of PLCgamma1 in T cells: a new insight into old domains. *EMBO J* 25:774-784.

50. Zhang, W., J. Sloan-Lancaster, J. Kitchen, R. P. Trible, and L. E. Samelson. 1998. LAT: the ZAP-70 tyrosine kinase substrate that links T cell receptor to cellular activation. *Cell* 92:83-92.

51. Welsh, M., Z. Songyang, J. D. Frantz, T. Trub, K. A. Reedquist, T. Karlsson, M. Miyazaki, L. C. Cantley, H. Band, and S. E. Shoelson. 1998. Stimulation through the T cell receptor leads to interactions between SHB and several signaling proteins. *Oncogene* 16:891-901.

52. Deckert, M., S. Tartare-Deckert, J. Hernandez, R. Rottapel, and A. Altman. 1998. Adaptor function for the Syk kinases-interacting protein 3BP2 in IL-2 gene activation. *Immunity* 9:595-605.

53. Tuosto, L., F. Michel, and O. Acuto. 1996. p95vav associates with tyrosine-phosphorylated SLP-76 in antigen-stimulated T cells. *J Exp Med* 184:1161-1166.

54. Wu, J., D. G. Motto, G. A. Koretzky, and A. Weiss. 1996. Vav and SLP-76 interact and functionally cooperate in IL-2 gene activation. *Immunity* 4:593-602.

55. Tybulewicz, V. L., L. Ardouin, A. Prisco, and L. F. Reynolds. 2003. Vav1: a key signal transducer downstream of the TCR. *Immunol Rev* 192:42-52.

56. Singer, A. L., S. C. Bunnell, A. E. Obstfeld, M. S. Jordan, J. N. Wu, P. S. Myung, L. E. Samelson, and G. A. Koretzky. 2004. Roles of the proline-rich domain in SLP-76 subcellular localization and T cell function. *J Biol Chem* 279:15481-15490.

57. Bubeck Wardenburg, J., R. Pappu, J. Y. Bu, B. Mayer, J. Chernoff, D. Straus, and A. C. Chan. 1998. Regulation of PAK activation and the T cell cytoskeleton by the linker protein SLP-76. *Immunity* 9:607-616.

58. Bunnell, S. C., M. Diehn, M. B. Yaffe, P. R. Findell, L. C. Cantley, and L. J. Berg. 2000. Biochemical interactions integrating Itk with the T cell receptor-initiated signaling cascade. *J Biol Chem* 275:2219-2230.

59. Su, Y. W., Y. Zhang, J. Schweikert, G. A. Koretzky, M. Reth, and J. Wienands. 1999. Interaction of SLP adaptors with the SH2 domain of Tec family kinases. *Eur J Immunol* 29:3702-3711.

60. Lewis, C. M., C. Broussard, M. J. Czar, and P. L. Schwartzberg. 2001. Tec kinases: modulators of lymphocyte signaling and development. *Curr Opin Immunol* 13:317-325.

61. Yablonski, D., T. Kadlecek, and A. Weiss. 2001. Identification of a phospholipase C-gamma1 (PLC-gamma1) SH3 domain-binding site in SLP-76 required for T-cell receptor-mediated activation of PLC-gamma1 and NFAT. *Mol Cell Biol* 21:4208-4218.

62. Kumar, L., S. Feske, A. Rao, and R. S. Geha. 2005. A 10-aa-long sequence in SLP-76 upstream of the Gads binding site is essential for T cell development and function. *Proc Natl Acad Sci U S A* 102:19063-19068.

63. Musci, M. A., L. R. Hendricks-Taylor, D. G. Motto, M. Paskind, J. Kamens, C. W. Turck, and G. A. Koretzky. 1997. Molecular cloning of SLAP-130, an SLP-76-associated substrate of the T cell antigen receptor-stimulated protein tyrosine kinases. *J Biol Chem* 272:11674-11677.

64. da Silva, A. J., Z. Li, C. de Vera, E. Canto, P. Findell, and C. E. Rudd. 1997. Cloning of a novel T-cell protein FYB that binds FYN and SH2-domain-containing leukocyte protein 76 and modulates interleukin 2 production. *Proc Natl Acad Sci U S A* 94:7493-7498.

65. Sauer, K., J. Liou, S. B. Singh, D. Yablonski, A. Weiss, and R. M. Perlmutter. 2001. Hematopoietic progenitor kinase 1 associates physically and functionally with the adaptor proteins B cell linker protein and SLP-76 in lymphocytes. *J Biol Chem* 276:45207-45216.

66. Gonen, R., D. Beach, C. Ainey, and D. Yablonski. 2005. T cell receptor-induced activation of phospholipase C-gamma1 depends on a sequence-independent function of the P-I region of SLP-76. *J Biol Chem* 280:8364-8370.

67. Pawson, T., and J. D. Scott. 1997. Signaling through scaffold, anchoring, and adaptor proteins. *Science* 278:2075-2080.

68. Tomlinson, M. G., J. Lin, and A. Weiss. 2000. Lymphocytes with a complex: adapter proteins in antigen receptor signaling. *Immunol Today* 21:584-591.

69. Yokosuka, T., K. Sakata-Sogawa, W. Kobayashi, M. Hiroshima, A. Hashimoto-Tane, M. Tokunaga, M. L. Dustin, and T. Saito. 2005. Newly generated T cell receptor microclusters initiate and sustain T cell activation by recruitment of Zap70 and SLP-76. *Nat Immunol* 6:1253-1262.

70. Bunnell, S. C., D. I. Hong, J. R. Kardon, T. Yamazaki, C. J. McGlade, V. A. Barr, and L. E. Samelson. 2002. T cell receptor ligation induces the formation of dynamically regulated signaling assemblies. *J Cell Biol* 158:1263-1275.

71. Campi, G., R. Varma, and M. L. Dustin. 2005. Actin and agonist MHC-peptide complex-dependent T cell receptor microclusters as scaffolds for signaling. *J Exp Med* 202:1031-1036.

72. Harder, T., and M. Kuhn. 2000. Selective accumulation of raft-associated membrane protein LAT in T cell receptor signaling assemblies. *J Cell Biol* 151:199-208.

73. Krummel, M. F., and M. M. Davis. 2002. Dynamics of the immunological synapse: finding, establishing and solidifying a connection. *Curr Opin Immunol* 14:66-74.

74. Barda-Saad, M., A. Braiman, R. Titerence, S. C. Bunnell, V. A. Barr, and L. E. Samelson. 2005. Dynamic molecular interactions linking the T cell antigen receptor to the actin cytoskeleton. *Nat Immunol* 6:80-89.

75. Boerth, N. J., J. J. Sadler, D. E. Bauer, J. L. Clements, S. M. Gheith, and G. A. Koretzky. 2000. Recruitment of SLP-76 to the membrane and glycolipid-enriched membrane microdomains replaces the requirement for linker for activation of T cells in T cell receptor signaling. *J Exp Med* 192:1047-1058.

76. Yoder, J., C. Pham, Y. M. Iizuka, O. Kanagawa, S. K. Liu, J. McGlade, and A. M. Cheng. 2001. Requirement for the SLP-76 adaptor GADS in T cell development. *Science* 291:1987-1991.

77. Kikuchi, K., Y. Kawasaki, N. Ishii, Y. Sasaki, H. Asao, T. Takeshita, I. Miyoshi, N. Kasai, and K. Sugamura. 2001. Suppression of thymic development by the dominant-negative form of Gads. *Int Immunol* 13:777-783.

78. Kumar, L., V. Pivniouk, M. A. de la Fuente, D. Laouini, and R. S. Geha. 2002. Differential role of SLP-76 domains in T cell development and function. *Proc Natl Acad Sci U S A* 99:884-889.

79. Jordan, M. S., J. S. Maltzman, S. Kliche, J. Shabason, J. E. Smith, A. Obstfeld, B. Schraven, and G. A. Koretzky. 2007. In vivo disruption of T cell development by expression of a dominant-negative polypeptide designed to abolish the SLP-76/Gads interaction. *Eur J Immunol* 37:2961-2972.

80. Klee, C. B., H. Ren, and X. Wang. 1998. Regulation of the calmodulin-stimulated protein phosphatase, calcineurin. *J Biol Chem* 273:13367-13370.

81. Crabtree, G. R., and E. N. Olson. 2002. NFAT signaling: choreographing the social lives of cells. *Cell* 109 Suppl:S67-79.

82. Macian, F. 2005. NFAT proteins: key regulators of T-cell development and function. *Nat Rev Immunol* 5:472-484.

83. Moran, O., M. W. Roessle, R. A. Mariuzza, and N. Dimasi. 2008. Structural features of the full-length adaptor protein GADS in solution determined using small-angle X-ray scattering. *Biophys J* 94:1766-1772.

84. Liu, Q., D. Berry, P. Nash, T. Pawson, C. J. McGlade, and S. S. Li. 2003. Structural basis for specific binding of the Gads SH3 domain to an RxxK motif-containing SLP-76 peptide: a novel mode of peptide recognition. *Mol Cell* 11:471-481.

85. Harkiolaki, M., M. Lewitzky, R. J. Gilbert, E. Y. Jones, R. P. Bourette, G. Mouchiroud, H. Sondermann, I. Moarefi, and S. M. Feller. 2003. Structural basis for SH3 domain-mediated high-affinity binding between Mona/Gads and SLP-76. *EMBO J* 22:2571-2582.

86. Mayer, B. J. 2001. SH3 domains: complexity in moderation. *J Cell Sci* 114:1253-1263.

87. Zarrinpar, A., R. P. Bhattacharyya, and W. A. Lim. 2003. The structure and function of proline recognition domains. *Sci STKE* 2003:RE8.

88. Li, S. S. 2005. Specificity and versatility of SH3 and other proline-recognition domains: structural basis and implications for cellular signal transduction. *Biochem J* 390:641-653.

89. Faravelli, A., and N. Dimasi. 2006. Expression, refolding and crystallizations of the Grb2-like (GADS) C-terminal SH3 domain complexed with a SLP-76 motif peptide. *Acta Crystallogr Sect F Struct Biol Cryst Commun* 62:52-55.

90. Dimasi, N. 2007. Crystal structure of the C-terminal SH3 domain of the adaptor protein GADS in complex with SLP-76 motif peptide reveals a unique SH3-SH3 interaction. *Int J Biochem Cell Biol* 39:109-123.

91. Wright, P. E., and H. J. Dyson. 2009. Linking folding and binding. *Curr Opin Struct Biol* 19:31-38.

92. Dyson, H. J., and P. E. Wright. 2005. Intrinsically unstructured proteins and their functions. *Nat Rev Mol Cell Biol* 6:197-208.

93. Michie, A. M., and J. C. Zuniga-Pflucker. 2002. Regulation of thymocyte differentiation: pre-TCR signals and beta-selection. *Semin Immunol* 14:311-323.

94. Peschon, J. J., P. J. Morrissey, K. H. Grabstein, F. J. Ramsdell, E. Maraskovsky, B. C. Gliniak, L. S. Park, S. F. Ziegler, D. E. Williams, C. B. Ware, J. D. Meyer, and B. L. Davison. 1994. Early lymphocyte expansion is severely impaired in interleukin 7 receptor-deficient mice. *J Exp Med* 180:1955-1960.

95. Van De Wiele, C. J., J. H. Marino, B. W. Murray, S. S. Vo, M. E. Whetsell, and T. K. Teague. 2004. Thymocytes between the beta-selection and positive selection checkpoints are nonresponsive to IL-7 as assessed by STAT-5 phosphorylation. *J Immunol* 172:4235-4244.

96. Janeway, C. A., Jr. 1995. Ligands for the T-cell receptor: hard times for avidity models. *Immunol Today* 16:223-225.

97. Alam, S. M., P. J. Travers, J. L. Wung, W. Nasholds, S. Redpath, S. C. Jameson, and N. R. Gascoigne. 1996. T-cell-receptor affinity and thymocyte positive selection. *Nature* 381:616-620.

98. Baldwin, T. A., K. A. Hogquist, and S. C. Jameson. 2004. The fourth way? Harnessing aggressive tendencies in the thymus. *J Immunol* 173:6515-6520.

99. Dalheimer, S. L., L. Zeng, K. E. Draves, A. Hassaballa, N. N. Jiwa, T. D. Parrish, E. A. Clark, and T. M. Yankee. 2009. Gads-deficient thymocytes are blocked at the transitional single positive CD4+ stage. *Eur J Immunol* 39:1395-1404.

100. He, X., and D. J. Kappes. 2006. CD4/CD8 lineage commitment: light at the end of the tunnel? *Curr Opin Immunol* 18:135-142.

101. Germain, R. N. 2002. T-cell development and the CD4-CD8 lineage decision. *Nat Rev Immunol* 2:309-322.

102. Lundberg, K., W. Heath, F. Kontgen, F. R. Carbone, and K. Shortman. 1995. Intermediate steps in positive selection: differentiation of CD4+8int TCRint thymocytes into CD4-8+TCRhi thymocytes. *J Exp Med* 181:1643-1651.

103. Suzuki, H., J. A. Punt, L. G. Granger, and A. Singer. 1995. Asymmetric signaling requirements for thymocyte commitment to the CD4+ versus CD8+ T cell lineages: a new perspective on thymic commitment and selection. *Immunity* 2:413-425.

104. Lucas, B., and R. N. Germain. 1996. Unexpectedly complex regulation of CD4/CD8 coreceptor expression supports a revised model for CD4+CD8+ thymocyte differentiation. *Immunity* 5:461-477.

105. Berry, D. M., S. J. Benn, A. M. Cheng, and C. J. McGlade. 2001. Caspase-dependent cleavage of the hematopoietic specific adaptor protein Gads alters signalling from the T cell receptor. *Oncogene* 20:1203-1211.

106. Yankee, T. M., K. E. Draves, M. K. Ewings, E. A. Clark, and J. D. Graves. 2001. CD95/Fas induces cleavage of the GrpL/Gads adaptor and desensitization of antigen receptor signaling. *Proc Natl Acad Sci U S A* 98:6789-6793.

107. Puga, I., A. Rao, and F. Macian. 2008. Targeted cleavage of signaling proteins by caspase 3 inhibits T cell receptor signaling in anergic T cells. *Immunity* 29:193-204.

108. Strober, W., B. Kelsall, and T. Marth. 1998. Oral tolerance. *J Clin Immunol* 18:1-30.

109. Garside, P., and A. M. Mowat. 2001. Oral tolerance. *Semin Immunol* 13:177-185.

110. Kaji, T., S. Hachimura, W. Ise, and S. Kaminogawa. 2003. Proteome analysis reveals caspase activation in hyporesponsive CD4 T lymphocytes induced in vivo by the oral administration of antigen. *J Biol Chem* 278:27836-27843.

111. Asai, K., S. Hachimura, M. Kimura, T. Toraya, M. Yamashita, T. Nakayama, and S. Kaminogawa. 2002. T cell hyporesponsiveness induced by oral administration of

ovalbumin is associated with impaired NFAT nuclear translocation and p27kip1 degradation. *J Immunol* 169:4723-4731.

112. Hachimura, S., T. Kaji, K. Asai, W. Ise, T. Nakayama, and S. Kaminogawa. 2004. Hyporesponsiveness of CD4 T cells induced in oral tolerance is maintained by selective impairment in the TCR-induced calcium/NFAT signaling pathway resulting from caspase activation. *Ann N Y Acad Sci* 1029:344-345.

113. Kettner, A., V. Pivniouk, L. Kumar, H. Falet, J. S. Lee, R. Mulligan, and R. S. Geha. 2003. Structural requirements of SLP-76 in signaling via the high-affinity immunoglobulin E receptor (Fc epsilon RI) in mast cells. *Mol Cell Biol* 23:2395-2406.

114. Saitoh, S., S. Odom, G. Gomez, C. L. Sommers, H. A. Young, J. Rivera, and L. E. Samelson. 2003. The four distal tyrosines are required for LAT-dependent signaling in FcepsilonRI-mediated mast cell activation. *J Exp Med* 198:831-843.

115. Wu, J. N., M. S. Jordan, M. A. Silverman, E. J. Peterson, and G. A. Koretzky. 2004. Differential requirement for adapter proteins Src homology 2 domain-containing leukocyte phosphoprotein of 76 kDa and adhesion- and degranulation-promoting adapter protein in FcepsilonRI signaling and mast cell function. *J Immunol* 172:6768-6774.

116. Yamasaki, S., M. Takase-Utsugi, E. Ishikawa, M. Sakuma, K. Nishida, T. Saito, and O. Kanagawa. 2008. Selective impairment of FcepsilonRI-mediated allergic reaction in Gads-deficient mice. *Int Immunol* 20:1289-1297.

117. Zhang, E. Y., A. Y. Chen, and B. T. Zhu. 2009. Mechanism of dinitrochlorobenzene-induced dermatitis in mice: role of specific antibodies in pathogenesis. *PLoS One* 4:e7703.

118. Boomer, J. S., and T. H. Tan. 2005. Functional interactions of HPK1 with adaptor proteins. *J Cell Biochem* 95:34-44.

119. Hu, M. C., W. R. Qiu, X. Wang, C. F. Meyer, and T. H. Tan. 1996. Human HPK1, a novel human hematopoietic progenitor kinase that activates the JNK/SAPK kinase cascade. *Genes Dev* 10:2251-2264.

120. Kiefer, F., L. A. Tibbles, M. Anafi, A. Janssen, B. W. Zanke, N. Lassam, T. Pawson, J. R. Woodgett, and N. N. Iscove. 1996. HPK1, a hematopoietic protein kinase activating the SAPK/JNK pathway. *EMBO J* 15:7013-7025.

121. Liu, S. K., C. A. Smith, R. Arnold, F. Kiefer, and C. J. McGlade. 2000. The adaptor protein Gads (Grb2-related adaptor downstream of Shc) is implicated in coupling hemopoietic progenitor kinase-1 to the activated TCR. *J Immunol* 165:1417-1426.

122. Lewitzky, M., M. Harkiolaki, M. C. Domart, E. Y. Jones, and S. M. Feller. 2004. Mona/Gads SH3C binding to hematopoietic progenitor kinase 1 (HPK1) combines an atypical SH3 binding motif, R/KXXK, with a classical PXXP motif embedded in a polyproline type II (PPII) helix. *J Biol Chem* 279:28724-28732.

123. Shui, J. W., J. S. Boomer, J. Han, J. Xu, G. A. Dement, G. Zhou, and T. H. Tan. 2007. Hematopoietic progenitor kinase 1 negatively regulates T cell receptor signaling and T cell-mediated immune responses. *Nat Immunol* 8:84-91.

124. Nishida, K., and T. Hirano. 2003. The role of Gab family scaffolding adapter proteins in the signal transduction of cytokine and growth factor receptors. *Cancer Sci* 94:1029-1033.

125. Bouscary, D., C. Lecoq-Lafon, S. Chretien, S. Zompi, S. Fichelson, O. Muller, F. Porteu, I. Dusanter-Fourt, S. Gisselbrecht, P. Mayeux, and C. Lacombe. 2001. Role of Gab

proteins in phosphatidylinositol 3-kinase activation by thrombopoietin (Tpo). *Oncogene* 20:2197-2204.

126. Lock, L. S., I. Royal, M. A. Naujokas, and M. Park. 2000. Identification of an atypical Grb2 carboxyl-terminal SH3 domain binding site in Gab docking proteins reveals Grb2-dependent and -independent recruitment of Gab1 to receptor tyrosine kinases. *J Biol Chem* 275:31536-31545.

127. Yamasaki, S., K. Nishida, M. Sakuma, D. Berry, C. J. McGlade, T. Hirano, and T. Saito. 2003. Gads/Grb2-mediated association with LAT is critical for the inhibitory function of Gab2 in T cells. *Mol Cell Biol* 23:2515-2529.

128. Bourgin, C., R. P. Bourette, S. Arnaud, Y. Liu, L. R. Rohrschneider, and G. Mouchiroud. 2002. Induced expression and association of the Mona/Gads adapter and Gab3 scaffolding protein during monocyte/macrophage differentiation. *Mol Cell Biol* 22:3744-3756.

129. Holgado-Madruga, M., D. R. Emlet, D. K. Moscatello, A. K. Godwin, and A. J. Wong. 1996. A Grb2-associated docking protein in EGF- and insulin-receptor signalling. *Nature* 379:560-564.

130. Ueno, E., T. Haruta, T. Uno, I. Usui, M. Iwata, A. Takano, J. Kawahara, T. Sasaoka, O. Ishibashi, and M. Kobayashi. 2001. Potential role of Gab1 and phospholipase C-gamma in osmotic shock-induced glucose uptake in 3T3-L1 adipocytes. *Horm Metab Res* 33:402-406.

131. Takeda, K., Y. Harada, R. Watanabe, Y. Inutake, S. Ogawa, K. Onuki, S. Kagaya, K. Tanabe, H. Kishimoto, and R. Abe. 2008. CD28 stimulation triggers NF-kappaB activation through the CARMA1-PKCtheta-Grb2/Gads axis. *Int Immunol* 20:1507-1515.

132. Watanabe, R., Y. Harada, K. Takeda, J. Takahashi, K. Ohnuki, S. Ogawa, D. Ohgai, N. Kaibara, O. Koiwai, K. Tanabe, H. Toma, K. Sugamura, and R. Abe. 2006. Grb2 and Gads exhibit different interactions with CD28 and play distinct roles in CD28-mediated costimulation. *J Immunol* 177:1085-1091.

133. Okkenhaug, K., L. Wu, K. M. Garza, J. La Rose, W. Khoo, B. Odermatt, T. W. Mak, P. S. Ohashi, and R. Rottapel. 2001. A point mutation in CD28 distinguishes proliferative signals from survival signals. *Nat Immunol* 2:325-332.

134. Schneider, H., and C. E. Rudd. 2008. CD28 and Grb-2, relative to Gads or Grap, preferentially co-operate with Vav1 in the activation of NFAT/AP-1 transcription. *Biochem Biophys Res Commun* 369:616-621.

135. Pages, F., M. Ragueneau, S. Klasen, M. Battifora, D. Couez, R. Sweet, A. Truneh, S. G. Ward, and D. Olive. 1996. Two distinct intracytoplasmic regions of the T-cell adhesion molecule CD28 participate in phosphatidylinositol 3-kinase association. *J Biol Chem* 271:9403-9409.

136. Neel, B. G., H. Gu, and L. Pao. 2003. The 'Shp'ing news: SH2 domain-containing tyrosine phosphatases in cell signaling. *Trends Biochem Sci* 28:284-293.

137. O'Reilly, A. M., and B. G. Neel. 1998. Structural determinants of SHP-2 function and specificity in Xenopus mesoderm induction. *Mol Cell Biol* 18:161-177.

138. Kwon, J., C. K. Qu, J. S. Maeng, R. Falahati, C. Lee, and M. S. Williams. 2005. Receptor-stimulated oxidation of SHP-2 promotes T-cell adhesion through SLP-76-ADAP. *EMBO J* 24:2331-2341.

139. Mustelin, T., S. Rahmouni, N. Bottini, and A. Alonso. 2003. Role of protein tyrosine phosphatases in T cell activation. *Immunol Rev* 191:139-147.

140. Feng, G. S. 1999. Shp-2 tyrosine phosphatase: signaling one cell or many. *Exp Cell Res* 253:47-54.

141. Hur, E. M., M. Son, O. H. Lee, Y. B. Choi, C. Park, H. Lee, and Y. Yun. 2003. LIME, a novel transmembrane adaptor protein, associates with p56lck and mediates T cell activation. *J Exp Med* 198:1463-1473.

142. Brdickova, N., T. Brdicka, P. Angelisova, O. Horvath, J. Spicka, I. Hilgert, J. Paces, L. Simeoni, S. Kliche, C. Merten, B. Schraven, and V. Horejsi. 2003. LIME: a new membrane Raft-associated adaptor protein involved in CD4 and CD8 coreceptor signaling. *J Exp Med* 198:1453-1462.

143. Palacios, E. H., and A. Weiss. 2004. Function of the Src-family kinases, Lck and Fyn, in T-cell development and activation. *Oncogene* 23:7990-8000.

144. Xia, C., Z. Bao, F. Tabassam, W. Ma, M. Qiu, S. Hua, and M. Liu. 2000. GCIP, a novel human grap2 and cyclin D interacting protein, regulates E2F-mediated transcriptional activity. *J Biol Chem* 275:20942-20948.

145. Sonnenberg-Riethmacher, E., T. Wustefeld, M. Miehe, C. Trautwein, and D. Riethmacher. 2007. Maid (GCIP) is involved in cell cycle control of hepatocytes. *Hepatology* 45:404-411.

146. Ma, W., X. Xia, L. J. Stafford, C. Yu, F. Wang, G. LeSage, and M. Liu. 2006. Expression of GCIP in transgenic mice decreases susceptibility to chemical hepatocarcinogenesis. *Oncogene* 25:4207-4216.

147. Lee, I., S. Y. Yeom, S. J. Lee, W. K. Kang, and C. Park. 2010. A novel senescence-evasion mechanism involving Grap2 and Cyclin D interacting protein inactivation by Ras

associated with diabetes in cancer cells under doxorubicin treatment. *Cancer Res* 70:4357-4365.

148. Ludwig, L., H. Kessler, C. Hoang-Vu, H. Dralle, G. Adler, B. O. Boehm, and R. M. Schmid. 2003. Grap-2, a novel RET binding protein, is involved in RET mitogenic signaling. *Oncogene* 22:5362-5366.

149. Jhiang, S. M. 2000. The RET proto-oncogene in human cancers. *Oncogene* 19:5590-5597.

150. Hansford, J. R., and L. M. Mulligan. 2000. Multiple endocrine neoplasia type 2 and RET: from neoplasia to neurogenesis. *J Med Genet* 37:817-827.

151. Wu, J. N., and G. A. Koretzky. 2004. The SLP-76 family of adapter proteins. *Semin Immunol* 16:379-393.

152. Fu, C., and A. C. Chan. 1997. Identification of two tyrosine phosphoproteins, pp70 and pp68, which interact with phospholipase Cgamma, Grb2, and Vav after B cell antigen receptor activation. *J Biol Chem* 272:27362-27368.

153. Bourgin, C., R. Bourette, G. Mouchiroud, and S. Arnaud. 2000. Expression of Mona (monocytic adapter) in myeloid progenitor cells results in increased and prolonged MAP kinase activation upon macrophage colony-stimulating factor stimulation. *FEBS Lett* 480:113-117.

154. Gotoh, N., A. Tojo, and M. Shibuya. 1996. A novel pathway from phosphorylation of tyrosine residues 239/240 of Shc, contributing to suppress apoptosis by IL-3. *EMBO J* 15:6197-6204.

155. Lindholm, C. K., M. L. Henriksson, B. Hallberg, and M. Welsh. 2002. Shb links SLP-76 and Vav with the CD3 complex in Jurkat T cells. *Eur J Biochem* 269:3279-3288.

156. Zhu, M., E. Janssen, K. Leung, and W. Zhang. 2002. Molecular cloning of a novel gene encoding a membrane-associated adaptor protein (LAX) in lymphocyte signaling. *J Biol Chem* 277:46151-46158.

157. Asazuma, N., J. I. Wilde, O. Berlanga, M. Leduc, A. Leo, E. Schweighoffer, V. Tybulewicz, C. Bon, S. K. Liu, C. J. McGlade, B. Schraven, and S. P. Watson. 2000. Interaction of linker for activation of T cells with multiple adapter proteins in platelets activated by the glycoprotein VI-selective ligand, convulxin. *J Biol Chem* 275:33427-33434.

158. Odunayo, A., J. R. Dodam, M. E. Kerl, and A. E. DeClue. 2010. Immunomodulatory effects of opioids. *J Vet Emerg Crit Care (San Antonio)* 20:376-385.

159. Dhawan, B. N., F. Cesselin, R. Raghubir, T. Reisine, P. B. Bradley, P. S. Portoghese, and M. Hamon. 1996. International Union of Pharmacology. XII. Classification of opioid receptors. *Pharmacol Rev* 48:567-592.

160. Schug, S. A., D. Zech, and S. Grond. 1992. Adverse effects of systemic opioid analgesics. *Drug Saf* 7:200-213.

161. Waldhoer, M., S. E. Bartlett, and J. L. Whistler. 2004. Opioid receptors. *Annu Rev Biochem* 73:953-990.

162. Lopez, A., and L. Salome. 2009. Membrane functional organisation and dynamic of mu-opioid receptors. *Cell Mol Life Sci* 66:2093-2108.

163. Inturrisi, C. E. 2002. Clinical pharmacology of opioids for pain. *Clin J Pain* 18:S3-13.

164. Janson, W., and C. Stein. 2003. Peripheral opioid analgesia. *Curr Pharm Biotechnol* 4:270-274.

165. Barry, U., and Z. Zuo. 2005. Opioids: old drugs for potential new applications. *Curr Pharm Des* 11:1343-1350.

166. Mehrishi, J. N., and I. H. Mills. 1983. Opiate receptors on lymphocytes and platelets in man. *Clin Immunol Immunopathol* 27:240-249.

167. Bidlack, J. M. 2000. Detection and function of opioid receptors on cells from the immune system. *Clin Diagn Lab Immunol* 7:719-723.

168. Krueger, H. M., N. B. Eddy, M. Sumwalt, and National research council (U.S.). Committee on drug addiction. 1941. *The pharmacology of the opium alkaloids*. U.S. Govt. print. off., Washington,.

169. McCarthy, L., M. Wetzel, J. K. Sliker, T. K. Eisenstein, and T. J. Rogers. 2001. Opioids, opioid receptors, and the immune response. *Drug Alcohol Depend* 62:111-123.

170. Sacerdote, P. 2008. Opioid-induced immunosuppression. *Curr Opin Support Palliat Care* 2:14-18.

171. Eisenstein, T. K., and M. E. Hilburger. 1998. Opioid modulation of immune responses: effects on phagocyte and lymphoid cell populations. *J Neuroimmunol* 83:36-44.

172. Flores, L. R., S. M. Wahl, and B. M. Bayer. 1995. Mechanisms of morphine-induced immunosuppression: effect of acute morphine administration on lymphocyte trafficking. *J Pharmacol Exp Ther* 272:1246-1251.

173. Hernandez, M. C., L. R. Flores, and B. M. Bayer. 1993. Immunosuppression by morphine is mediated by central pathways. *J Pharmacol Exp Ther* 267:1336-1341.

174. Vallejo, R., O. de Leon-Casasola, and R. Benyamin. 2004. Opioid therapy and immunosuppression: a review. *Am J Ther* 11:354-365.

175. Roy, S., J. Wang, J. Kelschenbach, L. Koodie, and J. Martin. 2006. Modulation of immune function by morphine: implications for susceptibility to infection. *J Neuroimmune Pharmacol* 1:77-89.

176. Bryant, H. U., E. W. Bernton, J. R. Kenner, and J. W. Holaday. 1991. Role of adrenal cortical activation in the immunosuppressive effects of chronic morphine treatment. *Endocrinology* 128:3253-3258.

177. Freier, D. O., and B. A. Fuchs. 1994. A mechanism of action for morphine-induced immunosuppression: corticosterone mediates morphine-induced suppression of natural killer cell activity. *J Pharmacol Exp Ther* 270:1127-1133.

178. Ayala, A., C. D. Herdon, D. L. Lehman, C. M. DeMaso, C. A. Ayala, and I. H. Chaudry. 1995. The induction of accelerated thymic programmed cell death during polymicrobial sepsis: control by corticosteroids but not tumor necrosis factor. *Shock* 3:259-267.

179. Tarcic, N., H. Ovadia, D. W. Weiss, and J. Weidenfeld. 1998. Restraint stress-induced thymic involution and cell apoptosis are dependent on endogenous glucocorticoids. *J Neuroimmunol* 82:40-46.

180. DePasquale-Jardieu, P., and P. J. Fraker. 1980. Further characterization of the role of corticosterone in the loss of humoral immunity in zinc-deficient A/J mice as determined by adrenalectomy. *J Immunol* 124:2650-2655.

181. Khalid, B. A., P. Pearce, I. G. Barr, D. Fraillon, B. H. Toh, and J. W. Funder. 1983. Dexamethasone induces different cellular protein synthetic responses in PNA+ and PNA- mouse thymocyte subpopulations. *J Immunol* 130:115-120.

182. Gruber, J., R. Sgonc, Y. H. Hu, H. Beug, and G. Wick. 1994. Thymocyte apoptosis induced by elevated endogenous corticosterone levels. *Eur J Immunol* 24:1115-1121.

183. Ku, G., and O. N. Witte. 1986. Corticosteroid-resistant bone marrow-derived B lymphocyte progenitor for long term in vitro cultures. *J Immunol* 137:2802-2807.

184. Garvy, B. A., L. E. King, W. G. Telford, L. A. Morford, and P. J. Fraker. 1993. Chronic elevation of plasma corticosterone causes reductions in the number of cycling cells of the B lineage in murine bone marrow and induces apoptosis. *Immunology* 80:587-592.

185. Laakko, T., and P. Fraker. 2002. Rapid changes in the lymphopoietic and granulopoietic compartments of the marrow caused by stress levels of corticosterone. *Immunology* 105:111-119.

186. Sabbele, N. R., A. Van Oudenaren, H. Hooijkaas, and R. Benner. 1987. The effect of corticosteroids upon murine B cells in vivo and in vitro as determined in the LPS-culture system. *Immunology* 62:285-290.

187. Arora, P. K., E. Fride, J. Petitto, K. Waggie, and P. Skolnick. 1990. Morphine-induced immune alterations in vivo. *Cell Immunol* 126:343-353.

188. LeVier, D. G., J. A. McCay, M. L. Stern, L. S. Harris, D. Page, R. D. Brown, D. L. Musgrove, L. F. Butterworth, K. L. White, Jr., and A. E. Munson. 1994. Immunotoxicological profile of morphine sulfate in B6C3F1 female mice. *Fundam Appl Toxicol* 22:525-542.

189. Hilburger, M. E., M. W. Adler, T. J. Rogers, and T. K. Eisenstein. 1997. Morphine alters macrophage and lymphocyte populations in the spleen and peritoneal cavity. *J Neuroimmunol* 80:106-114.

190. Franchi, S., A. E. Panerai, and P. Sacerdote. 2007. Buprenorphine ameliorates the effect of surgery on hypothalamus-pituitary-adrenal axis, natural killer cell activity and metastatic colonization in rats in comparison with morphine or fentanyl treatment. *Brain Behav Immun* 21:767-774.

191. Gomez-Flores, R., and R. J. Weber. 2000. Differential effects of buprenorphine and morphine on immune and neuroendocrine functions following acute administration in the rat mesencephalon periaqueductal gray. *Immunopharmacology* 48:145-156.

192. Briggs, F. N., and P. L. Munson. 1955. Studies on the mechanism of stimulation of ACTH secretion with the aid of morphine as a blocking agent. *Endocrinology* 57:205-219.

193. George, R., and E. L. Way. 1955. Studies on the mechanism of pituitary-adrenal activation by morphine. *Br J Pharmacol Chemother* 10:260-264.

194. Gomes, C., T. H. Svensson, and G. Trolin. 1976. Effects of morphine on central catecholamine turnover, blood pressure and heart rate in the rat. *Naunyn Schmiedebergs Arch Pharmacol* 294:141-147.

195. Vogel, W. H., J. Miller, K. H. DeTurck, and B. K. Routzahn, Jr. 1984. Effects of psychoactive drugs on plasma catecholamines during stress in rats. *Neuropharmacology* 23:1105-1108.

196. Hall, D. M., J. L. Suo, and R. J. Weber. 1998. Opioid mediated effects on the immune system: sympathetic nervous system involvement. *J Neuroimmunol* 83:29-35.

197. Flores, L. R., K. L. Dretchen, and B. M. Bayer. 1996. Potential role of the autonomic nervous system in the immunosuppressive effects of acute morphine administration. *Eur J Pharmacol* 318:437-446.

198. Boue, J., C. Blanpied, P. Brousset, N. Vergnolle, and G. Dietrich. 2011. Endogenous opioid-mediated analgesia is dependent on adaptive T cell response in mice. *J Immunol* 186:5078-5084.

199. Roy, S., J. Wang, S. Gupta, R. Charboneau, H. H. Loh, and R. A. Barke. 2004. Chronic morphine treatment differentiates T helper cells to Th2 effector cells by modulating transcription factors GATA 3 and T-bet. *J Neuroimmunol* 147:78-81.

200. Eisenstein, T. K., J. J. Meissler, Jr., T. J. Rogers, E. B. Geller, and M. W. Adler. 1995. Mouse strain differences in immunosuppression by opioids in vitro. *J Pharmacol Exp Ther* 275:1484-1489.

201. Grimm, M. C., A. Ben-Baruch, D. D. Taub, O. M. Howard, J. H. Resau, J. M. Wang, H. Ali, R. Richardson, R. Snyderman, and J. J. Oppenheim. 1998. Opiates transdeactivate chemokine receptors: delta and mu opiate receptor-mediated heterologous desensitization. *J Exp Med* 188:317-325.

202. Szabo, I., M. A. Wetzel, N. Zhang, A. D. Steele, D. E. Kaminsky, C. Chen, L. Y. Liu-Chen, F. Bednar, E. E. Henderson, O. M. Howard, J. J. Oppenheim, and T. J. Rogers. 2003. Selective inactivation of CCR5 and decreased infectivity of R5 HIV-1 strains mediated by opioid-induced heterologous desensitization. *J Leukoc Biol* 74:1074-1082.

203. Samelson, L. E. 2002. Signal transduction mediated by the T cell antigen receptor: the role of adapter proteins. *Annu Rev Immunol* 20:371-394.

204. Kersh, E. N., S. M. Kaech, T. M. Onami, M. Moran, E. J. Wherry, M. C. Miceli, and R. Ahmed. 2003. TCR signal transduction in antigen-specific memory CD8 T cells. *J Immunol* 170:5455-5463.

205. Teixeiro, E., M. A. Daniels, S. E. Hamilton, A. G. Schrum, R. Bragado, S. C. Jameson, and E. Palmer. 2009. Different T cell receptor signals determine CD8+ memory versus effector development. *Science* 323:502-505.

206. Farber, D. L. 2009. Biochemical signaling pathways for memory T cell recall. *Semin Immunol* 21:84-91.

207. Alam, S. M., G. M. Davies, C. M. Lin, T. Zal, W. Nasholds, S. C. Jameson, K. A. Hogquist, N. R. Gascoigne, and P. J. Travers. 1999. Qualitative and quantitative differences in T cell receptor binding of agonist and antagonist ligands. *Immunity* 10:227-237.

208. Yachi, P. P., J. Ampudia, T. Zal, and N. R. Gascoigne. 2006. Altered peptide ligands induce delayed CD8-T cell receptor interaction--a role for CD8 in distinguishing antigen quality. *Immunity* 25:203-211.

209. Koniaras, C., F. R. Carbone, W. R. Heath, and A. M. Lew. 1999. Inhibition of naive class I-restricted T cells by altered peptide ligands. *Immunol Cell Biol* 77:318-323.

210. Buckley, A. F., C. T. Kuo, and J. M. Leiden. 2001. Transcription factor LKLF is sufficient to program T cell quiescence via a c-Myc--dependent pathway. *Nat Immunol* 2:698-704.

211. Trumpp, A., Y. Refaeli, T. Oskarsson, S. Gasser, M. Murphy, G. R. Martin, and J. M. Bishop. 2001. c-Myc regulates mammalian body size by controlling cell number but not cell size. *Nature* 414:768-773.

212. Huang, C. Y., A. L. Bredemeyer, L. M. Walker, C. H. Bassing, and B. P. Sleckman. 2008. Dynamic regulation of c-Myc proto-oncogene expression during lymphocyte development revealed by a GFP-c-Myc knock-in mouse. *Eur J Immunol* 38:342-349.

213. Geng, Y., Q. Yu, E. Sicinska, M. Das, R. T. Bronson, and P. Sicinski. 2001. Deletion of the p27Kip1 gene restores normal development in cyclin D1-deficient mice. *Proc Natl Acad Sci U S A* 98:194-199.

214. Dang, C. V. 1999. c-Myc target genes involved in cell growth, apoptosis, and metabolism. *Mol Cell Biol* 19:1-11.

215. Yusuf, I., and D. A. Fruman. 2003. Regulation of quiescence in lymphocytes. *Trends Immunol* 24:380-386.

216. Crabtree, G. R. 1989. Contingent genetic regulatory events in T lymphocyte activation. *Science* 243:355-361.

217. Hardt, C. 1987. Activation of murine CD8+ lymphocytes: two distinct signals regulate c-myc and interleukin 2 receptor RNA expression. *Eur J Immunol* 17:1711-1717.

218. Dose, M., I. Khan, Z. Guo, D. Kovalovsky, A. Krueger, H. von Boehmer, K. Khazaie, and F. Gounari. 2006. c-Myc mediates pre-TCR-induced proliferation but not developmental progression. *Blood* 108:2669-2677.

219. Zehn, D., S. Y. Lee, and M. J. Bevan. 2009. Complete but curtailed T-cell response to very low-affinity antigen. *Nature* 458:211-214.

220. Germain, R. N., and I. Stefanova. 1999. The dynamics of T cell receptor signaling: complex orchestration and the key roles of tempo and cooperation. *Annu Rev Immunol* 17:467-522.

221. Rosette, C., G. Werlen, M. A. Daniels, P. O. Holman, S. M. Alam, P. J. Travers, N. R. Gascoigne, E. Palmer, and S. C. Jameson. 2001. The impact of duration versus extent

of TCR occupancy on T cell activation: a revision of the kinetic proofreading model. *Immunity* 15:59-70.

222. Bachmann, M. F., E. Sebzda, T. M. Kundig, A. Shahinian, D. E. Speiser, T. W. Mak, and P. S. Ohashi. 1996. T cell responses are governed by avidity and co-stimulatory thresholds. *Eur J Immunol* 26:2017-2022.

223. Tsukamoto, H., A. Irie, Y. Z. Chen, K. Takeshita, J. R. Kim, and Y. Nishimura. 2006. TCR ligand avidity determines the mode of B-Raf/Raf-1/ERK activation leading to the activation of human CD4+ T cell clone. *Eur J Immunol* 36:1926-1937.

224. Sloan-Lancaster, J., A. S. Shaw, J. B. Rothbard, and P. M. Allen. 1994. Partial T cell signaling: altered phospho-zeta and lack of zap70 recruitment in APL-induced T cell anergy. *Cell* 79:913-922.

225. Madrenas, J., R. L. Wange, J. L. Wang, N. Isakov, L. E. Samelson, and R. N. Germain. 1995. Zeta phosphorylation without ZAP-70 activation induced by TCR antagonists or partial agonists. *Science* 267:515-518.

226. Wulfing, C., J. D. Rabinowitz, C. Beeson, M. D. Sjaastad, H. M. McConnell, and M. M. Davis. 1997. Kinetics and extent of T cell activation as measured with the calcium signal. *J Exp Med* 185:1815-1825.

227. Pivniouk, V., E. Tsitsikov, P. Swinton, G. Rathbun, F. W. Alt, and R. S. Geha. 1998. Impaired viability and profound block in thymocyte development in mice lacking the adaptor protein SLP-76. *Cell* 94:229-238.

228. Clements, J. L., B. Yang, S. E. Ross-Barta, S. L. Eliason, R. F. Hrstka, R. A. Williamson, and G. A. Koretzky. 1998. Requirement for the leukocyte-specific adapter protein SLP-76 for normal T cell development. *Science* 281:416-419.

229. Zhang, W., C. L. Sommers, D. N. Burshtyn, C. C. Stebbins, J. B. DeJarnette, R. P. Trible, A. Grinberg, H. C. Tsay, H. M. Jacobs, C. M. Kessler, E. O. Long, P. E. Love, and L. E. Samelson. 1999. Essential role of LAT in T cell development. *Immunity* 10:323-332.

230. Bird, J. J., D. R. Brown, A. C. Mullen, N. H. Moskowitz, M. A. Mahowald, J. R. Sider, T. F. Gajewski, C. R. Wang, and S. L. Reiner. 1998. Helper T cell differentiation is controlled by the cell cycle. *Immunity* 9:229-237.

231. Oehen, S., and K. Brduscha-Riem. 1998. Differentiation of naive CTL to effector and memory CTL: correlation of effector function with phenotype and cell division. *J Immunol* 161:5338-5346.

232. Bachmann, M. F., M. Barner, A. Viola, and M. Kopf. 1999. Distinct kinetics of cytokine production and cytolysis in effector and memory T cells after viral infection. *Eur J Immunol* 29:291-299.

233. Opferman, J. T., B. T. Ober, and P. G. Ashton-Rickardt. 1999. Linear differentiation of cytotoxic effectors into memory T lymphocytes. *Science* 283:1745-1748.

234. Kaech, S. M., and R. Ahmed. 2001. Memory CD8+ T cell differentiation: initial antigen encounter triggers a developmental program in naive cells. *Nat Immunol* 2:415-422.

235. van Stipdonk, M. J., E. E. Lemmens, and S. P. Schoenberger. 2001. Naive CTLs require a single brief period of antigenic stimulation for clonal expansion and differentiation. *Nat Immunol* 2:423-429.

236. van Stipdonk, M. J., G. Hardenberg, M. S. Bijker, E. E. Lemmens, N. M. Droin, D. R. Green, and S. P. Schoenberger. 2003. Dynamic programming of CD8+ T lymphocyte responses. *Nat Immunol* 4:361-365.

237. Zhang, E. Y., B. L. Parker, and T. M. Yankee. 2011. Gads Regulates the Expansion Phase of CD8+ T Cell-Mediated Immunity. *J Immunol* 186:4579-4589.

238. Singh, A., A. Jatzek, E. H. Plisch, R. Srinivasan, J. Svaren, and M. Suresh. 2010. Regulation of memory CD8 T-cell differentiation by cyclin-dependent kinase inhibitor p27Kip1. *Mol Cell Biol* 30:5145-5159.

239. Joshi, N. S., W. Cui, A. Chandele, H. K. Lee, D. R. Urso, J. Hagman, L. Gapin, and S. M. Kaech. 2007. Inflammation directs memory precursor and short-lived effector CD8(+) T cell fates via the graded expression of T-bet transcription factor. *Immunity* 27:281-295.

240. Ahmed, R., M. J. Bevan, S. L. Reiner, and D. T. Fearon. 2009. The precursors of memory: models and controversies. *Nat Rev Immunol* 9:662-668.

241. Ahmed, R., and D. Gray. 1996. Immunological memory and protective immunity: understanding their relation. *Science* 272:54-60.

242. Shackelford, P. G., and R. D. Feigin. 1977. Listeria revisited. *Am J Dis Child* 131:391-392.

243. Cossart, P. 2007. Listeriology (1926-2007): the rise of a model pathogen. *Microbes Infect* 9:1143-1146.

244. Schlech, W. F., 3rd, P. M. Lavigne, R. A. Bortolussi, A. C. Allen, E. V. Haldane, A. J. Wort, A. W. Hightower, S. E. Johnson, S. H. King, E. S. Nicholls, and C. V. Broome. 1983. Epidemic listeriosis--evidence for transmission by food. *N Engl J Med* 308:203-206.

245. Swaminathan, B., and P. Gerner-Smidt. 2007. The epidemiology of human listeriosis. *Microbes Infect* 9:1236-1243.

246. Aoshi, T., J. A. Carrero, V. Konjufca, Y. Koide, E. R. Unanue, and M. J. Miller. 2009. The cellular niche of Listeria monocytogenes infection changes rapidly in the spleen. *Eur J Immunol* 39:417-425.

247. Conlan, J. W. 1996. Early pathogenesis of Listeria monocytogenes infection in the mouse spleen. *J Med Microbiol* 44:295-302.

248. Neuenhahn, M., K. M. Kerksiek, M. Nauerth, M. H. Suhre, M. Schiemann, F. E. Gebhardt, C. Stemberger, K. Panthel, S. Schroder, T. Chakraborty, S. Jung, H. Hochrein, H. Russmann, T. Brocker, and D. H. Busch. 2006. CD8alpha+ dendritic cells are required for efficient entry of Listeria monocytogenes into the spleen. *Immunity* 25:619-630.

249. Waite, J. C., I. Leiner, P. Lauer, C. S. Rae, G. Barbet, H. Zheng, D. A. Portnoy, E. G. Pamer, and M. L. Dustin. 2011. Dynamic imaging of the effector immune response to listeria infection in vivo. *PLoS Pathog* 7:e1001326.

250. Unanue, E. R. 1997. Studies in listeriosis show the strong symbiosis between the innate cellular system and the T-cell response. *Immunol Rev* 158:11-25.

251. Ladel, C. H., I. E. Flesch, J. Arnoldi, and S. H. Kaufmann. 1994. Studies with MHC-deficient knock-out mice reveal impact of both MHC I- and MHC II-dependent T cell responses on Listeria monocytogenes infection. *J Immunol* 153:3116-3122.

252. Pope, C., S. K. Kim, A. Marzo, D. Masopust, K. Williams, J. Jiang, H. Shen, and L. Lefrancois. 2001. Organ-specific regulation of the CD8 T cell response to Listeria monocytogenes infection. *J Immunol* 166:3402-3409.

253. Kaech, S. M., J. T. Tan, E. J. Wherry, B. T. Konieczny, C. D. Surh, and R. Ahmed. 2003. Selective expression of the interleukin 7 receptor identifies effector CD8 T cells that give rise to long-lived memory cells. *Nat Immunol* 4:1191-1198.

254. Ibegbu, C. C., Y. X. Xu, W. Harris, D. Maggio, J. D. Miller, and A. P. Kourtis. 2005. Expression of killer cell lectin-like receptor G1 on antigen-specific human CD8+ T lymphocytes during active, latent, and resolved infection and its relation with CD57. *J Immunol* 174:6088-6094.

255. Sarkar, S., V. Kalia, W. N. Haining, B. T. Konieczny, S. Subramaniam, and R. Ahmed. 2008. Functional and genomic profiling of effector CD8 T cell subsets with distinct memory fates. *J Exp Med* 205:625-640.

256. Prlic, M., and M. J. Bevan. 2008. Exploring regulatory mechanisms of CD8+ T cell contraction. *Proc Natl Acad Sci U S A* 105:16689-16694.

257. Smith-Garvin, J. E., J. C. Burns, M. Gohil, T. Zou, J. S. Kim, J. S. Maltzman, E. J. Wherry, G. A. Koretzky, and M. S. Jordan. 2010. T-cell receptor signals direct the composition and function of the memory CD8+ T-cell pool. *Blood* 116:5548-5559.

258. Obar, J. J., M. J. Molloy, E. R. Jellison, T. A. Stoklasek, W. Zhang, E. J. Usherwood, and L. Lefrancois. 2010. CD4+ T cell regulation of CD25 expression controls development of short-lived effector CD8+ T cells in primary and secondary responses. *Proc Natl Acad Sci U S A* 107:193-198.

259. Williams, M. A., A. J. Tyznik, and M. J. Bevan. 2006. Interleukin-2 signals during priming are required for secondary expansion of CD8+ memory T cells. *Nature* 441:890-893.

260. Bachmann, M. F., P. Wolint, S. Walton, K. Schwarz, and A. Oxenius. 2007. Differential role of IL-2R signaling for CD8+ T cell responses in acute and chronic viral infections. *Eur J Immunol* 37:1502-1512.

261. Pipkin, M. E., J. A. Sacks, F. Cruz-Guilloty, M. G. Lichtenheld, M. J. Bevan, and A. Rao. 2010. Interleukin-2 and inflammation induce distinct transcriptional programs that promote the differentiation of effector cytolytic T cells. *Immunity* 32:79-90.

262. Kalia, V., S. Sarkar, S. Subramaniam, W. N. Haining, K. A. Smith, and R. Ahmed. 2010. Prolonged interleukin-2Ralpha expression on virus-specific CD8+ T cells favors terminal-effector differentiation in vivo. *Immunity* 32:91-103.

263. Schluns, K. S., W. C. Kieper, S. C. Jameson, and L. Lefrancois. 2000. Interleukin-7 mediates the homeostasis of naive and memory CD8 T cells in vivo. *Nat Immunol* 1:426-432.

264. Masopust, D., S. J. Ha, V. Vezys, and R. Ahmed. 2006. Stimulation history dictates memory CD8 T cell phenotype: implications for prime-boost vaccination. *J Immunol* 177:831-839.

265. Kandula, S., and C. Abraham. 2004. LFA-1 on CD4+ T cells is required for optimal antigen-dependent activation in vivo. *J Immunol* 173:4443-4451.

266. Wang, Y., D. Li, R. Nurieva, J. Yang, M. Sen, R. Carreno, S. Lu, B. W. McIntyre, J. J. Molldrem, G. B. Legge, and Q. Ma. 2009. LFA-1 affinity regulation is necessary for the activation and proliferation of naive T cells. *J Biol Chem* 284:12645-12653.

267. Varga, G., N. Nippe, S. Balkow, T. Peters, M. K. Wild, S. Seeliger, S. Beissert, M. Krummen, J. Roth, C. Sunderkotter, and S. Grabbe. 2010. LFA-1 contributes to signal I

of T-cell activation and to the production of T(h)1 cytokines. *J Invest Dermatol* 130:1005-1012.

268. Chirathaworn, C., J. E. Kohlmeier, S. A. Tibbetts, L. M. Rumsey, M. A. Chan, and S. H. Benedict. 2002. Stimulation through intercellular adhesion molecule-1 provides a second signal for T cell activation. *J Immunol* 168:5530-5537.

269. Kohlmeier, J. E., L. M. Rumsey, M. A. Chan, and S. H. Benedict. 2003. The outcome of T-cell costimulation through intercellular adhesion molecule-1 differs from costimulation through leucocyte function-associated antigen-1. *Immunology* 108:152-157.

270. Kohlmeier, J. E., M. A. Chan, and S. H. Benedict. 2006. Costimulation of naive human CD4 T cells through intercellular adhesion molecule-1 promotes differentiation to a memory phenotype that is not strictly the result of multiple rounds of cell division. *Immunology* 118:549-558.

271. Hogg, N., I. Patzak, and F. Willenbrock. 2011. The insider's guide to leukocyte integrin signalling and function. *Nat Rev Immunol* 11:416-426.

272. Evans, R., I. Patzak, L. Svensson, K. De Filippo, K. Jones, A. McDowall, and N. Hogg. 2009. Integrins in immunity. *J Cell Sci* 122:215-225.

273. Benoit, M., and C. Selhuber-Unkel. 2011. Measuring cell adhesion forces: theory and principles. *Methods Mol Biol* 736:355-377.

274. Argenbright, L. W., and R. W. Barton. 1992. Interactions of leukocyte integrins with intercellular adhesion molecule 1 in the production of inflammatory vascular injury in vivo. The Shwartzman reaction revisited. *J Clin Invest* 89:259-272.

275. Malik, A. B. 1993. Endothelial cell interactions and integrins. *New Horiz* 1:37-51.

276. Muller, W. A. 2003. Leukocyte-endothelial-cell interactions in leukocyte transmigration and the inflammatory response. *Trends Immunol* 24:327-334.

277. Dustin, M. L. 2009. The cellular context of T cell signaling. *Immunity* 30:482-492.

278. Wang, Y., K. Shibuya, Y. Yamashita, J. Shirakawa, K. Shibata, H. Kai, T. Yokosuka, T. Saito, S. Honda, S. Tahara-Hanaoka, and A. Shibuya. 2008. LFA-1 decreases the antigen dose for T cell activation in vivo. *Int Immunol* 20:1119-1127.

279. Kinashi, T. 2005. Intracellular signalling controlling integrin activation in lymphocytes. *Nat Rev Immunol* 5:546-559.

280. McEver, R. P., and C. Zhu. 2010. Rolling cell adhesion. *Annu Rev Cell Dev Biol* 26:363-396.

281. Dustin, M. L., and T. A. Springer. 1989. T-cell receptor cross-linking transiently stimulates adhesiveness through LFA-1. *Nature* 341:619-624.

282. Baker, R. G., C. J. Hsu, D. Lee, M. S. Jordan, J. S. Maltzman, D. A. Hammer, T. Baumgart, and G. A. Koretzky. 2009. The adapter protein SLP-76 mediates "outside-in" integrin signaling and function in T cells. *Mol Cell Biol* 29:5578-5589.

283. Finkelstein, L. D., Y. Shimizu, and P. L. Schwartzberg. 2005. Tec kinases regulate TCR-mediated recruitment of signaling molecules and integrin-dependent cell adhesion. *J Immunol* 175:5923-5930.

284. Dustin, M. L., T. G. Bivona, and M. R. Philips. 2004. Membranes as messengers in T cell adhesion signaling. *Nat Immunol* 5:363-372.

285. Li, D., J. J. Molldrem, and Q. Ma. 2009. LFA-1 regulates CD8+ T cell activation via T cell receptor-mediated and LFA-1-mediated Erk1/2 signal pathways. *J Biol Chem* 284:21001-21010.

286. Ye, Z., M. Shi, S. Xu, and J. Xiang. 2010. LFA-1 defect-induced effector/memory CD8+ T cell apoptosis is mediated via Bcl-2/Caspase pathways and associated with downregulation of CD27 and IL-15R. *Mol Immunol* 47:2411-2421.

287. Grumont, R., P. Lock, M. Mollinari, F. M. Shannon, A. Moore, and S. Gerondakis. 2004. The mitogen-induced increase in T cell size involves PKC and NFAT activation of Rel/NF-kappaB-dependent c-myc expression. *Immunity* 21:19-30.

288. Villalba, M., K. Bi, J. Hu, Y. Altman, P. Bushway, E. Reits, J. Neefjes, G. Baier, R. T. Abraham, and A. Altman. 2002. Translocation of PKC[theta] in T cells is mediated by a nonconventional, PI3-K- and Vav-dependent pathway, but does not absolutely require phospholipase C. *J Cell Biol* 157:253-263.

289. Thebault, S., and J. Ochoa-Garay. 2004. Characterization of TCR-induced phosphorylation of PKCtheta in primary murine lymphocytes. *Mol Immunol* 40:931-942.

290. Marampon, F., C. Ciccarelli, and B. M. Zani. 2006. Down-regulation of c-Myc following MEK/ERK inhibition halts the expression of malignant phenotype in rhabdomyosarcoma and in non muscle-derived human tumors. *Mol Cancer* 5:31.

291. Lacorazza, H. D., and J. Nikolich-Zugich. 2004. Exclusion and inclusion of TCR alpha proteins during T cell development in TCR-transgenic and normal mice. *J Immunol* 173:5591-5600.

292. Niederberger, N., K. Holmberg, S. M. Alam, W. Sakati, M. Naramura, H. Gu, and N. R. Gascoigne. 2003. Allelic exclusion of the TCR alpha-chain is an active process requiring TCR-mediated signaling and c-Cbl. *J Immunol* 170:4557-4563.

293. Waterhouse, P., J. M. Penninger, E. Timms, A. Wakeham, A. Shahinian, K. P. Lee, C. B. Thompson, H. Griesser, and T. W. Mak. 1995. Lymphoproliferative disorders with early lethality in mice deficient in Ctla-4. *Science* 270:985-988.

294. Freeman, G. J., A. J. Long, Y. Iwai, K. Bourque, T. Chernova, H. Nishimura, L. J. Fitz, N. Malenkovich, T. Okazaki, M. C. Byrne, H. F. Horton, L. Fouser, L. Carter, V. Ling, M. R. Bowman, B. M. Carreno, M. Collins, C. R. Wood, and T. Honjo. 2000. Engagement of the PD-1 immunoinhibitory receptor by a novel B7 family member leads to negative regulation of lymphocyte activation. *J Exp Med* 192:1027-1034.

295. Latchman, Y., C. R. Wood, T. Chernova, D. Chaudhary, M. Borde, I. Chernova, Y. Iwai, A. J. Long, J. A. Brown, R. Nunes, E. A. Greenfield, K. Bourque, V. A. Boussiotis, L. L. Carter, B. M. Carreno, N. Malenkovich, H. Nishimura, T. Okazaki, T. Honjo, A. H. Sharpe, and G. J. Freeman. 2001. PD-L2 is a second ligand for PD-1 and inhibits T cell activation. *Nat Immunol* 2:261-268.

296. Harper, K., C. Balzano, E. Rouvier, M. G. Mattei, M. F. Luciani, and P. Golstein. 1991. CTLA-4 and CD28 activated lymphocyte molecules are closely related in both mouse and human as to sequence, message expression, gene structure, and chromosomal location. *J Immunol* 147:1037-1044.

297. Carreno, B. M., and M. Collins. 2002. The B7 family of ligands and its receptors: new pathways for costimulation and inhibition of immune responses. *Annu Rev Immunol* 20:29-53.

298. Chen, L. 2004. Co-inhibitory molecules of the B7-CD28 family in the control of T-cell immunity. *Nat Rev Immunol* 4:336-347.

299. Zou, W., and L. Chen. 2008. Inhibitory B7-family molecules in the tumour microenvironment. *Nat Rev Immunol* 8:467-477.

300. Nunes, J. A., A. Truneh, D. Olive, and D. A. Cantrell. 1996. Signal transduction by CD28 costimulatory receptor on T cells. B7-1 and B7-2 regulation of tyrosine kinase adaptor molecules. *J Biol Chem* 271:1591-1598.

301. Thummler, K., J. Leipe, A. Ramming, H. Schulze-Koops, and A. Skapenko. 2010. Immune regulation by peripheral suppressor T cells induced upon homotypic T cell/T cell interactions. *J Leukoc Biol* 88:1041-1050.

302. Eisenstein, T. K., R. T. Rahim, P. Feng, N. K. Thingalaya, and J. J. Meissler. 2006. Effects of opioid tolerance and withdrawal on the immune system. *J Neuroimmune Pharmacol* 1:237-249.

303. Wang, J., R. A. Barke, J. Ma, R. Charboneau, and S. Roy. 2008. Opiate abuse, innate immunity, and bacterial infectious diseases. *Arch Immunol Ther Exp (Warsz)* 56:299-309.

304. Bryant, H. U., E. W. Bernton, and J. W. Holaday. 1987. Immunosuppressive effects of chronic morphine treatment in mice. *Life Sci* 41:1731-1738.

305. Bryant, H. U., E. W. Bernton, and J. W. Holaday. 1988. Morphine pellet-induced immunomodulation in mice: temporal relationships. *J Pharmacol Exp Ther* 245:913-920.

306. Sei, Y., K. Yoshimoto, T. McIntyre, P. Skolnick, and P. K. Arora. 1991. Morphine-induced thymic hypoplasia is glucocorticoid-dependent. *J Immunol* 146:194-198.

307. Freier, D. O., and B. A. Fuchs. 1993. Morphine-induced alterations in thymocyte subpopulations of B6C3F1 mice. *J Pharmacol Exp Ther* 265:81-88.

308. Plum, J., M. De Smedt, A. Billiau, H. Heremans, G. Leclercq, and B. Tison. 1991. IFN-gamma reverses IL-4 inhibition of fetal thymus growth in organ culture. *J Immunol* 147:50-54.

309. Ueno, T., C. Liu, T. Nitta, and Y. Takahama. 2005. Development of T-lymphocytes in mouse fetal thymus organ culture. *Methods Mol Biol* 290:117-133.

310. Loder, F., B. Mutschler, R. J. Ray, C. J. Paige, P. Sideras, R. Torres, M. C. Lamers, and R. Carsetti. 1999. B cell development in the spleen takes place in discrete steps and is determined by the quality of B cell receptor-derived signals. *J Exp Med* 190:75-89.

311. Cho, B. K., V. P. Rao, Q. Ge, H. N. Eisen, and J. Chen. 2000. Homeostasis-stimulated proliferation drives naive T cells to differentiate directly into memory T cells. *J Exp Med* 192:549-556.

312. Goldrath, A. W., L. Y. Bogatzki, and M. J. Bevan. 2000. Naive T cells transiently acquire a memory-like phenotype during homeostasis-driven proliferation. *J Exp Med* 192:557-564.

313. Murali-Krishna, K., and R. Ahmed. 2000. Cutting edge: naive T cells masquerading as memory cells. *J Immunol* 165:1733-1737.

314. Clarke, S. R., and A. Y. Rudensky. 2000. Survival and homeostatic proliferation of naive peripheral CD4+ T cells in the absence of self peptide:MHC complexes. *J Immunol* 165:2458-2464.

315. Tanchot, C., A. Le Campion, S. Leaument, N. Dautigny, and B. Lucas. 2001. Naive CD4(+) lymphocytes convert to anergic or memory-like cells in T cell-deprived recipients. *Eur J Immunol* 31:2256-2265.

316. Cohen, J. J., and R. C. Duke. 1984. Glucocorticoid activation of a calcium-dependent endonuclease in thymocyte nuclei leads to cell death. *J Immunol* 132:38-42.

317. Radtke, F., A. Wilson, S. J. Mancini, and H. R. MacDonald. 2004. Notch regulation of lymphocyte development and function. *Nat Immunol* 5:247-253.

318. Robey, E. A., and J. A. Bluestone. 2004. Notch signaling in lymphocyte development and function. *Curr Opin Immunol* 16:360-366.

319. Huang, E. Y., A. M. Gallegos, S. M. Richards, S. M. Lehar, and M. J. Bevan. 2003. Surface expression of Notch1 on thymocytes: correlation with the double-negative to double-positive transition. *J Immunol* 171:2296-2304.

320. Fiorini, E., E. Merck, A. Wilson, I. Ferrero, W. Jiang, U. Koch, F. Auderset, E. Laurenti, F. Tacchini-Cottier, M. Pierres, F. Radtke, S. A. Luther, and H. R. Macdonald. 2009. Dynamic regulation of notch 1 and notch 2 surface expression during T cell development and activation revealed by novel monoclonal antibodies. *J Immunol* 183:7212-7222.

321. Deftos, M. L., Y. W. He, E. W. Ojala, and M. J. Bevan. 1998. Correlating notch signaling with thymocyte maturation. *Immunity* 9:777-786.

322. Bryant, H. U., B. C. Yoburn, C. E. Inturrisi, E. W. Bernton, and J. W. Holaday. 1988. Morphine-induced immunomodulation is not related to serum morphine concentrations. *Eur J Pharmacol* 149:165-169.

323. Roy, S., J. H. Wang, S. Balasubramanian, Sumandeep, R. Charboneau, R. Barke, and H. H. Loh. 2001. Role of hypothalamic-pituitary axis in morphine-induced alteration in thymic cell distribution using mu-opioid receptor knockout mice. *J Neuroimmunol* 116:147-155.

324. Vines, R. L., M. S. Coleman, and J. J. Hutton. 1980. Reappearance of terminal deoxynucleotidyl transferase containing cells in rat bone marrow following corticosteroid administration. *Blood* 56:501-509.

325. Yin, D., D. Tuthill, R. A. Mufson, and Y. Shi. 2000. Chronic restraint stress promotes lymphocyte apoptosis by modulating CD95 expression. *J Exp Med* 191:1423-1428.

326. Yin, D., R. A. Mufson, R. Wang, and Y. Shi. 1999. Fas-mediated cell death promoted by opioids. *Nature* 397:218.

327. Wang, J., R. Charboneau, R. A. Barke, H. H. Loh, and S. Roy. 2002. Mu-opioid receptor mediates chronic restraint stress-induced lymphocyte apoptosis. *J Immunol* 169:3630-3636.

328. Lundin, P., and B. Jarplid. 1973. Effects of corticosteroid and radiation on lymphoid tissue in mice. Comparisons and mutual interactions. *Lymphology* 6:158-166.

329. Bach, J. F., D. Duval, M. Dardenne, J. C. Salomon, T. Tursz, and C. Fournier. 1975. The effects of steroids on T cells. *Transplant Proc* 7:25-30.

330. Batra, K. V., L. M. Elrod, and R. Schrek. 1966. Species differences in the in vitro sensitivity of lymphocytes to prednisolone and x-rays. *J Pharmacol Exp Ther* 152:525-528.

331. Nieto, M. A., and A. Lopez-Rivas. 1992. Glucocorticoids activate a suicide program in mature T lymphocytes: protective action of interleukin-2. *Ann N Y Acad Sci* 650:115-120.

332. Perandones, C. E., V. A. Illera, D. Peckham, L. L. Stunz, and R. F. Ashman. 1993. Regulation of apoptosis in vitro in mature murine spleen T cells. *J Immunol* 151:3521-3529.

333. Aderjan, R., S. Hofmann, G. Schmitt, and G. Skopp. 1995. Morphine and morphine glucuronides in serum of heroin consumers and in heroin-related deaths determined by HPLC with native fluorescence detection. *J Anal Toxicol* 19:163-168.

334. Rook, E. J., J. M. van Ree, W. van den Brink, M. J. Hillebrand, A. D. Huitema, V. M. Hendriks, and J. H. Beijnen. 2006. Pharmacokinetics and pharmacodynamics of high doses of pharmaceutically prepared heroin, by intravenous or by inhalation route in opioid-dependent patients. *Basic Clin Pharmacol Toxicol* 98:86-96.

335. Zubkova, I., H. Mostowski, and M. Zaitseva. 2005. Up-regulation of IL-7, stromal-derived factor-1 alpha, thymus-expressed chemokine, and secondary lymphoid tissue chemokine gene expression in the stromal cells in response to thymocyte depletion: implication for thymus reconstitution. *J Immunol* 175:2321-2330.

336. von Freeden-Jeffry, U., P. Vieira, L. A. Lucian, T. McNeil, S. E. Burdach, and R. Murray. 1995. Lymphopenia in interleukin (IL)-7 gene-deleted mice identifies IL-7 as a nonredundant cytokine. *J Exp Med* 181:1519-1526.

337. Maki, K., S. Sunaga, Y. Komagata, Y. Kodaira, A. Mabuchi, H. Karasuyama, K. Yokomuro, J. I. Miyazaki, and K. Ikuta. 1996. Interleukin 7 receptor-deficient mice lack gammadelta T cells. *Proc Natl Acad Sci U S A* 93:7172-7177.

338. Ramos-Casals, M., M. Garcia-Carrasco, M. P. Brito, A. Lopez-Soto, and J. Font. 2003. Autoimmunity and geriatrics: clinical significance of autoimmune manifestations in the elderly. *Lupus* 12:341-355.

339. Dorshkind, K., E. Montecino-Rodriguez, and R. A. Signer. 2009. The ageing immune system: is it ever too old to become young again? *Nat Rev Immunol* 9:57-62.

340. Williams, K. M., F. T. Hakim, and R. E. Gress. 2007. T cell immune reconstitution following lymphodepletion. *Semin Immunol* 19:318-330.

341. Askenasy, E. M., N. Askenasy, and J. J. Askenasy. 2010. Does lymphopenia preclude restoration of immune homeostasis? The particular case of type 1 diabetes. *Autoimmun Rev* 9:687-690.

342. Kang, S. J., H. E. Liang, B. Reizis, and R. M. Locksley. 2008. Regulation of hierarchical clustering and activation of innate immune cells by dendritic cells. *Immunity* 29:819-833.

343. Pham, N.-L., V. Badovinac, and J. Harty. 2011. Differential role of "signal 3" inflammatory cytokines in regulating CD8 T cell expansion and differentiation in vivo. *Frontiers in Immunology* 2:Article 4.

344. Haring, J. S., V. P. Badovinac, and J. T. Harty. 2006. Inflaming the CD8+ T cell response. *Immunity* 25:19-29.

345. Mescher, M. F., J. M. Curtsinger, P. Agarwal, K. A. Casey, M. Gerner, C. D. Hammerbeck, F. Popescu, and Z. Xiao. 2006. Signals required for programming effector and memory development by CD8+ T cells. *Immunol Rev* 211:81-92.

346. Rubinstein, M. P., N. A. Lind, J. F. Purton, P. Filippou, J. A. Best, P. A. McGhee, C. D. Surh, and A. W. Goldrath. 2008. IL-7 and IL-15 differentially regulate CD8+ T-cell subsets during contraction of the immune response. *Blood* 112:3704-3712.

347. Obar, J. J., and L. Lefrancois. 2010. Early events governing memory CD8+ T-cell differentiation. *Int Immunol* 22:619-625.

348. Casey, K. A., and M. F. Mescher. 2007. IL-21 promotes differentiation of naive CD8 T cells to a unique effector phenotype. *J Immunol* 178:7640-7648.

349. Khanna, K. M., J. T. McNamara, and L. Lefrancois. 2007. In situ imaging of the endogenous CD8 T cell response to infection. *Science* 318:116-120.

350. Kambayashi, T., E. Assarsson, B. J. Chambers, and H. G. Ljunggren. 2001. Cutting edge: Regulation of CD8(+) T cell proliferation by 2B4/CD48 interactions. *J Immunol* 167:6706-6710.

351. Wong, P., and E. G. Pamer. 2001. Cutting edge: antigen-independent CD8 T cell proliferation. *J Immunol* 166:5864-5868.

352. Mercado, R., S. Vijh, S. E. Allen, K. Kerksiek, I. M. Pilip, and E. G. Pamer. 2000. Early programming of T cell populations responding to bacterial infection. *J Immunol* 165:6833-6839.

353. Prlic, M., G. Hernandez-Hoyos, and M. J. Bevan. 2006. Duration of the initial TCR stimulus controls the magnitude but not functionality of the CD8+ T cell response. *J Exp Med* 203:2135-2143.

354. Sanchez-Madrid, F., P. Simon, S. Thompson, and T. A. Springer. 1983. Mapping of antigenic and functional epitopes on the alpha- and beta-subunits of two related mouse glycoproteins involved in cell interactions, LFA-1 and Mac-1. *J Exp Med* 158:586-602.

355. Harning, R., C. Myers, and V. J. Merluzzi. 1993. Monoclonal antibodies to lymphocyte function-associated antigen-1 inhibit invasion of human lymphoma and metastasis of murine lymphoma. *Clin Exp Metastasis* 11:337-342.

356. Harning, R., J. Pelletier, K. Lubbe, F. Takei, and V. J. Merluzzi. 1991. Reduction in the severity of graft-versus-host disease and increased survival in allogenic mice by treatment with monoclonal antibodies to cell adhesion antigens LFA-1 alpha and MALA-2. *Transplantation* 52:842-845.

357. Heagy, W., C. Waltenbaugh, and E. Martz. 1984. Potent ability of anti-LFA-1 monoclonal antibody to prolong allograft survival. *Transplantation* 37:520-523.

358. Driessens, M. H., P. van Hulten, A. Zuurbier, G. La Riviere, and E. Roos. 1996. Inhibition and stimulation of LFA-1 and Mac-1 functions by antibodies against murine CD18. Evidence that the LFA-1 binding sites for ICAM-1, -2, and -3 are distinct. *J Leukoc Biol* 60:758-765.

359. Gultner, S., T. Kuhlmann, A. Hesse, J. P. Weber, C. Riemer, M. Baier, and A. Hutloff. 2010. Reduced Treg frequency in LFA-1-deficient mice allows enhanced T effector differentiation and pathology in EAE. *Eur J Immunol* 40:3403-3412.

360. Ding, Z. M., J. E. Babensee, S. I. Simon, H. Lu, J. L. Perrard, D. C. Bullard, X. Y. Dai, S. K. Bromley, M. L. Dustin, M. L. Entman, C. W. Smith, and C. M. Ballantyne. 1999. Relative contribution of LFA-1 and Mac-1 to neutrophil adhesion and migration. *J Immunol* 163:5029-5038.

361. Bose, T., and L. Lefrancois. 2011. The role of {beta}2 integrins in host immune responses to bacterial infection. *J Immunol* 186:112.26.

362. Scholer, A., S. Hugues, A. Boissonnas, L. Fetler, and S. Amigorena. 2008. Intercellular adhesion molecule-1-dependent stable interactions between T cells and dendritic cells determine CD8+ T cell memory. *Immunity* 28:258-270.

363. Binnerts, M. E., and Y. van Kooyk. 1999. How LFA-1 binds to different ligands. *Immunol Today* 20:240-245.

364. Ostermann, G., K. S. Weber, A. Zernecke, A. Schroder, and C. Weber. 2002. JAM-1 is a ligand of the beta(2) integrin LFA-1 involved in transendothelial migration of leukocytes. *Nat Immunol* 3:151-158.

365. Marzo, A. L., K. D. Klonowski, A. Le Bon, P. Borrow, D. F. Tough, and L. Lefrancois. 2005. Initial T cell frequency dictates memory CD8+ T cell lineage commitment. *Nat Immunol* 6:793-799.

366. Hao, Y., N. Legrand, and A. A. Freitas. 2006. The clone size of peripheral CD8 T cells is regulated by TCR promiscuity. *J Exp Med* 203:1643-1649.

367. Gurung, P., B. M. Young, R. A. Coleman, S. Wiechert, L. E. Turner, N. B. Ray, T. J. Waldschmidt, K. L. Legge, and R. T. Cook. 2009. Chronic ethanol induces inhibition of antigen-specific CD8+ but not CD4+ immunodominant T cell responses following Listeria monocytogenes inoculation. *J Leukoc Biol* 85:34-43.

368. Seo, S. K., H. Y. Jeong, S. G. Park, S. W. Lee, I. W. Choi, L. Chen, and I. Choi. 2008. Blockade of endogenous B7-H1 suppresses antibacterial protection after primary Listeria monocytogenes infection. *Immunology* 123:90-99.

369. Pamer, E. G., A. J. Sijts, M. S. Villanueva, D. H. Busch, and S. Vijh. 1997. MHC class I antigen processing of Listeria monocytogenes proteins: implications for dominant and subdominant CTL responses. *Immunol Rev* 158:129-136.

370. Schnupf, P., and D. A. Portnoy. 2007. Listeriolysin O: a phagosome-specific lysin. *Microbes Infect* 9:1176-1187.

371. Bahjat, K. S., N. Meyer-Morse, E. E. Lemmens, J. A. Shugart, T. W. Dubensky, D. G. Brockstedt, and D. A. Portnoy. 2009. Suppression of cell-mediated immunity following recognition of phagosome-confined bacteria. *PLoS Pathog* 5:e1000568.

372. McCoy, J. L., R. B. Herberman, E. B. Rosenberg, F. C. Donnelly, P. H. Levine, and C. Alford. 1973. 51 Chromium-release assay for cell-mediated cytotoxicity of human leukemia and lymphoid tissue-culture cells. *Natl Cancer Inst Monogr* 37:59-67.

373. Peterson, E. J., M. L. Woods, S. A. Dmowski, G. Derimanov, M. S. Jordan, J. N. Wu, P. S. Myung, Q. H. Liu, J. T. Pribila, B. D. Freedman, Y. Shimizu, and G. A. Koretzky. 2001. Coupling of the TCR to integrin activation by Slap-130/Fyb. *Science* 293:2263-2265.

374. Griffiths, E. K., C. Krawczyk, Y. Y. Kong, M. Raab, S. J. Hyduk, D. Bouchard, V. S. Chan, I. Kozieradzki, A. J. Oliveira-Dos-Santos, A. Wakeham, P. S. Ohashi, M. I. Cybulsky, C. E. Rudd, and J. M. Penninger. 2001. Positive regulation of T cell activation and integrin adhesion by the adapter Fyb/Slap. *Science* 293:2260-2263.

375. Peterson, E. J. 2003. The TCR ADAPts to integrin-mediated cell adhesion. *Immunol Rev* 192:113-121.

376. Myung, P. S., G. S. Derimanov, M. S. Jordan, J. A. Punt, Q. H. Liu, B. A. Judd, E. E. Meyers, C. D. Sigmund, B. D. Freedman, and G. A. Koretzky. 2001. Differential

requirement for SLP-76 domains in T cell development and function. *Immunity* 15:1011-1026.

377. Dustin, M. L., and J. A. Cooper. 2000. The immunological synapse and the actin cytoskeleton: molecular hardware for T cell signaling. *Nat Immunol* 1:23-29.

378. Zhang, J., A. Shehabeldin, L. A. da Cruz, J. Butler, A. K. Somani, M. McGavin, I. Kozieradzki, A. O. dos Santos, A. Nagy, S. Grinstein, J. M. Penninger, and K. A. Siminovitch. 1999. Antigen receptor-induced activation and cytoskeletal rearrangement are impaired in Wiskott-Aldrich syndrome protein-deficient lymphocytes. *J Exp Med* 190:1329-1342.

379. Snapper, S. B., F. S. Rosen, E. Mizoguchi, P. Cohen, W. Khan, C. H. Liu, T. L. Hagemann, S. P. Kwan, R. Ferrini, L. Davidson, A. K. Bhan, and F. W. Alt. 1998. Wiskott-Aldrich syndrome protein-deficient mice reveal a role for WASP in T but not B cell activation. *Immunity* 9:81-91.

380. Krause, M., A. S. Sechi, M. Konradt, D. Monner, F. B. Gertler, and J. Wehland. 2000. Fyn-binding protein (Fyb)/SLP-76-associated protein (SLAP), Ena/vasodilator-stimulated phosphoprotein (VASP) proteins and the Arp2/3 complex link T cell receptor (TCR) signaling to the actin cytoskeleton. *J Cell Biol* 149:181-194.